Estimating sauropod body mass and gait

by the analysis of recent and fossil tetrapod tracks with photogrammetry and soil mechanics

Sashima Läbe

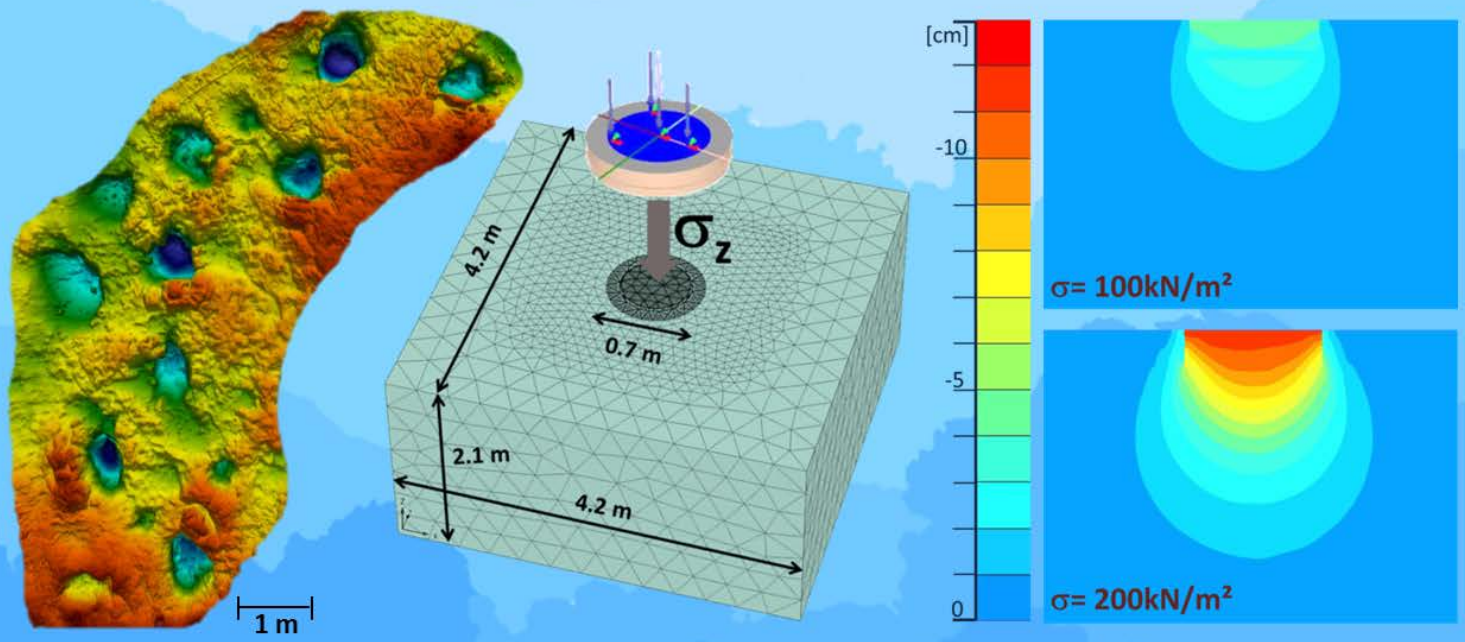

Estimating sauropod body mass and gait
by the analysis of recent and fossil tetrapod tracks with photogrammetry and soil mechanics

Dissertation
zur
Erlangung des Doktorgrades (Dr. rer. nat.)
der
Mathematisch-Naturwissenschaftlichen Fakultät
der
Rheinischen Friedrich-Wilhelms-Universität Bonn

vorgelegt von
Sashima Läbe
aus
Hannover

Bonn 2017

Anfertigung mit Genehmigung der Mathematisch-Naturwissenschaftlichen Fakultät der Rheinischen Friedrich-Wilhelms-Universität Bonn

1. Gutachter: Prof. Dr. P. Martin Sander

2. Gutachter: Prof. Dr. Thomas Martin

Tag der Promotion: 28.07.2017

Erscheinungsjahr: 2017

Für Jonathan, ein Dinobuch.

Front cover (from left to right, see Chapter 6 for details): Color depth map of the Copper Ridge sauropod trackway. Finite element analysis model. Vertical displacement in lateral view of the finite element analysis model.

Back cover: Silhouette of *Diplodocus carnegii* by Scott Hartman. The image has been changed and reused under Creative Commons Attribution 3.0 Unported license.

Acknowledgements

First of all, I wish to thank my supervisor P. Martin Sander for continuously encouraging and supporting me during my research. I really appreciate being part of his working group. I am grateful for his advice and expertise on my way becoming a researcher and I also thank him for his courageous efforts during field work.

I thank Thomas Martin for kindly being the second reviewer, as well as Thorsten Geisler-Wierwille, and Christa E. Müller, who kindly agreed on being part of the dissertation committee.

I thank the Studienstiftung des deutschen Volkes and the Andrea von Braun Stiftung for providing generous scholarships that funded my research and related fieldwork.

This dissertation would not have been possible without many researchers, who I wish to thank for their support: I thank Tom Schanz for introducing me to soil mechanics and giving me the opportunity to conduct parts my research in his lab. Holger Preuschoft is thanked for introducing me to biomechanics and for sharing his interest in the study of extant horses with me. I thank Ulrich Witzel for getting this project started years ago. Kathrin Kienapfel is thanked for letting me participate in her horse research, which taught me a great deal on biomechanics. I thank Christoph Schmüdderich, who kindly provided support and instructions of the finite element analyses. Negar Rahemi, Hanna Haase, and Michael Skubisch are thanked for their support in all kinds of soil mechanical questions. I thank Heinrich Mallison for introducing me to photogrammetry. For supporting my fieldwork I wish to thank Benjamin Englich, Nils Knötschke, Angelika Leipner, and Octávio Mateus. I am grateful for inspiration, collaboration, and support from Thomas Barciaga, Matteo Belvedere, Peter L. Falkingham, Yvonne Lins, Martin G. Lockley, and Neffra Matthews.

I am very grateful to Jessica Mitchell and wish to express my earnest thanks to her for being a wonderful office mate and friend. Without her support, knowledge, motivation, and proof reading pages by pages, I never would have become the researcher I am now. For fruitful discussions and his great expertise on dinosaur tracks, I am thankful to Jens Lallensack. My peers of AGSander, I thank you all for contributing to this inspiring working atmosphere. Without help from the technical staff, it would not be possible to finish this dissertation. Thus, I am grateful to Baran Demir, Olaf Dülfer, Peter Göddertz, Dagmar Hambach, Kay Heitplatz, Dorothea Kranz, Carola Kubus, Beate Mühlens-Scaramuzza, Georg Oleschinski, and Rainer Schwarz.

To my dear fiends Marianne Koch, Jeffrey Power, Kristian Remes, Achim Schermann, Leonie Schwermann, Andreas Temme, Katja Waskow, and Sarah Wilker, I thank you all wholeheartedly for your friendship, support, and all cheering ups during my entire dissertation. My friends from my tap dance group are also thanked for helping me finding the right "steps" during the last few years.

To Seela and Siegfried Läbe, I am fortunate having wonderful, supportive, understanding, and loving parents – Thank you for everything. I thank my beloved companion, friend and field partner Thorsten Plogschties for his ongoing support and company during all kinds of adventures, endeavors, and travels. My special and heartfelt thanks go to my dear son Jonathan. His love makes me stronger and he always reminds me to enjoy life against all odds.

Summary

This dissertation presents an analysis of recent and fossil tracks with quantitative and interdisciplinary methods for estimating the body mass and locomotion of a sauropod trackmaker. By employing methods from natural and engineering sciences, this research demonstrates that interdisciplinary research on tetrapod tracks can provide insights beyond conventional paleontological research. The novelty in this dissertation is that it brings aspects from traditional vertebrate ichnology together with modern methods and considerations from biomechanics and soil mechanics to gain additional information about sauropod paleobiology.

Track and trackways are structures left behind by an animal. Their formation is dependent on the substrate (i.e., soil or sediment) that contains the tracks, as well as the anatomy and locomotion of the trackmaker. Fossil tracks can provide a great deal of information about the extinct trackmaker, such as type, size, speed, behavior, and even pathologies. Although, it would be intuitive to think that the body mass of the trackmaker can also be determined from tracks, this has not been done before. Particularly, since body mass, which, for example, can reach record-breaking values in the case of the sauropod dinosaurs, is one of the fundamental attributes of any animal. Common mass estimation methods require body fossils for reconstructing density/volume or to make scaling relationships from long bones. However, body fossils are usually not available in most tracksites due to preservation conditions. Thus, estimating the weight of the trackmaker from its tracks, both extant and extinct, is the object of research in this dissertation.

For determining the exact geometry and dimensions of both recent and fossil tracks, precise documentation is required. Photogrammetry is a method from geodesy that has proved to be very useful for vertebrate ichnology. It uses digital images to generate three-dimensional (3D) models. The interpretability of these 3D models is improved by the geological method of vertical exaggeration, which stretches the vertical axis of a model to visualize previously unseen structures in the tracks. Applying vertical exaggeration is novel to vertebrate ichnology and reveals important information of the trackmaker from its tracks, such as travel direction and anatomical details of the hands and feet.

To test if estimating the weight from fossil tracks is feasible, studying recent trackmakers for calibration is necessary. Elephants are the largest living land animals and often used as living analogs to the extinct sauropod dinosaurs. Elephant footprints are digitized and used as the basis of a numerical simulation (finite element analysis), constrained by the substrate

properties. The load required to generate these footprints was reconstructed and the elephant's weight was back calculated. Although, weight estimation for a recent trackmaker is possible with an error of about 15%, careful assessment of the influence of the trackmaker's locomotion is also important. For fossil trackmakers, precise evaluation of the locomotion, let alone the gait, is difficult to ascertain from tracks. The main gaits, such as walk, trot, pace, and gallop, are determined by studying horses, which make them a prime example for understanding locomotion from tracks. Together with basic estimations of the trackmaker's size, it is possible to estimate the gait from tracks. Different gaits also mean varying distribution of the mass among the limbs during locomotion, which is of particular interest for any mass estimation approach on tracks. For instance, the fraction of the weight distributed on the hindlimbs is high when the center of mass of the animal is positioned posteriorly and low when the position of the center of mass is positioned anteriorly.

Considering all these influencing factors, mass estimation and reconstruction of movement are possible from recent, as well from fossil tracks. For example, in the case of a 150 million year old sauropod trackway, the mass of the trackmaker was estimated to be about 16 tonnes, which is in good agreement with other mass estimates from body fossils. With these results, this research intends to provide a foundation for future applications of the gait and mass estimation approaches based on tracks, and hopes to inspire others to employ interdisciplinary methods to tetrapod tracks to exploit their, often underestimated, high information content.

Contents

CHAPTER 1

Introduction

Long before the first scientists researched vertebrate tracks, starting in the 19th century (e.g., Kaup, 1835; Hitchcock, 1836; Tagart, 1846; Hitchcock, 1848, 1858; Jones, 1862; Hitchcock, 1865; Struckmann, 1880), animal tracking was vital to our prehistoric ancestors. Even today, hunters, foresters, and tribal people make use of animal traces, as well as animal conservationists, who use the interpretation of footprints for tracking endangered species (e.g., Alibhai et al., 2008). Much of this long-held knowledge on animal tracking has been applied to the research on dinosaur tracks, the field of dinosaur ichnology, on which many descriptive studies had been carried out to report new tracksites and to name new tracks in recent decades (e.g., in Gillette and Lockley, 1989) to about the end of the 20th century. Since then, it has been increasingly recognized that vertebrate ichnology needs to go beyond the descriptive to harvest the wealth of information contained in fossil tracks left by four-footed animals on the surface of this planet for the last 320 million years.

1.1. TERMINOLOGY

In contrast to traditional and descriptive studies mentioned above, this interdisciplinary dissertation involves several methods from geosciences and engineering, such as photogrammetry, sediment analysis, soil mechanical finite element analysis, and biomechanical considerations on locomotion. Obviously, during interdisciplinary work multiple science cultures and terminologies meet each other, which require an understanding on the used terms. The ichnological terminology used here follows that of Marty et al. (2016), who provided a glossary of terms relevant for dinosaur ichnology. With this glossary, the authors simplified the communication in vertebrate ichnology, since formerly missing general agreement on terms was often a source of confusion.

However, for easier understanding and better readability, the most important terms are introduced here. The terms *track/s* and *imprint/s* are used for substrate deformation formed by a single autopodium or multiple autopodia of a *trackmaker*, which is the animal that left tracks behind. A sequence of multiple imprints/tracks of one trackmaker is termed a *trackway*. Particularly for *quadruped* trackmakers (movement on four limbs), such as sauro-

pods, in contrast to *biped* trackmakers (movement on two limbs, the hind limbs), such as humans, distinguishing between tracks of anterior and posterior limbs is required: *Footprint/s* is used for *pes/pedēs* (foot) tracks, and *manus/manūs* (hand) tracks refer to the anterior autopodium. Measurements of manus and pes tracks are used for calculating the *heteropody index*, which, for example, is used for identifying a sauropod trackmaker (Lockley, 1989; Lockley et al., 1994; Santos et al., 1994; Lockley, 2007).

Chapters dealing with the movement of the trackmaker (Chapter 4 and Chapter 5), frequently use the following terms: the movement of an animal involving its limbs to progress over the land surface is meant by the term *locomotion*. Different types of repeating cycles of limb movement are termed *gaits*, such as walk, trot, pace, amble, and gallop (cf. Muybridge, 1899). The term *walking* not only means that the trackmaker goes from A to B, but that it employed a *walk*, which is a slow gait that requires alternating *stance phases* (ground contact) of two and three limbs.

For the chapters where methods from soil mechanics are employed (Chapter 3 and Chapter 5), the term *substrate* stands for the medium that contains the tracks. Since this is a multi-methodological and interdisciplinary approach, substrate can represent both, the *sediment* from a geological perspective, as well as *soil* from a soil mechanical perspective.

For the weight estimation approach (Chapter 3 and Chapter 6), the term *dynamic component* refers to the locomotion of the trackmaker, while *static component* is due to the trackmaker's weight. Note that the terms *body mass* and *weight* are interchangeably used in this dissertation. The proper physical term for an amount of matter is *mass*, while *weight* is technically a force exerted to an object by acceleration of gravity. The weight estimation approaches explicitly consider the acceleration and forces exerted on the substrate by the trackmaker during track formation. Thus, it was refrained from strictly distinguishing both terms.

1.2. TRACKS AND TRACKWAYS – WHAT ARE THEY GOOD FOR?

The dinosaur track record provides valuable information about aspects of the trackmaker that are unavailable in body fossils, such as the behavior of the trackmaker by observing the direction of travel or the co-occurrence with other trackways (e.g., Day, Upchurch et al., 2002; Lockley et al., 2002; Myers and Fiorillo, 2009; Bibi et al., 2012). Moreover, the trackmaker's size (Thulborn, 1990), locomotion (Gatesy et al., 1999; Day, Norman et al., 2002), and speed (Alexander, 1976) can be revealed from its tracks. The track distribution and assemblages can also provide information about the paleoenvironment (Lockley et al., 1986; Marty, 2008; Falkingham et al., 2012; Santos et al., 2013).

Tracks of the long-necked dinosaurs (sauropods) are particularly interesting, since they can reach impressive sizes, such as the more than 1.5 m long sauropod tracks from the Lower

Cretaceous Broome Sandstone, Australia (Salisbury et al., 2017). Sauropod trackmakers were the largest terrestrial creatures that have ever lived on Earth (Upchurch, 1995; Curry Rogers and Wilson, 2005; Sander and Clauss, 2008; Klein et al., 2011; Sander et al., 2011; Sander, 2013). With a length of about one fifth of the Australian ones, the sauropod tracks, for example, from the Upper Jurassic Avelino tracksite, Portugal (Lockley and dos Santos, 1993) and Barkhausen tracksite, Germany (Kaever and de Lapparent, 1974; Friese, 1979) belong to the smallest sauropods.

1.3. INTERPRETATIVE STUDIES ON DINOSAUR TRACKS

Beginning with the new millennium, a new phase in dinosaur ichnology started going beyond the traditional descriptive approach. To gain more insights on track formation, many researchers employed animal and laboratory experimental approaches (Manning, 2004; Milàn, 2006; Jackson et al., 2009, 2010; Platt et al., 2012; Falkingham and Gatesy, 2014; White et al., 2017) and quantitative computer simulation, such as the method of finite element analysis (FEA). FEA allows for modelling of physical processes with simulated materials behaving in a natural manner. With such methods, the geotechnical aspect of tracks was investigated (Margetts et al., 2005; Margetts et al., 2006; Falkingham et al., 2011b; Falkingham et al., 2014; Sanz et al., 2016), for example, to infer paleobiological features of the trackmaker (Falkingham et al., 2009; Falkingham et al., 2011a; Schanz et al., 2013).

Vertebrate tracks are complex structures in the sediments (Manning, 2004). To understand the information contained in tracks, not only the anatomy of the trackmaker has to be considered, but also its locomotion, and the substrate in which the tracks are found (Padian and Olsen, 1984; Falkingham, 2014). This requires a deeper interpretation of the track record with interdisciplinary methodology to provide further paleobiological insights on the trackmaker.

1.4. AIM OF THIS DISSERTATION

The dissertation consists of a succession of six chapters and a final synthesis that are directly associated with each other (Figure 1.1). The objective of this dissertation is to investigate the potential of tracks for making paleobiological interpretations, such as the locomotion (types of gaits) and the body mass of fossil sauropod trackmakers, with interdisciplinary and multi-methodological approaches. Therefore, three-dimensional (3D) documentation of tracks and studies on extant trackmakers, such as the horse (Kienapfel et al., 2014; Chapter 4) and elephant (Schanz et al., 2013; Chapter 3), set the stage for the quantitative research on sauropod trackmakers. The dissertation focusses on sauropod tracks, since their dynamics are assumed to be low (e.g., Preuschoft et al., 2011) and their foot anatomy is easily approximated. The results of this dissertation extend previous knowledge (see section 1.3) in terms of combining the anatomy seen in digital track models, the loco-

motion estimated from footfall patterns in trackways, and the penetration of the autopodium into the substrate with soil mechanical methods, particularly in view on sauropod trackmakers. However, the work on quantitative track interpretations with interdisciplinary methods is in its infancy and has room for development in future studies on other trackmakers, both fossil and extant.

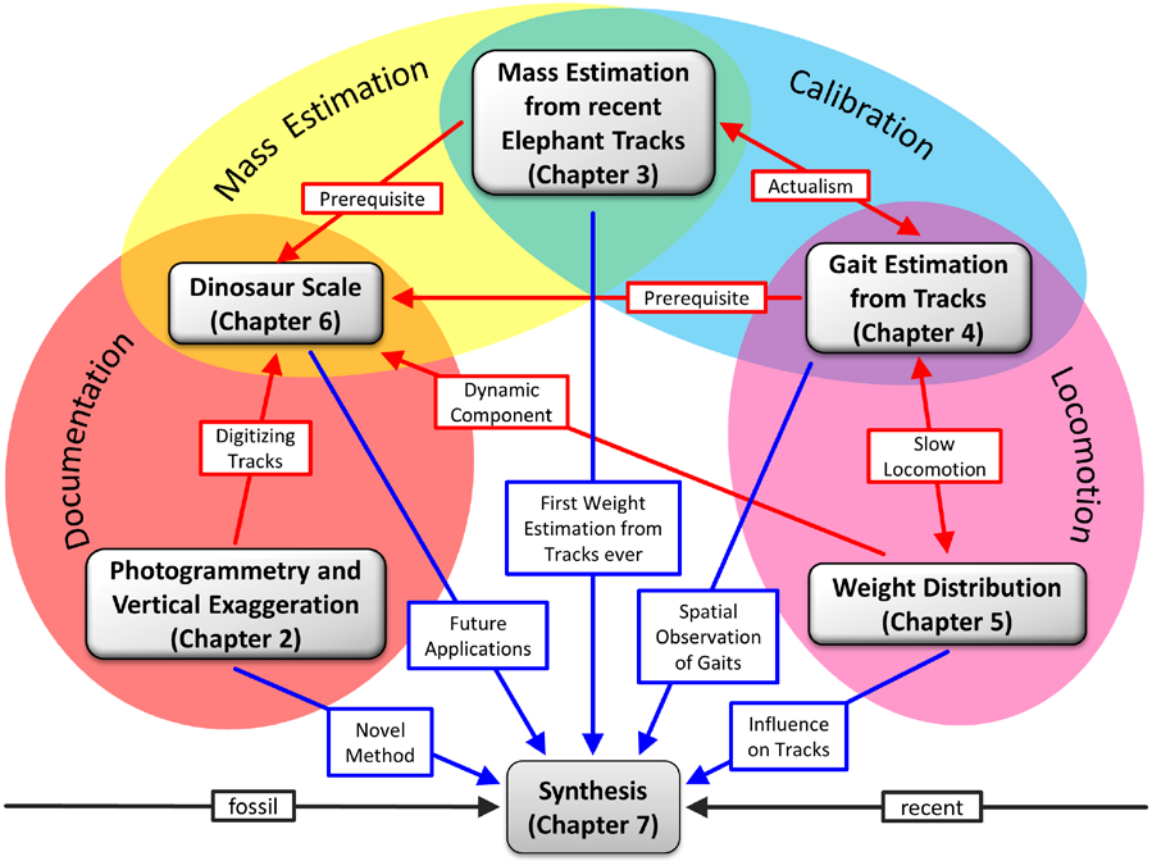

Figure 1.1: The "big picture" overview of all dissertation chapters (excluding this introduction). Each chapter is imbedded in a larger context (documentation, mass estimation, calibration, locomotion), whereby Chapters 3, 4 and 6 mark combinations of overlapping fields. Chapters on fossil tracks are on the left side, while recent track chapters are right (black arrows). Red arrows indicate interactions between chapters. Blue arrows reflect the overall implications from evidence from disparate fields for the final synthesis. Note that the grey boxes show keywords of chapters instead of full chapter titles.

1.5. DESCRIPTION OF CHAPTERS

1.5.1 Chapter 2

This chapter focuses on the digitizing method photogrammetry and the manipulation of 3D models with vertical exaggeration using sauropod tracks of four localities with mostly poor preservation for the purpose of extending previous knowledge and the possible scientific data obtainable at these localities (e.g., Läbe, unpubl. b; Chapter 6). For vertical exaggeration, the vertical axis of a 3D model is stretched while the horizontal axes remain unmodified. This chapter highlights the benefits of vertical exaggeration to gain additional information for interpreting tracks, such as track depth, direction of travel, and details of anat-

omy. With that, Chapter 2 extends the scope of photogrammetry as documentation technique (e.g., Matthews et al., 2006; Mallison and Wings, 2014) to a valuable tool for track interpretation, since structures in tracks are revealed that were unseen with conventional methods. Although the manipulation of elevation in 3D models is frequently applied in the field of geology, for example, for visualizing thin sediment layers in cross sections, the application of vertical exaggeration is a novelty in the field of vertebrate ichnology. Chapter 2 has been submitted for publication and is now under revision. It is single-authored by the doctoral candidate (author contributions are provided at the end of the chapter).

1.5.2 Chapter 3

This chapter reports on a new method for interpreting recent tracks quantitatively for estimating body mass in contrast to existing methods that use scaling relationships and volume/density reconstructions from body fossils. The required load to produce a track of an extant elephant trackmaker is simulated with 3D, soil mechanical FEA based measurements of the original tracks and substrate properties. The weight of the trackmaker can be estimated with an error of about 15%. Compared to other studies that employed advanced geotechnical methods for modelling of vertebrate tracks (e.g., Margetts et al., 2005; Margetts et al., 2006; Falkingham et al., 2010; Falkingham et al., 2011a; Sanz et al., 2016), Chapter 3 is the first study to have ever estimated the body mass of trackmaker from its tracks. Chapter 3 is a collaboration of multiple authors from various subjects. It has been published in the scientific journal *PlosOne* (author contributions are provided at the end of the chapter).

1.5.3 Chapter 4

Looking at a trackway, one intuitively would think that the gait of the trackmaker should be reconstructable from its tracks. Compared to classical literature on gaits that studied gaits as function of time (e.g., Muybridge, 1899; Howell, 1944; Hildebrand, 1965; Gray, 1968; Hildebrand, 1989), Chapter 4 focusses on the spatial distribution of tracks (e.g., Renders, 1984; Thompson et al., 2007) to provide a comprehensive distinction between several gaits (cf. Chapter 7). Thus, for the first time, Chapter 4 tests if the pattern of imprints along a trackway can indicate the gait used by the trackmaker with regard to future application on fossil tracks. Since horse gaits are a prime example for highly standardized gaits because of the demands of sport completion recent horses are studied for this work. Different gaits, for example, walk, trot, and gallop, show different footfall patterns in the trackways, such as in the stride lengths. Since the locomotion of fossil trackmakers is still difficult to investigate, this knowledge is necessary for a novel way of interpreting fossil tracks to estimate the gait of a fossil trackmaker (e.g., Läbe, unpubl. a; Chapter 5). This chapter has been published in the scientific journal *Fossil Record*. The first two authors contributed equally to this paper that was supervised by the senior (last) author (author contributions are provided at the end of the chapter).

1.5.4 Chapter 5

Chapter 5 deals with the distribution of weight among the limbs during locomotion, since this knowledge is necessary for the analysis of tracks, and illustrates, for the first time, how the insights of the study by Kienapfel et al. (2014; Chapter 4) are applied to a fossil trackmaker (sauropod with indications of a walking locomotion). By considering the position of the center of mass in an animal and the employed gait that is reflected in a combination of several limb support scenarios (e.g., two in the walk), a weight distribution factor is calculated. As mentioned above, locomotion will affect track formation and is therefore relevant for weight estimation approaches using tracks, such as applied by Schanz et al. (2013; Chapter 3) and Läbe (unpubl. b; Chapter 6). In addition to previous consideration of weight distribution (Henderson, 2006; Schanz et al., 2013), Chapter 5 focuses on slow locomotion during walking in view of a reduced dynamic component assumed for sauropods (Preuschoft et al., 2011).

1.5.5 Chapter 6

A case study on a sauropod trackway from the Morrison Formation presented in Chapter 6 combines all previous dissertation chapters to test if the weight of a sauropod trackmaker can be estimated from fossil tracks based on the concepts introduced by Schanz et al. (2013; Chapter 3) by integrating the digital documentation technique by Läbe (in revision; Chapter 2) as well as considerations on locomotion (Kienapfel et al., 2014; Chapter 4; Läbe, unpubl. a; Chapter 5). Compared to previous studies employing a similar method (Sanz et al., 2016), Chapter 6 better meets the challenge of estimating the weight of a fossil trackmaker by using a more advanced material model for the FEA simulation and by focusing more on the portion of locomotion during track formation. Although, the results of this study are comparable to other sauropod mass estimates, which provide independent confirmation of very high sauropod body masses, still, careful assessment of required parameters, such as the dynamic component of the trackmaker and the properties of the substrate, is necessary. However, this chapter marks a first step towards the application of the method by Schanz et al. (2013) on fossil trackmakers, which is particularly valuable for localities where body fossils, required for conventional mass estimation techniques, are scanty.

1.5.6 Chapter 7

This chapter provides the synthesis of my dissertation and is written for publication as a review paper. The chapter deals with the developments in vertebrate ichnology from early descriptive research to today's interdisciplinary methods and discusses the previous dissertation chapters with respect to their overall contribution to vertebrate ichnology (Figure 1.1). Historical and conventional track literature is comprehensively reviewed, whereby the technological improvements in track documentation, such as described in Chapter 2, is mentioned in detail. A special interest of this synthesis lies on paleobiological interpreta-

tions about trackmakers based on evidence from disparate fields of study. The chapter agrees with previous studies that trackmakers locomotion is constrained by body mass (e.g., Preuschoft et al., 2011) and that both affect track formation together with substrate properties (Padian and Olsen, 1984; Falkingham, 2014). However, the innovation of the synthesis, likewise of the present dissertation, is that not only soil mechanics and digital documentation are considered for understanding track formation, but also locomotion of the trackmaker is included to gain novel paleobiological insights.

1.6. REFERENCES

Alexander, R. M. 1976. Estimates of speeds of dinosaurs. Nature 261:129–130.

Alibhai, S. K., Z. C. Jewell, and P. R. Law. **2008**. A footprint technique to identify white rhino *Ceratotherium simum* at individual and species levels. Endangered Species Research 4:205–218.

Bibi, F., B. Kraatz, N. Craig, M. Beech, M. Schuster, and A. Hill. **2012**. Early evidence for complex social structure in Proboscidea from a late Miocene trackway site in the United Arab Emirates. Biology Letters 8(4):670–673.

Curry Rogers, K., and J. A. Wilson (eds.). **2005**. The Sauropods - Evolution and Paleobiology. University of California Press, Berkeley, 349 pp.

Day, J. J., D. B. Norman, P. Upchurch, and H. P. Powell. **2002**. Dinosaur locomotion from a new trackway. Nature 415(6871):494–495.

Day, J. J., P. Upchurch, D. B. Norman, A. S. Gale, and H. P. Powell. **2002**. Sauropod trackways, evolution, and behavior. Science 296(5573):1659.

Falkingham, P. L. 2014. Interpreting ecology and behaviour from the vertebrate fossil track record. Journal of Zoology 292(4):222–228.

Falkingham, P. L., K. T. Bates, and P. D. Mannion. **2012**. Temporal and palaeoenvironmental distribution of manus- and pes-dominated sauropod trackways. Journal of the Geological Society 169(4):365–370.

Falkingham, P. L., K. T. Bates, L. Margetts, and P. L. Manning. **2011a**. Simulating sauropod manus-only trackway formation using finite-element analysis. Biology Letters 7:142–145.

Falkingham, P. L., K. T. Bates, L. Margetts, and P. L. Manning. **2011b**. The 'Goldilocks' effect: preservation bias in vertebrate track assemblages. Journal of the Royal Society Interface 8(61):1142–1154.

Falkingham, P. L., and S. M. Gatesy. **2014**. The birth of a dinosaur footprint: subsurface 3D motion reconstruction and discrete element simulation reveal track ontogeny. Proceedings of the National Academy of Sciences of the United States of America 111(51):18279–18284.

Falkingham, P. L., J. Hage, and M. Baker. **2014**. Mitigating the Goldilocks effect: the effects of different substrate models on track formation potential. Royal Society Open Science 1(3):1–9.

Falkingham, P. L., L. Margetts, and P. L. Manning. **2010**. Fossil vertebrate tracks as paleopenetrometers: confounding effects of foot morphology. Palaios 25(6):356–360.

Falkingham, P. L., L. Margetts, I. M. Smith, and P. L. Manning. **2009**. Reinterpretation of palmate and semi-palmate (webbed) fossil tracks; insights from finite element modelling. Palaeogeography, Palaeoclimatology, Palaeoecology 271(1-2):69–76.

Friese, H. 1979. Die Saurierfährten von Barkhausen im Wiehengebirge. Veröffentlichungen des Landkreises Osnabrück 1:1–36.

Gatesy, S. M., K. M. Middleton, F. A. J. Jr, and N. H. Shubin. **1999**. Three-dimensional preservation of foot movements in Triassic theropod dinosaurs. Nature 399(6732):141–144.

Gillette, D. D., and M. G. Lockley (eds.). **1989**. Dinosaur Tracks and Traces. Cambridge University Press, Cambridge, 476 pp.

Gray, J. 1968. How Animals Move. Cambridge University Press, Cambridge.

Henderson, D. M. 2006. Burly gaits: centers of mass, stability, and the trackways of sauropod dinosaurs. Journal of Vertebrate Paleontology 26(4):907–921.

Hildebrand, M. 1965. Symmetrical gaits of horses. Science 150(3697):701–708.

Hildebrand, M. 1989. The quadrupedal gaits of vertebrates. Bioscience 39(11):766–775.

Hitchcock, E. 1836. Ornithichnology – description of the foot marks of birds (Ornithichnites) on New Red Sandstone in Massachusetts. American Journal of Science 29:307–340.

Hitchcock, E. 1848. An attempt to discriminate and describe the animals that made the fossil footmarks of the United States, and especially of New England. Memoirs of the American Academy of Arts and Science 3:129–256.

Hitchcock, E. 1858. Ichnology of New England: A Report on the Sandstone of the Connecticut Valley, Especially its Fossil Footmarks. W. White, Boston, Mass., 232 pp.

Hitchcock, E. 1865. Supplement to the Ichnology of New England. Wright and Potter State Printers, Boston, Mass., 96 pp.

Howell, A. B. 1944. Speed in Animals. University of Chicago Press, Chicago, 270 pp.

Jackson, S. J., M. A. Whyte, and M. Romano. **2009**. Laboratory-controlled simulations of dinosaur footprints in sand: A key to understanding vertebrate track formation and preservation. Palaios 24(4):222–238.

Jackson, S. J., M. A. Whyte, and M. Romano. **2010**. Range of experimental dinosaur (*Hypsilophodon foxii*) footprints due to variation in sand consistency: how wet was the track? Ichnos 17(3):197–214.

Jones, T. R. 1862. Trails, tracks, and surface-markings. The Geologist 5(04):128–139.

Kaever, M., and A. F. de Lapparent. **1974**. Les traces de pas de Dinosaures du Jurassique de Barkhausen (Basse Saxe, Allemagne). Bulletin de la Société Géologique de France 16:516–525.

Kaup, J. J. 1835. Mittheilungen, an Professor Bronn gerichtet. Thier-Fährten von Hildburghausen: *Chirotherium* oder *Chirosaurus.* Neues Jahrbuch für Mineralogie, Geognosie, Geologie und Petrefaktenkunde:327–328.

Kienapfel, K., S. Läbe, and H. Preuschoft. **2014**. Do tracks yield reliable information on gaits? – Part 1: The case of horses. Fossil Record 17:59–67.

Klein, N., K. Remes, C. T. Gee, and P. M. Sander (eds.). **2011**. Biology of the Sauropod Dinosaurs - Understanding the Life of Giants. Life of the Past. Indiana University Press, Bloomington, 331 pp.

Läbe, S. unpubl. a. Do tracks yield reliable information on gaits? – Part 2: Thoughts on the weight distribution of sauropod dinosaurs during walking. Doctoral thesis 2017(Chapter 5).

Läbe, S. unpubl. b. The dinosaur scale: interpreting sauropod tracks with a soil mechanical approach for body mass estimation with thoughts on weight distribution among the limbs during walking. Doctoral thesis 2017(Chapter 6).

Läbe, S. in revision. Vertical exaggeration of 3D surface models highlights additional detail in vertebrate tracks: an example from the photogrammetry of sauropod tracks. Journal of Paleontological Techniques (2017).

Lockley, M., A. S. Schulp, C. A. Meyer, G. Leonardi, and D. Kerumba Mamani. **2002**. Titanosaurid trackways from the Upper Cretaceous of Bolivia: evidence for large manus, wide-gauge locomotion and gregarious behaviour. Cretaceous Research 23(3):383–400.

Lockley, M. G. 1989. Summary and Prospectus; pp. 441–447 in D. D. Gillette and M. G. Lockley (eds.), Dinosaur Tracks and Traces. Cambridge University Press, Cambridge, 476 pp.

Lockley, M. G. 2007. The morphodynamics of dinosaurs, other archosaurs, and their trackways: holistic insights into relationships between feet, limbs, and the whole body. SEPM Special Publication 88:27–51.

Lockley, M. G., and V. F. dos Santos. **1993**. A preliminary report on sauropod trackways from the Avelino site, Sesimbra region, Upper Jurassic Portugal. Gaia: Revista de Geociências 6:38–42.

Lockley, M. G., J. O. Farlow, and C. A. Meyer. **1994**. *Brontopodus* and *Parabrontopodus* ichnogen. nov. and the significance of wide- and narrow-gauge sauropod trackways. Gaia: Revista de Geociências 10:135–145.

Lockley, M. G., K. J. Houk, and N. K. Prince. **1986**. North America's largest dinosaur trackway site: implications for Morrison Formation paleoecology. Geological Society of America Bulletin 97(10):1163–1176.

Mallison, H., and O. Wings. **2014**. Photogrammetry in paleontology - a practical guide. Journal of Paleontological Techniques 12:1–31.

Manning, P. L. 2004. A new approach to the analysis and interpretation of tracks: examples from the dinosauria. Geological Society of London Special Publications 228:94–123.

Margetts, L., J. Leng, I. M. Smith, and P. L. Manning. **2006**. Parallel Three Dimensional Finite Element Analysis of Dinosaur Trackway Formation; pp. 743–749 in H. F. Schweiger (ed.), Numerical Methods in Geotechnical Engineering: Proceedings of the Sixth European Conference on Numerical Methods in Geotechnical Engineering. Balkema-proceedings and monographs in engineering, water and earth sciences. Taylor & Francis, London, 1678 pp.

Margetts, L., I. M. Smith, J. Leng, and P. L. Manning. **2005**. Simulating dinosaur trackway formation; pp. 1–4 in E. Oñate and D. R. J. Owen (eds.), VIII International Conference on Computational Plasticity (COMPLAS). CIMNE, Barcelona.

Marty, D. 2008. Sedimentology, taphonomy, and ichnology of Late Jurassic dinosaur tracks from the Jura carbonate platform (Chevenez—Combe Ronde tracksite, NW Switzerland): insights into the tidal-flat palaeoenvironment and dinosaur diversity, locomotion, and palaeoecology. GeoFocus 21:1–278.

Marty, D., P. L. Falkingham, and A. Richter. **2016**. Dinosaur Track Terminology: A Glossary of Terms; pp. 399–402 in P. L. Falkingham, D. Marty, and A. Richter (eds.), Dinosaur Tracks - The Next Steps. Life of the Past. Indiana University Press, Bloomington, 413 pp.

Matthews, N. A., T. A. Noble, and B. H. Breithaupt. **2006**. The application of photogrammetry, remote sensing and geographic information systems (GIS) to fossil resource management. New Mexico Museum of Natural History and Science Bulletin 34:119–131.

Milàn, J. 2006. Variations in the morphology of emu (*Dromaius novaehollandiae*) tracks reflecting differences in walking pattern and substrate consistency: ichnotaxonomic implications. Palaeontology 49(2):405–420.

Muybridge, E. 1899. Animals in Motion. Chapman & Hall, London, 264 pp.

Myers, T. S., and A. R. Fiorillo. **2009**. Evidence for gregarious behavior and age segregation in sauropod dinosaurs. Palaeogeography, Palaeoclimatology, Palaeoecology 274(1-2):96–104.

Padian, K., and P. E. Olsen. **1984**. The fossil trackway *Pteraichnus*: not pterosaurian, but crocodilian. Journal of Paleontology 58(1):178–184.

Platt, B. F., S. T. Hasiotis, and D. R. Hirmas. **2012**. Empirical determination of physical controls on megafaunal footprints formation through neoichnological experiments with elephants. Palaios 27:725–737.

Preuschoft, H., B. Hohn, S. Stoinski, and U. Witzel. **2011**. Why so huge? Biomechanical Reasons for the Acquisition of Large Size in Sauropod and Theropod Dinosaurs;

pp. 197–218 in N. Klein, K. Remes, C. T. Gee, and P. M. Sander (eds.), Biology of the Sauropod Dinosaurs - Understanding the Life of Giants. Life of the Past. Indiana University Press, Bloomington, 331 pp.

Renders, E. 1984. The gait of *Hipparion* sp. from fossil footprints in Laetoli, Tanzania. Nature 308:179–181.

Salisbury, S. W., A. Romilio, M. C. Herne, R. T. Tucker, and J. P. Nair. **2017**. The dinosaurian ichnofauna of the Lower Cretaceous (Valanginian–Barremian) Broome Sandstone of the Walmadany Area (James Price Point), Dampier Peninsula, Western Australia. Journal of Vertebrate Paleontology 36(6, suppl.):1–152.

Sander, P. M. 2013. An evolutionary cascade model for sauropod dinosaur gigantism - overview, update and tests. PLoS ONE 8(10):1–23.

Sander, P. M., A. Christian, M. Clauss, R. Fechner, C. T. Gee, E.-M. Griebeler, H.-C. Gunga, J. Hummel, H. Mallison, S. F. Perry, H. Preuschoft, O. W. M. Rauhut, K. Remes, T. Tütken, O. Wings, and U. Witzel. **2011**. Biology of the sauropod dinosaurs: the evolution of gigantism. Biological Reviews 86:117–155.

Sander, P. M., and M. Clauss. **2008**. Sauropod gigantism. Science 322(5899):200–201.

Santos, V. F., P. M. Callapez, and N. P. Rodrigues. **2013**. Dinosaur footprints from the Lower Cretaceous of the Algarve Basin (Portugal): new data on the ornithopod palaeoecology and palaeobiogeography of the Iberian Peninsula. Cretaceous Research 40:158–169.

Santos, V. F. d., M. G. Lockley, C. A. Meyer, J. Carvalho, A. Galopim de Carvalho, and J. J. Moratalla. **1994**. A new sauropod tracksite from the Middle Jurassic of Portugal. Gaia: Revista de Geociências 10:5–13.

Sanz, E., A. Arcos, C. Pascual, and I. M. Pidal. **2016**. Three-dimensional elasto-plastic soil modelling and analysis of sauropod tracks. Acta Palaeontologica Polonica 61(2):387–402.

Schanz, T., Y. Lins, H. Viefhaus, T. Barciaga, S. Läbe, H. Preuschoft, U. Witzel, and P. M. Sander. **2013**. Quantitative interpretation of tracks for determination of body mass. PLoS ONE 8(10):1–12.

Struckmann, C. 1880. Vorläufige Nachricht über das Vorkommen großer, vogelähnlicher Thierfährten (Ornithoidichnites) im Hastingssandsteine von Bad Rehburg bei Hannover. Neues Jahrbuch für Mineralogie, Geologie und Paläontologie 1:125–128.

Tagart, E. 1846. On markings in the Hastings Sand Beds near Hastings, supposed to be the footprints of birds. Quarterly Journal of the Geological Society 2(1-2):267.

Thompson, M. E., R. S. White, and G. S. Morgan. **2007**. Pace versus trot: can medium speed gait be determined from fossil trackways? New Mexico Museum of Natural History and Science Bulletin 42:309–314.

Thulborn, T. 1990. Dinosaur Tracks. Chapman and Hall, New York, 410 pp.

Upchurch, P. 1995. The evolutionary history of sauropod dinosaurs. Philosophical Transactions of the Royal Society B: Biological Sciences 349(1330):365–390.

White, M. A., A. G. Cook, and S. J. Rumbold. **2017**. A methodology of theropod print replication utilising the pedal reconstruction of *Australovenator* and a simulated paleo-sediment. PeerJ 5(4):1-19.

CHAPTER 2

Vertical exaggeration of 3D surface models highlights additional detail in vertebrate tracks: an example from the photogrammetry of sauropod tracks

Läbe, S. *Journal of Paleontological Techniques*. Submitted 2016. In revision.

2.1. ABSTRACT

Photogrammetry is used in many paleontological studies for generating three-dimensional (3D) surface models of specimens. Specifically, the documentation of dinosaur trackways benefits from the advances in photogrammetry because extensive trackways can be entirely digitized without perspective distortion. However, the preservation and condition of the majority of tracks is not always sufficient for detailed study, making interpretations difficult. By applying the visualization method of vertical exaggeration to sauropod tracks, this study shows more accurate interpretations of photogrammetric 3D models. In vertical exaggeration, the vertical axis of a 3D model is stretched in order to accentuate subtle structures of the track surface. In the case of the Jurassic Avelino tracksite (Portugal), Copper Ridge Dinosaur tracksite (Utah, USA), Barkhausen tracksite (Germany), and the Cretaceous Münchehagen tracksite (Germany), additional track details were revealed by using vertical exaggeration with the aid of the photogrammetry software Agisoft PhotoScan, and the two visualization tools CloudCompare and ParaView. Moreover, questionable tracks were re-evaluated and further supported with this method. Vertical exaggeration can be a useful tool for improving the interpretability of poorly preserved tracksites, not only of sauropod tracks, but of any vertebrate tracksite. The method of vertical exaggeration is common in geology for visualizing topography; for vertebrate ichnology, vertical exaggeration is a novel method.

2.2. INTRODUCTION

The information contained in vertebrate tracks is of high value, not only for today's foresters and hunters, but also for researchers. Specifically, fossilized tracks of extinct animals occur more often than body fossils, and provide additional, and sometimes the only information, about an extinct taxon, its behavior, and locomotion. Among fossil tracks, dinosaur tracks are of great interest to gain more information about this extinct group of animals. Sauropod tracks are particularly remarkable because of their size; after all, they are produced from the largest land animals of all time. For examples, the largest sauropod tracks were found in the Lower Cretaceous Broome Sandstone, Australia, with a length of single pes print measuring 170 cm (Salisbury et al., 2017).

Many examples of sauropod ichnofossils have been found over the world like *Parabrontopodus* (Lockley et al., 1994), which is a narrow-gauged, high heteropody ichnotaxon attributed to non-macronarian neosauropods, and *Brontopodus* (Farlow et al., 1989), which is a wide-gauged, low heteropody ichnotaxon attributed to macronarians (Farlow, 1992; Lockley et al., 1994; Wilson and Carrano, 1999; Wilson, 2005). In cases where tracks can be associated with body fossils, dinosaur tracks might be used to identify the trackmaker based on apomorphic traits (Wright, 2005). Additionally, trackways provide insights into the trackmaker's locomotion based on the stance that is bipedal or quadrupedal, and speed estimations (Alexander, 1976). Even the weight can be estimated from tracks, as this was shown with footprints of an extant elephant by Schanz et al. (2013).

However, to interpret and analyze vertebrate tracks, sufficient documentation needs to be carried out (cf. Thulborn, 1990, Lockley, 1991b). The classical way of documenting dinosaur tracks and trackways is two-dimensional. In the field, the morphologies of the tracks are usually drawn with chalk on the actual track and then sketched on paper or, alternatively, the track surface was covered with transparent film and each track was traced through the film. Sketching is usually a valuable and fast method for documentation, if a grid for precise measurements of the tracks is included. However, the researcher risks incorporation of a perspective distortion into the sketch because of the single point of view of the observer, which could lead to a misinterpretation of the tracks. The second approach by tracing the tracks through film will produce a more precise redrawing of the tracks in the original size. Still, it is in 2D and might produce space-consuming datasets, considering the enormous size of some dinosaur trackways. In any case, both methods are useful for ichnological documentation, but it has to be considered that they are usually affected by field conditions and, more importantly, by the interpretations and experiences of the executing researcher. This is a general issue in ichnology. For instance, interpretation problems might occur already with drawing the track outlines in the field. Falkingham (2016) and Lallensack (2016) have already discussed this issue proposing a possible solution. Their ap-

proaches using the projection of the track topography to contour lines helps with the objective determination of tracks outlines. However, this approach requires a three-dimensional (3D) model of the track.

2.2.1 The use and development of digital ichnology

In the beginning of the 21st Century, the application of 3D methods for digitally documenting dinosaur tracks was a major novelty in ichnology. The technique of laser scanning was applied on dinosaur tracks and many researchers found this to be an accurate method to document dinosaur footprints, trackways, and entire tracksites (Bates, Breithaupt et al., 2008; Bates, Manning et al., 2008; Bates et al., 2009; Adams et al., 2010; Bates et al., 2010; Platt et al., 2010). Shortly after that, photogrammetry was introduced in vertebrate ichnology as an alternative method (Matthews and Breithaupt, 2001; Breithaupt et al., 2004; Breithaupt et al., 2006; Matthews et al., 2006; Bates, Breithaupt et al., 2008; Breithaupt and Matthews, 2011). However, with increasing availability of open-source software and powerful workstations photogrammetry has become the preferred method in recent years.

Photogrammetry is a well-known technique first used in geodesy for taking measurements from photographs. What has started with a method from a single photograph in the 19th century (Grimm, 2007; Matthews et al., 2016) has now turned into a multidimensional application based on multiple photos. A study by Matthews, Noble and Breithaupt (2016) illustrates the advantages of photogrammetry for vertebrate ichnology and provides detailed information about the history, the general workflow, and implications for digital collection and management of fossil vertebrate tracks. The benefits of this modern method are not only a faster and more precise data collection, but also that the interpretability of tracks is noticeably enhanced as well. Photogrammetry is a non-destructive and effective method for 3D digitization of objects, irrespective of their size, to capture them entirely and distortion-free with moderate effort. The application is user-friendly, because the tools required are commonplace, namely camera and computer.

From photos, textured 3D models of the objects are generated by a computer-assisted workflow in order to digitize and study them in a more standardized fashion. With the technological progress of the past few years and the affordable costs of hardware and software, photogrammetry has become an often applied documenting method - a multitool for numerous paleontological questions (Falkingham, 2012; Mallison and Wings, 2014). For example, photogrammetry was employed for paleobotanical documentation of a Carboniferous forest (Fernández-Lozano and Gutiérrez-Alonso, 2017) or for reconstructing the body mass of sauropod dinosaurs (Stoinski et al., 2011). Many authors use photogrammetry for documenting newly discovered and already well-known dinosaur tracksites; for example, the Early Cretaceous Dinosaur Ridge tracksite, Colorado, USA (Matthews and Breithaupt, 2001), the Middle Jurassic Red Gulch Dinosaur Tracksite, Wyoming, USA

(Breithaupt et al., 2004), and the Lower Jurassic Coste dell'Anglone tracksite in Italy (Petti et al., 2008), where photogrammetry, laser scanning and standard documentation methods were compared. From photogrammetric 3D models of dinosaur tracks, measurements and detailed descriptions can be obtained, for example, for the analysis with geometric morphometrics (Lallensack et al., 2016). Tracksites, which do not exist anymore, because of weathering or destruction, can be digitally reconstructed based on historic photographs thanks to photogrammetry (Falkingham et al., 2014). McCrea et al. (2015) and Razzolini et al. (2016) even applied photogrammetry to unusual trackway configurations, which they attributed to pathologies in the dinosaur's locomotor abilities.

Tracksites with good or excellent preservation, such as tracks with a high numerical scale of quality described by Belvedere and Farlow (2016), which include true tracks, skin impressions or claw marks, are rare. In many tracksites, the tracks are preserved as undertracks, meaning that the original walking surface is no longer preserved, and generally considered lacking in necessary details for further analysis.

The purpose of this study is to describe and to examine an approach that enhances details of moderately to poorly preserved tracks (including undertracks). 3D sauropod track models, which were generated with photogrammetry, were selectively manipulated by using the visualization technique of vertical exaggeration. Vertical exaggeration is a commonly employed method in geology and geomorphology to visualize cross sections and topography. The main principle of vertical exaggeration is that the scale of the z-axis in a 3D model is increased relative to the horizontal axis to create a vertical stretching. Vertical exaggeration is a valuable technique to emphasize subtle features of tracks and to reveal very shallow tracks, improving the interpretation and documentation of dinosaur ichnofossils.

2.3. MATERIAL AND METHODS

The current study involves the documentation and re-interpretation of four known and well-described sauropod tracksites, which show a wide range in preservation quality, track depth, and post-imprint modification. The tracksites were thoroughly studied and photographed in the field. The tracks were analyzed with photogrammetry and 3D visualizing software to generate 3D models to interpret the tracks and their distribution on the track surface, described below.

2.3.1 Sauropod track localities

The Upper Jurassic Avelino tracksite or Pedreira do Avelino (Figure 2.1A) was discovered by M.T. Antunes in 1976 (Antunes and Mateus, 2003) and thoroughly described by Lockley and dos Santos (1993). The tracksite is located in a former quarry near Sesimbra, 30 km south of Lisbon, Portugal, and was designated as a national monument in 1997. Multiple sauropod tracks are located on three levels in the stratigraphic section (Lockley and dos

Santos, 1993), which dips 30° to the North. The present study focusses on the 10 x 15 m primary track surface. The sediment of the track surface consists of micritic limestone of Kimmeridgian age, belonging to the Azóia Unit Limestone (Lourinhã Formation) (Lockley and dos Santos, 1993; Meyer and Pittman, 1994) that was deposited on a carbonate platform (Lockley and Meyer, 2000) or in a transitional coastal environment (Castanera et al., 2014). In general, the quality of the tracks varies on the track surface. The tracks were attributed to the *Parabrontopodus* type (Lockley and dos Santos, 1993), and were made by individuals of different sizes, with the length measurements of the pes tracks ranging from 30 cm to 100 cm (Lockley and dos Santos, 1993; Santos et al., 2008; Castanera et al., 2014).

The Upper Jurassic Copper Ridge Dinosaur tracksite, also known as Valley City tracksite (Lockley, 1991b; Lockley and Hunt, 1995; Foster, 2015; Hunt-Foster et al., 2016) is situated north of the town of Moab, Utah, USA, and close to Arches National Park (Figure 2.1B). The site is interpreted for the public and located on land managed by the Bureau of Land Management. The sediments are fluvial and lie within the Salt Wash Member of the Morrison Formation. One sauropod trackway and two theropod trackways are exposed on the track surface. McCrea et al. (2015) analyzed a theropod trackway from the Copper Ridge Dinosaur tracksite using photogrammetry because of its unusual arrangement, attributed to a limping trackmaker. The present study focusses on the sauropod trackway in which the tracks form a turning pattern, one of the few instances known in the sauropod track record (Ishigaki and Matsumoto, 2009). The preservation of the sauropod tracks is poor, which might be due to decades of exposure since the discovery of the tracks. The sauropod trackway was so far considered to consist mainly of pes tracks with the manus tracks being overprinted.

The Upper Jurassic Barkhausen tracksite is located near the town of Osnabrück, Germany (Figure 2.1C). The tracksite is middle Kimmeridgian in age and contains two trackways of three-toed dinosaurs and eight sauropod trackways (Friese, 1979). The track locality is accessible to the public and protected by a shelter. The sand and siltstone layer of the track-bearing surface dips 60° north. The track surface was entirely documented with photogrammetry. The leftmost sauropod trackway is the best preserved and shows comparatively deep tracks of both manus and pes, from which the best preserved set of a right manus and pes track was selected to carry out further analysis in this study. The pes track length is on average about 30 cm, and it is assumed that they were made by small individuals (cf. trackmaker size classes after Marty, 2008). The tracks vary in depth and quality. The sauropod dinosaur tracks were termed *Elephantopoides barkhausensis* by Kaever and de Lapparent (1974). However, after a re-evaluation of the site, the ichnotaxon is considered to be *Parabrontopodus* (Lockley et al., 1994). For the Barkhausen tracksite, some contradictive, partly dubious, literature is available (see discussion and clarification in Lallensack et al., 2015).

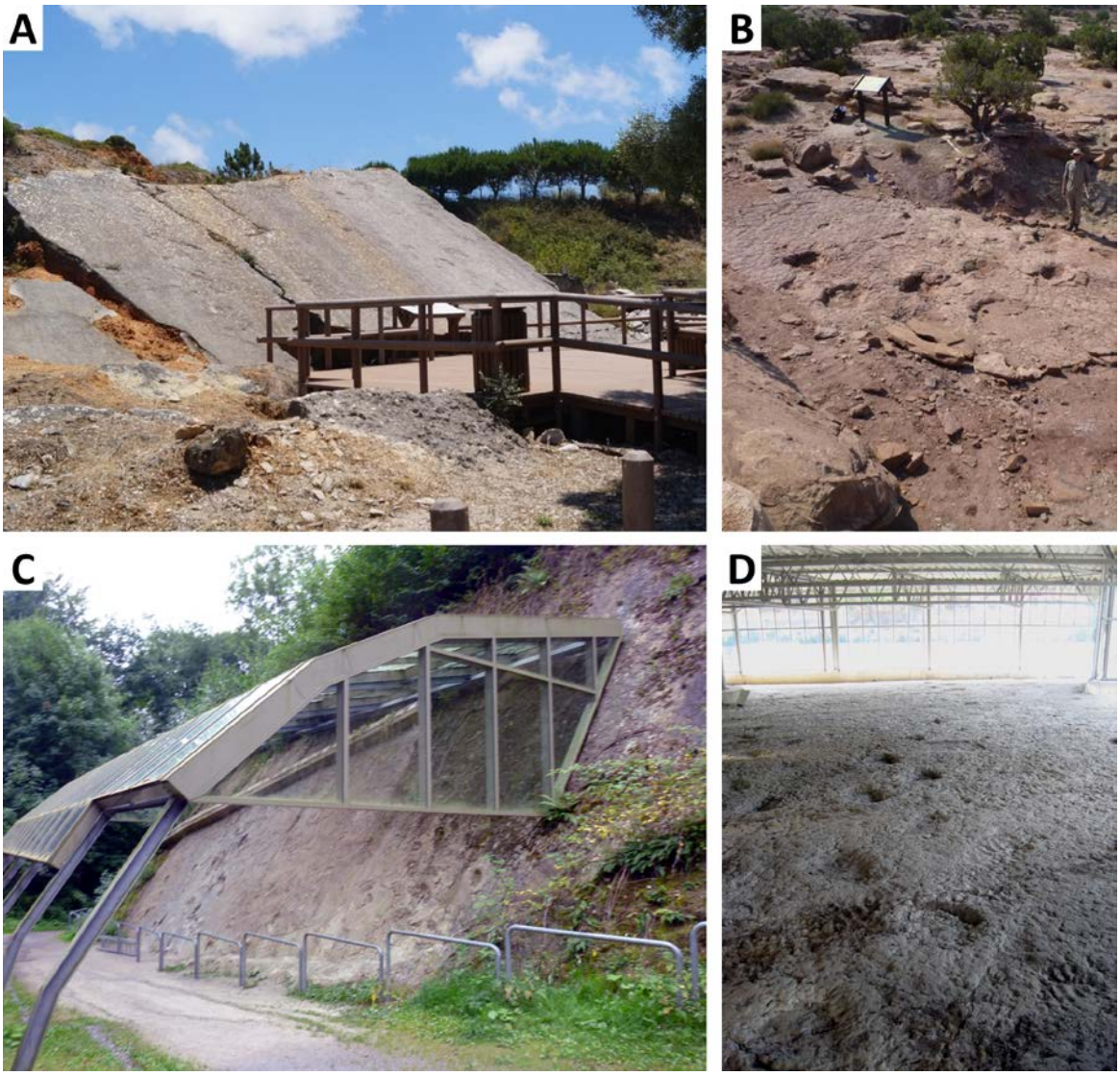

Figure 2.1: Overview of all digitized sauropod tracksites of this study. All tracksites are in situ, accessible to the public and additional information for visitors is provided onsite. A. The main track surface of the Upper Jurassic Avelino tracksite, Portugal, exposes eight sauropod trackways. B. At the Upper Jurassic Copper Ridge Dinosaur tracksite, Utah, USA, a single curved sauropod trackway is preserved. C. Multiple sauropod trackways are exposed on the Upper Jurassic Barkhausen tracksite, Germany, which are protected by a shelter. D. At Münchehagen, Germany, multiple sauropod tracksites are located in a dinosaur theme park and protected by a large shelter.

The Lower Cretaceous Münchehagen tracksite is located within the Dinopark (Dinosaurier-Freilichtmuseum Münchehagen), near Hannover, Germany (Figure 2.1D). The main tracksite is a natural heritage and protected by a closed shelter in the Dinopark. Sauropod tracks are distributed all over the tracksite and form up to seven individual trackways (Fischer, 1998). The sauropod tracks were described and named *Rotunichnus muenchehagensis* (Hendricks, 1981), but they seem to be more related to the *Brontopodus*-type (Lockley et al., 1994; Lockley et al., 2004). The main track surface in the Dinopark had already been studied with photogrammetry in order to document the tracks digitally. With this methodology, undiscovered manus tracks within the sauropod trackways were revealed (Englich, 2013). In addition, the shape, morphology, and variability of the Münchehagen

theropod and ornithopod tracks were recently investigated using photogrammetric data (Lallensack et al., 2016; Wings et al., 2016). Here, the focus lies on one sauropod trackway for testing the method of vertical exaggeration.

2.3.2 Methodology

For photogrammetry, the photos were taken from different positions and angles around the tracks with an overlap of around 66% from one photo to the other, in order to generate all-encompassing 3D models. The number of photos taken depends on the area to be covered by the photos. The photos for photogrammetry were taken in JPEG format with a Sony Alpha 58 DSLT camera (23.6 x 15.7 mm APS-C sensor, 18-55 mm lens, 4.44 x 4.44 µm pixel size), a canon EOS 1000D DSLR camera (22.2 x 14.8 mm APS-C sensor, 18 mm lens, 5.72 x 5.72 µm pixel size), and a Panasonic Lumix DMC FT-3 compact camera (6.08 x 4.56 mm CCD sensor, 4.9 mm lens, 1.51 x 1.51 µm pixel size). Since some of the studied track surfaces are tilted, the photo capture was carried out as optimally as possible without any additional support of a crane or drone. Nonetheless, the captured photos led to adequate 3D models. Depending on the tracksite, the average height above the tracks where photos were taken ranges between 1.2 m and 3.12 m. Two different kinds of scale bars were chosen and placed directly on the track surface: a custom two-meter yardstick for linear measurements and a wooden cube with an edge length of ten centimeters to calibrate the 3D model along the three spatial axes, with the exception of the Münchehagen trackway model where only the yardstick was used.

For the photogrammetric digitization of the sauropod tracks the commercial software Agisoft PhotoScan, v. 1.3.1. Professional Edition (www.agisoft.com), was used. Although other open-source software for photogrammetry is available, the rationale for using PhotoScan was that it was the most effective and user-friendly software for this study. Mallison and Wings (2014) have presented their experiences with PhotoScan in a practical guide, which I followed accordingly. The basic workflow in Agisoft PhotoScan begins by importing the photographs of the tracks, then adding masks to the images, thus, excluding unnecessary details on the photos, such as vegetation or people, and subsequently excluding them from the calculation of the 3D model. From these photos, the software detects common points, based on trigonometric algorithms and structure from motion technique. This photo alignment process results in a sparse point cloud. After that, the dense point cloud is produced in a separated data generation step, which provides the foundation for a solid surface model (Figure 2.2A). The chosen accuracy for the alignment in PhotoScan was high, except in the Münchehagen model, which was aligned with medium accuracy. The photogrammetric models were computed on a workstation at the University of Bonn (Windows 10, Intel Core i7 CPU 3.60 GHz, 64 GB RAM, 2x NVIDIA Geforce GTX 690 graphics board) with a high to ultra-high reconstruction quality.

Although PhotoScan provides georeferencing, this was not applied to the models, since it requires high GPS accuracy, which was not obtained for these tracksites, as they cover areas of only 2 m² to 36 m². Instead, local coordinates were assigned to the models based on the scale bars. The error of the scale bar measurements is between 1 mm for the Avelino tracksite and 3 mm for the Münchehagen tracksite. The accuracy of the resulting model can be assessed from the ground sample distance (GSD), which is based on the resolution of the camera sensor, focal length of the lens and the distance to the track surface (cf. Matthews et al., 2016). In all cases, the GSD is below one millimeter per pixel. Details of calculation and the chosen settings for each model can be seen in Table 2.1. The 3D models were exported in Stanford PLY file format for further processing.

Table 2.1: Overview of calculation details and settings for the generation of the 3D models with Agisoft PhotoScan for each sauropod tracksite.

	Avelino	Copper Ridge	Barkhausen	Münchehagen
Number of photos	45	101	15	27
Camera	Sony Alpha SLT-A58	Panasonic Lumix DMC-FT3	Canon EOS 1000D	Panasonic Lumix DMC-FT3
Image resolution	5456 x 3632	4000 x 3000	3888 x 2592	4000 x 3000
Average height of photo capture [m]	3.12	2.78	1.57	1.2
Use of masks	yes	yes	no	no
Number of points in sparse point cloud	457,095	275,954	98,483	21,993
Number of points in dense point cloud	38,354,988	116,897,747	20,987,151	27,920,209
Chosen alignment accuracy	high	high	high	medium
Chosen reconstruction quality	high	ultra-high	ultra-high	high
Calculation time [h : min]	01:31	08:24	00:25	00:33
Ground sample distance [mm/pixel]	0.641	0.851	0.469	0.363
Estimated error of scale bars [m]	0.001	0.02	0.03	0.03

With help of the open-source software CloudCompare, v. 2.5.3.beta (www.danielgm.net/cc), the models were aligned to the horizontal x-y plane by the working step “bounding box PCA fit”, which allows for direct comparisons between models, as each model was oriented in the exact same way for the following steps. The aligned 3D models were edited with the 3D visualizing freeware ParaView, v.4.2.0. (www.paraview.org), for exaggeration and generating color depth maps. For the color depth maps, the function “elevation” was applied in z-direction to each 3D model to generate a color-coded model based on the original topography of the tracks; in general, blue

hues indicate deep parts or low elevation in the models and red hues indicate shallow parts or high elevation in the models. The crucial step for this study was to apply vertical exaggeration to the models. Using the function "transform" in ParaView, the scale of the vertical axis is increased relative to the horizontal axes; 3D models are stretched along the z-axis (the axis orthogonal to the plane of the track surface) to emphasize subtle features of the tracks and to reveal very shallow tracks. The models were vertically transformed by factors of two, five, and ten times. Based on the vertically exaggerated models, sitemaps were drawn and the tracks were re-interpreted.

2.4. RESULTS

2.4.1 Avelino tracksite (Figure 2.2)

The tracks are very shallow and therefore difficult to see under field conditions. In the solid surface 3D model (Figure 2.2B) that is without texture, the tracks do not appear very pronounced. Most tracks show a displacement rim, which makes them recognizable at all. In Figure 2.2C, the color depth map visualizes the trackways more distinctly; individual tracks can be assigned to trackways more easily. In some areas, parts of the thin sedimentary layers appear to be eroded, revealing some of the tracks to be preserved on different sedimentary levels. In comparison with the unmodified model (Figure 2.2B), the application of a ten-fold vertical exaggeration (Figure 2.2D) improves the visibility of very shallow tracks. In Figure 2.2E, the track surface interpretation from 1993 by Lockley and dos Santos was included to compare with a detailed sitemap (Figure 2.2F) drawn from the vertical exaggerated model and color depth maps. In total, 143 tracks were counted. Most of them belong either to the four trackways previously described by Lockley and dos Santos (1993; Figure 2.2E), or to four other trackways, which were additionally identified on the track surface after model improvement with vertical exaggeration. Walking direction of trackway 5 was determined (arrows in Figure 2.2F), since it shows manus and pes impressions. The tracks of trackways 6 through 8 are very faint and incomplete, so that manus and pes prints could not be distinguished adequately to determine direction of travel, but they are clear enough to confirm they belong to the trackways.

2.4.2 Copper Ridge Dinosaur tracksite (Figures 2.3 and 2.4)

The track surface shows a turning sauropod trackway. In Figure 2.4A, the solid surface model of the trackway is illustrated, which seems to be pes-dominated. The five-fold exaggerated color depth map (Figure 2.4B) shows that the length and width as well as the depth of the footprints vary across the track surface. Of particular interest in Figure 2.4B, some additional structures were highlighted, which are very faintly imprinted into the former sediment; some of these additional tracks were identified as possible manus tracks.

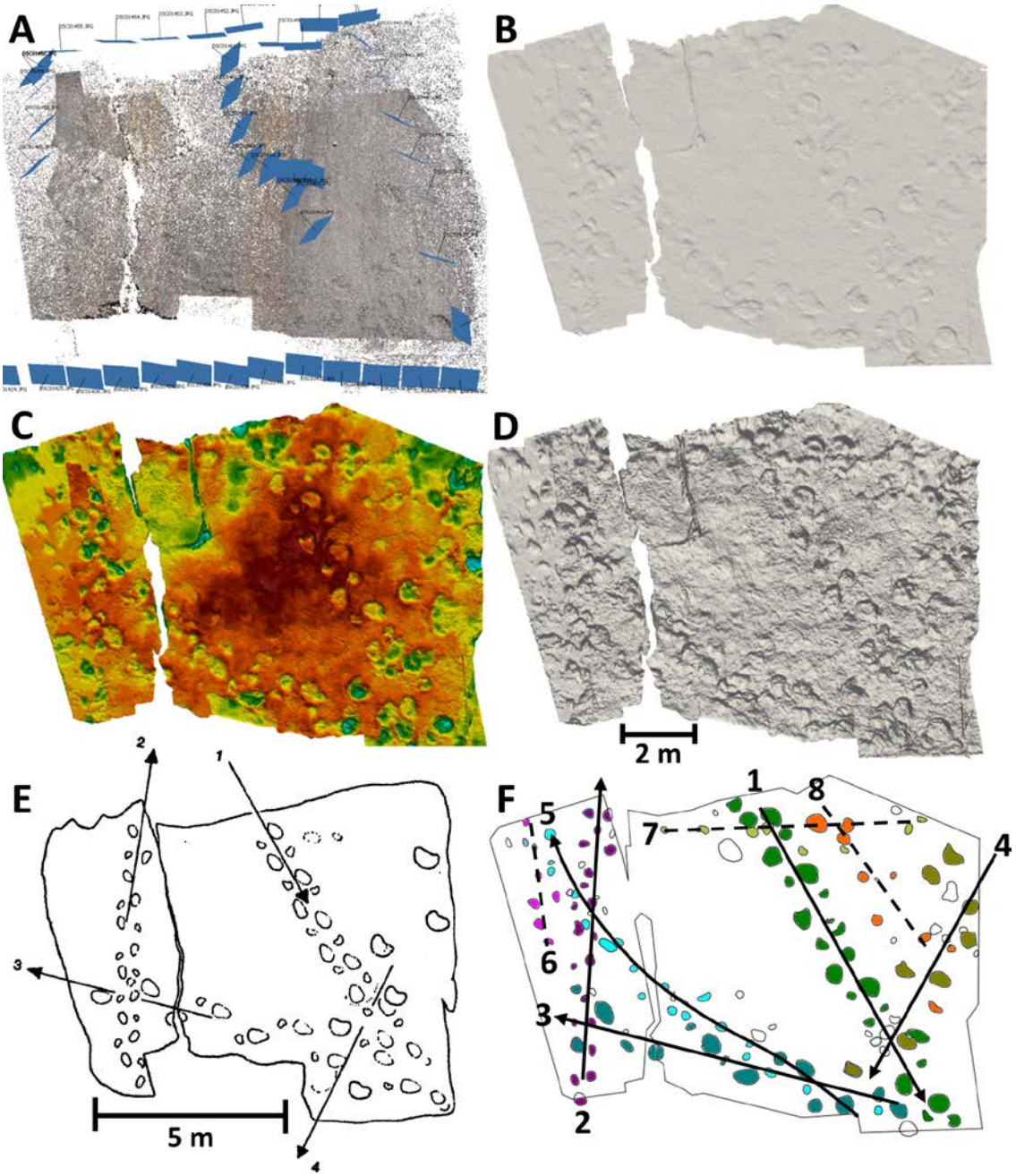

Figure 2.2: 3D models and interpretation of the Avelino tracksite, Portugal. A. Sparse point cloud and camera positions of photos (blue rectangles with file names) taken for model generation in Agisoft PhotoScan. B. The solid surface 3D model illustrates the very shallow tracks. C. To increase visibility, the depths of the track surface are mapped, whereby red indicates the highest areas and blue lowest areas. D. The 10x vertical exaggeration of the model improves visibility of the shallow tracks. E. Previous interpretation and sitemap from 1993 (modified after Lockley and dos Santos, 1993). F. New sitemap and interpretation based on color depth map and vertical exaggeration. Four additional footfall patterns were recognized from the improved model, and the many footprints add up to entire trackways, although they are still incomplete and walking direction cannot be determined yet.

In Figure 2.4C, the trackway is seen in lateral view with a two-fold vertical exaggeration, showing that the pes tracks are imprinted more deeply anteriorly. The trackmaker was traveling northwards and made the turn to the northeast, as Ishigaki and Matsumoto (2009) had already stated. In Figure 2.4D, the interpreted sitemap of the trackway is given, illus-

trating the preserved manus and pes tracks of the trackway. The sitemap was also compared with the previous interpretations by Ishigaki and Matsumoto (2009) given in Figure 2.4E. Many of the manus track positions (dotted lines in Figure 2.4E) formerly reconstructed and discussed by Ishigaki and Matsumoto (2009) could be confirmed and refined here.

In Figure 2.3A-B, the manus track M2 and the pes track P2 are illustrated in a photo from the original tracks and the exaggerated color depth map. The manus track M2 is one of the few reported manus tracks from the tracksite (Lockley, 1991b; Lockley and Hunt, 1995; Ishigaki and Matsumoto, 2009). The M2 is well recognizable in the field by its roundish shape, although it is still sealed with sediment. The next manus and pes track set in the trackway consist of M3 and P3 (Figure 2.3C-D). The position of M3 was formerly reconstructed by Ishigaki and Matsumoto (2009), and is now visualized by vertical exaggeration and the color depth map. Although it is not as clear as the M2 and difficult to find in the field, it is recognizable from its roundish shape in the exaggerated color depth maps.

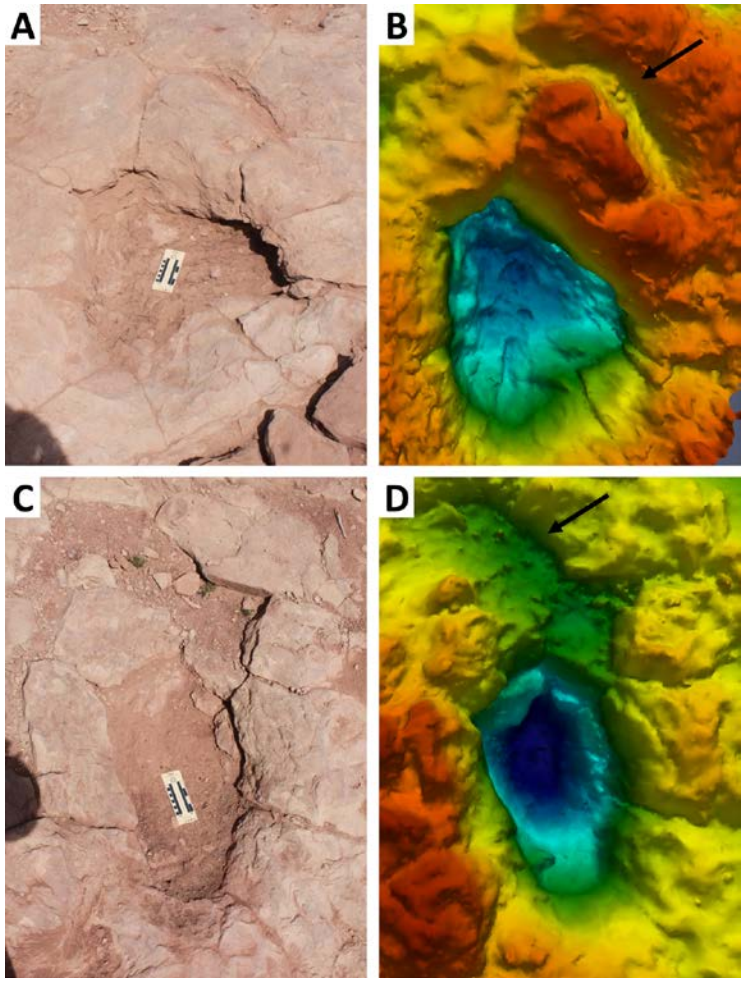

Figure 2.3: Manus and pes track sets from the Copper Ridge Dinosaur tracksite. A. Photo of the right manus track M2 (arrow) and the pes track P2. B. Vertical exaggerated color depth map of the 3D model of M2 and P2. C. Photo of the left manus track M3 (arrow) and the pes track P3. D. Vertical exaggerated color depth map of the 3D model of M3 and P3. Scale bar in A. and C. is 10 cm (or ca. 4 inch). Photos provided by courtesy of P. Martin Sander.

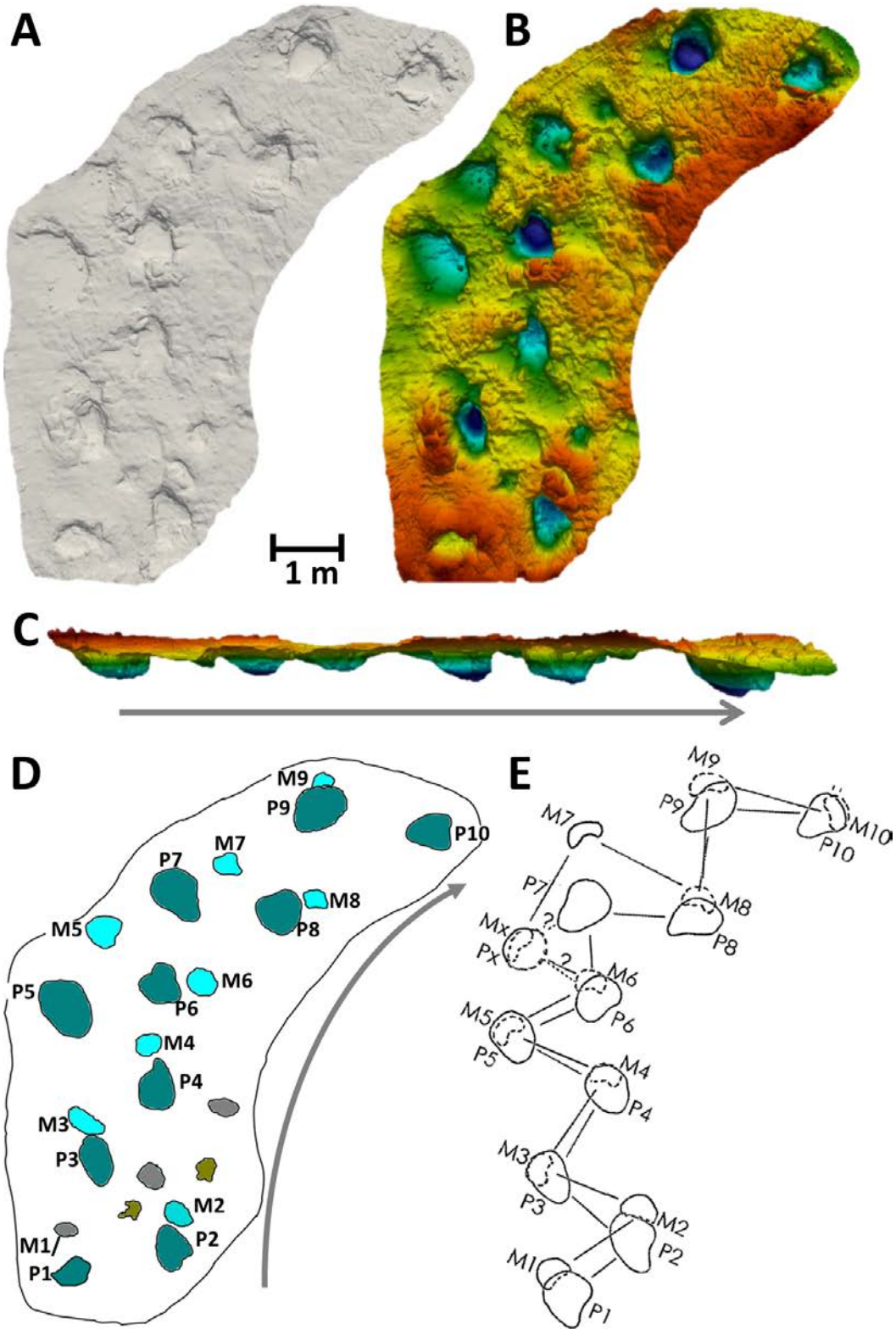

Figure 2.4: 3D models of the turning sauropod trackway at the Copper Ridge Dinosaur tracksite, Utah, USA. A. Photogrammetric solid surface model of the trackway. B. Color depth map of the 5x vertical exaggeration showing that the dimensions as well as the depth of the footprints vary over the track surface. Red indicates the highest areas and blue lowest areas in the model. C. Lateral view of a 2x vertically exaggerated color-coded model indicating the walking direction of the sauropod trackmaker. D. Sitemap of the trackway. Dark blue are pes tracks, and visualized manus tracks are light blue. Tracks in other colors do not belong to the sauropod trackway. E. Previous interpretation (modified after Ishigaki and Matsumoto, 2009 and Lockley, 1991a) for comparison with new interpretation. M = manus track. P= pes track. Tracks drawn as dotted lines were not observed but reconstructed by Ishigaki and Matsumoto (2009).

2.4.3 Barkhausen tracksite (Figure 2.5)

In the field, most of the tracks at the Barkhausen tracksite are well visible, as most of them show displacement rims. The entire tracksite is strewn with cracks from the treatment with cement in order to preserve the tracks from weathering (Friese, 1979), which makes distinguishing between natural and artificial structures difficult. The 3D model of the best preserved manus and pes track set is given in Figure 2.5A as a color-coded five-fold vertical exaggerated 3D model viewed from above. The anterior part of the pes track is noticeably more deeply imprinted than the posterior part. Figure 2.5B shows lateral views of the model in three different intensities of vertical exaggeration. The deep impression of the anterior part of the pes track is particularly visible in the 10x exaggerated model, whereas in the others it is not that obvious. The deep impression might be the claw impression of digit I, which is of interest because it may help identify a possible trackmaker for the Barkhausen tracksite.

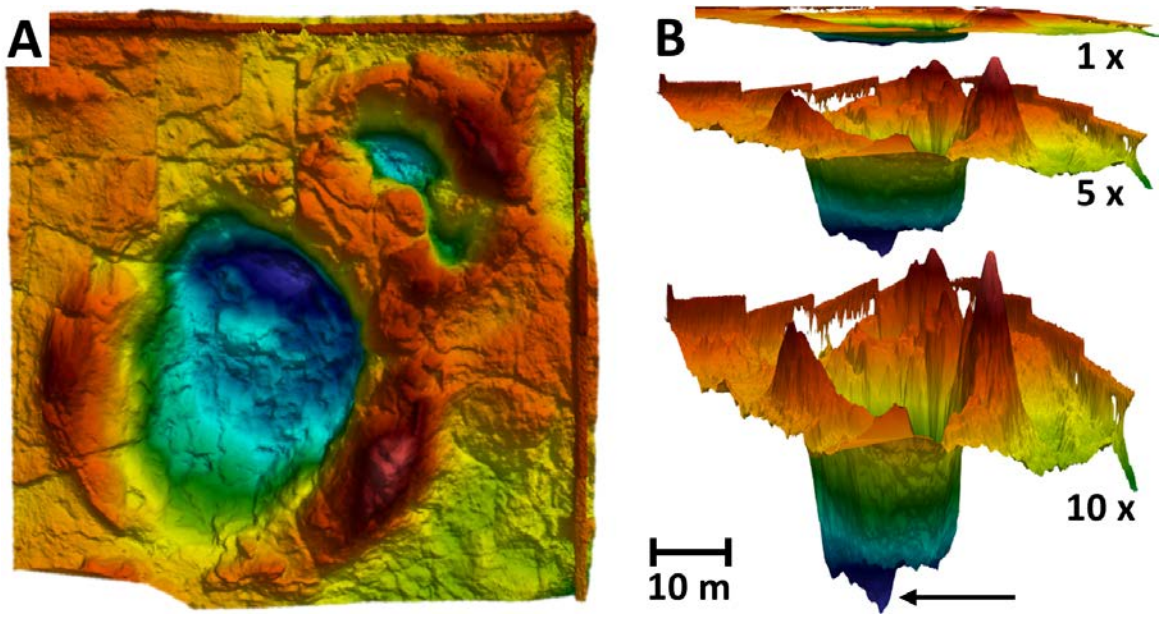

Figure 2.5: A well-preserved set of a right manus and pes track from a sauropod trackway at Barkhausen, Germany. A. The 5x vertically exaggerated color-coded model viewed from above, whereby the highest areas are red and the lowest areas are blue. Depth of the tracks, displacement rims around it, cracks and other structures are notably enhanced in this model. B Comparison of lateral posterior views of models with 1x, 5x, and 10x vertical exaggeration: Only the 10x view reveals the impression of the pedal claw of digit I (arrow).

2.4.4 Münchehagen trackway (Figure 2.6)

A partial sauropod trackway from the protected natural heritage site at Münchehagen was digitized (Figure 2.6). The trackway model with a five-fold vertical exaggeration shows 17 pes and nine manus tracks (Figure 2.6A - B). The preservation of the individual tracks and wave ripple marks on the track surface varies along the trackway. Pes tracks are clearly visible throughout the entire trackway. In the middle part of the model in Figure 2.6A, the red area lacks manus tracks. As already seen in the original trackway, this part is surround-

ed by cracks and has a different surface structure without ripple marks. In Figure 2.6C, the lateral view of the non-exaggerated model is illustrated. However, compared to the lateral view of the five-fold exaggerated model (Figure 2.6D), the actual depth of the sauropod manus and pes prints is more recognizable. It also shows that the red area is elevated compared to the main track level.

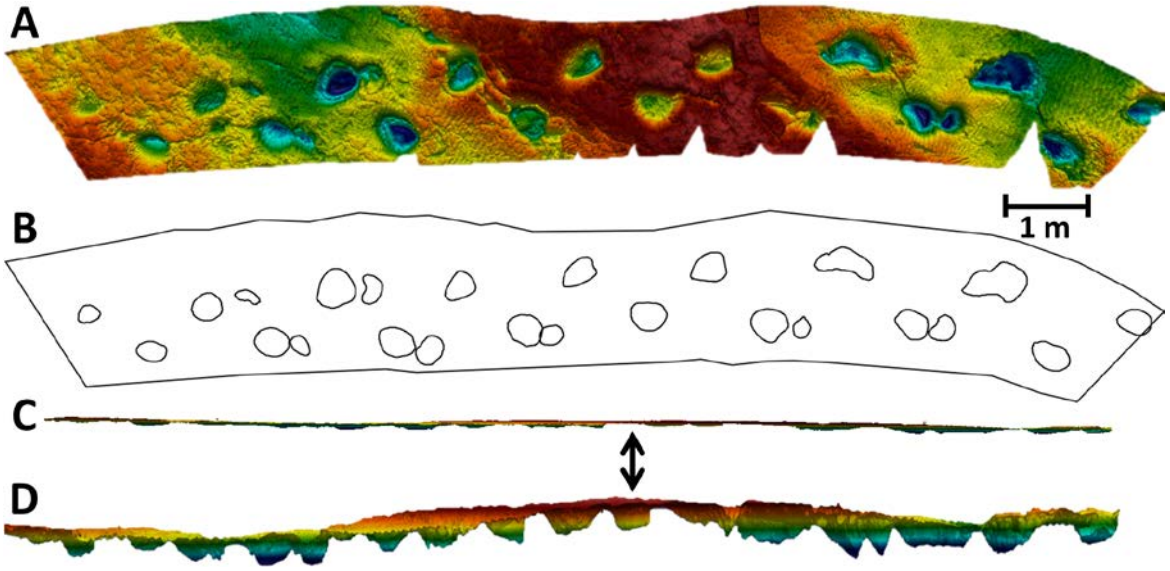

Figure 2.6: Partial sauropod trackway with manus and pes tracks from Münchehagen, Germany. A. Color depth map with 5x vertical exaggeration in top view showing that the preservation of the individual tracks and wave ripple marks varies along the course of the trackway. The pes tracks are well visible throughout the trackway, whereas manus tracks are sometimes lacking. B. Sitemap for the sauropod trackway illustrating the footfall pattern of the trackmaker. C. Lateral view of the trackway without vertical exaggeration. D. The lateral view of the five-fold exaggerated model illustrates elevation variation. Specifically, the red area lacks manus tracks, because they are still covered by a sediment layer (arrow). In this part, more preparation of the trackway is needed to uncover the manus tracks.

2.5. DISCUSSION

In the last few years, photogrammetry and other 3D methods have substantially contributed to research in paleontology. Specifically in vertebrate ichnology, the increasing use of digitization improved interpretations based on 3D surface models (e.g., Matthews and Breithaupt, 2001; Petti et al., 2008; Falkingham, 2012; Mallison and Wings, 2014; Matthews et al., 2016).

In the present study, 3D models were manipulated using vertical exaggeration along with a color depth map. For this research, four well-known tracksites were chosen, since reassessing previously studied tracks with different techniques is valuable for ensuring the results are scientifically rigorous. Although the studied tracksites suffer from erosion after decades of exposure since their discovery and description, photogrammetry and vertical exaggeration can be used as additional and supporting tools for gaining further information. In the following sections, the advantages and disadvantages of the application of vertical exaggeration on 3D models will be discussed.

2.5.1 Visibility of tracks

The vertical exaggeration along with a color depth map of 3D models is able to extend the visualization and traceability of structures for the observer and visualizes structures in a more comprehensive way. Vague structures in the 3D models can either be assigned to tracks or trackways by vertical exaggeration, or excluded from the interpretation because the morphology differs considerably from a plausible track-like shape.

In the Avelino tracksite (Figure 2.2), the preservation of tracks and trackways is poor, since the manus and pes tracks are very shallow and do not contain many details, apart from the footfall pattern. Previous research on the Avelino tracksite (Lockley and dos Santos, 1993) was able to find in total 108 tracks (Figure 2.2E), from which four narrow-gauged sauropod trackways were identified on the main track surface and an additional one on a separate, dislocated slab of the same stratigraphic level at a distance of 28 meters. It has to be acknowledged that so many tracks were detected with conventional methods (e.g., sketching) by Lockley and dos Santos (1993), although the majority of the tracks at the Avelino tracksite are very faint and only visible under very good lighting conditions in the field.

With the application of vertical exaggeration and color depth maps on the 3D models of the tracksite, this study was able to reveal more than 30 additional sauropod tracks on the main track surface, all together representing at least eight trackways of sauropods (Figure 2.2F). This illustrates that with vertical exaggeration in combination with color depth maps of the 3D models, the visibility of tracks with poor preservation can be improved (pers. comm. Martin G. Lockley). Tracks and structures that were questionable based on conventional documentation methods can be re-examined with the manipulation of the 3D models to help confirm or reject interpretations.

2.5.2 Advantages of the lateral view

The vertical exaggeration works for both, lateral and top down views of the model, depending on which track detail is of interest to the researcher. In the top down view, the vertical exaggeration works best in combination with color depth maps of the 3D models. However, the strength of vertical exaggeration is the visualization in the lateral view, as the tracks are treated more in a geological way as cross-sections (e.g., Figure 2.6C-D).

In some tracksites, determining the direction of travel of the trackmaker is difficult, due to poor preservation. In the case of the Barkhausen tracksite, many authors who studied the tracksite suggested conflicting interpretations. Kaever and de Lapparent (1974), for example, interpreted the walking direction of the sauropod trackmaker to be heading South, whereas Lockley and Meyer (2000) correctly found the walking direction to be northwards. In such cases, and possibly for isolated tracks, the lateral view of trackway models might be helpful because changes in depth of the tracks in lateral view may indicate direc-

tionality. Although, the walking direction in the sauropod trackway of the Copper Ridge Dinosaur tracksite was never doubted, the lateral view in Figure 2.4C nicely shows that the tracks are deeper in the anterior part. Note that the walking direction is not obvious in the Münchehagen trackway (Figure 2.6D). This is because many tracks are still infilled with sediment and not fully prepared. In case of the Avelino tracksite, the walking direction of the trackmaker could not be identified in some of the trackways. Thus, it is not known if the trackways have a preferred direction, as also mentioned by Castanera et al. (2014). Gregarious behavior might possibly be inferred in the case of trackways 2 and 6, as the tracks were made by small individuals, which tended to travel in groups (Myers and Fiorillo, 2009; Castanera et al., 2014).

2.5.3 Implications for trackmaker identification and locomotion

Additional data from 3D model manipulation with vertical exaggeration might be useful for future studies on trackmaker behavior and locomotion. A study by Ishigaki and Matsumoto (2009) analyzed the pes-dominated turning trackway of the Copper Ridge sauropod trackmaker and reconstructed the possible locations of the missing manus tracks. For the unusual turning pattern in the trackway, the position of the manus tracks is of particular interest for the locomotion of the trackmaker. Many of the reconstructed manus track positions (dotted lines in Figure 2.4E; Figure 2.3) could be supported and verified by the new visualization in the 3D model. The Mx/Px track from Ishigaki and Matsumoto (2009) is now attributed to be the manus track M5 corresponding to the pes P5 (Figure 2.4D-E) and the M7 from the previous work is located closer to the corresponding pes track P7. The resulting footfall pattern in the Copper Ridge trackway (Figure 2.4D) shows short step lengths and ipsilateral manus and pes prints placed together. The manus prints are placed in front of the pes. This might indicate the gait of the trackmaker, for example, a slow walk (Läbe et al. unpubl. data). Although additional manus tracks were highlighted, the trackway is still considered to be pes-dominated, meaning that the pes prints are deeper imprinted than the manus prints. This could be an argument for a higher distribution of weight on the hind limbs due to a posterior position of the centre of mass (cf. Henderson, 2006).

In the case of the well-preserved set of a manus and pes track from the Barkhausen tracksite (Figure 2.5), the claw impression of digit I is explicitly visualized through the analysis of the 3D model. This might be used in future research for trackmaker identification, as little work has been on this aspect for this tracksite. In case of the Avelino tracksite, this paper agrees with the results of other researchers that these tracks are undertracks and that the right most trackway (trackway 4 in Figure 2.2E-F) is manus-dominated (Lockley and dos Santos, 1993; Castanera et al., 2013).

2.5.4 Missing tracks?

In the case of the Münchehagen tracksite, it was stated formerly that the majority of manus tracks is not preserved (Lockley et al., 2004). Since the track surface and the tracks show

sedimentary structures, such as wave ripple marks, it was previously argued that the sauropod trackmakers were swimming and therefore only pes tracks were imprinted to the sediment (Fischer, 1998). Although the majority of the manus tracks are difficult to find on the original track surface, Englich (2013) however, discovered that the majority of manus tracks is still preserved, but infilled and sealed with sediments and that some of the tracks were simply overlooked in the past. Cracks along the track surface had been patched up with cement for maintenance, which additionally hinders an easy interpretation of the site. The hypothesis by Englich (2013) could be supported in the present study, as the comparison of the original tracks with exaggerated models in lateral view shows. In Figure 2.7, the elevated red area of the middle part of Figure 2.6 is enlarged.

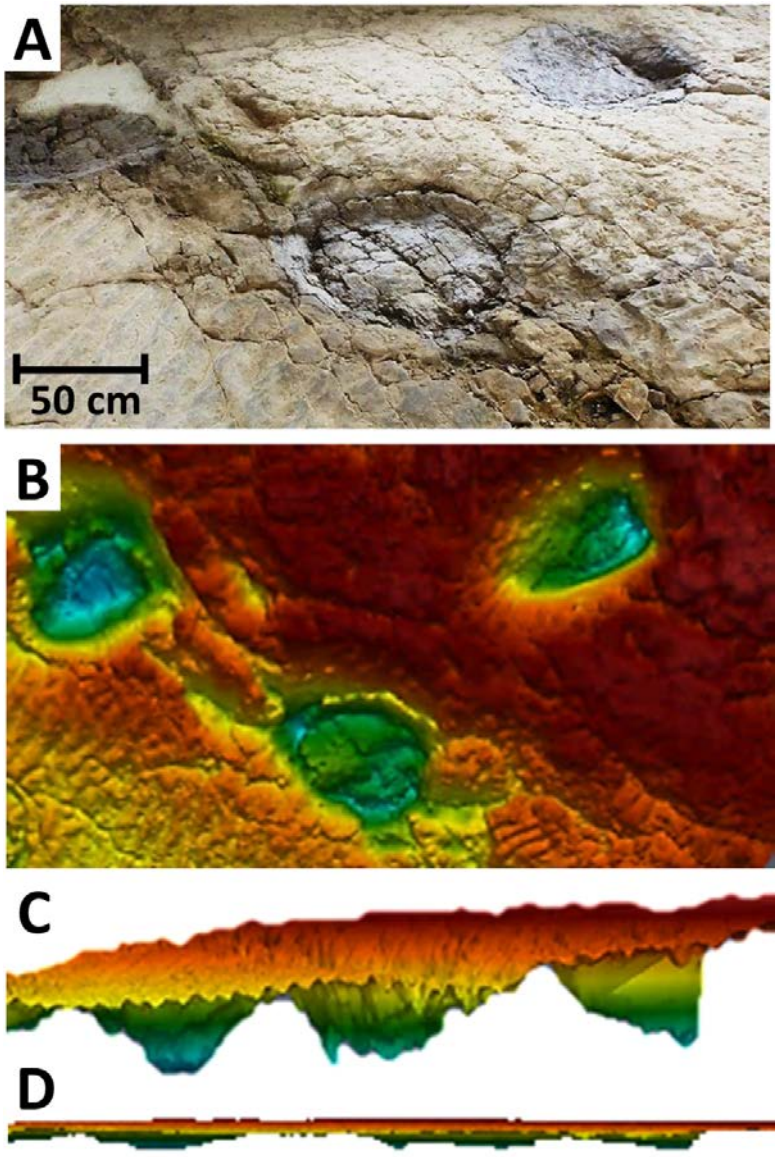

Figure 2.7: Transition between the parts of the trackway where manus tracks are preserved to the region where they are not in the Münchehagen trackway. A. Photo of the original tracks. B. Vertical exaggerated color depth map of the 3D model in view from above (enlarged from Figure 2.6A). C. Lateral view of the 5x exaggerated color-coded 3D model. D. Lateral view of the unexaggerated model.

The focus is on the transition between the part of the surface where manus tracks are preserved to the region where they are not. From the photo (Figure 2.7A), three pes tracks and a diagonal crack, which occur frequently in these rocks because of salt tectonics, are visible. The color depth map (Figure 2.7B) shows that on the right side of the crack the area is elevated, which is particularly visible in the lateral view in Figure 2.7C. In the 3D model with vertical exaggeration, a sediment layer could be observed, which is overlying the track surface. Thus, in this area of the site, more preparation of the trackway is needed to uncover the manus tracks.

2.5.5 Potential problems and recommendations for the work with vertical exaggeration

As the proposed method conducts manipulation of 3D models in order to visualize additional structures, the potential of errors needs to be understood and minimized. Artifacts that develop during any step of the processing of the photogrammetric model could easily be propagated and even increased into the vertical exaggerated model, and therefore be misinterpreted as feature of the tracks. To minimize errors in the photogrammetric process, it is necessary to work very thoroughly; for example, the proper use of scale bars during photo capture of the object. With the use of proper and thorough procedures from photo capture to model creation, photogrammetry can provide accurate and dependable models with negligible error. The software Agisoft PhotoScan can provide an error estimation and recent studies (e.g., Matthews et al., 2016) have discussed in detail ways to detect and reduce error.

It is unavoidable that with increasing vertical exaggeration of the tracks in the 3D model, other structures, like surface cracks or debris on the track surface become exaggerated as well. In that case, it might be difficult to distinguish between real structures and irrelevant other structures. Therefore, the best and most effective factors for vertical exaggeration for the purpose of highlighting additional detail in the tracks appear to be 5x and 10x in the top down view, and 2x to 5x in the lateral view. With excessive vertical exaggerations, the analysis of the model is distorted, since exaggerated irrelevant structures, such as cracks and debris, hide the structures, which are of interest.

Researchers, who want to apply vertical exaggeration in the future, should, however be aware that this method is a manipulation of the original 3D model. If new information is obtained, it should be confirmed by the careful crosschecking with the original material or photographs. When interpreting the vertically exaggerated model, appropriate care should be taken to not mistake true structures of the object with morphologies due to errors as described above. For instance, marginal structures of the model, which the observer did not observe under field conditions at all, are likely to be artifacts, since a lack of points in the points cloud and distortion might occur in these parts of the model. For the application of

vertical exaggeration, only 3D models of very good quality and sufficient accuracy (cf. Table 2.1) should be used.

Before applying vertical exaggeration, it is recommended to first study the original tracks, then the 3D model without any kind of manipulation. In most cases, valuable information regarding the tracks is already gained at this stage. However, to exhaust the full potential of the information contained in the tracks, the vertical exaggeration with color depth mapping can be applied to the model. Comparing models with different vertical exaggerations (e.g., Figure 2.5B) is useful for finding the optimal exaggeration to interpret very subtle structures.

In future studies, the combined approach of vertical exaggeration and color depth maps of 3D models could be applied to other vertebrate and invertebrate tracksites, providing further insights into locomotion and behavior of animals throughout evolutionary history. Vertical exaggeration will not only be applicable to photogrammetry, but also to any kind of 3D model. In terms of the research on ichnology, 3D models from laser scanning might also be suitable for manipulation with vertical exaggeration.

2.6. CONCLUSION

In this study, photogrammetric 3D models of sauropod tracks were manipulated using vertical exaggeration with the intention of improving the detail of subtle track features and uncovering undocumented features of trackways. Although commonly applied in geological studies for visualizing topography and cross section, the application of vertical exaggeration is a novelty in the field of vertebrate ichnology. The findings of this study using vertical exaggeration of the models are not only in good agreement with interpretations of previous research on the selected track localities, but also extend them. In all four studied track localities, the manipulated 3D models used here broaden the understanding of the trackway and the individual tracks. The additional details discovered by vertical exaggeration along with color depth maps will lead to more accurate and detailed interpretations. The presence of questionable tracks from former trackway interpretations are confirmed in most cases and locomotion patterns can be better resolved. The direction of trackways can be interpreted more accurately, since there is no bias due to perspective distortion. This approach of vertical exaggeration demonstrates the value of re-interpreting known tracks, even if those were considered as poorly preserved. For vertical exaggeration, the best and most effective factors for improving the visibility of tracks appear to be 2x to 10x. With the easily applicable approach of vertical exaggeration, re-interpretation of tracks and insights into paleobiological questions such as locomotion and behavior of the trackmaker can be obtained.

2.7. ACKNOWLEDGEMENTS

I thank the developers of the freeware used in this paper, to make it freely available so that it could be used for this research. The BLM office in Moab is thanked for providing further information about the Copper Ridge Dinosaur tracksite, since the site is managed by the BLM. P. M. Sander (Universität Bonn) is thanked for providing photographs of the Copper Ridge Dinosaur tracksite, which were used for an earlier version of the photogrammetry, thankfully provided by H. Mallison (Museum für Naturkunde Berlin). I thank T. Plogschties (Universität Bonn) for greatly supporting data collection at the Copper Ridge Dinosaur tracksite and Avelino tracksite. Octávio Mateus (Universidade Nova de Lisboa, Museu da Lourinhã) is thanked for providing additional information about the Avelino tracksite. I thank A. Leipner (Museum am Schölerberg) and B. Englich (Dinosaurierpark Münchehagen) for support during the field work at the Barkhausen tracksite. N. Knötschke (Dinosaurierpark Münchehagen) is thanked for the access to the tracksite in the protected part of the Dinopark Münchehagen. I thank Martin G. Lockley (University of Colorado) for discussing the preliminary results of this study. For discussion, advice, and improving the manuscript, I wish to thank J. Mitchell, J. N. Lallensack and P. M. Sander (Universität Bonn). The comments and suggestions of Neffra Matthews, an anonymous reviewer, and the editor Matteo Belvedere greatly improved the manuscript. Finally, I wish to thank the German Academic Scholarship Foundation (Studienstiftung des deutschen Volkes) for generous funding.

2.8. AUTHOR CONTRIBUTIONS

Conceived and designed the experiments: SL. Performed the experiments: SL. Analyzed the data: SL. Contributed reagents/materials/analysis tools: SL. Wrote the paper: SL.

2.9. REFERENCES

Adams, T. L., C. Strganac, M. J. Polcyn, and L. L. Jacobs. **2010**. High resolution three-dimensional laser-scanning of the type specimen of *Eubrontes* (?) *glenrosensis* Shuler, 1935, from the Comanchean (Lower Cretaceous) of Texas: implications for digital archiving and preservation. Palaeontologia Electronica 13(3):1–11.

Alexander, R. M. 1976. Estimates of speeds of dinosaurs. Nature 261:129–130.

Antunes, M. T., and O. Mateus. **2003**. Dinosaurs of Portugal. Comptes Rendus Palevol 2(1):77–95.

Bates, K. T., B. H. Breithaupt, P. L. Falkingham, N. A. Matthews, D. Hodgetts, and P. L. Manning. **2008**. Integrated LiDAR and photogrammetric documentation of the Red Gulch Dinosaur Tracksite (Wyoming, USA); pp. 101–103 in S. E. Foss, L. Cavin, T. Brown, J. I. Kirkland, and V. L. Santucci (eds.), Proceedings of the Eighth Conference

on Fossil Resources, St. George, Utah. BLM Regional Paleontologist, Salt Lake City, Utah.

Bates, K. T., P. L. Falkingham, D. Hodgetts, J. O. Farlow, B. H. Breithaupt, M. O'Brien, N. Matthews, W. I. Sellers, and P. L. Manning. **2009**. Digital imaging and public engagement in palaeontology. Geology Today 25(4):134–139.

Bates, K. T., P. L. Falkingham, F. Rarity, D. Hodgetts, A. Purslow, and P. L. Manning. **2010**. Application of high-resolution laser scanning and photogrammetric techniques to data acquisition, analysis and interpretation in palaeontology. International Archives of Photogrammetry, Remote Sensing and Spatial Information Sciences 38:68–73.

Bates, K. T., P. L. Manning, B. Vila, and D. Hodgetts. **2008**. Three-dimensional modelling and analysis of dinosaur trackways. Palaeontology 51(4):999–1010.

Belvedere, M., and J. O. Farlow. **2016**. The Numerical Scale for Quantifying the Quality of Preservation of Vertebrate Tracks; pp. 92–98 in P. L. Falkingham, D. Marty, and A. Richter (eds.), Dinosaur Tracks - The Next Steps. Life of the Past. Indiana University Press, Bloomington, 413 pp.

Breithaupt, B. H., and N. A. Matthews. **2011**. Photogrammetric ichnology: state-of-the-art digital data analysis of paleontological resources in North America, Europe, Asia, and Africa. Journal of Vertebrate Paleontology Program and Abstracts 2011:77.

Breithaupt, B. H., N. A. Matthews, and T. A. Noble. **2004**. An integrated approach to three-dimensional data collection at dinosaur tracksites in the Rocky Mountain West. Ichnos 11(1-2):11–26.

Breithaupt, B. H., E. H. Southwell, T. Adams, and N. A. Matthews. **2006**. The Red Gulch dinosaur tracksite: public participation in the conservation and management of a world-class paleontological site. New Mexico Museum of Natural History and Science Bulletin 34:10.

Castanera, D., B. Vila, N. L. Razzolini, P. L. Falkingham, J. I. Canudo, P. L. Manning, and À. Galobart. **2013**. Manus track preservation bias as a key factor for assessing trackmaker identity and quadrupedalism in basal ornithopods. PLoS ONE 8(1):1–13.

Castanera, D., B. Vila, N. L. Razzolini, V. F. Santos, C. Pascual, and J. I. Canudo. **2014**. Sauropod trackways of the Iberian Peninsula: palaeoetological and palaeoenvironmental implications. Journal of Iberian Geology 40(1):49–59.

Englich, B. 2013. Neuaufnahme unterkretazischer Fährten sauropoder Dinosaurier im Naturdenkmal "Saurierfährten Münchehagen". Unpublished diploma thesis, University of Bonn, Bonn, 65 pp.

Falkingham, P. L. 2012. Acquisition of high resolution three-dimensional models using free, open-source, photogrammetric software. Palaeontologia Electronica 15(1):1-15.

Falkingham, P. L. 2016. Applying Objective Methods to Subjective Track Outlines; pp. 73–80 in P. L. Falkingham, D. Marty, and A. Richter (eds.), Dinosaur Tracks - The Next Steps. Life of the Past. Indiana University Press, Bloomington, 413 pp.

Falkingham, P. L., K. T. Bates, and J. O. Farlow. **2014**. Historical photogrammetry: Bird's Paluxy River dinosaur chase sequence digitally reconstructed as it was prior to excavation 70 years ago. PLoS ONE 9(4):1–5.

Farlow, J. O. 1992. Sauropod tracks and trackmakers: integrating the ichnological and skeletal records. Zubia 10:89–138.

Farlow, J. O., J. G. Pittman, and J. M. Hawthorne. **1989**. *Brontopodus birdi,* Lower Cretaceous Sauropod Footprints from the U.S. Gulf Coastal Plain; pp. 371–394 in D. D. Gillette and M. G. Lockley (eds.), Dinosaur Tracks and Traces. Cambridge University Press, Cambridge, 476 pp.

Fernández-Lozano, J., and G. Gutiérrez-Alonso. **2017**. The Alejico Carboniferous forest: a 3D-terrestrial and UAV-assisted photogrammetric model for geologic heritage preservation. Geoheritage 9(2):163–173.

Fischer, R. 1998. Die Saurierfährten im Naturdenkmal Münchehagen. Mitteilungen aus dem Institut für Geologie und Paläontologie der Universität Hannover 37:3–59.

Foster, J. R. 2015. Theropod dinosaur ichnogenus *Hispanosauropus* identified from the Morrison Formation (Upper Jurassic), Western North America. Ichnos 22(3-4):183–191.

Friese, H. 1979. Die Saurierfährten von Barkhausen im Wiehengebirge. Veröffentlichungen des Landkreises Osnabrück 1:1–36.

Grimm, A. 2007. The origin of the term photogrammetry. Photogrammetric Week '07 51:53–60.

Henderson, D. M. 2006. Burly gaits: centers of mass, stability, and the trackways of sauropod dinosaurs. Journal of Vertebrate Paleontology 26(4):907–921.

Hendricks, A. 1981. Die Saurierfährte von Münchehagen bei Rehburg-Loccum (NW-Deutschland). Abhandlungen aus dem Landesmuseum für Naturkunde Münster in Westfalen 43:3–22.

Hunt-Foster, R. K., M. G. Lockley, A. R. C. Milner, J. R. Foster, N. A. Matthews, B. H. Breithaupt, and J. A. Smith. **2016**. Tracking dinosaurs in BLM Canyon Country, Utah. Geology of the Intermountain West 3:67–100.

Ishigaki, S., and Y. Matsumoto. **2009**. "Off-tracking"-like phenomenon observed in the turning sauropod trackway from the Upper Jurassic of Morocco. Memoir of the Fukui Prefectural Dinosaur Museum 8:1–10.

Kaever, M., and A. F. de Lapparent. **1974**. Les traces de pas de Dinosaures du Jurassique de Barkhausen (Basse Saxe, Allemagne). Bulletin de la Société Géologique de France 16:516–525.

Lallensack, J. N. 2016. An objective method for the generation of footprint outlines. Journal of Vertebrate Paleontology Program and Abstracts, 2016:171.

Lallensack, J. N., P. M. Sander, N. Knötschke, and O. Wings. **2015**. Dinosaur tracks from the Langenberg Quarry (Late Jurassic, Germany) reconstructed with historical photogrammetry: evidence for large theropods soon after insular dwarfism. Palaeontologia Electronica 18.2.31A:1–34.

Lallensack, J. N., A. H. van Heteren, and O. Wings. **2016**. Geometric morphometric analysis of intratrackway variability: a case study on theropod and ornithopod dinosaur trackways from Münchehagen (Lower Cretaceous, Germany). PeerJ 4:1-52.

Lockley, M., and A. P. Hunt. **1995**. Dinosaur Tracks and Other Fossil Footprints of the Western United States. Columbia University Press, New York, 360 pp.

Lockley, M. G. 1991a. The dinosaur footprint renaissance. Modern Geology 16:139–160.

Lockley, M. G. 1991b. Tracking Dinosaurs - A New Look at an Ancient World. Cambridge University Press, Cambridge, 237 pp.

Lockley, M. G., and V. F. dos Santos. **1993**. A preliminary report on sauropod trackways from the Avelino site, Sesimbra region, Upper Jurassic Portugal. Gaia: Revista de Geociências 6:38–42.

Lockley, M. G., J. O. Farlow, and C. A. Meyer. **1994**. *Brontopodus* and *Parabrontopodus* ichnogen. nov. and the significance of wide- and narrow-gauge sauropod trackways. Gaia: Revista de Geociências 10:135–145.

Lockley, M. G., and C. Meyer. **2000**. Dinosaur Tracks and Other Fossil Footprints of Europe. Columbia University Press, New York, 341 pp.

Lockley, M. G., J. L. Wright, and D. Thies. **2004**. Some observations on the dinosaur tracks at Münchehagen (Lower Cretaceous), Germany. Ichnos 11(3-4):261–274.

Mallison, H., and O. Wings. **2014**. Photogrammetry in paleontology - a practical guide. Journal of Paleontological Techniques 12:1–31.

Marty, D. 2008. Sedimentology, taphonomy, and ichnology of Late Jurassic dinosaur tracks from the Jura carbonate platform (Chevenez—Combe Ronde tracksite, NW Switzerland): insights into the tidal-flat palaeoenvironment and dinosaur diversity, locomotion, and palaeoecology. GeoFocus 21:1–278.

Matthews, N. A., and B. H. Breithaupt. **2001**. Close-range photogrammetry experiments at Dinosaur Ridge. The Mountain Geologist 38(3):147–153.

Matthews, N. A., T. A. Noble, and B. H. Breithaupt. **2006**. The application of photogrammetry, remote sensing and geographic information systems (GIS) to fossil resource management. New Mexico Museum of Natural History and Science Bulletin 34:119–131.

Matthews, N. A., T. A. Noble, and B. H. Breithaupt. **2016**. Close-Range Photogrammetry for 3-D Ichnology: The Basics of Photogrammetric Ichnology; pp. 28–55 in P. L. Falkingham, D. Marty, and A. Richter (eds.), Dinosaur Tracks - The Next Steps. Life of the Past. Indiana University Press, Bloomington, 413 pp.

McCrea, R. T., D. H. Tanke, L. G. Buckley, M. G. Lockley, J. O. Farlow, L. Xing, N. A. Matthews, C. W. Helm, S. G. Pemberton, and B. H. Breithaupt. **2015**. Verte-

brate ichnopathology: pathologies inferred from dinosaur tracks and trackways from the Mesozoic. Ichnos 22(3-4):235–260.

Meyer, C. A., and J. G. Pittman. **1994**. A comparison between the *Brontopodus* ichnofacies of Portugal, Switzerland and Texas. Gaia: Revista de Geociências 10:125–133.

Myers, T. S., and A. R. Fiorillo. **2009**. Evidence for gregarious behavior and age segregation in sauropod dinosaurs. Palaeogeography, Palaeoclimatology, Palaeoecology 274(1-2):96–104.

Petti, F. M., M. Avanzini, M. Belvedere, M. de Gasperi, P. Ferretti, S. Girardi, F. Remondino, and R. Tomasoni. **2008**. Digital 3D modelling of dinosaur footprints by photogrammetry and laser scanning techniques: integrated approach at the Coste dell'Anglone tracksite (Lower Jurassic, Southern Alps, Northern Italy). Studi Trentini di Scienze Naturali - Acta Geologica 83:303–315.

Platt, B. F., S. T. Hasiotis, and D. R. Hirmas. **2010**. Use of low-cost multistripe laser triangulation (MLT) scanning technology for three-dimensional, quantitative paleoichnological and neoichnological studies. Journal of Sedimentary Research 80(7):590–610.

Razzolini, N. L., B. Vila, I. Díaz-Martínez, P. L. Manning, and À. Galobart. **2016**. Pes shape variation in an ornithopod dinosaur trackway (Lower Cretaceous, NW Spain): New evidence of an antalgic gait in the fossil track record. Cretaceous Research 58:125–134.

Salisbury, S. W., A. Romilio, M. C. Herne, R. T. Tucker, and J. P. Nair. **2017**. The dinosaurian ichnofauna of the Lower Cretaceous (Valanginian–Barremian) Broome Sandstone of the Walmadany Area (James Price Point), Dampier Peninsula, Western Australia. Journal of Vertebrate Paleontology 36(6, suppl.):1–152.

Santos, V. F. d., C. M. d. Silva, and L. A. Rodrigues. **2008**. Dinosaur track sites from Portugal: scientific and cultural significance. Oryctos 8:77–88.

Schanz, T., Y. Lins, H. Viefhaus, T. Barciaga, S. Läbe, H. Preuschoft, U. Witzel, and P. M. Sander. **2013**. Quantitative interpretation of tracks for determination of body mass. PLoS ONE 8(10):1–12.

Stoinski, S., T. Suthau, and H.-C. Gunga. **2011**. Reconstructing Body Volume and Surface Area of Dinosaurs Using Laser Scanning and Photogrammetry; pp. 94–104 in N. Klein, K. Remes, C. T. Gee, and P. M. Sander (eds.), Biology of the Sauropod Dinosaurs - Understanding the Life of Giants. Life of the Past. Indiana University Press, Bloomington, 331 pp.

Thulborn, T. 1990. Dinosaur Tracks. Chapman and Hall, New York, 410 pp.

Wilson, J. A. 2005. Integrating ichnofossil and body fossil records to estimate locomotor posture and spatiotemporal distribution of early sauropod dinosaurs: a stratocladistic approach. Paleobiology 31(3):400–423.

Wilson, J. A., and M. T. Carrano. **1999**. Titanosaurs and the origin of "wide-gauge" trackways: a biomechanical and systematic perspective on sauropod locomotion. Paleobiology 25(2):252–267.

Wings, O., J. N. Lallensack, and H. Mallison. **2016**. The Early Cretaceous Dinosaur Trackways in Münchehagen (Lower Saxony, Germany): 3-D Photogrammetry as Basis for Geometric Morphometric Analysis of Shape Variation and Evaluation of Material Loss during Excavation; pp. 57–70 in P. L. Falkingham, D. Marty, and A. Richter (eds.), Dinosaur Tracks - The Next Steps. Life of the Past. Indiana University Press, Bloomington, 413 pp.

Wright, J. L. 2005. Steps in Understanding Sauropod Biology; pp. 252–280 in K. Curry Rogers and J. A. Wilson (eds.), The Sauropods - Evolution and Paleobiology. University of California Press, Berkeley, 349 pp.

CHAPTER 3

Quantitative interpretation of tracks for determination of body mass

Schanz, T., Y. Lins, H. Viefhaus, T. Barciaga, **S. Läbe**, H. Preuschoft, U. Witzel, and P. M. Sander. 2013. *PLoS ONE* 8(10):1-12.

3.1. ABSTRACT

To better understand the biology of extinct animals, experimentation with extant animals and innovative numerical approaches have grown in recent years. This research project uses principles of soil mechanics and a neoichnological field experiment with an African elephant to derive a novel concept for calculating the mass (i.e., the weight) of an animal from its footprints. We used the elephant's footprint geometry (i.e., vertical displacements, diameter) in combination with soil mechanical analyses (i.e., soil classification, soil parameter determination in the laboratory, Finite Element Analysis (FEA) and gait analysis) for the back analysis of the elephant's weight from a single footprint. In doing so we validated the first component of a methodology for calculating the weight of extinct dinosaurs. The field experiment was conducted under known boundary conditions at the Zoological Gardens Wuppertal with a female African elephant. The weight of the elephant was measured and the walking area was prepared with sediment in advance. Then the elephant was walked across the test area, leaving a trackway behind. Footprint geometry was obtained by laser scanning. To estimate the dynamic component involved in footprint formation, the velocity the foot reaches when touching the subsoil was determined by the Digital Image Correlation (DIC) technique. Soil parameters were identified by performing experiments on the soil in the laboratory. FEA was then used for the back calculation of the elephant's weight. With this study, we demonstrate the adaptability of using footprint geometry in combination with theoretical considerations of loading of the subsoil during a walk and soil mechanical methods for prediction of trackmakers weight.

3.2. INTRODUCTION

Since the first massive bones of sauropods were discovered, many scientists have investigated how these animals evolved to their gigantic size (Sander and Clauss, 2008; Klein et al., 2011; Sander et al., 2011). Analyses and interpretation of sauropod gigantism are essential for the understanding of evolutionary constraints and how these constraints impact Earth's geological and biological history. Bones of sauropods, of course, are not their only remains in the fossil record, but the second most common evidence for their former existence are footprints and entire trackways. The track record is important because it provides anatomical details and locomotion patterns of the trackmaker. Unlike bones, which are often transported, trace fossils are autochthonous and provide unequivocal information about the actual habitat of the trackmaker. The enormous tracks of gigantic sauropod dinosaurs occur in sediments from the Late Triassic (Lockley et al., 2001) to Cretaceous all over the world (Wright, 2005): for example in tidal flat deposits of the Paluxy River tracksite in Texas, USA (Farlow et al., 1989), in fluvial deposits (Barnes and Lockley, 1994; Foster and Lockley, 2006) and in lacustrine carbonate sediments of the Morrison Formation (Lockley et al., 1986; Prince and Lockley, 1989) or in lagoonal deposits in Münchehagen, Germany (Fischer, 1998; Lockley et al., 2004). A comprehensive listing and review is found in Mannion and Upchurch (2010).

In the past, mostly descriptive studies of tracks were done, but currently the focus is on understanding the paleobiology of the trackmaker. In general, it is possible to estimate anatomical details like hip heights (Henderson, 2003) of the trackmaker from the tracks or to estimate walking velocity from measurements of pace and stride (Alexander, 1976; Thulborn, 1990; Alexander, 2006). Modern vertebrate ichnology deals with experiments on living animals (e.g., Milàn, 2006; Platt et al., 2012), artificial indenters in the laboratory (e.g., Manning, 2004; Jackson et al., 2010), and computer-aided approaches (e.g., Henderson, 2006; Falkingham et al., 2011a). Common methods for calculating body mass based on body volume and density were done with models (Colbert, 1962), 3D scanning (Gunga et al., 2007; Gunga et al., 2008), or numerical methods (Henderson, 1999). Current numerical studies (Falkingham et al., 2009; Falkingham et al., 2010; Falkingham et al., 2011b; Bates et al., 2013) have as their main objective to qualitatively better understand the kinematics of the foot indenting the subsoil and to relate subsoil properties to footprint quality and preservation.

Quantitative approaches to dinosaur footprints offer the perspective of addressing a fundamental question in dinosaur paleobiology, i.e., mass estimation. However, a reliable quantitative method for weight reconstruction from dinosaur footprints has not been developed so far, even though this is of major importance, especially for gigantic sauropods (Campione and Evans, 2012).

Here we introduce an approach for weight estimation based on footprint geometry using soil mechanical concepts. These can be used to back calculate the load applied to the subsoil by the trackmaker's feet. The geometry of the footprint (i.e., vertical displacements and diameter) is strongly influenced by the applied stress and the constitutive characteristics of the subsoil. Note that we use the term "geometry" in a different way than in the literature on dinosaur ichnology where it refers to the parameters of entire trackways. However, we only study the individual footprint, not the trackway. The value of the stress applied to the subsoil depends on the weight of the dinosaur (i.e., a static component) as well as on the deceleration that the dinosaur foot experiences when coming into contact with the subsoil (i.e., a dynamic component). In addition, biomechanical aspects, such as gait and weight distribution among the four limbs of the trackmaker, have to be taken into account when dealing with this problem. An important step towards the application of the soil-mechanical approach to fossil footprints is the validation by work on extant tracks, also known as the actualistic approach in paleontology. The African elephant (*Loxodonta africana*) is the largest terrestrial animal today, just as the sauropods were in the Mesozoic. Considering elephants and sauropods show similarities in foot morphology, quadrupedality and massive, graviportal limbs, elephants have often been included as recent analogs in sauropod research (e.g., Henderson, 2006; Platt et al., 2012). The field part of our study was conducted at the Zoological Gardens Wuppertal, Germany. Briefly, after weighing an African elephant cow was walked across a prepared sand bed to produce footprints. Based on the footprint geometry, gait analysis, and soil mechanical properties of the subsoil, the Finite Element Analysis (FEA) was adopted to back calculate the weight of the elephant. For simplicity, in this analysis we only consider layered subsoil properties that are homogenous within each layer. We are aware that the situation in track formation often is much more complex, especially for a foot penetrating soft layers in a large deformation type of kinematics before finding resistance at a competent layer below (see Gatesy, 2003; Falkingham et al., 2011b). For this study we focus on sand as subsoil material because in a next step we will target sauropod footprints preserved in sandstones.

Well known sauropod track sites in sandstones are the Late Jurassic sites of Barkhausen (Kaever and de Lapparent, 1974; Diedrich, 2011) and Copper Ridge (Utah, USA) (Barnes and Lockley, 1994; Ishigaki and Matsumoto, 2009), and the Early Cretaceous site of Münchehagen (Fischer, 1998; Lockley et al., 2004), also Germany. Barkhausen shows several trackways of relatively small sauropods together with one theropod trackway in fine-grained sand. The surface on which the animals walked is well preserved as indicated by the distinctive sediment bulges caused by the feet. The same applies to the Copper Ridge site which was made by a large sauropod that walked on a 15 cm thick bed of medium sand underlain by a mudstone. The Münchehagen site records numerous long trackways impressed in a 25 cm thick medium sandstone also underlain by a mudstone. Some of the tracks are partially eroded at this site, making them unsuitable for the soil mechanical ap-

proach to weight estimation. However, note that this paper only reports on a first step in methods development, showing that weight estimation from footprints is possible. Considerably more research is necessary before reliable results can be obtained for sauropods, let alone other dinosaurs. Note also that elephants and sauropods are particularly suitable for this approach because of their graviportal stance and locomotion and their simple foot morphology.

3.3. METHODS AND MATERIALS

For the present research, FEA, gait analysis and Digital Image Correlation (DIC) technique were carried out, the specifics of both of which are described below. The subsoil used in the field experiment was classified and soil parameters were determined with precision by performing several experiments in the laboratory. These parameters were needed as input parameters in the FEA simulations.

3.3.1 Finite element analysis (FEA) using an advanced constitutive soil model

For the numerical simulation of the observed elephant footprint geometry (i.e., vertical displacements and diameter) FEA was used. In routine soil mechanics applications we normally derive settlements from the applied load. However, in the current study, we took the opposite approach by applying a specific type of so called back analysis (inverse analysis) in order to determine the load from the settlements. Inverse analysis is a well-established tool in soil mechanics (for an overview see Knabe et al., 2013). The FEA code used in this study considers three spatial dimensions and was originally developed for the analysis of deformations in geotechnical applications. Soil behavior is simulated in a non-linear elastic- plastic manner. Several soil models, for example, the Mohr-Coulomb model and the hardening soil model (Schanz et al., 1999) that differ in accuracy, are implemented in the FEA code to model the mechanical behavior of soil. The Mohr-Coulomb model is an elastic-plastic material model that assumes a constant stiffness of the material (i.e., the stiffness of the soil) with the depth. However, this condition is generally not met by the mechanical behavior of soils. The Mohr-Coulomb model is mostly used in initial approaches to numerical modeling of soil mechanical behavior only, but it is physically wrong for solving deformation problems as in this research.

A more realistic material model for the simulation of the behavior of different types of soil is the hardening soil model. When soil is subjected to primary loading, it shows an increase in stiffness with increasing stress and develops an irreversible plastic strain. In contrast to the Mohr-Coulomb model, the hardening soil model implements the stress dependent stiffness behavior of the soils, i.e., the hardening of the soil is taken into account. In addition to the material parameters used in the Mohr-Coulomb model, i.e., friction angle ϕ [°], cohesion c [kN/m^2], dilatancy ψ [°], the hardening soil model requires further input parameters. These include the stiffness modulus E_{oed} [kN/m^2] for primary compression loading (de-

rived from one-dimensional compression tests), the unloading and reloading stiffness modulus E_{ur} [kN/m^2] (derived from one-dimensional compression tests), as well as the deviatoric stiffness E_{50} [kN/m^2] (derived from triaxial tests). In reality, all loading conditions and loading directions may occur simultaneously, depending on the spatial position of an observation point. Therefore a constitutive model as used in this study is required that automatically analyzes the loading conditions and applies the relevant stiffness. Considering the fact that stiffnesses may vary by a factor of 7 to 10, we have to admit that less realistic soil models than the hardening soil model cannot be used for quantitative analyses. The required input parameters were determined in standard soil mechanics laboratory experiments that we performed with the material used as subsoil in the elephant field experiment.

3.3.2 Method of digital image correlation (DIC)

As noted, the stress transmitted to the subsoil during animal walking has a dynamic and a static component. Subsoil deformation is a consequence of the maximum load, which either corresponds to the maximum static load $\sigma_{stat,max}$ or to the sum of dynamic load and the corresponding static load $\sigma_{dyn+stat}$. To determine the velocity of the elephant's foot at the time of contact with the subsurface, the DIC technique was used. The elephant's walk was recorded by a high speed camera (Casio Exilim EX-F1, 60 frames per second) and deformation of pixel clusters (Figure 3.1) was analyzed for the defined time interval (see Röchter, 2011 for details of the DIC technique). The velocity vectors obtained by the DIC technique permit calculation of the dynamic stress applied to the subsoil based on Equation (3.1):

$$\sigma_{dyn} = \frac{m \cdot v_1^2}{2 \cdot s \cdot A} \tag{3.1}$$

where m [kg] is the mass in motion (i.e., the weight distributed over the limb considered); v_1 [m/s] is the velocity of the mass (i.e., the velocity of the limb) on impact on the subsoil; s [m] is the path of deceleration (i.e., the deformation of the subsoil); and A [m^2] is the area of the foot obtained from footprint geometry. If the state of dynamic loading corresponds to the maximum load, a factor f_{dyn} [–] can be obtained that relates $\sigma_{dyn+stat}$ to σ_{stat} (Equation (3.2)):

$$f_{dyn} = \frac{\sigma_{dyn+stat}}{\sigma_{stat}} \tag{3.2}$$

Thus, in Equation (3.3) the stresses determined by FEA (i.e., $\sigma_{dyn+stat}$) can then be related to the weight of the elephant:

$$m_e = \frac{\sigma_{dyn+stat} \cdot A}{f_{dyn} \cdot g \cdot f_{wd}} \tag{3.3}$$

where m_e [kg] is the mass of the elephant; g [m/s^2] is the acceleration of gravity; and f_{wd} [–] is the factor given in Equation (3.4) considering weight distribution on the limbs, i.e., gait, by relating the mass carried by the particular limb (m_{limb} [kg]) to the total mass (m_{tot} [kg]):

$$f_{wd} = \frac{m_{limb}}{m_{tot}} \tag{3.4}$$

In summary, the factors f_{wd} [–] and f_{wd} [–] differ for varying loading situations (i.e., combination of footfalls and walking velocity), but do not depend on the total mass of the elephant. Thus, application of Equation (3.3) to weight estimation of any other animal requires considerations of the anatomical characteristics and locomotion patterns of the trackmaker.

3.3.3 3D scanner

Footprint geometry was captured with a portable laser scanner designed and constructed for this purpose. The scanner (see Figure 3.2) covers an area of 800 x 800 mm. The 3D surface scan provides very precise (±75 μm) information of the settlements in the subsoil produced by the weight of the elephant. This information is later needed for calculating the weight of the elephant using FEA.

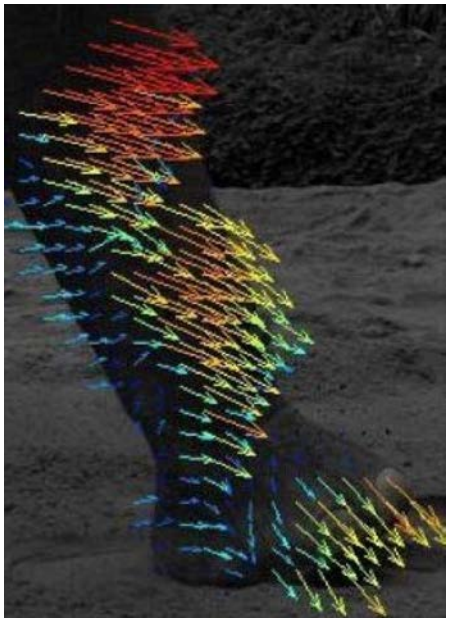

Figure 3.1: Vectors of displacement of elephant's forelimb obtained by DIC technique. The vectors illustrate the amount (length and color of arrows) and direction (orientation of arrows) of displacement.

Figure 3.2: 3D laser scanner developed and custom-built for recording animal tracks. The scanner covers an area of 800 x 800 mm.

3.3.4 Classification of the soil used and derivation of soil parameters

It is important to note that the general approach (including its accuracy) suggested in this paper does not depend on the type of subsoil. Different constitutive models are available and well validated in soil mechanics to consider, for example, cohesive soils or low permeability soils including consolidation analysis (Knabe et al., 2012). The sediment used in the neoichnological experiment was the so called Rhine sand. The grain-size distribution of Rhine sand is given in Figure 3.3. As can be seen from the grain-size distribution curve, grain-sizes range between 0.1 and 4.0 mm in diameter. The estimated coefficient of curvature $C_c = d_{30}^2/(d_{60} \cdot d_{10})$ and the coefficient of uniformity $C_u = d_{60}/d_{10}$, lead to the conclusion that the sediment is a poorly graded medium sand. Based on Hazen's formula (Hazen, 1892), a permeability coefficient of k = 0.0003 m/s was calculated. The loose density was found to be ρ_{min} = 1.51 g/cm^3, and the dense density was found to be ρ_{max} = 1.79 g/cm^3, which correspond to a loose void ratio of e_{max} = 0.75 and a dense void ratio of e_{min} = 0.48.

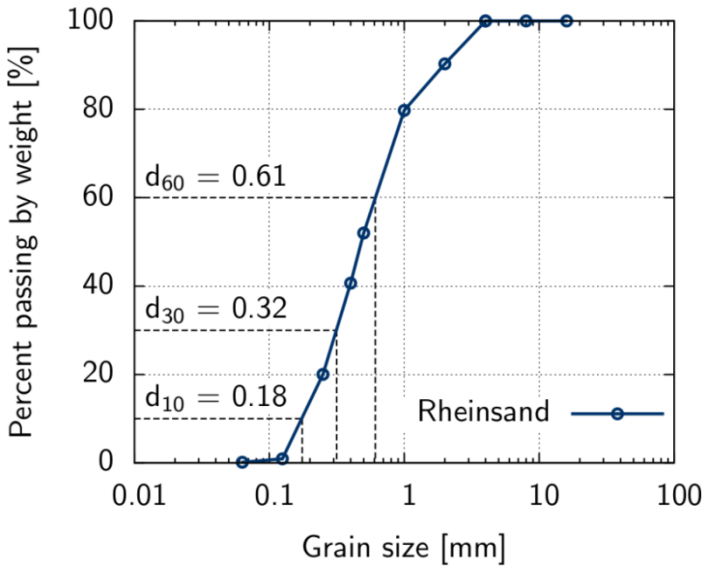

Figure 3.3: Grain-size distribution of Rhine sand. Grain sizes are given for characteristic values, i.e., for 10% (d_{10}), 30% (d_{30}), and 60% (d_{60}) of the sand passing the corresponding mesh size by weight.

Several tests are available in soil mechanics to measure the stress-strain behavior of a soil, for example, the isotropic compression test, the one-dimensional compression test, the triaxial test, and the direct shear test (Lambe et al., 1969).

In the present study, the stress-strain behavior of the soil was investigated using a one-dimensional compression and rebound test. This type of test is performed in conventional oedometer cells. Results derived from the one-dimensional compression and rebound test conducted on Rhine sand are shown in Figure 3.4 and Figure 3.5. This test includes the application of stress to a soil sample along the vertical axis, while the strain in the horizontal direction is restricted. To determine stress-strain behavior, the one-dimensional com-

pression and rebound test is often used because it is simple to perform. We also used this test because the strain condition in the soil sample is approximately similar to the situation in the center of the load generated by the elephant's foot on the subsoil. Important parameters derived from one-dimensional compression test are the stiffness moduli E_{oed} [kN/m^2] and E_{ur} [kN/m^2] that describe the stress dependent stiffness in a soil (Schanz and Vermeer, 1998). The stress dependent stiffness moduli E_{oed} and E_{ur} can be calculated based on Equation (3.5), where E_{oed}^{ref} is the reference stiffness modulus for initial loading and E_{ur}^{ref} is the reference stiffness modulus for the unloading/reloading path determined for a reference stress σ_{ref} = 100 kN/m^2 and m is a dimensionless parameter (Ohde, 1939; Schanz, 1998):

$$E_{oed} = E_{oed}^{ref} \cdot \left(\frac{\sigma}{\sigma_{ref}}\right)^m \quad E_{ur} = E_{ur}^{ref} \cdot \left(\frac{\sigma}{\sigma_{ref}}\right)^m \tag{3.5}$$

The parameter m and the normalized stiffness modulus E_{oed}^{ref} and E_{ur}^{ref} are derived from a regression analysis that is presented in the diagram in Figure 3.5. To linearize the function of vertical net stress against strain ε (σ), the logarithm of the strain ln (ε) and the logarithm of the normalized stress $ln(\sigma/\sigma_{ref})$ is used (Equation (3.6)):

$$ln(\varepsilon) = \alpha \cdot ln\left(\frac{\sigma}{\sigma_{ref}}\right) + \beta \quad E_{oed,ur}^{ref} = \frac{1}{\alpha} \cdot \frac{\sigma_{ref}}{exp^{\beta}} \quad m = 1 - \alpha \tag{3.6}$$

where α and β are the slope and the intersection with the y-axis, respectively.

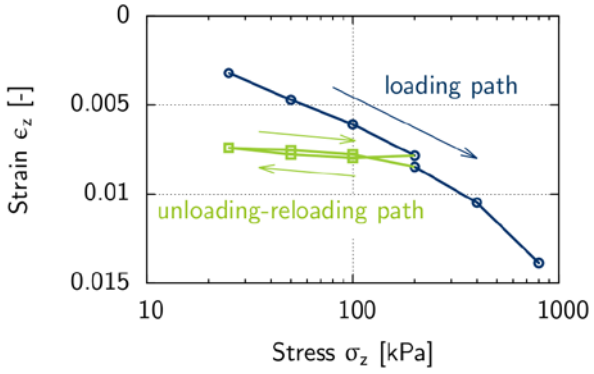

Figure 3.4: One dimensional compression and rebound test results for Rhine sand with an initial density of e = 0.6. Initial loading was conducted towards a value of 200 kPa followed by an unloading-reloading path down to 25 kPa. Initial loading was then continued towards a value of 800 kPa.

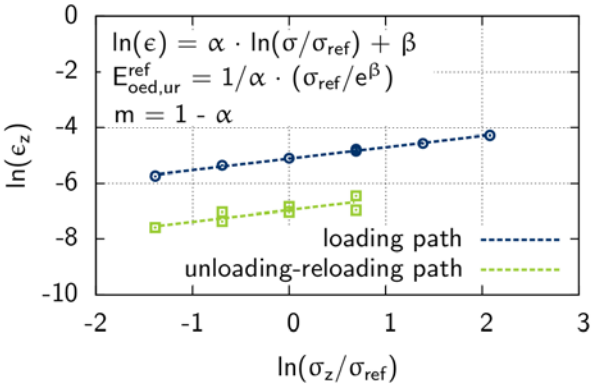

Figure 3.5: One dimensional compression and rebound regression analysis for Rhine sand with an initial density of e = 0.6. Parameters a and b of linear functions for initial loading and unloading-reloading path lead to the stiffness value E_{oed}^{ref} and E_{ur}, respectively.

A triaxial test was performed to predict shear parameters such as friction angle, cohesion and angle of dilatancy (Schanz and Vermeer, 1996). Triaxial tests are conducted in a cell, where a cylindrical sample is subjected to a confining pressure σ_3 (radial stress). Increasing axial stress σ_1 is applied to the sample by a vertical loading that causes shear failure in

the sample. Figure 3.6 and Figure 3.7 show results derived from triaxial tests conducted on Rhine sand at a cell pressure of σ_3 = 50, 100, 150 kN/m^2 (i.e., the confining pressure), where maximum shear stress is plotted against effective normal stress (Figure 3.6), and deviatoric stress is plotted against axial strain (Figure 3.7). Based on Equation (3.7), the initial loading of the soil was described by the stress-dependent secant stiffness E_{50} [kN/m^2] (Figure 3.7) that is the secant stiffness over the first 50% of the deviatoric stress:

$$E_{50} = E_{50}^{ref} \cdot \left(\frac{\sigma_3}{\sigma_{ref}} \right)^m \tag{3.7}$$

where E_{50}^{ref} is the stress-dependent secant stiffness at reference stress σ_{ref} = 100 kN/m^2. The friction angle was calculated from the maximum shear stress-effective normal stress diagram (see Figure 3.6) between the x-axis and the linear function through the points of maximum shear stress. The linear function intersects with the point of origin and leads to a cohesion value c = 0 kN/m^2.

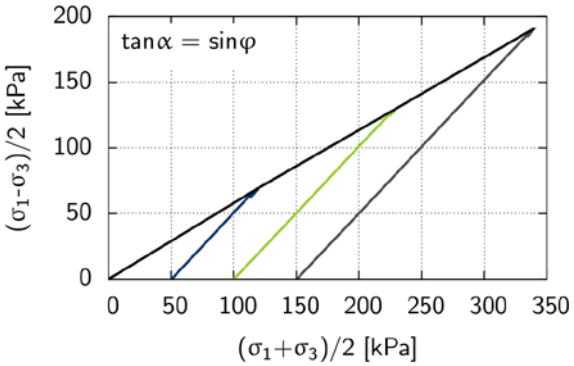

Figure 3.6: Triaxial test results for the determination of shear parameters of Rhine sand with an initial density of e = 0.6. Black line: Maximum shear stress is plotted against effective normal stress associated with cohesion c [kN/m2] and friction angle ϕ [°]. Blue, green and grey line: Stress paths for experiments conducted at 50 kN/m2, 100 kN/m2, and 150 kN/m2 confining pressure, respectively.

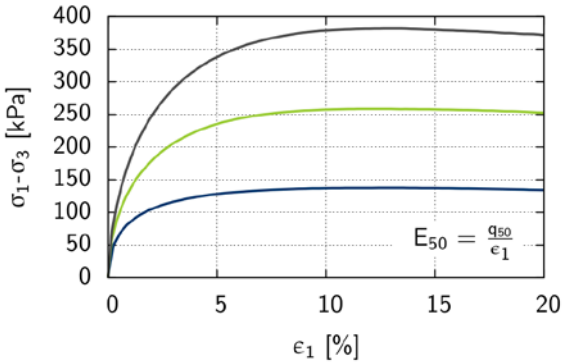

Figure 3.7: Triaxial test results for the determination of stiffness E_{50} [kN/m2] of Rhine sand with an initial density of e = 0.6. Blue, green and grey line: Deviatoric stress is plotted against axial strain for experiments conducted at 50 kN/m2, 100 kN/m2, and 150 kN/m2 confining pressure, respectively. The stiffness E_{50} is the secant stiffness over the first 50% of the deviatoric stress.

The hardening soil model parameters determined from triaxial and oedometer tests for Rhine sand with an initial density e = 0.6 (average density of Rhine sand in the field) are summarized in Table 3.1. For this type of subsoil material, i.e. sand, water content is of no significance, because additional strength and stiffness from capillary pressure is in the range of a few kN/m^2 only. Also, permeability of the sand is so high that undrained conditions during loading do not have to be considered.

Table 3.1: Hardening soil model parameters.

Parameter	Rhine sand
m [–]	0.4
E_{oed}^{ref} [MN/m^2]	42
E_{ur}^{ref} [MN/m^2]	208
ϕ [°]	35
ψ [°]	5
c [kN/m^2]	0
E_{50}^{ref} [MN/m^2]	42

3.3.5 Field experiment

The field experiment was carried out in the Zoological Gardens Wuppertal, Germany, with the tame African elephant cow Sweeny walking on a sand bed prepared in advance.

Because our goal was to back calculate the elephant's weight from a single footprint, some considerations on the gaits of elephants are in order here. Elephants differ remarkably from large hooved mammals in their locomotor repertoire by being confined to symmetrical gaits. In view of their great size (up to 5.5 tons), it is not clear whether this confinement depends on their unique size and thus is relevant for sauropods, or on some other reason. A simple theoretical consideration (detailed e.g., in Preuschoft et al., 2011) may help. The speed reached in any gait is defined by the distance covered in one step cycle ('stride length') multiplied by cycle frequency. Since limb length as well as excursion angles are limited, great step lengths can only be reached by intercalating phases of suspension without ground contact into each step cycle. In combination with step frequency, this leads to a shortening of the ground contacts. Because the sum of impulses exchanged between the animal and the ground must be equal to its constantly acting body weight, the immediate consequence of a suspension phase are increased ground reaction forces. To avoid exceeding the strength limits of the limbs, suspension phases must be kept short or eliminated completely. In Christian et al. (1999) the authors have calculated the ground reaction forces in dependence of the intervals available for ground contacts. According to these calculations, the mass of large sauropods alone compelled them to have used elastic damping mechanisms in order to avoid dangerous stressing of limbs even during a walk. This would have excluded the option of a further shortening of ground contact intervals which are typical for asymmetric gaits.

The gaits used by elephants for slow locomotion is a walk, the walk being a 4-beat rhythm with intervals between footfalls of 25% of cycle duration. To move faster, elephants change to a gait very similar to an 'amble' (a 4-beat rhythm with higher frequency than the walk) by elongating their steps (Christian et al., 1999; Hutchinson et al., 2003). This is

possible by intercalating a phase without ground contact, first with the hindlimbs and then with the forelimbs. This step elongation seems to be facilitated by marked elastic up and down-movements of the heavy head (Christian et al., 1999).

Before the experiment the weight of Sweeny was carefully measured using the special scale kept in the elephant enclosure for this purpose. As can be seen in Figure 3.8, the weight was measured under several conditions to determine the weight borne by each limb of the elephant. The following loads were measured: A. The elephant was standing with all limbs on the scale (m = 2530 kg). B. The load carried by both hindlimbs (m = 1125 kg). C. The load carried by both forelimbs (m = 1530 kg). And D. The load carried by one forelimb (m = 1390 kg). If it is known from biomechanical considerations how the weight of the moving trackmaker is distributed on its limbs and which type of gait was used during track formation (according to f_{dyn} and f_{wd} in Equation (3.3)), analysis of just one print will be sufficient for determining the trackmakers weight.

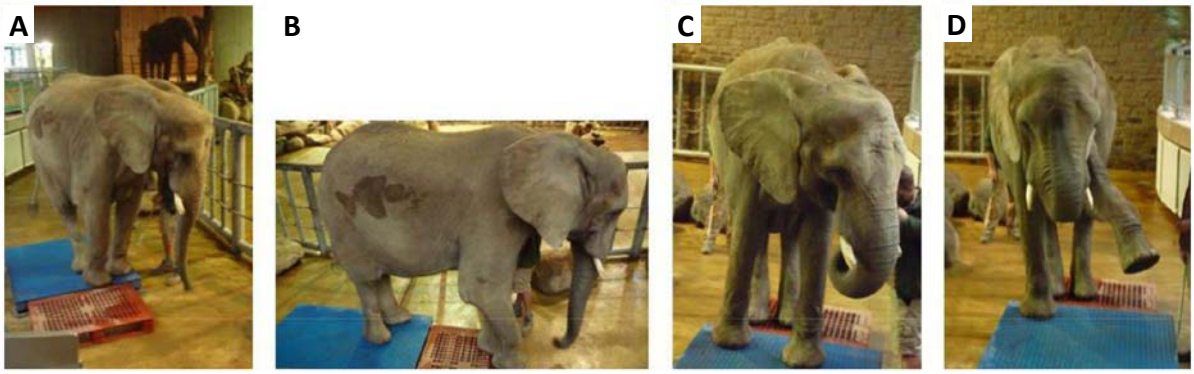

Figure 3.8: Weighing the elephant cow Sweeny. The following loads were measured: A. The elephant was standing with all limbs on the scale (m = 2530 kg). B. The load carried by both hindlimbs (m = 1125 kg). C. The load carried by both forelimbs (m = 1530 kg). D. The load carried by one forelimb (m = 1390 kg).

Prior to the experiment, a test field had been prepared for the elephant to cross. This consisted of an excavation in the elephant enclosure of 5.25 m in length, 2.20 m in width, and 0.90 m in depth, which was refilled with the experimental subsoil. The sand fill was prepared in three layers with each layer being compacted with a hand-pulled roller after dumping into the test field. Soil samples were obtained from the prepared test field by manual sampling with a metal tube and taken to the lab to determine density and water content. Dry density and water content of the samples are given in Figure 3.9. The average dry density was found to be ρ_d = 1.6 g/cm^3. Homogeneity was an important experimental condition for the volume of soil influenced by the loading. This volume can be estimated as a cube with a side length of about twice the relevant loading dimension, which was foot diameter in our case. As noted, the subsoil was put into place in three layers, and each of these layers was verified for the target void ratio.

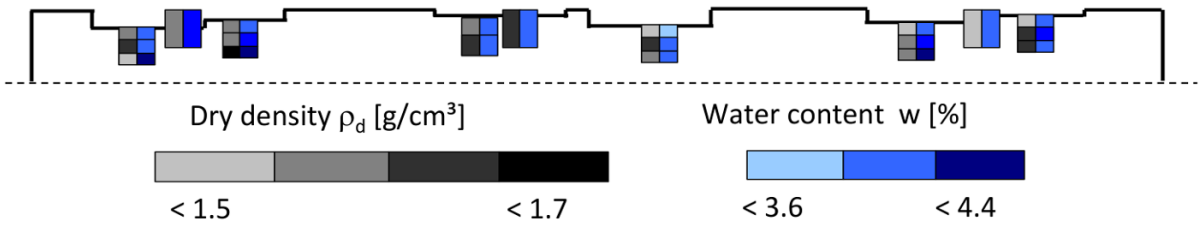

Figure 3.9: Results of dry density and water content profile measurements. Soil samples were obtained from the prepared test field by manual sampling with a metal tube. Samples were taken inside and outside several footprints, indicated by differing sampling depths, i.e., differing starting points of the top of the tube. Footprints are displayed schematically, for detailed information see Figure 3.11.

The elephant enclosure and the location of the test field is shown in Figure 3.10. Guided by one of her keepers, Sweeny walked across the test field during the experiment and left several footprints in the sand bed. A total of six footprints were scanned using the 3D laser scanner (see Figure 3.11). The area of the forefeet and hindfeet is about the same, whereas lengths ratio of forefeet to hindfeet is about 0.85, and the widths ratio is about 1.18. Visual analysis of the actual footprints and of the scanned prints indicates that the loading area is the same as the area imprinted on the subsoil. However, for practical reasons, we restricted the FEA to the footprints of the forelimbs. Based on the 3D scanner results, average footprint length is 0.32 m, average width is 0.30 m, and the average depths of the three scanned forefoot impressions is 0.020 m, 0.021 m, and 0.026 m, respectively.

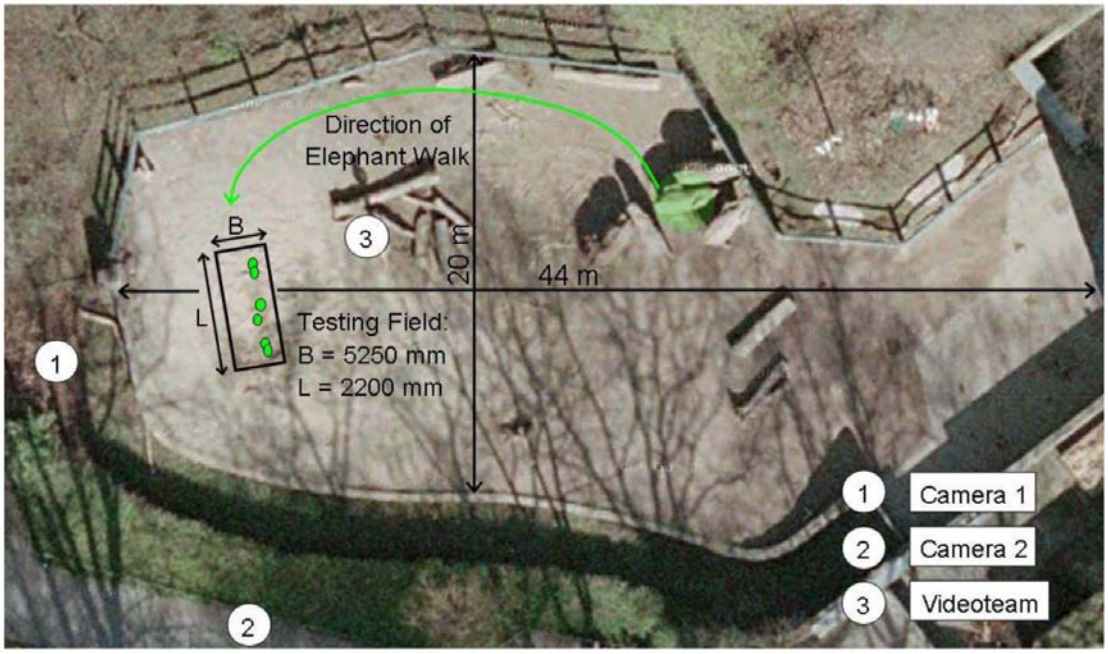

Figure 3.10: Satellite image of elephant enclosure (and elephants) at the Zoological Gardens Wuppertal including the testing field (www.google.de). Positions of the scanned footprints are marked in green within the prepared testing field.

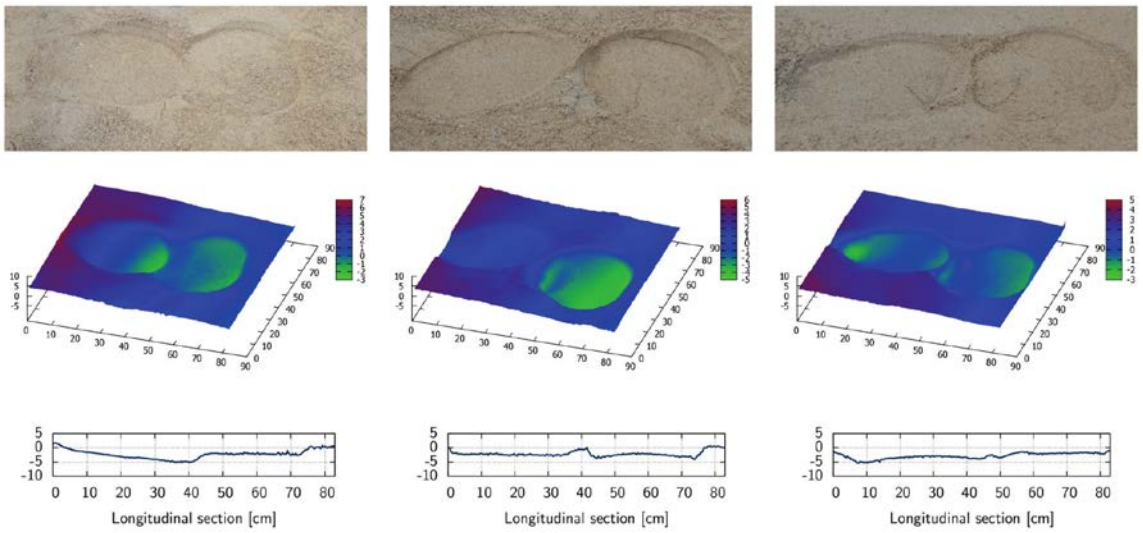

Figure 3.11: Capture of elephant footprints geometry using 3D laser scanner. A total of six footprints were scanned, i.e., three pairs, each of them consisting of one forefoot imprint (right) and one hindfoot imprint (left). Each pair is pictured by a photograph (top), 3D surface plot (center), and a 2D longitudinal section plot (bottom).

3.4. RESULTS

Our 3D FEA model consists of a soil volume 2 m in width, 2 m in length and 1 m in depth and a circular plate 0.32 m in diameter that simulates the elephant's forefoot. Since the rigid plate differs from the soft sole of the elephant's foot, the numerical results for the vertical deformation were multiplied by a factor of 1/0.75 based on the DIN 4019-1 (1979) standard to take into account the flexible loading characteristics produced by the foot. The geometry of the FE model, including the mesh generated, is given in Figure 3.12. The boundary conditions were set to the bottom of the model volume being fully fixed. The sides of the model were vertically unconstrained but fixed in all other directions. To simulate the subsoil-foot interaction, interfaces were introduced into the model around the circular plate. The outer interface were assigned the normal parameters of the subsoil, but reduced soil parameters were assigned to the inner interface to model smooth contact between the subsoil and the elephant's foot. The numerical simulation is a forward simulation, i.e., stress is applied through the plate to the soil, and then the settlements are derived. As described above, the hardening soil model was used for describing the mechanical behavior of the soil. The model input parameters were experimentally determined as described above.

Two approaches were used in the numerical simulations. The first approach included the numerical simulation of the vertical displacements of the subsoil by the elephant's weight. The calculation is based on the results of the gait analysis, the application of the DIC technique, and the elephant's weight. The numerical simulation was performed using several phases. The initial phase included the generation of initial conditions in the soil, i.e., the configuration of the initial geometry and the initial stress state (e.g., effective stresses, state

parameters). In the second phase, the circular plate was activated, without applying stress to the soil. In the following phases, the stresses induced by the weight of the elephant were applied successively. From the sequence of footfalls in the elephant walk (see Figure 3.13), four scenarios of static loading were simulated as loads applied to the circular plate simulating the elephant's forefoot.

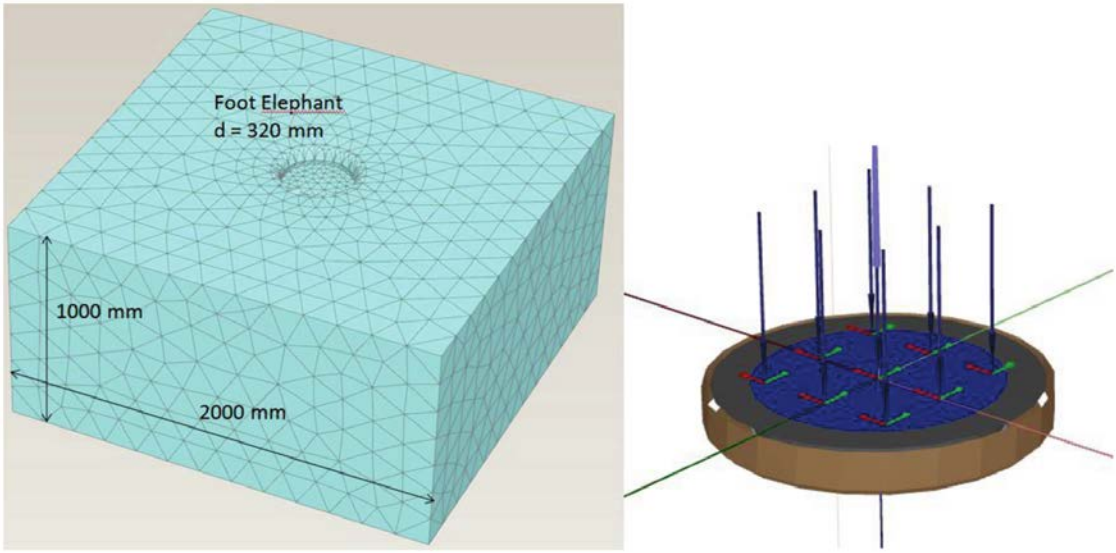

Figure 3.12: Geometry and generated mesh of the FEA model and interfaces. See text for a detailed description of the model.

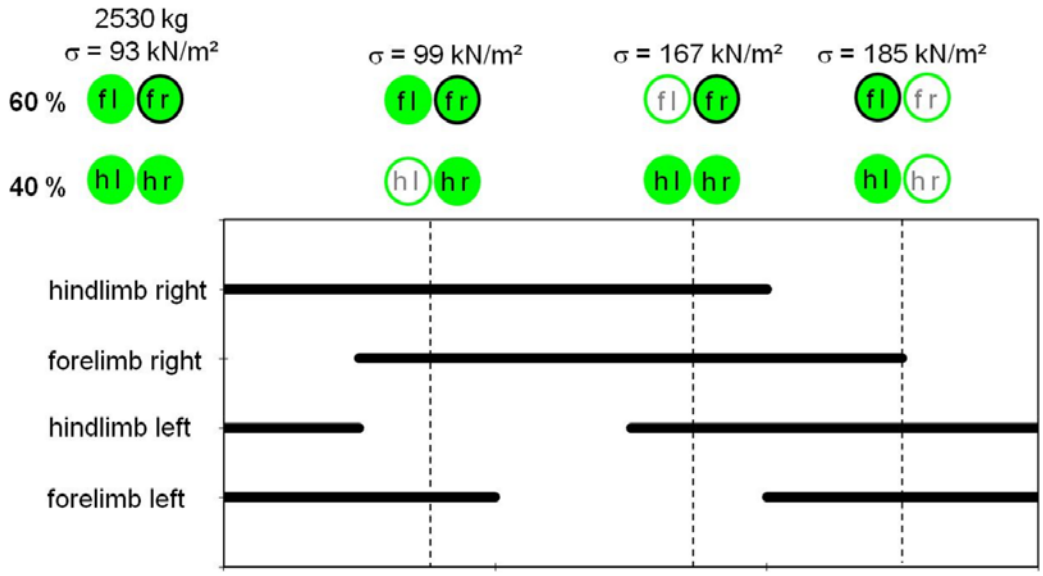

Figure 3.13: Sequence of footfalls in elephant walk after Genin et al. (2010). The static loading conditions (loading steps 1 to 4) simulated by FEA are marked and quantified within the sequence. The leftmost loading step is loading step 1, with the elephant at a standstill. Black bars indicate ground contact of the respective foot. fl = left forefoot, fr = right forefoot, hl = left hindfoot, hr = right hindfoot. See text for a detailed description of the loading steps.

Application of a stress of $\sigma = 93$ kN/m^2 (loading step 1) simulated the standing elephant (i.e., the weight is distributed to all four limbs, where 60% of the weight is carried by the

forelimbs and 40% is carried by the hindlimbs). Loading step 2 (σ = 99 kN/ m^2) simulated the load on one forelimb with both forelimbs touching the ground but one hindlimb not touching the ground. Loading step 3 (σ = 166 kN/m^2) simulated the load on one forelimb with the other not touching the ground but both hindlimbs touching the ground. Loading step 4, representing the maximum static stress σ_{max} = 185 kN/m^2 below the forefoot, simulated only one forelimb and one hindlimb touching the ground, as when the animal was progressing in a walk. In a final step (loading step 5), we added the dynamic component of the foot to the model by introducing the relevant stress $\sigma_{stat} + \sigma_{dyn}$ for the simulation of the settlements, i.e., the sum of the static stress of loading step 2 and the dynamic stress (Equation (3.8)):

$$\sigma_{stat} + \sigma_{dyn} = \sigma_{stat+dyn} \rightarrow 99\ kN/m^2 + 245\ kN/m^2 = 344\ kN\ /\ m^2 \tag{3.8}$$

The factors f_{dyn} and f_{wd}, which determine the stresses applied during the loading steps according to Equation (3.3) are summarized in Table 3.2.

Table 3.2: Factors f_{wd} and f_{dyn} determining total mass distribution on the limbs during the elephant's walk.

	Forelimb	**Hindlimb**
f_{wd}		
4 limbs	0.3	0.2
3 limbs (2 fore-, 1 hind-)	0.32	0.36
3 limbs (1 fore-, 2 hind-)	0.54	0.23
2 limbs (1 fore-, 1 hind-)	0.6	0.4
f_{dyn}	3.5	1.6

The results of the numerical simulation are shown in Figure 3.14 and Figure 3.15, in which the vertical deformations are presented. For loading step 1, a deformation u = 0.003 m was calculated, loading step 2 resulted in a deformation of u = 0.004 m, loading step 3 in a deformation of u = 0.007 m, and loading step 4 in a deformation of u = 0.008 m. As expected the largest deformation was found for loading step 5 with u = 0.018 m.

In order to determine the weight of a dinosaur based on back analysis of vertical settlements, a second approach was developed. In this approach, numerical simulations were carried out for Rhine sand subsoil with relative densities of I_D = 0.22; 0.41; 0.59; 0.81; 1.00 and applied stresses of σ = 50; 100; 150; 200; 250; 300; 350; 400 kN/m^2, respectively. The relative density is calculated in Equation (3.9):

$$I_D = \left(\frac{e_{max} - e}{e_{max} - e_{min}}\right) \tag{3.9}$$

where e_{max} and e_{min} are the maximum and minimum void ratio of the soil and e is the void ratio of the soil. For each simulation, hardening soil model parameters were calculated from experimental results carried out on Rhine sand samples with the appropriate void ratio.

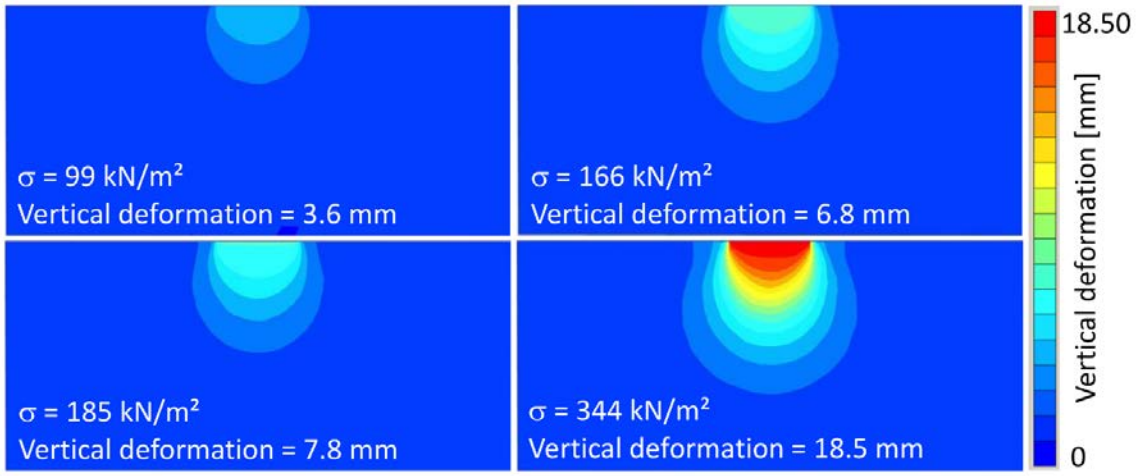

Figure 3.14: Vertical sections of FEA model at loading steps 2 to 5. Colors indicate amount of deformation.

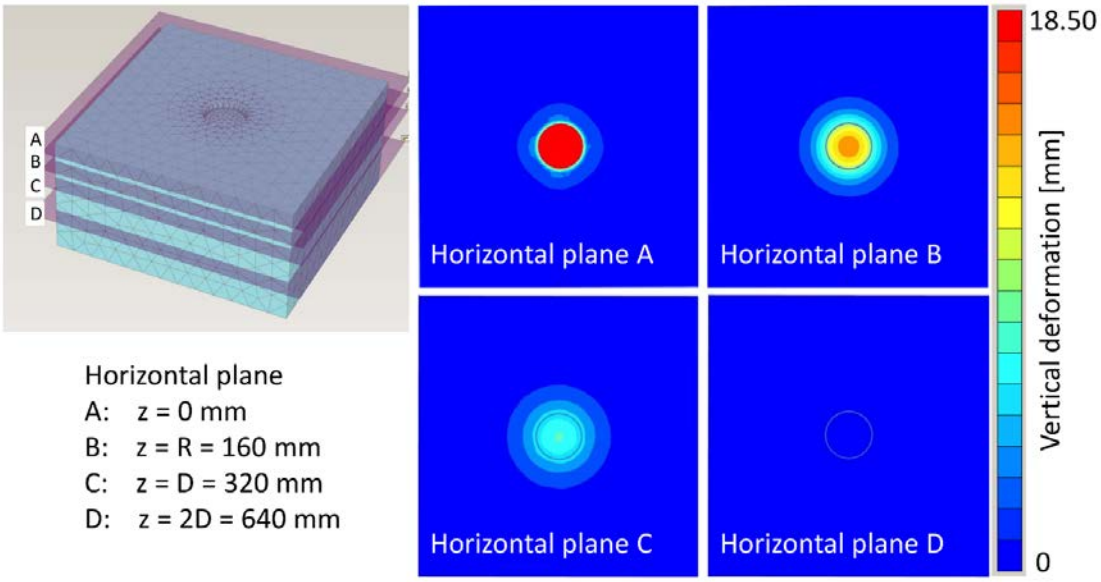

Figure 3.15: Four horizontal sections of FEA model of loading step 5. Horizontal plane A is at surface, horizontal plane B is at the depth of the radius R of the circular plate that was loaded to simulate the elephant's foot, horizontal plane C is at the depth of the diameter D of the circular plate, and horizontal plane D is at twice the depth of the diameter D of the circular plate. Colors indicate amount of deformation.

In Figure 3.16 and Figure 3.17, the results of the second approach are presented that allows determination of the stress applied to a specific subsoil and thus the total mass of an animal (see Equation (3.3)). To use the diagram, only two values have to be known: the relative density of the subsoil I_D [–] and footprint geometry (i.e., vertical displacement and diameter). In the case of the elephant's footprints, the relative density of the subsoil was found to

be between 0.30 and 0.47, and measured vertical displacements were between 0.020 m and 0.026 m. Using these results as input values in the diagram in Figure 3.16, applied stress with an average value of about 360 kN/m^2 can be obtained. Using Equation (3.3), an average mass of about 2635 kg can be back-calculated from the geometry of the elephant footprints and the relative density of the soil.

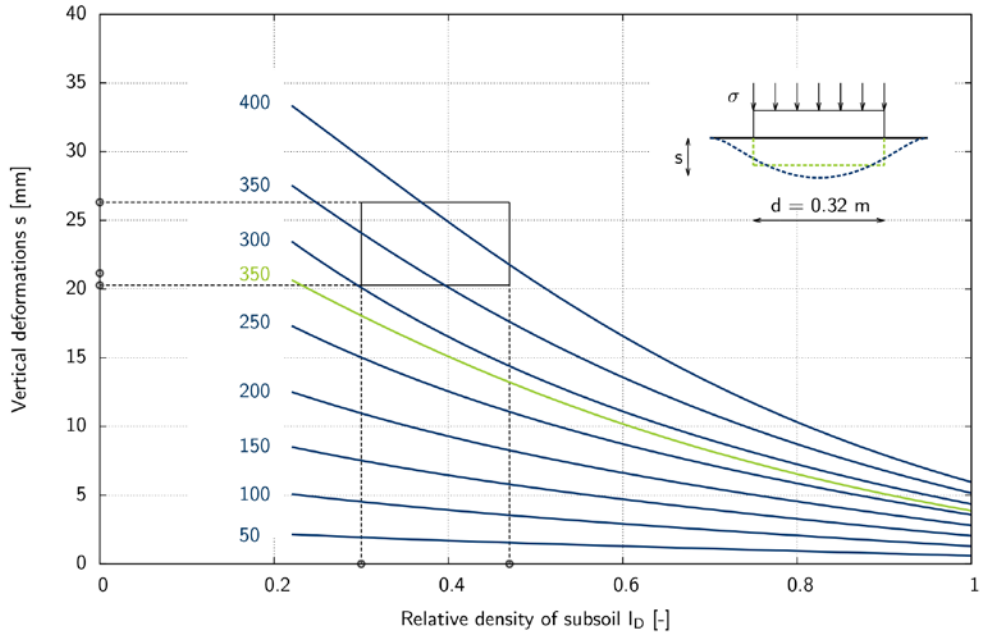

Figure 3.16: 2D-plot of relative density versus settlements for back analysis of applied stress σ [kN/m2] by FEA for a circular plate (d = 0.32 m). The diagram applies to subsoil conditions of Rhine sand. According to the deformation characteristics illustrated at the top right corner of the diagram, blue curves apply to the flexible loading characteristics of the elephant's foot, and the green curve (σ = 350 kN/m2 ≈ loading step 5) applies to rigid loading characteristics used in the FEA model. The relationship is detailed in the text. The range of stresses that can be back- calculated from in situ conditions of relative density of subsoil I_D (0.3 and 0.47) and measured values of σ (20.28 mm, 21.16 mm, and 26.32 mm) is marked by a box.

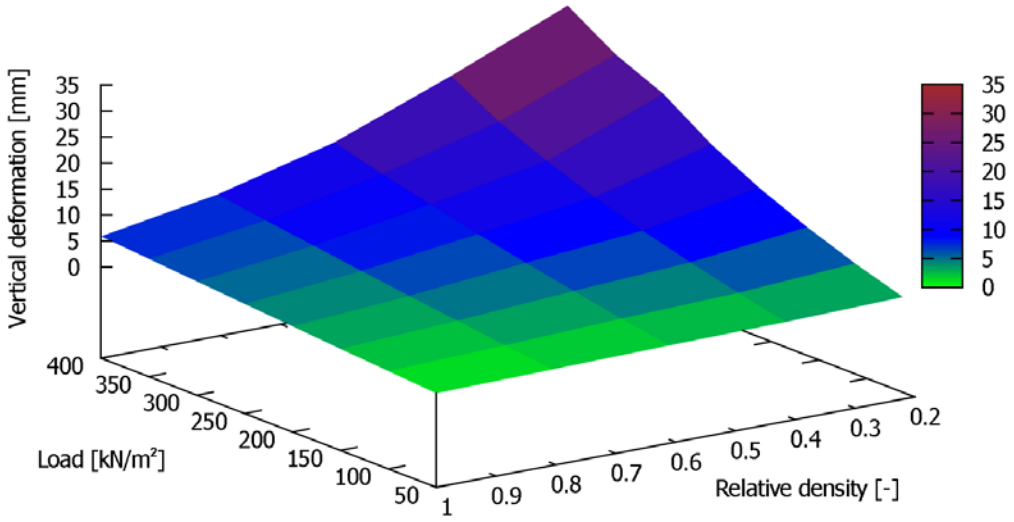

Figure 3.17: 3D-plot of relative density versus settlements for back analysis of applied stress σ [kN/m2] by FEA for a circular plate (d = 0.32 m). The diagram applies to subsoil conditions of Rhine sand. This diagram can be used to estimate the load having produced a fossil footprint if the original subsoil parameters were the same as our experimental subsoil, Rhine sand.

3.5. DISCUSSION

The present study illustrates the successful application of soil mechanical concepts to the quantitative interpretation of the soil deformation represented by footprints. Two aspects have to be taken into account accurately: (1) the simulation of the behavior of the subsoil using corresponding soil parameters and (2) the relationship between applied stress and total mass of the animal. The constitutive soil model used in this study for FEA describes soil behavior in a most realistic manner since it takes into account stress and loading direction dependent soil stiffness. The geometry, initial conditions and boundary conditions of the model, as well asthe input parameters characterizing soil behavior, influence the results of subsoil deformation and have to be accurately identified. The present research study indicates that the dynamic component of the trackmaker has a significant influence on subsoil deformation. A factor of approximately 3.5 relating $\sigma_{stat} + \sigma_{dyn}$ to σ_{stat} was identified using the DIC technique to quantify the velocity of the elephant's foot when coming into contact with the subsoil. The outcome of our numerical simulation is that the average vertical displacement u_{Exp} = 0.022 m measured in the field experiment is in good agreement with the numerically calculated vertical displacement u_{FEA} = 0.018 m as a result of the maximum applied stress $\sigma_{stat} + \sigma_{dyn}$.

3.6. CONCLUSIONS

We conclude that a reliable method for weight reconstruction from footprints has been developed, implemented and validated. Our inverse approach, as shown in Figure 3.16 and 17, allows the stress applied to a specific subsoil to be determined. In addition, the total weight of an animal (see Equation (3.3)) can be determined with an error of about 15%.

Our work represents a first step in the direction of back calculating the weight of extinct animals such as sauropod dinosaurs from their footprint. However, several additional footprint and subsoil characteristics have to be considered before reliable results can be obtained for fossils. These include geological processes that alter the original subsoil deformation such as the (1) influence of overburden pressure on subsoil deformations after the footprint was created, (2) identification of the type of fossil footprint (i.e., undertrack, overtrack, true track), (3) surface weathering, and (4) the soil profile, including constitutive parameters and layering of the subsoil. Accordingly, in ongoing research using micro-CT analysis, realistic stiffness parameters of fossil subsoils are estimated from the granulometric properties of the rock in which the footprint is preserved. It thus is clear that detailed sedimentological study must precede the soil mechanical approach in the study of sauropod footprints.

3.7. ACKNOWLEDG9MENTS

The authors thank the Zoological Gardens Wuppertal (Wuppertal, Germany) for permitting and supporting the field experiment with the elephant cow Sweeny. We thank Dr. Ulrich Schürer, Dr. Arne Lawrence and the staff of the elephant house for their kind assistance on the research project. Finally, we thank R. Hodge for correcting the English and the academic editor Peter Dodson, the reviewer Peter Falkingham and the anonymous reviewer for their helpful reviews and comments.

3.8. AUTHOR CONTRIBUTIONS

Conceived and designed the experiments: TS YL UW PMS. Performed the experiments: TS YL HV UW SL. Analyzed the data: TS YL HV HP. Contributed reagents/materials/analysis tools: TB. Wrote the paper: TS YL HV SL HP PMS.

3.9. REFERENCES

Alexander, R. M. 1976. Estimates of speeds of dinosaurs. Nature 261:129–130.

Alexander, R. M. 2006. Dinosaur biomechanics. Proceedings of the Royal Society B: Biological Sciences 273(1596):1849–1855.

Barnes, F. A., and M. G. Lockley. **1994**. Trackway evidence for social sauropods from the Morrison Formation, eastern Utah (USA). Gaia: Revista de Geociências 10:37–41.

Bates, K. T., R. Savage, T. C. Pataky, S. A. Morse, E. Webster, P. L. Falkingham, L. Ren, Z. Qian, D. Collins, M. R. Bennett, J. McClymont, and R. H. Crompton. **2013**. Does footprint depth correlate with foot motion and pressure? Journal of the Royal Society Interface 10(83):1–12.

Campione, N. E., and D. C. Evans. **2012**. A universal scaling relationship between body mass and proximal limb bone dimensions in quadrupedal terrestrial tetrapods. BMC Biology 10(60):1–21.

Christian, A., R. H. G. Müller, G. Christian, and H. Preuschoft. **1999**. Limb swinging in elephants and giraffes and implications for the reconstruction of limb movements and speed estimates in large dinosaurs. Mitteilungen aus dem Museum für Naturkunde in Berlin, Geowissenschaftliche Reihe 2:81–90.

Colbert, E. H. 1962. The weights of dinosaurs. American Museum Novitates 2076:1–16.

Diedrich, C. 2011. Upper Jurassic tidal flat megatracksites of Germany - coastal dinosaur migration highways between European islands, and a review of the dinosaur footprints. Palaeobiodiversity and Palaeoenvironments 91:129–155.

DIN 4019-1. **1979**. Setzungsberechnungen bei lotrechter, mittiger Belastung. Deutsches Institut für Normung e.V.

Falkingham, P. L., K. T. Bates, L. Margetts, and P. L. Manning. **2011a**. Simulating sauropod manus-only trackway formation using finite-element analysis. Biology Letters 7:142–145.

Falkingham, P. L., K. T. Bates, L. Margetts, and P. L. Manning. **2011b**. The 'Goldilocks' effect: preservation bias in vertebrate track assemblages. Journal of the Royal Society Interface 8(61):1142–1154.

Falkingham, P. L., L. Margetts, and P. L. Manning. **2010**. Fossil vertebrate tracks as paleopenetrometers: confounding effects of foot morphology. Palaios 25(6):356–360.

Falkingham, P. L., L. Margetts, I. M. Smith, and P. L. Manning. **2009**. Reinterpretation of palmate and semi-palmate (webbed) fossil tracks; insights from finite element modelling. Palaeogeography, Palaeoclimatology, Palaeoecology 271(1-2):69–76.

Farlow, J. O., J. G. Pittman, and J. M. Hawthorne. **1989**. *Brontopodus birdi,* Lower Cretaceous Sauropod Footprints from the U.S. Gulf Coastal Plain; pp. 371–394 in D. D. Gillette and M. G. Lockley (eds.), Dinosaur Tracks and Traces. Cambridge University Press, Cambridge, 476 pp.

Fischer, R. 1998. Die Saurierfährten im Naturdenkmal Münchehagen. Mitteilungen aus dem Institut für Geologie und Paläontologie der Universität Hannover 37:3–59.

Foster, J. R., and M. G. Lockley. **2006**. The vertebrate ichnological record of the Morrison Formation (Upper Jurassic, North America). New Mexico Museum of Natural History and Science Bulletin 36:203–216.

Gatesy, S. 2003. Direct and indirect track features: what sediment did a dinosaur touch? Ichnos 10(2-4):91–98.

Genin, J. J., P. A. Willems, G. A. Cavagna, R. Lair, and N. C. Heglund. **2010**. Biomechanics of locomotion in Asian elephants. Journal of Experimental Biology 213(5):694–706.

Gunga, H.-C., T. Suthau, A. Bellmann, A. Friedrich, T. Schwanebeck, S. Stoinski, T. Trippel, K. Kirsch, and O. Hellwich. **2007**. Body mass estimations for *Plateosaurus engelhardti* using laser scanning and 3D reconstruction methods. Naturwissenschaften 94:623–630.

Gunga, H.-C., T. Suthau, A. Bellmann, S. Stoinski, A. Friedrich, T. Trippel, K. Kirsch, and O. Hellwich. **2008**. A new body mass estimation of *Brachiosaurus brancai* Janensch, 1914 mounted and exhibited at the Museum of Natural History (Berlin, Germany). Fossil Record 11(1):33–38.

Hazen, A. 1892. Some physical properties of sands and gravels, with special reference to their use in filtration. 24th Annual Rep, Massachusetts State Board od Health:539–556.

Henderson, D. M. 1999. Estimating the masses and centers of mass of extinct animals by 3-D mathematical slicing. Paleobiology 25(1):88–106.

Henderson, D. M. 2003. Footprints, trackways, and hip heights of bipedal dinosaurs – testing hip height predictions with computer models. Ichnos 10:99–114.

Henderson, D. M. 2006. Burly gaits: centers of mass, stability, and the trackways of sauropod dinosaurs. Journal of Vertebrate Paleontology 26(4):907–921.

Hutchinson, J. R., D. Famini, R. Lair, and R. Kram. **2003**. Biomechanics: are fast-moving elephants really running? Nature 422(6931):493–494.

Ishigaki, S., and Y. Matsumoto. **2009**. "Off-tracking"-like phenomenon observed in the turning sauropod trackway from the Upper Jurassic of Morocco. Memoir of the Fukui Prefectural Dinosaur Museum 8:1–10.

Jackson, S. J., M. A. Whyte, and M. Romano. **2010**. Range of experimental dinosaur (*Hypsilophodon foxii*) footprints due to variation in sand consistency: how wet was the track? Ichnos 17(3):197–214.

Kaever, M., and A. F. de Lapparent. **1974**. Les traces de pas de Dinosaures du Jurassique de Barkhausen (Basse Saxe, Allemagne). Bulletin de la Société Géologique de France 16:516–525.

Klein, N., K. Remes, C. T. Gee, and P. M. Sander (eds.). **2011**. Biology of the Sauropod Dinosaurs - Understanding the Life of Giants. Life of the Past. Indiana University Press, Bloomington, 331 pp.

Knabe, T., M. Datcheva, T. Lahmer, F. Cotecchia, and T. Schanz. **2013**. Identification of constitutive parameters of soil using an optimization strategy and statistical analysis. Computers and Geotechnics 49:143–157.

Knabe, T., H. F. Schweiger, and T. Schanz. **2012**. Calibration of constitutive parameters by inverse analysis for a geotechnical boundary problem. Canadian Geotechnical Journal 49(2):170–183.

Lambe, T. W., Whitman, and R. V. 1969. Soil Mechanics. John Wiley & Sons Inc., 576 pp.

Lockley, M. G., K. J. Houk, and N. K. Prince. **1986**. North America's largest dinosaur trackway site: implications for Morrison Formation paleoecology. Geological Society of America Bulletin 97(10):1163–1176.

Lockley, M. G., J. L. Wright, A. P. Hunt, and S. G. Lucas. **2001**. The Late Triassic sauropod track record comes into focus: old legacies and new paradigms. Guidebook New Mexico Geological Society 52:181-190.

Lockley, M. G., J. L. Wright, and D. Thies. **2004**. Some observations on the dinosaur tracks at Münchehagen (Lower Cretaceous), Germany. Ichnos 11(3-4):261–274.

Manning, P. L. 2004. A new approach to the analysis and interpretation of tracks: examples from the dinosauria. Geological Society of London Special Publications 228:94–123.

Mannion, P. D., and P. Upchurch. **2010**. A quantitative analysis of environmental associations in sauropod dinosaurs. Paleobiology 36(2):253–282.

Milàn, J. 2006. Variations in the morphology of emu (*Dromaius novaehollandiae*) tracks reflecting differences in walking pattern and substrate consistency: ichnotaxonomic implications. Palaeontology 49(2):405–420.

Ohde, J. 1939. Zur Theorie der Druckverteilung im Baugrund. Bauingenieur 20:93–99.

Platt, B. F., S. T. Hasiotis, and D. R. Hirmas. **2012**. Empirical determination of physical controls on megafaunal footprints formation through neoichnological experiments with elephants. Palaios 27:725–737.

Preuschoft, H., B. Hohn, S. Stoinski, and U. Witzel. **2011**. Why so huge? Biomechanical Reasons for the Acquisition of Large Size in Sauropod and Theropod Dinosaurs; pp. 197–218 in N. Klein, K. Remes, C. T. Gee, and P. M. Sander (eds.), Biology of the Sauropod Dinosaurs - Understanding the Life of Giants. Life of the Past. Indiana University Press, Bloomington, 331 pp.

Prince, N. K., and M. G. Lockley. **1989**. The Sedimentology of the Purgatoire tracksite Region, Morrison Formation of Southeastern Colorado; pp. 155–163 in D. D. Gillette and M. G. Lockley (eds.), Dinosaur Tracks and Traces. Cambridge University Press, Cambridge, 476 pp.

Röchter, L. 2011. Systeme paralleler Scherbänder unter Extension im ebenen Verformungszustand. Ph.D. thesis, Ruhr-Universität Bochum.

Sander, P. M., A. Christian, M. Clauss, R. Fechner, C. T. Gee, E.-M. Griebeler, H.-C. Gunga, J. Hummel, H. Mallison, S. F. Perry, H. Preuschoft, O. W. M. Rauhut, K. Remes, T. Tütken, O. Wings, and U. Witzel. **2011**. Biology of the sauropod dinosaurs: the evolution of gigantism. Biological Reviews 86:117–155.

Sander, P. M., and M. Clauss. **2008**. Sauropod gigantism. Science 322(5899):200–201.

Schanz, T. 1998. Zur Modellierung des mechanischen Verhaltens von Reibungsmaterialien. Institut für Geotechnik, Universität Stuttgart: Mitteilung 45:1–155.

Schanz, T., and P. A. Vermeer. **1996**. Angles of friction and dilatancy of sand. Géotechnique 46(1):145–151.

Schanz, T., and P. A. Vermeer. **1998**. On the Stiffness of Sands; pp. 383–387 in R. J. Jardine, M. C. R. Davies, D. W. Hight, A. K. C. Smith, and S. E. Stallebrass (eds.), Prefailure Deformation Behaviour of Geomaterials. Thomas Telford, London.

Schanz, T., P. A. Vermeer, and P. G. Bonnier. **1999**. The Hardening Soil Model: Formulation and Verification; pp. 1–16 in R. B. J. Brinkgreve (ed.), Beyond 2000 in Computational Geotechnics - 10 Years of PLAXIS International. CRC Press, Rotterdam, 328 pp.

Thulborn, T. 1990. Dinosaur Tracks. Chapman and Hall, New York, 410 pp.

Wright, J. L. 2005. Steps in Understanding Sauropod Biology; pp. 252–280 in K. Curry Rogers and J. A. Wilson (eds.), The Sauropods - Evolution and Paleobiology. University of California Press, Berkeley, 349 pp.

CHAPTER 4

Do tracks yield reliable information on gaits? – Part 1: The case of horses

Kienapfel, K., **S. Läbe**, and H. Preuschoft. 2014. *Fossil Record*, 17:59–67.

4.1. ABSTRACT

During their lifetime animals leave many tracks and traces behind, which can provide insights into the animals' behaviour. Single footprints of extant vertebrates are frequently found in sediments all over the world, often arranged into trackways. The study of footprints and trackways lead to interpretations about the mode of locomotion of the trackmaker. Here we show an approach to identify gaits from tracks.

A series of experiments with horses was performed to determine whether gaits could be identified on the basis of fossil trackways, for example, those left behind by sauropod dinosaurs of the Mesozoic era or Tertiary mammals, to unveil their locomotor abilities. The generally valid rules for quadrupedal locomotion were taken into consideration. Symmetrical gaits result in very similar trackways; a further differentiation can be made by application of statistics on step lengths, excursion angles and overstepping.

A clear difference exists between the trot and the pace. These rapid, symmetric gaits imply high ground reaction forces (GRF) because of their long phases of aerial suspension at higher speeds. The resulting GRF seem to be too high to be sustained by the limb bones of huge graviportal animals like sauropods. Unfortunately, most of these factors are rarely available in the case of fossil tracks. Likewise, the asymmetrical, springing gaits can be excluded for sauropods because of the enormous GRF. Provided that limb length as well as trunk length can be approximated, and left and right, as well as forefoot and hindfoot imprints can be discriminated, the symmetrical gaits (walk, amble, pace, trot) used when making a trackway can be discerned.

4.2. INTRODUCTION

Footprints of extinct animals are quite common in earth history and can be found in sedimentary rocks all over the world, often arranged into trackways of many metres in length. Apart from mostly descriptive approaches, the study of fossil footprints and trackways

today raises two major questions: which animal was the trackmaker and what can we learn about the mode of its locomotion?

One aim of research on footprints and trackways is to apply and to verify a soil mechanical concept to predict the weight of the trackmaker and the direction and shifting of ground reaction forces (GRF), using footprint geometry and the soil mechanical properties of the subsoil by application of finite element analysis (Schanz et al., 2013). Another aim is to apply our knowledge of the mode of locomotion of extant taxa on the footfall pattern in trackways of extinct taxa and to estimate gait as postulated by Thompson et al. (2007). The present study focuses on this second aspect, determining gaits with the aid of a thoroughly investigated living analogue.

Locomotion, in general, can be performed by cyclic or rhythmic repetition of the same sequence of movements, where the footfall sequences define the gaits (see below). Locomotion can also be acyclic, like in leaping. Large animals prefer cyclic locomotion because the available muscle force is limited and they require effective use of resources to save energy (Borelli, 1680, clearly shown and explained in Hildebrand and Goslow, 2003). In contrast, smaller masses permit and even favour acyclic locomotion (Günther, 1989; Günther et al., 1991) because they allow rapid bursts of speed, or more technically speaking, very high accelerations. Within limits, at a given speed, the rhythm of the gait remains constant. This allows the use of pendulous movements to save energy.

One of the most obvious traits of trackways discriminates between "wide-gauge tracks" and "narrow-gauge tracks", which means the distance of the imprints according to a middle line between right and left imprints (Farlow, 1992; Lockley et al., 1994; Henderson, 2006). In extant taxa, wide-gauge tracks can be found in lizards and in crocodiles, while narrow-gauge tracks, such as those of horses (with 15–20 cm), are usually less than the width of two imprints side by side (own observations; Gray, 1968). The width of the trackway is in part coupled with the posture of the limbs, which can either be sprawled that is abducted in the shoulder and hip joints by keeping the stylopodia more or less horizontal in a lateral direction (such as in many extant reptiles, newts and egg-laying mammals, e.g., Christian, 1995 and Preuschoft et al., 2007), or extended and moving more or less in a parasagittal plane (such as in quadrupedal, especially cursorial mammals).

Like track width, the gaits of extinct mammals or dinosaurs can hardly be deduced from single footprints, but may be derived from a trackway consisting of several footprints in sequence of one individual. A number of gait variants can be distinguished among living animals. The terminology used to describe gaits is mainly derived from horses which have been well investigated (Hildebrand, 1965). A basic characteristic of any cyclic locomotion is symmetry or asymmetry (Howell, 1944), the latter occurring in the "springing gaits". Among the symmetrical gaits, "striding" gaits have duty factors of more than 50% of cycle length. The cycle length, but not the foreswing period, is shortened in the pace-like walk.

The walk may follow a “lateral sequence” (like in horses), or a “diagonal sequence” (like in crocodiles, lizards and primates; see Hildebrand, 1976; Hildebrand and Goslow, 2003). The diagonal footings make the latter similar to the trot, which, however, is characterized by phases of aerial suspension – like the pace – and duty factors of less than 50% of cycle length and subsequent long steps. The amble is similar to the walk, but its frequency is greater. At higher speeds there may occur phases without ground contact of either the fore- or the hindlimbs.

In the literature, the description of gaits is primarily based on the variation of footfall sequence over time. Their variation in space, as can be seen in the footfall pattern available in trackways, is mostly ignored. One of the rare exceptions is Smith (1912 cited by Gray, 1968), who documented tracks similar to our results. Trackways document the distribution of footprints in space, and time is one of the unknown factors. One distinction between the gaits trot and pace is characterised by the pattern of footfalls in space.

Among the asymmetrical gaits, two variants can be discriminated. The relatively large cursorial mammals, as well as monkeys and apes (Arms et al., 2002; Preuschoft, 2002) prefer the canter, or gallop, with one phase of aerial suspension. A second phase of aerial floating (“extended”) occurs in smaller cursorial mammals at higher speeds. Small- sized mammals, like cats, dogs or hares most often use the half bound. While the number of suspension phases depends on size and on speed, the canter offers somewhat elongated ground contacts; GRF are, therefore, moderate and in each cycle the animal has the chance to re-accelerate or to change direction.

Nearly all large hooved mammals, carnivores, even crocodiles and limbed squamates use very similar gaits. Notable exceptions are the graviportal elephants, as their repertoire of locomotion is confined to symmetrical gaits (Christian, Müller et al., 1999; Hutchinson et al., 2003; Hutchinson et al., 2006). With regard to their superior size (in the case of male African elephant up to 5.5 tons, in contrast to other heavyweights, e.g., rhino – 2.2 tons, hippo – 1.5 tons, giraffe – 1.2 tons, or crocodile – 1 ton; cf. Fechner, 2009), it is unclear, whether this speciality depends on their size or on any other reason.

A simple theoretical consideration by Preuschoft et al. (2011) may help: the speed reached in any gait is defined by distance covered in one cycle multiplied by the frequency of the cycle. Since limb length as well as excursion angles are limited (see below), great step lengths can only be reached, if phases of suspension without ground contact are intercalated into each cycle. In combination with the given frequency, this leads to shortening of the ground contacts. The immediate consequences of phases of suspension are increased GRF, because the sum of impulses exchanged between the animal and the ground must be equal to the constantly acting body weight. Christian, Heinrich et al. (1999) calculated the GRF, which are dependent on the intervals available for ground contacts. According to their calculations, the mass of large sauropods alone compels them to use elastic damping mecha-

nisms to avoid dangerous stressing of limbs even while walking. This means that any further shortening of contact intervals must be excluded, which are, for example, typical for asymmetric gaits.

Some basic information about quadrupedal locomotion must be kept in mind: in all kinds of tetrapod locomotion (Preuschoft et al., 1994), the limbs are either swung forward (swing phase) or used for support (stance phase). The swing phase follows the law of the pendulum, and consequently sets limits to the frequency, since the time period (T) equals the product of the square root of the length (l) over the acceleration (g) and two times π :

$$T = 2\pi \sqrt{\frac{l}{g}}$$

A marked flexion during foreswing, as well as the lightweight construction of the distal parts of the limbs, are means to reduce pendulum length and to increase frequency. In the stance phase, the limbs behave like an inverted pendulum. The distance (y) covered during each step depends on the excursion angle (α) and limb length (l):

$$y = l \sin \alpha$$

In cursorial mammals the functional length of limbs is maximised by long metapodials (Preuschoft et al., 1994) and in hooved mammals by the inclusion of phalanges into the length of the limb. In the extreme case of horses, which are highly adapted to a cursorial lifestyle, only the tip of the distal phalanx transmits GRF between substrate and the animal's body and needs a local reinforcement in the form of a sturdy toe tip cover. In addition, the extended posture of the joints contributes to limb length.

During steady-state locomotion, the GRF follow a constant pattern in all quadrupeds as well as bipeds (e.g., Adachi et al., 1996; Li et al., 1996; Lee et al., 1999; Fischer and Lilje, 2011). The vertical force component follows a parabolic curve, while the horizontal force component decelerates in the first part of the stance and re-accelerates in the second. If horizontal and vertical force components are combined, the resulting GRF will change direction and size during each stance phase. The animals place their stance limbs close to this resultant GRF. Hence the carpal/tarsal, elbow/knee, and shoulder/hip joints are keeping the lever arms of the load short. Any deviation of the limbs from the GRF leads to greater torques particularly in the shoulder and hip joints and, therefore, requires more energy. This fact sets strict limits to the excursion angles of the limbs and step lengths, if limb lengths are given. It also explains why heavy animals prefer small excursion angles, and rather short steps, especially at slow speeds.

Considerable differences in movements may occur between steady-state locomotion at constant speed and phases of acceleration and deceleration. Because of the energy that is required for accelerating and decelerating, all extant large animals show a strong tendency to keep their speed at a constant level as well as changes of direction.

To infer the gait used from the observed tracks, we have analysed the trackways of horses moving in the most common gaits: walk (4-beat rhythm with intervals between footfalls of 25% of cycle duration), trot (2-beat rhythm, in which hind hooves and contralateral fore hooves make ground contact nearly at the same time), amble (or *tölt*, a 4-beat rhythm with higher frequency than the walk), pace (2-beat rhythm, like the trot, but with lateral, instead of diagonal supports), canter (German: Galopp, a 3-beat rhythm). Because of the demands of sport competitions, horse gaits (as well as body shapes) are highly standardised, and therefore a limited sample of horses can provide a reliable reference.

4.3. METHODS AND MATERIALS

A straight runway of 20 m, 25 m or 50 m (depending on the local facilities) in length and 1 m in width was prepared and marked. In the direction of movement, the starting line of the runway was used as a reference or zero line, as well as the limitation of the runway parallel to the direction of movement, in order to measure the distribution of the imprints like in a coordinate system. In total, 11 horses of different breeds and sizes (Table 4.1) were ridden along these runways.

Table 4.1: Horses (vertical) and gaits (horizontal) under investigation, including the speed of the run.

Horse	**Height [m]**	**Gait and speed [m/s]**									
		Slow walk	Fast walk	Slow trot	Rapid trot	Slow canter	Fast gallop	Slow amble	Rapid amble	Running pace	*Schweine-pass*
German warmblood	1.68	1.1	1.6	2.6	4.6		6.1				
German sad-dle horse	1.50	1.2	1.5	3.0	4.3	4.6	6.9				
German warmblood	1.64	1.45			2.5						
Icelandic horse	1.35									6.3	
Icelandic horse	1.38									8.8	
Icelandic horse	1.38									10.2	
Saddle-bred	1.65							3.2	4.4		
Paso Fino	1.65					3.3		1.3			
Icelandic horse	1.37	1.7						2.9	3.6		
Aegidien-berger	1.42							3.1	4.0		
Icelandic horse	1.35										2.5

One difficulty in the analyses of tracks of horses and other cursorial animals is the similarity of the anterior (manus) and posterior (pes) hoofprints. The runs were recorded on video to identify the imprints from the footfall pattern, as well as to document the velocity and

the gait used. Instead of measuring step and stride lengths, which are used as common indicators in track literature, the distribution of all hoofprints was measured in reference to the zero line, using the tips of the hoofprints as indicators (Figure 4.1 and Figure 4.2).

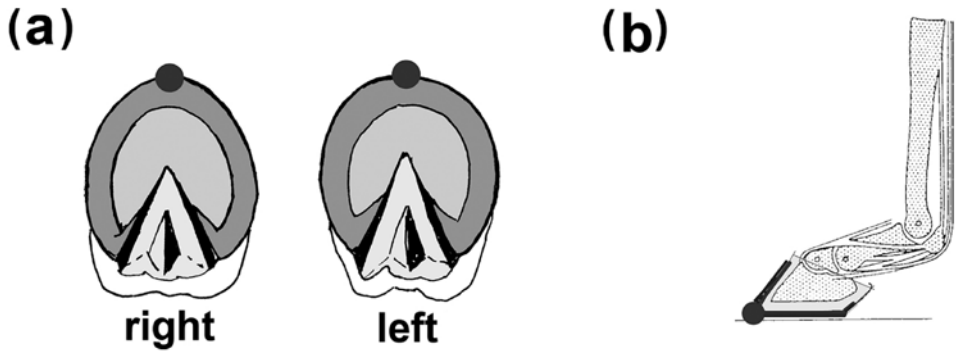

Figure 4.1: Horse hooves. (a) Hind hoof and fore hoof of a horse seen from below; (b) Longitudinal section through the mechanically relevant elements of the autopodium. The hoof is shown during the middle of the stance phase, while highest loads are acting. Dots at the tips of the hooves are indicating the points used for track measurement. The difference between the imprints of hind hoof and fore hooves is not obvious, so that both are hardly discernible in most tracks.

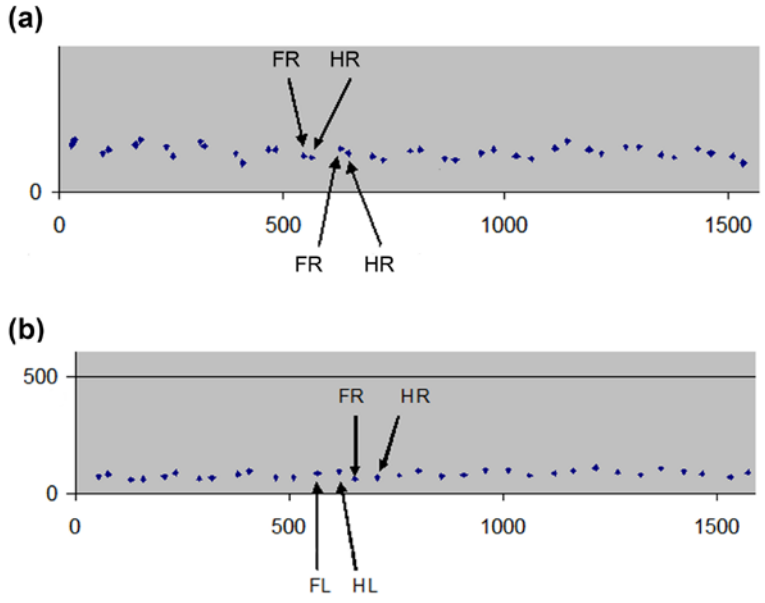

Figure 4.2: Raw data of two randomly chosen trackways; horizontal axis: distance covered in cm. (a) Slow tölt (i.e., amble); (b) Fast tölt of an Icelandic horse; FR – front right; HR – hind right; FL – front left; HL – hind left. ¢KŜ K2ℕÎ2yűl·f l·Èλă ăK2ǿă űKŜ Řλăúl·yÕŜ Ŏ2ØŜℕŜŘ λy˝ŎY℗

4.4. RESULTS

The pattern of hoofprints along the trackways includes step length and track width. This is applicable to all limb postures. Horses, like all cursorial mammals, move their limbs more or less in a parasagittal plane, and produce trackways, which are as narrow as one and a half hooves placed side by side.

In spite of their narrowness, no "crossing over" was observed; the left imprints were constantly placed further to the left than the right ones and vice versa. Rather than following a straight line, the horses sway from side to side forming a trackway with lateral deviations. The amplitudes of these fluctuations – against expectation – are independent of the speed of locomotion. As expected, the number of cycles on the runway becomes smaller with increasing speed and with the size of the horses (Table 4.2). The running pace of Icelandic ponies cannot be taken as an equivalent for trotting, because of its high speed, which is even faster than the canter of these small horses.

Table 4.2: Average number of gait cycles of horses with different wither heights in different gaits on a runway of 20 m.

	Height > 1.50 m; in cycles per 20 m	**Height < 1.40 m; in cycles per 20 m**
Walk	11	12
Amble	8.35	11.5
Trot	7.7	–
Canter	5.7	9
Running pace	–	6

In the walk (Figure 4.4), the placement of ipsilateral hoofprints shows three variants: first, the hind hooves touch the ground behind the spots where the fore hooves just have been. This is rarely practiced, especially in laming horses, or horses with very short legs in proportion to their body length. Second, hind hooves are put down at exactly the same place (capping, cf. Thompson et al., 2007). This occurs at moderate speeds. If walking becomes more rapid, hind hooves are placed clearly in front of the prints of the fore hooves (overstepping; Figure 4.2). Step length increases with walking speed and with size. As shown in Figure 4.3, the longer the legs are in proportion to the distance between shoulder and hip joints (trunk length), the more often occurs overstepping.

In the *tölt* of Icelandic horses and in similar gaits (amble) of bigger horses (Figure 4.5), step lengths are greater than in the walk, and the overstepping of hindlimbs is more apparent. At very high speeds, the hoofprints are no longer grouped in pairs of one fore and one hind, but evenly spaced along the whole trackway. Contralateral hooves may be placed closer together than the hoofprints of the same side (similar to the pace, see below).

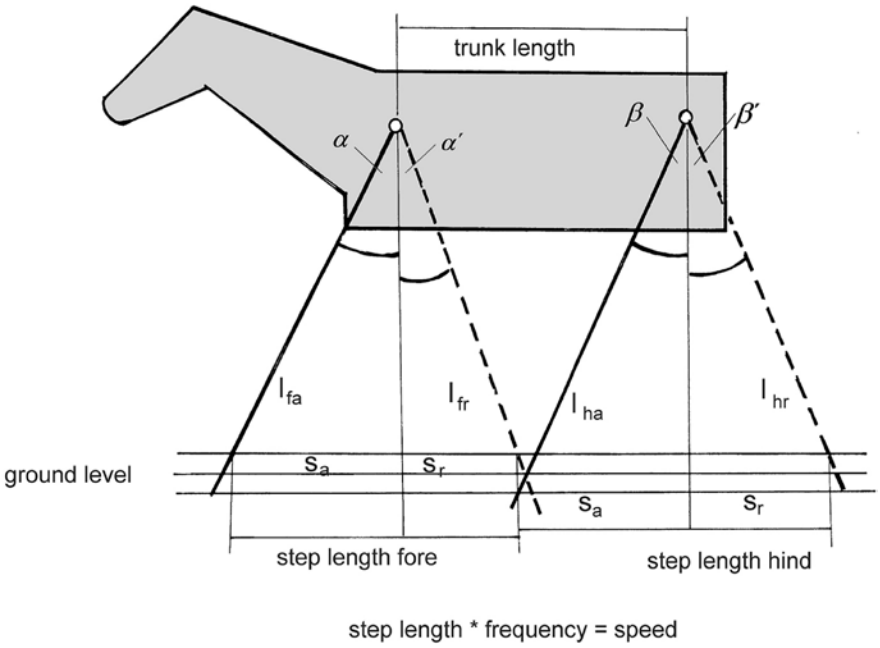

Figure 4.3: Relationship between trunk length and length of the limbs. The extremities are reduced to their "functional limb lengths". Step length (*s*) is the product of excursion angles (*α* or *β*) and limb lengths (for example $s = \sin \alpha\ l_{fa} + \alpha' \sin \alpha'\ l_{fr}$). The longer the limbs, the lower the ground level below the animal, and the greater the distance (*s*) covered during each step, without any change of trunk length. The uppermost ground level indicates a lagging of the hind hoof behind the imprint of the fore hoof; the middle level indicates capping; the lowermost indicates overstepping. Excursion angles (*α* and *β*) are determined by the resultant GRF. Among living mammals, *α* usually is greater than *α′*, while *β* is commonly smaller than *β′*; l_{fa} – left forelimb in anteversion; l_{fr} – left forelimb in retroversion; l_{ha} – left hind in anteversion; l_{hr} – left hind in retroversion.

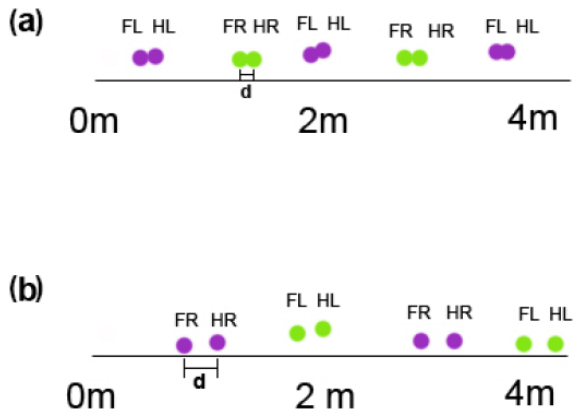

Figure 4.4: Typical tracks produced in the walk. The faster the walk (and the longer the limbs and the shorter the trunk), the greater is the distance (d) between the ipsilateral front- and hind hooves (i.e., the degree of overstepping increases); horizontal axis: distance covered in m. (a) Slow walk and (b) Fast walk of a German warmblood.

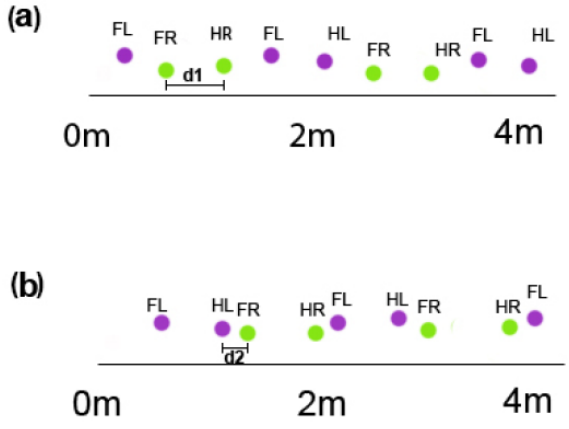

Figure 4.5: Typical track produced in the *tölt* (amble) of an Icelandic horse. In the amble the overstepping (d1) is greater than in the walk and the contralateral hoofprints are close to each other at fast speeds (d2). This is similar to the pace. (a) Slow *tölt*; (b) fast *tölt*.

In the trot (Figure 4.6), the hoofprints are grouped in pairs, formed by ipsilateral limbs. Again three variants are possible: anterior imprints set in front of posterior imprints, cap-

ping and overstepping. The first can be observed rarely, especially at very slow speeds, and was not documented in this study. Capping can be observed in low and sometimes normal speeds (Figure 4.6b). Overstepping is the result of great step lengths and becomes more marked at higher speeds (Figure 4.6a). The really large step lengths are reached by intervals of aerial floating.

The running pace of Icelandic horses looks similar to the trot, but the paired prints are from contralateral sides, so that the seeming "overstepping" is performed by contralateral rather than ipsilateral hooves (Figure 4.7).

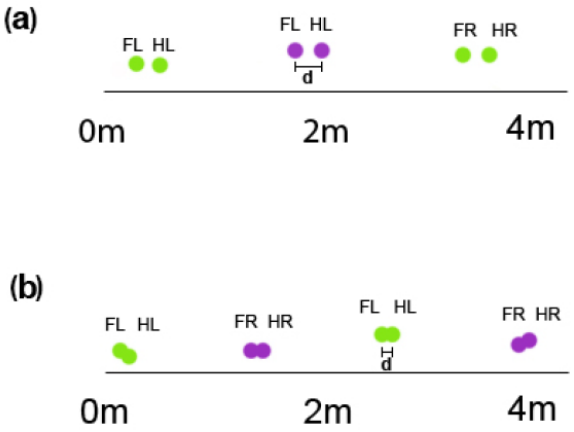

Figure 4.6: Typical tracks produced in the trot of a German warmblood. With higher speed, the overstepping (d) of the ipsilateral hind hoof is increasing. (b) Slow trot: the hind hoof is placed right on top of the fore hoof imprint (capping); (a) fast (extended) trot, which leads to marked overstepping. A third possibility is the placing of the hind hoof in front of the fore hoof at very slow speed (this is rarely done and not shown here).

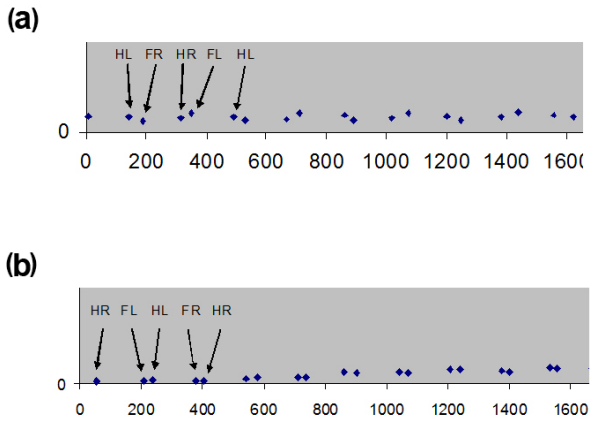

Figure 4.7: Part of the original tracks comparing fast running pace (a) and fast trot (b). In the running pace the contralateral hoofprints are grouped together with overstepping of the fore hoof over the contralateral hind hoof. In the trot the ipsilateral hoofprints are grouped with an overstepping of the front hoof over the ipsilateral hind hoof. The horizontal axis shows the distance covered in cm.

The pattern of hoofprints is completely different in the canter (German: *Galopp*; Figure 4.8), which also comprises three variants. In all of them, groups of four evenly spaced imprints are separated by slightly longer distances (Figure 4.8a). These longer distances correspond to support on the diagonal right hind hoof/left fore hoof, if the right limbs lead, and left hind hoof/right fore hoof if the left limbs lead. The track in Figure 4.8a shows the slowest canter, in which the trailing hind hoof does not reach the leading fore hoof ("understepping" in an atypical and not desired 4-beat rhythm). With growing speed, the distances between all imprints increase (Figure 4.8b), and the imprint of the right hind hoof covers the left fore hoof imprint in the left lead (in the right lead, the left hind hoof imprint would cap the right fore hoof imprint). In rare cases, this usually longer distance can be the same as the other distances between hoofprints so that the imprints are distributed evenly along the trackway. The fastest canter is characterised by an overstepping of the trailing hind hoof over the leading fore hoof. The higher the speed, the greater the distance (*d*) be-

tween the hoofprints. In many cases the hind hooves are placed slightly lateral to those of the forelimbs ("crabbing"). This obliquity is more pronounced than the distance between left and right limbs.

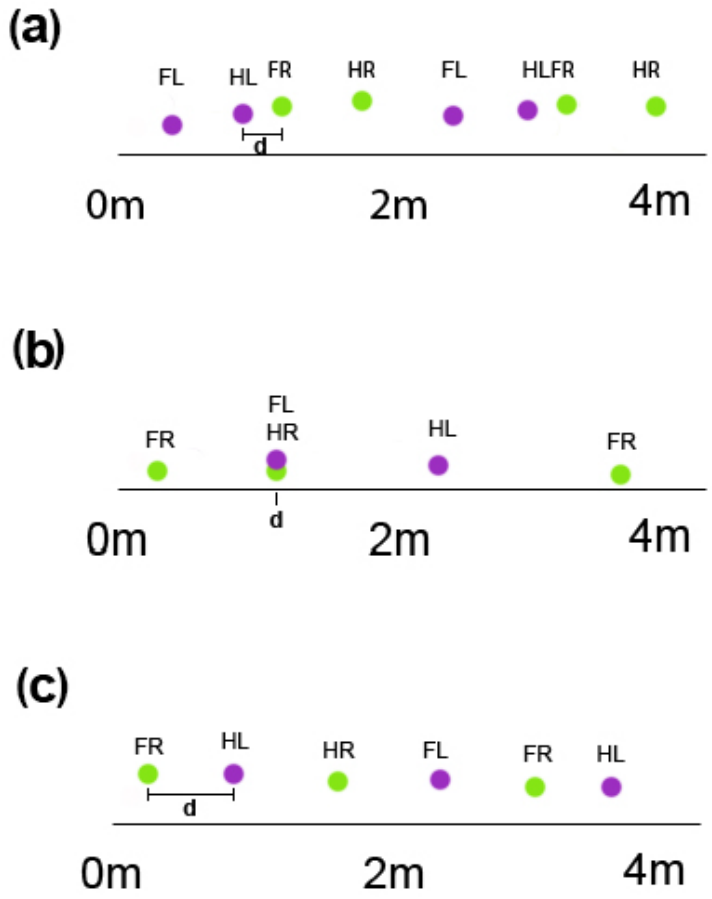

Figure 4.8: Typical footfall pattern of the canter (German: Galopp) in its three varieties. (a) Right lead of a Paso Fino at slow speed; (b) Left lead of a German warmblood horse at normal speed; (c) Right lead of a medium sized German saddle horse at fast speed. The stride length increases with increasing speed. The Paso Fino places the hind hooves between the imprints of the fore hooves, because of slow speed. The warmblood has the same limb length as the Paso Fino, but it is placing the hind hooves beneath the prints of the fore hooves, because of higher speed. The German saddle horse is medium sized and places the hind hooves in front of the fore hooves. With increasing speed in the canter, the separation between all four hoofprints becomes clearer (in the example of right lead the group HL, HR, FL, FR.).

4.5. DISCUSSION

The small number of experimental animals is acceptable in view of the highly standardised locomotor patterns in the various breeds of horses. A dominating aim of horse breeding is performance with the same kinematic characteristics and the same sequence of footfalls. This is also the basis for any success in equine sports. In the following discussion, three aspects are emphasised: first the relation between mechanics and footprints in the case of horses, second the parallels to elephants and third the general conditions for the interpretation of tracks left by quadrupeds.

4.5.1 Footprint mechanics

The number of cycles on the runway (20 m) differs with gait, speed and body size (Table 4.2). As a whole, the hoofprints are arranged evenly along the trackways, and so document a nearly continuous support of the body against gravity. Interruptions of support by phases of aerial floating entail enlarged GRF, but are not directly visible from the tracks. Distances (step lengths) between footings of the same limb depend on limb lengths and the excursion angles. Exceptionally long step lengths within a trackway can be derived from increased excursion angles. All symmetrical gaits produce very similar trackways.

The trackways are surprisingly narrow: 10–20 cm is less than the width of two hooves placed side by side. This of course has to do with the high level of motor coordination in cursorial mammals. Swaying (fluctuation) from one side to the other occurs, as well as crabbing. Both seem to be without relationship to speed or gaits – with exception of the canter, where crabbing occurs more often and more pronounced than in other gaits. We have not found any reduction of track width ("straddle") with increasing speed, as postulated by Thompson et al. (2007).

The intervals between points, where support is given to the mass, are quite long in the trot and the pace, indicating long phases of aerial floating. The canter, by contrast, shows more continuous support of body mass. This may be one reason for changing from trot to canter in horses that have the choice and the preference of the canter over trot on slippery or rough ground. On this particular point, canter or gallop show clear differences to the commonly known half bound of, for example, hares, which contains long phases of aerial suspension.

Determining the arrangement of hoofprints in the case of horses is more difficult than in many other animals, because all four hooves are very similar to each other in shape. If left and right as well as fore and hind can be discriminated, the pace can be identified in contrast to the other symmetrical gaits. Alexander (2003) published "computer generated trackways" of a horse where the pace and trot were identical. The authors of several former studies concluded that gaits cannot be derived from tracks (e.g., Dagg, 1974). Thompson et al. (2007) studied fossil camelids and identified the pairs of imprints as ipsilateral. They used the distances between the first (fore) and the second (hind) imprints (that is the degree of overstepping) as a criterion for trot or pace. Doing so, they did not make full use of the available information about gaits in extant animals. According to our results, however, these pairs in the pace consist of contralateral, not ipsilateral hoofprints, in contrast to the trot. In the trackways of the same individual, the extent of overstepping seems to depend exclusively on its speed. To estimate gaits and speeds of the fossil camelids, an admittedly rough comparison can be drawn to our systematically collected data on horse gaits (Streitlein and Preuschoft, 1987). On a 60 m runway, three typical and successful German warmblood horses showed average stride lengths of 244 cm (speed of 3.23 m/s) in the slow

("collected") trot, and 348 cm (speed 4.91 m s−1) in *Mitteltrab* (which can be translated as "extended trot"). In the first gait, fore hooves are capped by the hind hooves, in the latter, faster gait, overstepping by 3–5 cm is essential. Obviously, the stride lengths of the fossil camelids, which varied from 101 cm (in the larger forms 168 cm) to 207 cm, are much shorter than those of our horses. Since the forefoot imprints of the camelids varied from 9 cm ×14 cm and from 17 cm ×20 cm, the conclusion seems adequate that these animals have been roughly of the same size class as our horses. This would imply that the fossil camelids did neither trot nor pace, but rather used the comfortable and safe walk. This notion is confirmed by the results obtained by van der Sluijs et al. (2010), on New World camels. Llama and alpaca clearly preferred a pace-like walk while moving at speeds of 1.13 m s−1 ± 0.12 m or 0.97 m s−1 ± 0.15 m, respectively, and could by no means be induced to use a trot or true pace at all. Instead, they changed directly from walk into canter. The stride lengths of llama walking varied between 53 to 106 ± 8 cm, depending on speed that is near the lower border of the fossils.

Traits which are seen as important for horses, like overstepping, depend on the relation between trunk length and limb length. If both factors are unknown, the observation loses its value for characterizing the gait, unless independent information is available. Fechner (2009) discusses overstepping in the case of a probable trackmaker that definitely had long hind and shorter forelimbs.

4.5.2 Parallels to elephants

Elephants use the walk for slow locomotion. If not in a hurry, they extend the stance phases (Christian, Müller et al., 1999). The foreswing of each limb follows the laws of the pendulum, and thus requires a given time interval. If this time interval is shorter than the animal needs, the least energy-consuming option is elongating the stance phase between the foreswings. The least energy-consuming speed is given by a continuous sequence of swing phases of each pair of limbs. For more rapid locomotion, elephants increase frequency and step length, but both factors reach narrow limits. To move even faster, elephants change to a gait very similar to the "amble" (Christian, Müller et al., 1999; Hutchinson et al., 2003; Hutchinson et al., 2006), by elongation of the steps. This is possible by intercalating a phase without ground contact first of the hindlimbs then of the forelimbs. This step elongation seems to be facilitated by marked elastic up and down-movements of the heavy head (Christian, Müller et al., 1999). Gambaryan (1974) illustrated this gait, in his Figure 11, but called it a "fast walk" without putting emphasis on the phases without ground contact of either the hindlimbs or the forelimbs.

The foot construction of the elephants is well known through a recent publication of Weissengruber et al. (2006) and the feet of sauropods seem to be similar to those of elephants, in having soft cushions for weight transmission parallel to the metapodials. The narrow-

ness of hindfoot imprints is often observed in relation to the broader forelimb imprints. This parallels hooves of horses and the feet of camels.

4.5.3 Conditions for the interpretation of tracks

Among the variables which influence the number of footprints per given distance (step length, aerial floating, excursion angle), the size, as indicator of limb and trunk length can be estimated, whereas speed and gait are the unknown values. The area of the imprints should be proportional to body size, provided that the construction of the foot, for example, hoof, paw with or without claws, soft cushion, such as in elephants (or camels), is known. This latter factor may well be visible from the footprints or from morphological analysis of the possible trackmaker's foot skeleton. In contrast to horses, the imprints of fore- and hindlimbs of quadrupedal dinosaurs can usually be identified; they differ markedly in shape, size and depth. Concerning these traits, the interpretation of a fossil trackway is fairly reliable.

The sequence of imprints along the trackway provides some information about the gait used (symmetrical, asymmetrical). Step length in relation to estimated limb length helps to find phases without ground contact. Identification of gaits like amble (i.e., *tölt*) from trackways is only possible, if limb length (height at withers, height of hip joint) as well as trunk length are known or can be approximated. If long trackways with at least 5 footprints are available, a discrimination between the symmetrical gaits may be possible from a trackway.

The narrow width of the trackways seems at a first glance to be characteristic for mammals, especially cursorials. However, it should not be overlooked that animals with sprawling limbs can also walk on a narrow track. The chameleons are outstanding examples of this locomotion type and use it especially when walking along branches. Their rather extended joints contribute to increasing functional limb lengths. The next step of this investigation is the application of this knowledge to fossil tracks to reveal the mode of locomotion of extinct taxa (Läbe et al., 2013).

4.6. CONCLUSIONS

The arrangement of imprints along trackways provides valuable information about the gait (symmetrical versus asymmetrical) used by the trackmaker. Provided that the size of the trackmaker is known or can be approximated, in particular concerning lengths of limbs in relation to trunk length, the "symmetrical gaits" walk and amble can be discriminated from trot or pace. The bigger and heavier the trackmaker, the greater the vertical component of the ground reaction force and the narrower the excursion angle. If the limb lengths can be estimated or are known, step lengths greater than a reasonable estimate of the excursion angle indicate a phase of aerial suspension, which is typical of trot and pace, as well as fast

amble. If several characteristics of a trackway are combined with estimated body size and estimated limb lengths and excursion angles, and if at least 5 subsequent footprints of a trackway are available, an identification of the gait may be possible.

4.7. ACKNOWLEDGEMENTS

This investigation was prompted and sponsored by the DFG Research Unit "Biology of Sauropod Dinosaurs: the Evolution of Gigantism". It has the publication no. 157. We thank the whole group for stimulating discussions. Our special thanks go to Walter Feldmann, Agidienberg, for providing his facilities and horses (Icelandic horses, Aegidienberger, American Saddlebred and Paso Fino) for the investigation of variants of amble, paso llano and running pace. The authors would like to thank Jessica Mitchell (University of Bonn) for improving the English, the editors of this journal, and two anonymous reviewers for their reviews and comments.

4.8. AUTHOR CONTRIBUTIONS

Conceived and designed the experiments: HP. Performed the experiments: KK SL HP. Analyzed the data: KK SL HP. Wrote the paper: KK SL HP. KK and SL contributed equally to this paper.

4.9. REFERENCES

Adachi, K., S. Nishizawa, and B. Endo. **1996**. The trajectory of the point of application of the resultant force of body mass and walking speeds. Folia Primatologica 66:160–180.

Alexander, R. M. 2003. How Animals Move. Focus Multimedia Ltd.

Arms, A., D. Voges, H. Preuschoft, and M. Fischer. **2002**. Arboreal locomotion in small New-World monkeys. Zeitschrift für Morphologie und Anthropologie 83:243–263.

Borelli, G. A. 1680. De motu animalium ex principio mechanico statico. Rome.

Christian, A. 1995. Zur Biomechanik der Lokomotion vierfüßiger Reptilien, besonders der Squamata. Courier Forschungsinstitut Senckenberg 108:1–58.

Christian, A., W.-D. Heinrich, and W. Golder. **1999**. Posture and mechanics of the forelimbs of *Brachiosaurus brancai* (Dinosauria: Sauropoda). Mitteilungen aus dem Museum für Naturkunde in Berlin, Geowissenschaftliche Reihe 2:63–73.

Christian, A., R. H. G. Müller, G. Christian, and H. Preuschoft. **1999**. Limb swinging in elephants and giraffes and implications for the reconstruction of limb movements and speed estimates in large dinosaurs. Mitteilungen aus dem Museum für Naturkunde in Berlin, Geowissenschaftliche Reihe 2:81–90.

Dagg, A. I. 1974. The locomotion of the camel (*Camelus dromedarius*). Journal of Zoology 174:67–78.

Farlow, J. O. 1992. Sauropod tracks and trackmakers: integrating the ichnological and skeletal records. Zubia 10:89–138.

Fechner, R. 2009. Morphofunctional evolution of the pelvic girdle and limb of saurischian dinosaurs on the lineage to sauropod dinosaurs. Ph.D. thesis, Universität München.

Fischer, M. S., and K. E. Lilje. **2011**. Hunde in Bewegung. Franckh Kosmos Verlag, Stuttgart.

Gambaryan, P. P. 1974. How Animals Run. John Wiley & Sons Inc., New York.

Gray, J. 1968. How Animals Move. Cambridge University Press, Cambridge.

Günther, M. M. 1989. Funktionsmorphologische Untersuchungen am Sprungverhalten mehrerer Halbaffen. Ph.D. thesis, Freie Universität Berlin.

Günther, M. M., H. Preuschoft, H. Ishida, and Y. Nakano. **1991**. Can Prosimian-like Leaping be Considered a Preadaptation to Bipedal Walking in Hominids?; pp. 153–165 in S. Matano, R. H. Tuttle, H. Ishida, and M. Goodman (eds.), Topics in Primatology. 3. University of Tokyo Press, Tokyo.

Henderson, D. M. 2006. Burly gaits: centers of mass, stability, and the trackways of sauropod dinosaurs. Journal of Vertebrate Paleontology 26(4):907–921.

Hildebrand, M. 1965. Symmetrical gaits of horses. Science 150(3697):701–708.

Hildebrand, M. 1976. Analysis of Tetrapod Gaits: General Consideration on Symmetrical Gaits; pp. 203–236 in R. M. Herman, S. Grillner, P. S. G. Stein, and D. G. Stuart (eds.), Neural Control of Locomotion. Plenum Press, New York.

Hildebrand, M., and G. E. Goslow. **2003**. Vergleichende und funktionelle Anatomie der Wirbeltiere. Springer, Berlin.

Howell, A. B. 1944. Speed in Animals. University of Chicago Press, Chicago, 270 pp.

Hutchinson, J. R., D. Famini, R. Lair, and R. Kram. **2003**. Biomechanics: are fast-moving elephants really running? Nature 422(6931):493–494.

Hutchinson, J. R., D. Schwerda, D. J. Famini, R. H. I. Dale, M. S. Fischer, and R. Kram. **2006**. The locomotor kinematics of Asian and African elephants: changes with speed and size. Journal of Experimental Biology 209(19):3812–3827.

Läbe, S., P. M. Sander, T. Schanz, H. Preuschoft, and U. Witzel. **2013**. Gait reconstruction from sauropod trackways using photogrammetry and soil mechanical finite element analysis: a case study from the middle Kimmeridgian Barkhausen tracksite. Journal of Vertebrate Paleontology (Program and Abstracts 2013):158.

Lee, D. V., J. E. Bertram, and R. J. Todhunter. **1999**. Acceleration and balance in trotting dogs. Journal of Experimental Biology 202(24):3565–3573.

Li, Y., R. H. Crompton, R. M. Alexander, M. M. Günther, and W. J. Wang. **1996**. Characteristics of ground reaction forces in normal and chimpanzee-like bipedal walking by humans. Folia Primatologica 66:137–159.

Lockley, M. G., J. O. Farlow, and C. A. Meyer. **1994**. *Brontopodus* and *Parabrontopodus* ichnogen. nov. and the significance of wide- and narrow-gauge sauropod trackways. Gaia: Revista de Geociências 10:135–145.

Preuschoft, H. 2002. What does "arboreal locomotion" mean exactly? And what are the relationships between "climbing", environment and morphology? Zeitschrift für Morphologie und Anthropologie 83:171–188.

Preuschoft, H., B. Hohn, S. Stoinski, and U. Witzel. **2011**. Why so huge? Biomechanical Reasons for the Acquisition of Large Size in Sauropod and Theropod Dinosaurs; pp. 197–218 in N. Klein, K. Remes, C. T. Gee, and P. M. Sander (eds.), Biology of the Sauropod Dinosaurs - Understanding the Life of Giants. Life of the Past. Indiana University Press, Bloomington, 331 pp.

Preuschoft, H., H. Witte, A. Christian, and S. Recknagel. **1994**. Körpergestalt und Lokomotion bei großen Säugetieren. Verhandlungen der Deutschen Zoologischen Gesellschaft 87(2):147–163.

Preuschoft, H., U. Witzel, B. Hohn, D. Schulte, and C. Distler. **2007**. Biomechanics of locomotion and body structure in varanids with special emphasis on the forelimbs. Mertensiella 16:59–78.

Schanz, T., Y. Lins, H. Viefhaus, T. Barciaga, S. Läbe, H. Preuschoft, U. Witzel, and P. M. Sander. **2013**. Quantitative interpretation of tracks for determination of body mass. PLoS ONE 8(10):1–12.

Smith, F. 1912. On Horse Tracks. Veterinary Physiology, Billiere. Tindall & Cox, London.

Streitlein, I., and H. Preuschoft. **1987**. Die Kinematik der Trabtempi von Reitpferden. Wissenschaftliche Publikationen der Deutschen Reiterlichen Vereinigung 9:20–65.

Thompson, M. E., R. S. White, and G. S. Morgan. **2007**. Pace versus trot: can medium speed gait be determined from fossil trackways? New Mexico Museum of Natural History and Science Bulletin 42:309–314.

van der Sluijs, L., M. Gerken, and H. Preuschoft. **2010**. Comparative analysis of walking gaits in South American camelids. Journal of Zoology 282(4):291–299.

Weissengruber, G. E., G. F. Egger, J. R. Hutchinson, H. B. Groenewald, L. Elsasser, D. Famini, and G. Forstenpointner. **2006**. The structure of the cushions in the feet of African elephants (*Loxodonta africana*). Journal of Anatomy 209(6):781–792.

CHAPTER 5

Do tracks yield reliable information on gaits? – Part 2: Thoughts on weight distribution among the limbs of sauropod dinosaurs during walking

5.1. ABSTRACT

Since the limbs of sauropod dinosaurs had to bear the high body mass of the animal, the distribution of weight among the limbs during locomotion is of great interest. Due to their gigantic body size and mass, it is common sense that safety and stability are very important parameters in sauropod locomotion, excluding most likely highly dynamic gaits with phases of aerial suspension. This chapter gives an overview of formerly discussed ways of locomotion of sauropod dinosaurs and focusses on the weight distribution among the limbs during locomotion. Apart from body fossils, ichnofossils provide insights into the locomotion of a trackmaker. Therefore, possible positions of the center of mass and types of limb support during walking locomotion, obtained from the footfall pattern of sauropod trackways, are discussed, in order to calculate the weight distribution factor f_{wd^*}. The weight distribution factor is important for track-based weight estimation approaches that simulate the load exerted by the trackmaker to form tracks.

5.2. INTRODUCTION

5.2.1 General introduction

Sauropod dinosaurs were the largest animals that ever existed on earth (Curry Rogers and Wilson, 2005; Sander and Clauss, 2008; Klein et al., 2011; Sander et al., 2011; Sander, 2013). Apart from their anatomy and physiology, their locomotion is of great interest, since their high body mass was borne on the limbs during standing and movement. To begin with, there are two ways of studying locomotion of any dinosaur on land: either on skeletal anatomy or on tracks, as a direct result of the trackmaker's locomotion. Hutchinson and Gatesy (2006) and Hutchinson et al. (2011) studied anatomy and physiology to investigate locomotor abilities of *Tyrannosaurus rex* with moments in the joints from computer generated muscle models. Through science history, the locomotion of the sauropodomorph dino-

saur *Plateosaurus engelhardti* underwent a change from facultative quadrupedal locomotion (e.g., Christian et al., 1996; Moser, 2003) to an obligatory bipedal one (Bonnan and Senter, 2007; Mallison, 2010a, 2010b; Mallison, 2011b). Mallison's work was based on computer models to investigate the body mass, posture and locomotion that confirmed results of Bonnan and Senter (2007). The approach chosen by Henderson (2006) to determine the gauge of sauropods, both narrow and wide, was based on the position of the center of mass (CM). He calculated a posteriorly positioned CM of 11.5% for *Diplodocus* and more anterior CM position of 37.4% for *Brachiosaurus* given as percentages of the glenoacetabular distance (with the acetabulum at 0% and the glenoid at 100%). Henderson's study with computer models confirmed prior hypotheses (cf. Farlow, 1992; Wilson and Carrano, 1999) that *Brachiosaurus* performed a stable locomotion when replicating a wide-gauge trackway, and that *Diplodocus* was more stable when performing a narrow-gauge trackway. The CM position of these two sauropods was also considered in a paper about rearing ability (Mallison, 2011c). The result was that rearing might have been feasible for *Diplodocus* but not for *Brachiosaurus*, because of the posterior CM positon of the former one. In the studies by Sellers et al. (2009) on *Edmontosaurus* and by Sellers et al. (2013) on *Argentinosaurus*, possible gaits were reconstructed based on criteria, such as stability, efficiency, and speed by using physical principles to generate algorithms for the simulation of muscles.

5.2.2 Quadrupedal locomotion on land

A quadrupedal gait is the way of limb movement during locomotion on land, which consists of a repeating cycle of the four moving limbs. A stride is covered by one limb moving forward and is separated into a stance phase, with the limb being in ground contact, and a swing phase, with the lifted limb moving forward (Howell, 1944; Hildebrand, 1965, 1976). A common classification of the basic gaits of quadruped tetrapods is the distinction between walk, trot and run. These gaits were already illustrated in the 19th century through rapid series photographs by Eadweard Muybridge (1899). The more up-to-date way for distinguishing locomotion is simply between walking and running by duty factor (Hildebrand, 1976, 1980; Biewener, 1983; Hildebrand, 1985, 1989), which is the fraction of the cycle when one particular foot touches the ground. A duty factor of 0.5 and higher indicates walking and below 0.5 running. Another way of distinguishing walking and running is the Froude number, a dimensionless speed measure (Alexander and Jayes, 1983; Gatesy and Biewener, 1991).

The terms symmetrical and asymmetrical (Howell, 1944; Hildebrand, 1989) are also used to describe gaits. A symmetrical gait is a harmonious locomotion, such as walk or trot, with even durations between the footfalls, whereas asymmetrical locomotion has uneven intervals, such as the gallop.

Hildebrand advanced the analysis and classification of gaits by developing a system to distinguish between gaits based on only two parameters of the stride phases (Hildebrand, 1965). He succeeded in bringing some order into a system of smooth transitions between several gaits, for example, between walking and running, or lateral and diagonal gaits. In horses, up to 39 symmetrical gaits can be observed, which rather are variations and specifications of walking and running (Hildebrand, 1965).

The slowest symmetrical gait is the walk; a 'lateral sequence singlefoot' or 'lateral sequence lateral couplet gait' according to Hildebrand's terminology (Hildebrand, 1965, 1985, 1989). The walk has a four-beat rhythm. The duty factor in the walk is ≥ 0.5 (Hildebrand, 1985). Possible types (stages) of limb support during the quadrupedal walk cycle are given as a simplified illustration in Figure 5.1. The walk has alternating supporting phases of two limbs (2LS = two-limb support) and three limbs (3LS = three-limb support) that are in stance phase at the same time. A cycle in the walk consists of eight phases ($t_1 - t_8$): one period for each of the four limbs in stance and swing phase (Howell, 1944; Hildebrand, 1989). The walk can be either lateral or diagonal (Hildebrand, 1976). The lateral walk, as performed by most quadrupeds including horses, starts with one hindlimb, followed by the ipsilateral (same side of the body) forelimb, then the contralateral (opposite side) hindlimb and finally the remaining contralateral forelimb. Among extant animals, the diagonal walk is performed, for example, by primates, crocodiles and lizards (Hildebrand, 1976; Hildebrand and Goslow, 2001). However, the lateral walk offers most stability, since the 3LS, which works like a tripod, creates larger areas of support, whereas in the diagonal walk the areas of support are smaller (Gray, 1944; Hildebrand, 1980).

5.2.3 Increase of speed

Several strategies exist for speed increase in quadrupedal locomotion (Preuschoft et al., 1994; Preuschoft et al., 2011; Kienapfel et al., 2014). A first stage is to increase the step length, but this is not boundlessly possible due to very high moments of torque acting on the proximal joints of the pectoral and pelvic girdle. Moreover, the excursion angle of the limb is limited by the degrees of freedom of the joints. Another strategy is the increase of the frequency of limb movement, as this is, for example, done in the amble (e.g., *tölt* as observed in Icelandic horses), which can be considered as a walk with a higher frequency. High frequency limb movements require an additional input of energy, since the limb acts like a physical pendulum that has to overcome momentums of inertia to swing and has a preferred frequency at which it is energy-optimized. In order to remain so, an increase in pendulum frequency cannot be carried out excessively. A further increase of speed can only be achieved by employing a gait that incorporates phases of aerial suspension, where none of the feet are in contact with the ground (Preuschoft et al., 1994; Preuschoft et al., 2011).

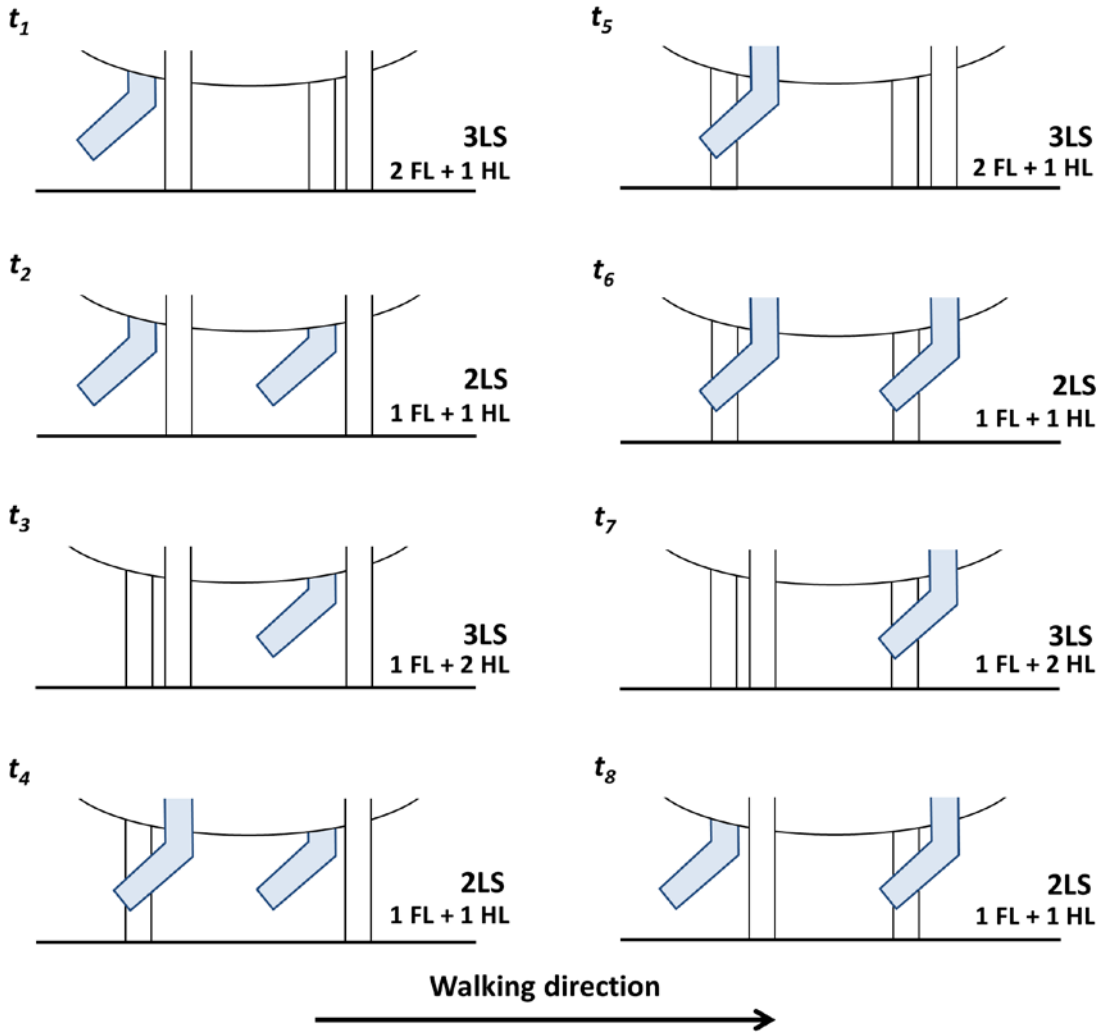

Figure 5.1: Simplified illustration of types of limb support during a walk cycle, subdivided into eight es ($t_1 - t_8$). The sequence starts with the left hindlimb and walking direction is from left to right. Abbreviations: 3LS = three-limb support of the body, 2LS = two-limb support of the body, HL = hindlimb, FL = forelimb.

Gaits with aerial suspension are the running trot (a two-beat rhythm with the contralateral forefoot and hindfoot in ground contact at the same time), the running pace (a two-beat rhythm with the ipsilateral forefoot and hindfoot in ground contact at the same time), or the gallop (or canter, a three-beat rhythm, which entails a sequence of hindfoot, then hindfoot with contralateral forefoot, and the remaining forefoot last) (Muybridge, 1899; Hildebrand, 1965; Alexander, 1984; Hildebrand, 1989). For example, elephants reach high speeds without a phase of aerial suspension by employing an amble and by shifting their CM vertically (Hutchinson et al., 2003; Hutchinson et al., 2006, 2006; Ren et al., 2008, 2008; Genin et al., 2010).

As noted by Pfau et al. (2011), the gait terminology of Hildebrand (1965, 1976, 1980, 1985, 1989) should be used to avoid confusion in describing and naming various gaits. In some publications, for instance, the pace was often referred to as amble gait (cf. Leonardi,

1987; Casanovas et al., 1997; Vila et al., 2013), which hinders the comparability and comprehensibility of literature.

Based on dinosaur trackways, the speed of the trackmaker can be calculated (Alexander, 1976; Thulborn, 1982; Alexander, 1985; Thulborn, 1990), although the accuracy is limited because of numerous sources of error (Alexander, 1991). Alexander (1976) has proposed a physical formula to calculate the speed of an extinct trackmaker from its tracks. The formula is $v = 0.25g^{0.5} \cdot s^{1.67} \cdot h^{-1.17}$ where v is the speed [m/s], g [m/s²] is the acceleration of gravity, s [m] is the stride length measured from the trackway, and h [m] is the hip height estimated from the pes track length. The formula is based on dynamic similarities of the strides produced in extant animals, like mammals, including humans, and birds, with those of extinct ones, such as dinosaurs. Alexander (1976) noted that dinosaurs were slower than mammals on average.

5.2.4 Dynamics of sauropod dinosaurs

However, out of all the gaits, which one was most likely employed by the gigantic sauropod dinosaurs, and what are the implications for the weight distribution among the limbs? Several studies have been carried out to assess the limb kinematics of sauropods based on ichnological and osteological evidence (Alexander, 1989; Wilson and Carrano, 1999; Riga, 2011; Vila et al., 2013). Based on forward dynamic computer simulations, Sellers et al. (2013) found that a three-dimensional model of the giant sauropod *Argentinosaurus* walked most stable at slow speed while employing a pace gait. The method presented by Sellers et al. (2013), demonstrated an unique simulation of how a sauropod could have moved. However, the authors acknowledged that further improvement of their approach is needed. The pace as a possible gait of sauropods was also proposed by Casanovas et al. (1997), Mezga et al. (2007), and Vila et al. (2013), based on ichnological data from Spain. In modern animals, the pace is usually performed at higher speeds, since it is unstable at lower speeds (Hildebrand, 1985). The CM position lies partly outside the area of support (see 5.2.2), leading to a 'tipping over' of the animal. This is an argument against the proposals of sauropods employing a pace, since the very high body mass of sauropods required safety and stability (see below) during locomotion.

Highly dynamic gaits with an aerial phase of suspension, such as gallop, trot and pace, have so far been excluded from possible gaits for the sauropod dinosaurs. Some authors concluded that the ability of fast locomotion is limited in sauropods, due to their high body mass. The ground reaction force on the animal while moving had been estimated for the stance phases by Christian et al. (1999), concluding that the high body mass of the sauropods led to enormous stresses in the limbs, which would have required a damping mechanism in the limbs to avoid injuries. Similar to those of elephants (Weissengruber et al., 2006), autopodial structures in sauropod feet might have damped the ground contacts, which though would lead to deceleration of the sauropod (pers. comm. H. Preuschoft,

2017). Preuschoft et al. (2011) also stressed the importance of safety and stability in the sauropod gait. From computer models of *Diplodocus* it was derived that the posterior CM position could have hindered the sauropod in fast acceleration (Mallison, 2011c). Based on these considerations, the dynamical component and dynamic gaits in the sauropod locomotion is assumed to be negligible.

5.2.5 Purpose

The aim of this chapter is to infer weight distribution among limbs during locomotion of a sauropod trackmaker based on theoretical consideration of sauropod locomotion. In combination with general considerations concerning sauropod locomotion (section 5.2.4), the weight distribution among the limbs can be derived from sauropod gaits estimated with the method by Kienapfel et al. (2014). The weight distribution is important for weight estimation methods that use footprints of a moving trackmaker, such as performed by Schanz et al. (2013) for an African elephant.

5.3. THE STUDY OF TRACKS TO INFER GAITS

Gaits are usually studied and described as functions of time, which is, however, not applicable to fossil tracks. Contrarily, a study by Kienapfel et al. (2014) aimed at inferring gait information from the footfall pattern seen in trackways, using the example of extant horses. The study was conducted with regard to future application on fossil trackmakers, such as sauropods. The authors were able to distinguish symmetrical versus asymmetrical gaits from horse tracks. Further, if the limb and trunk length of the trackmaker can be approximated, it is possible to differentiate between tracks generated during walk and amble from those tracks left by the pace and trot. From that study, the slow walk was distinguishable from all other gaits and was characterized by short strides with overprinting and minimal overstepping, and a close placing of ipsilateral manus and pes prints. An example of a walking Icelandic horse (data from Kienapfel et al., 2014) with a shoulder height of 1.37 m is illustrated in Figure 5.2. For fossil camelids, a similar approach was taken by Thompson et al. (2007), but the focus of this study was limited to the pace and trot.

5.3.1 Example for sauropod gait estimation based on the Barkhausen tracksite

For the first time, the insights of the study by Kienapfel et al. (2014; Chapter 4) were applied to a fossil trackmaker. As an example, a sauropod trackway from the Barkhausen tracksite, Germany (Läbe et al., 2013), was measured and compared with data from Kienapfel et al. (2014). The tracksite is of Upper Jurassic age (Kimmeridgian) and exposes trackways of eight sauropod dinosaurs and two tridactyl trackways (Kaever and de Lapparent, 1974; Friese, 1979; Lockley, Farlow et al., 1994). The sauropod trackways made by small individuals contain small pes and manus tracks, which vary in depth and quality. The sauropod trackway chosen from the Barkhausen tracksite is pes-dominated and consists of

five manus and pes track sets. The location of the manus and pes tracks within the sauropod trackway had been measured from a photogrammetric model (cf. Läbe, in revision) in order to plot their position into a coordinate system to investigate the footfall pattern according to Kienapfel et al. (2014). The average pes length is 37 cm and the stride length is 150 cm. From track measurements, a speed of about 3.5 km/h and a hip height of about 150 cm were estimated for the trackmaker based on formulas by Alexander (1976). Using the trackway gauge, which is narrow, and the heteropody index (i.e., manus/pes track ratio; Lockley, 1989; Lockley, Farlow et al., 1994), which is about 1:3, the trackway can be assigned to the ichnotaxon *Parabrontopodus* (Lockley, Farlow et al., 1994).

The sauropod trackway (Figure 5.2) shows small strides that the manus is always in front of the pes and that ipsilateral tracks are placed close together. In this regard, the Barkhausen tracks are comparable to the horse trackway. The limb length of the Barkhausen sauropod and Icelandic horse are comparable, although it has to be noted that for the sauropod trackmaker the hip height was estimated and for the horse the height at withers was measured (Kienapfel et al., 2014). The trunk length of the sauropod trackmaker cannot be estimated with certainty. However, since both trackways and the limb length of the trackmakers are comparable (Figure 5.2, in addition to negligible dynamics in sauropods in section 5.2.4), we argue that the Barkhausen trackway was produced by a slow walking sauropod trackmaker.

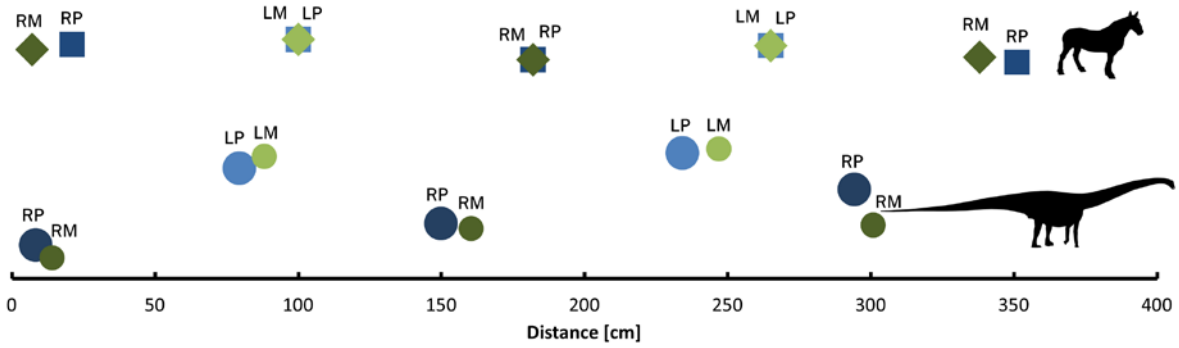

Figure 5.2: Comparison of trackways of a walking Icelandic horse with that of a sauropod from the Barkhausen tracksite, Germany. Abbreviations and colors: RP (dark blue) = right pes imprint, LP (light blue) = left pes imprint, RM (dark green) = right manus imprint, LM (light green) = left manus imprint.

5.3.2 Problems with this approach

Unfortunately, most of the required parameters can, at most, only be estimated in fossil tracks, which makes a reliable gait reconstruction somewhat speculative (Kienapfel et al., 2014; Stevens et al., 2016). While stride length can be measured directly from the tracks, the trackmaker hip height is estimated from length measurements of pes tracks. According to Alexander (1976), the equation $h \approx 4 \cdot PL$ can be applied, where h is the hip height and PL is the pes length. The apparent trunk length (glenoacetabular distance), which is required for gait determination according to Kienapfel et al. (2014), is a difficult parameter

to obtain from tracks. Leonardi (1987) has compiled three different equations from previous work (Soergel, 1925; Baird, 1952, 1954) to estimate the glenoacetabular distance of a trackmaker based on measurements of the trackway. Crucial for the application of these equations is that a gait has to be assumed, since the equations were formulated for the walking trot, lateral sequence walk and pace. By applying these equations (Soergel, 1925; Baird, 1952, 1954; Leonardi, 1987; Farlow et al., 1989), the glenoacetabular distance of the Barkhausen trackmaker was only roughly estimated to range between 1 m and 1.40 m. However, the formulas for estimating the glenoacetabular distance remain to be verified for any living trackmaker, which makes their application speculative.

5.4. WEIGHT DISTRIBUTION AMONG THE LIMBS

5.4.1 Possible types of limb support during walking locomotion

As noted previously, the high body mass of sauropod dinosaurs makes their mode of locomotion specifically interesting, because the weight had to be distributed over the limbs during movement. To infer weight distribution among the limbs, it is helpful to theoretically consider the possible types of limb support on which the weight was borne during locomotion. Depending on the gait, different types of limb support occur over a complete locomotion cycle, such as $t_1 - t_8$ in the walk. Types of support during locomotion are: four limb support (4LS), three limbs with main support either on the hindlimb pair (3 HLP) or on the forelimb pair (3 FLP), two limb support (2LS), one limb support (1LS), or no limbs (see Figure 5.1 and Figure 5.3).

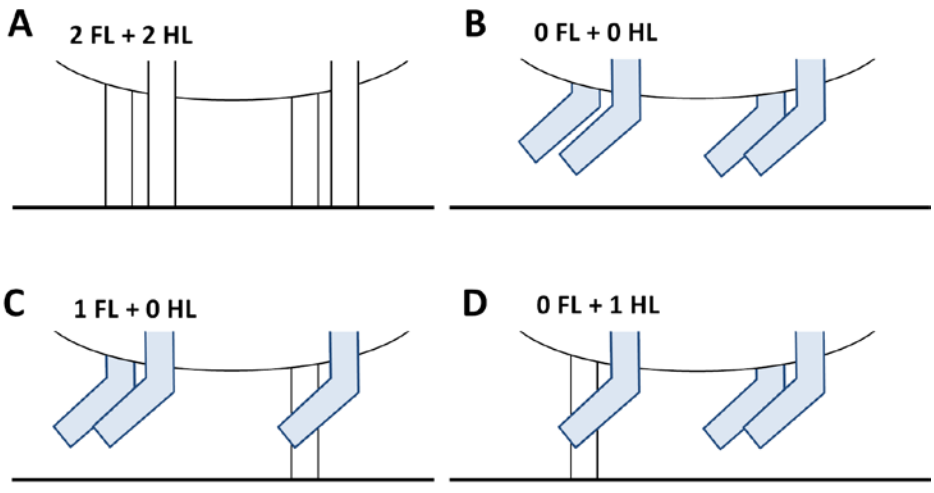

Figure 5.3: Types of limb support during walking, which are non-plausible and can be excluded in the case of sauropods. A. Standing posture. B. Phase of aerial suspension with no limbs touching the ground. C and D. One-limb support for forelimb and hindlimb, respectively. Abbreviations: FL = forelimb, HL = hindlimb.

Excluding dynamic gaits for sauropods (see section 5.2.4) also means that some types of limb support can most likely be excluded (Figure 5.3). The scenario in Figure 5.3B occurs

only during phases of aerial suspension in dynamic gaits, and the 1LS occurs usually directly before or after phases of aerial suspension (Figure 5.3C, D). A 4LS will occur when the trackmaker is standing still (Figure 5.3A) or in the walking trot, such as observed in lizards. The 2LS can be observed during various gaits, such as the walk, pace, trot and amble. Finally, the support on three limbs (3LS) usually occurs only during walking (Figure 5.1).

5.4.2 The position of the center of mass (CM)

The position of the CM of an animal is an important constraint for the weight distribution among the limbs during locomotion. In the approach for weight estimation from tracks by Schanz et al. (2013), an African elephant was studied. Although elephants are a popular analog to sauropods in terms of foot morphology and quadrupedality, they differ significantly in their weight distribution from sauropods. In elephants, the position of the CM lies with 60% very anteriorly: roughly spoken, the forelimbs bear about 60% of the weight (Henderson, 2004; Genin et al., 2010). This is due to the relatively high mass located in the head of the animal. Despite their long neck, diplodocid sauropods, for instance, are reconstructed to have their position of the CM much more posteriorly because of the small head and the heavily pneumatized, lightweight cervical column. According to Henderson (2004; 2006), the hindlimbs of *Diplodocus* would bear about 88.5% of the weight and the forelimbs 11.5%, whereas Alexander (1989) and Lockley and Rice (1990) assumed that the hindlimbs carried 78% of the weight. In *Brachiosaurus*, the CM is more anteriorly positioned at 37.4% (Henderson, 2006).

5.4.3 Determination of the weight distribution factor f_{wd^*}

In the study by Schanz et al. (2013), the weight distribution factor f_{wd} was empirically determined by weighing the elephant trackmaker and using the equation $f_{wd} = m_{limb}/m_{total}$, where m_{limb} is the mass carried on one particular limb and m_{total} is the total mass of the elephant. The CM of the elephant was anteriorly positioned at about 60% of the glenoacetabular distance. During locomotion, the weight of the swinging limb was redistributed to the other limbs remaining in stance phase. Schanz et al. (2013) assumed that 80% of the swinging limb weight was redistributed to the other limb of the same limb pair and 20% was redistributed to the other limb pair. For the present study, the same values were used for the redistribution of the weight of the swinging limb.

In this study, the weight distribution factor was calculated differently than f_{wd} (Schanz et al., 2013). The differences are based theoretical considerations and this new, adapted factor is therefore named f_{wd^*}. The weight distribution factor f_{wd^*} was calculated for different theoretical CM positions (section 5.4.2) and for different types of limb support (section 5.4.1), which are possible in different gaits. f_{wd^*} was calculated for 11.5% (the most posterior CM position), 20%, 37.4%, and 50% (the most anterior CM position).

Using the types of limb support and the different CM positions, the weight distribution factor can be calculated for each of these. The factor f_{wd^*} was calculated for one hindlimb since the sauropod trackways studied in this doctoral thesis are mostly pes-dominated. For 1LS, the factor is 1, since 100% of the total body weight is borne by one particular hindlimb. For the 2LS, with ipsi- or contralateral limbs, the factor is represented by CM position, since the weight is distributed between fore- and hindlimbs. For the 4LS, or the standstill, the factor of the 2LS is divided by two. Depending on whether the 3LS is supported by both forelimbs or hindlimbs, the fraction of the redistribution has to be considered (e.g., 80% or 20%). In Figure 5.4 and Table 5.1, the calculated weight distribution factors f_{wd^*} are given for four different CM positions and five types of limb support. Each of the four CM scenarios is illustrated in a bar plot in Figure 5.4, showing how the weight distribution varies during phase t_1 to t_8 during the locomotion cycle. A calculation example for a CM position of 11.5% for *Diplodocus* is also given in Table 5.1. The higher the value for f_{wd^*} is, the higher the fraction of the weight which is distributed on one hindlimb.

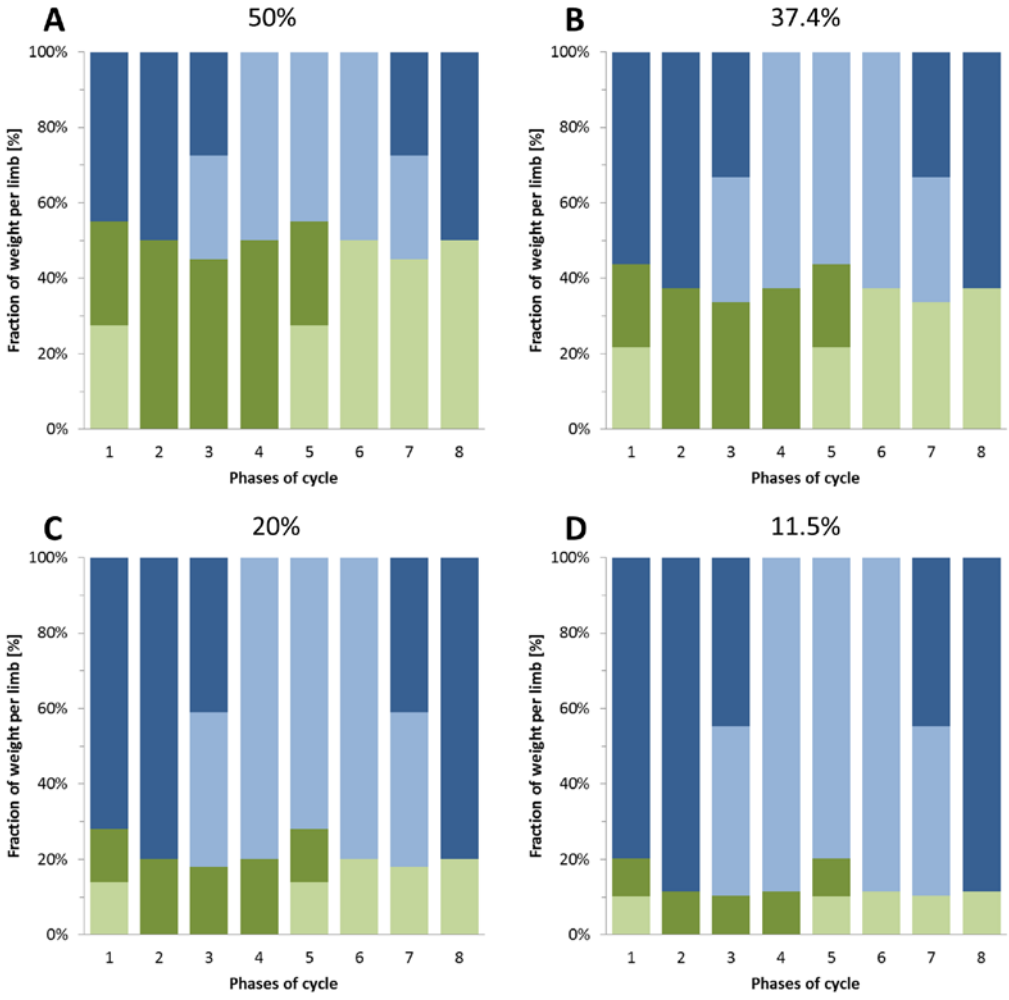

Figure 5.4: Weight distribution diagrams for different CM positions (A. 50%. B. 37.4%. C. 20%. D. 11.5%) over a complete cycle t_1 to t_8 with alternating 2LS and 3LS (x-axis). It can be seen that the fraction of weight borne on a limb (dark green = right forelimb, light green = left forelimb, dark blue = right hindlimb, light blue = left hindlimb) varies over the cycle.

Table 5.1: Weight distribution factors f_{wd^*} among limbs for four different CM positions and five different types of limb support, with a calculation example for a CM position of 11.5%. Factors are given as fractions and not as percentages.

Types of limb support	f_{wd^*}				Calculation example for CM position of 11.5%
	CM 11.5	20	37.4	50	
1	1	1	1	1	$= 1$
2	0.885	0.8	0.626	0.5	$= 0.885$
3 FLP	0.7965	0.7	0.5634	0.45	$= (0.885/2 \cdot 0.8) + 0.885/2$
3 HLP	0.4482	0.412	0.3317	0.275	$= (0.115/2 \cdot 0.1) + 0.115/2$
4	0.4425	0.4	0.313	0.25	$= 0.885/2$

5.5. DISCUSSION

For the weight estimation methods based on tracks by Schanz et al. (2013), two factors were employed for evaluating the dynamic force component exerted by the trackmaker during locomotion, namely the weight distribution factor and dynamic factor. In contrast to the present chapter, the weight distribution factor was empirically determined (Schanz et al., 2013, equation 4). The dynamic factor was determined from video recordings that, obviously, are not available for the trackmaker of fossil tracks.

The factor f_{wd^*} presented here is a theoretical consideration to obtain a weight distribution factor for approximating the dynamic component during slow walking. This factor is important and necessary for any study that examines substrate deformation caused by a walking quadruped and in particular for the weight estimation approach presented in Chapter 6 (Läbe, unpubl.). Since tracks are always a result of static (i.e., by the weight) and dynamic (i.e., by the locomotion) force exerted by the trackmaker (cf. Falkingham, 2014), the weight distribution factor f_{wd^*} is assumed to influence the load of the trackmaker on the substrate during track formation. The dynamic factor as used by Schanz et al. (2013) is assumed to be negligible because of limited dynamics in sauropods (section 5.2.4).

The work in this chapter doubtlessly contains many assumptions and care has to be taken when applying the factor f_{wd^*}, since both, the determination of the position of the CM and the types of limb support involve uncertainties. f_{wd^*} varies depending on the position of the CM and on the particular type of limb support, which, in turn, depends on the gait. To derive the position of the CM of the trackmaker from a trackway, gauge (Farlow, 1992; Lockley, Farlow et al., 1994; Wilson and Carrano, 1999; Romano et al., 2007), heteropody index (Lockley, 1989; Lockley, Farlow et al., 1994; Santos et al., 1994; Santos et al., 2009) and manus- or pes domination (Lockley, Pittman et al., 1994; Henderson, 2004; Henderson, 2006; Falkingham et al., 2012) have to be taken into consideration. The trackmaker's gait has to be approximated (Kienapfel et al., 2014), to infer the types of limb support from tracks.

In the example of the Barkhausen sauropod trackway (Figure 5.2), footfall pattern and speed estimates of about 3.5 km/h support a walking locomotion of the trackmaker. Speed estimation is easy with Alexander's formula, and results seem to be viable. However, physiology and metabolism of dinosaurs were different from extant mammals, and the formula should always be applied with care, as even Alexander clarified in a follow-up publication (Alexander, 1991). In addition, the calculated speeds appear to be too slow, considering the high metabolic rates of sauropods (Sander et al., 2011). Based on computer modeling presented by Mallison (2011a), it was hypothesized that dinosaurs could have combined high step frequencies with short strides to achieve higher speeds. A weakness of this approach is that animals normally do not move outside the pendulum resonance frequency, since this would not be energy efficient (Preuschoft et al., 1994; Preuschoft et al., 2011).

In the case of sauropods, it is generally assumed that they moved in a safe and stable way (Preuschoft et al., 2011) with bending stresses and rapid accelerations being minimized, as has been observed for other large mammals (McMahon, 1975; Biewener, 1989). This does not mean that sauropods were generally not able to move fast or to employ gaits with higher speeds, such as amble, pace and trot. Although footfall pattern of sauropod trackways show in most cases short strides and placement of ipsilateral manus and pes together with the manus in front of the pes, it might be possible that sauropods had, depending on speed or terrain, a larger repertoire of gaits, than it is conveyed by trackways.

Based on presented criteria, a walking locomotion of the trackmaker is supported including 2LS, 3HLP support and 3FLP support, from which the factor for 2LS is the highest value. However, the entire trackway and imprint positions have to be studied, since each imprint in a trackway has experienced all possible types of limb support during the entire walk cycle.

5.6. CONCLUSION

Since the footfall pattern in a trackway contains much information, studies such as the present chapter, the study by Thompson et al. (2007) and the work by Kienapfel et al. (2014) are valuable for further studies of a trackmaker's gait. For the first time, these insights were applied to a sauropod trackmaker. The understanding of the distribution of the weight among the limbs is important for gait estimation and for further understanding of the dynamics of a trackmaker. Here, the factor f_{wd^*} for weight distribution on hindlimbs of sauropod dinosaurs employing a walking gait was calculated based on the position of the center of mass and the types of limb support. Before f_{wd^*} is calculated, the gait has to be approximated according to Kienapfel et al. (2014), likewise the position of the center of mass. In general, the weight distribution is of interest for the estimation of the trackmaker's weight from its tracks, when besides the static force exerted by the trackmaker also the dynamic force has to be taken into account.

5.7. ACKNOWLEDGEMENTS

I thank Holger Preuschoft (Ruhr-Universität Bochum) and Jens N. Lallensack (Universität Bonn) for fruitful discussions and valuable comments on this manuscript. P.M. Sander and Jeffrey Power are thanked for improving the manuscript. The author was supported by the Studienstiftung des deutschen Volkes.

5.8. REFERENCES

Alexander, R. M. 1976. Estimates of speeds of dinosaurs. Nature 261:129–130.

Alexander, R. M. 1984. The gaits of bipedal and quadrupedal animals. The International Journal of Robotics Research 3(2):49-59.

Alexander, R. M. 1985. Mechanics of posture and gait of some large dinosaurs. Zoological Journal of the Linnean Society 83(1):1–25.

Alexander, R. M. 1989. Dynamics of Dinosaurs and Other Extinct Giants. Columbia University Press, New York, 167 pp.

Alexander, R. M. 1991. Doubts and assumptions in dinosaur mechanics. Interdisciplinary Science Reviews 16(2):175–181.

Alexander, R. M., and A. S. Jayes. **1983**. A dynamic similarity hypothesis for the gaits of quadrupedal mammals. Journal of Zoology 201:135–152.

Baird, D. 1952. Revision of the Pennsylvanian and Permian footprints *Limnopus*, *Allopus* and *Baropus*. Journal of Paleontology 26(5):832–840.

Baird, D. 1954. *Chirotherium lulli*, a pseudosuchian reptile from New Jersey. Bulletin of the Museum 111:166–194.

Biewener, A. A. 1983. Allometry of quadrupedal locomotion: the scaling of duty factor, bone curvature and limb orientation to body size. Journal of Experimental Biology 105:147–171.

Biewener, A. A. 1989. Scaling body support in mammals: limb posture and muscle mechanics. Science 245(4913):45–48.

Bonnan, M. F., and P. Senter. **2007**. Were the basal sauropodomorph dinosaurs *Plateosaurus* and *Massospondylus* habitual quadrupeds?; pp. 139–155 in P. M. Barrett and D. J. Batten (eds.), Evolution and palaeobiology of early Sauropodomorph dinosaurs. Special papers in palaeontology 77. Palaeontological Association, London.

Casanovas, M., A. Fernandez, F. Perez-Lorente, and J. V. Santafe. **1997**. Sauropod trackways from site El Sobaquillo (Munilla, La Rioja, Spain) indicate amble walking. Ichnos 5(2):101–107.

Christian, A., D. Koberg, and H. Preuschoft. **1996**. Shape of the pelvis and posture of the hindlimbs in *Plateosaurus*. Paläontologische Zeitschrift 70(3-4):591–601.

Christian, A., R. H. G. Müller, G. Christian, and H. Preuschoft. **1999**. Limb swinging in elephants and giraffes and implications for the reconstruction of limb movements

and speed estimates in large dinosaurs. Mitteilungen aus dem Museum für Naturkunde in Berlin, Geowissenschaftliche Reihe 2:81–90.

Curry Rogers, K., and J. A. Wilson (eds.). **2005**. The Sauropods - Evolution and Paleobiology. University of California Press, Berkeley, 349 pp.

Falkingham, P. L. 2014. Interpreting ecology and behaviour from the vertebrate fossil track record. Journal of Zoology 292(4):222–228.

Falkingham, P. L., K. T. Bates, and P. D. Mannion. **2012**. Temporal and palaeoenvironmental distribution of manus- and pes-dominated sauropod trackways. Journal of the Geological Society 169(4):365–370.

Farlow, J. O. 1992. Sauropod tracks and trackmakers: integrating the ichnological and skeletal records. Zubia 10:89–138.

Farlow, J. O., J. G. Pittman, and J. M. Hawthorne. **1989**. *Brontopodus birdi,* Lower Cretaceous Sauropod Footprints from the U.S. Gulf Coastal Plain; pp. 371–394 in D. D. Gillette and M. G. Lockley (eds.), Dinosaur Tracks and Traces. Cambridge University Press, Cambridge, 476 pp.

Friese, H. 1979. Die Saurierfährten von Barkhausen im Wiehengebirge. Veröffentlichungen des Landkreises Osnabrück 1:1–36.

Gatesy, S. M., and A. A. Biewener. **1991**. Bipedal locomotion: effects of speed, size and limb posture in birds and humans. Journal of Zoology 224(1):127–147.

Genin, J. J., P. A. Willems, G. A. Cavagna, R. Lair, and N. C. Heglund. **2010**. Biomechanics of locomotion in Asian elephants. Journal of Experimental Biology 213(5):694–706.

Gray, J. 1944. Studies in the mechanics of the tetrapod skeleton. Journal of Experimental Biology 20(2):88–116.

Henderson, D. M. 2004. Tipsy punters: sauropod dinosaur pneumaticity, buoyancy and aquatic habits. Proceedings of the Royal Society B 271(Suppl 4):180–183.

Henderson, D. M. 2006. Burly gaits: centers of mass, stability, and the trackways of sauropod dinosaurs. Journal of Vertebrate Paleontology 26(4):907–921.

Hildebrand, M. 1965. Symmetrical gaits of horses. Science 150(3697):701–708.

Hildebrand, M. 1976. Analysis of Tetrapod Gaits: General Consideration on Symmetrical Gaits; pp. 203–236 in R. M. Herman, S. Grillner, P. S. G. Stein, and D. G. Stuart (eds.), Neural Control of Locomotion. Plenum Press, New York.

Hildebrand, M. 1980. The adaptive significance of tetrapod gait selection. American Zoologist 20(1):255–267.

Hildebrand, M. 1985. Walking and Running; pp. 38–57 in M. Hildebrand, D. M. Bramble, L. F. Liem, and D. B. Wake (eds.), Functional Vertebrate Morphology. Harvard University Press, Cambridge Mass., 430 pp.

Hildebrand, M. 1989. The quadrupedal gaits of vertebrates. Bioscience 39(11):766–775.

Hildebrand, M., and G. E. Goslow. **2001**. Analysis of Vertebrate Structure. Wiley, New York, 635 pp.

Howell, A. B. 1944. Speed in Animals. University of Chicago Press, Chicago, 270 pp.

Hutchinson, J. R., K. T. Bates, J. Molnar, V. Allen, and P. J. Makovicky. **2011**. A computational analysis of limb and body dimensions in *Tyrannosaurus rex* with implications for locomotion, ontogeny, and growth. PLoS ONE 6(10):1–20.

Hutchinson, J. R., D. Famini, R. Lair, and R. Kram. **2003**. Biomechanics: are fast-moving elephants really running? Nature 422(6931):493–494.

Hutchinson, J. R., and S. M. Gatesy. **2006**. Beyond the bones. Nature 440:292–294.

Hutchinson, J. R., D. Schwerda, D. J. Famini, R. H. I. Dale, M. S. Fischer, and R. Kram. **2006**. The locomotor kinematics of Asian and African elephants: changes with speed and size. Journal of Experimental Biology 209(19):3812–3827.

Kaever, M., and A. F. de Lapparent. **1974**. Les traces de pas de Dinosaures du Jurassique de Barkhausen (Basse Saxe, Allemagne). Bulletin de la Société Géologique de France 16:516–525.

Kienapfel, K., S. Läbe, and H. Preuschoft. **2014**. Do tracks yield reliable information on gaits? – Part 1: The case of horses. Fossil Record 17:59–67.

Klein, N., K. Remes, C. T. Gee, and P. M. Sander (eds.). **2011**. Biology of the Sauropod Dinosaurs - Understanding the Life of Giants. Life of the Past. Indiana University Press, Bloomington, 331 pp.

Läbe, S. in revision. Vertical exaggeration of 3D surface models highlights additional detail in vertebrate tracks: an example from the photogrammetry of sauropod tracks. Journal of Paleontological Techniques (2017).

Läbe, S., P. M. Sander, T. Schanz, H. Preuschoft, and U. Witzel. **2013**. Gait reconstruction from sauropod trackways using photogrammetry and soil mechanical finite element analysis: a case study from the middle Kimmeridgian Barkhausen tracksite. Journal of Vertebrate Paleontology (Program and Abstracts 2013):158.

Leonardi, G. (ed.). **1987**. Glossary and Manual of Tetrapod Footprint Palaeoichnology. Departamento Nacional da Produção Mineral, Brazil, 137 pp.

Lockley, M. G. 1989. Summary and Prospectus; pp. 441–447 in D. D. Gillette and M. G. Lockley (eds.), Dinosaur Tracks and Traces. Cambridge University Press, Cambridge, 476 pp.

Lockley, M. G., J. O. Farlow, and C. A. Meyer. **1994**. *Brontopodus* and *Parabrontopodus* ichnogen. nov. and the significance of wide- and narrow-gauge sauropod trackways. Gaia: Revista de Geociências 10:135–145.

Lockley, M. G., J. G. Pittman, C. A. Meyer, and V. F. d. Santos. **1994**. On the common occurrence of manus-dominated sauropod trackways in Mesozoic carbonates. Gaia: Revista de Geociências 10:119–124.

Lockley, M. G., and A. Rice. **1990**. Did "*Brontosaurus*" ever swim out to sea?: evidence from brontosaur and other dinosaur footprints. Ichnos 1(2):81–90.

Mallison, H. 2010a. The digital *Plateosaurus* I: body mass, mass distribution and posture assessed using CAD and CAE on a digitally mounted complete skeleton. Palaeontologia Electronica 13(2):1–26.

Mallison, H. 2010b. The digital *Plateosaurus* II: An assessment of the range of motion of the limbs and vertebral column and of previous reconstructions using a digital skeletal mount. Acta Palaeontologica Polonica 55(3):433–458.

Mallison, H. 2011a. Fast moving dinosaurs: why our basic tenet is wrong. Journal of Vertebrate Paleontology (Program and Abstracts 2011):150.

Mallison, H. 2011b. *Plateosaurus* in 3D: How CAD Models and Kinetic–Dynamic Modeling Bring an Extinct Animal to Life; pp. 219–236 in N. Klein, K. Remes, C. T. Gee, and P. M. Sander (eds.), Biology of the Sauropod Dinosaurs - Understanding the Life of Giants. Life of the Past. Indiana University Press, Bloomington, 331 pp.

Mallison, H. 2011c. Rearing Giants: Kinetic–Dynamic Modeling of Sauropod Bipedal and Tripodal Poses; pp. 237–250 in N. Klein, K. Remes, C. T. Gee, and P. M. Sander (eds.), Biology of the Sauropod Dinosaurs - Understanding the Life of Giants. Life of the Past. Indiana University Press, Bloomington, 331 pp.

McMahon, T. A. 1975. Allometry and biomechanics: limb bones in adult ungulates. The American Naturalist 109(969):547-563.

Mezga, A., B. C. Tešović, and Z. Bajraktarević. **2007**. First record of dinosaurs in the Late Jurassic of the Adriatic-Dinaridic Carbonate Platform (Croatia). Palaios 22(2):188–199.

Moser, M. 2003. *Plateosaurus engelhardti* MEYER, 1837 (Dinosauria: Sauropodomorpha) aus dem Feuerletten (Mittelkeuper; Obertrias) von Bayern. Zitteliana, Reihe B 24:1–188.

Muybridge, E. 1899. Animals in Motion. Chapman & Hall, London, 264 pp.

Pfau, T., E. Hinton, C. Whitehead, A. Wiktorowicz-Conroy, and J. R. Hutchinson. **2011**. Temporal gait parameters in the alpaca and the evolution of pacing and trotting locomotion in the Camelidae. Journal of Zoology 283(3):193–202.

Preuschoft, H., B. Hohn, S. Stoinski, and U. Witzel. **2011**. Why so huge? Biomechanical Reasons for the Acquisition of Large Size in Sauropod and Theropod Dinosaurs; pp. 197–218 in N. Klein, K. Remes, C. T. Gee, and P. M. Sander (eds.), Biology of the Sauropod Dinosaurs - Understanding the Life of Giants. Life of the Past. Indiana University Press, Bloomington, 331 pp.

Preuschoft, H., H. Witte, A. Christian, and S. Recknagel. **1994**. Körpergestalt und Lokomotion bei großen Säugetieren. Verhandlungen der Deutschen Zoologischen Gesellschaft 87(2):147–163.

Ren, L., M. Butler, C. Miller, H. Paxton, D. Schwerda, M. S. Fischer, and J. R. Hutchinson. **2008**. The movements of limb segments and joints during locomotion in African and Asian elephants. Journal of Experimental Biology 211(18):3057.

Riga, B. J. 2011. Speeds and stance of titanosaur sauropods: analysis of *Titanopodus* tracks from the Late Cretaceous of Mendoza, Argentina. Anais da Academia Brasileira de Ciências 83(1):279–290.

Romano, M., M. A. Whyte, and S. J. Jackson. **2007**. Trackway ratio: a new look at trackway gauge in the analysis of quadrupedal dinosaur trackways and its implications for ichnotaxonomy. Ichnos 14(3-4):257–270.

Sander, P. M. 2013. An evolutionary cascade model for sauropod dinosaur gigantism - overview, update and tests. PLoS ONE 8(10):1–23.

Sander, P. M., A. Christian, M. Clauss, R. Fechner, C. T. Gee, E.-M. Griebeler, H.-C. Gunga, J. Hummel, H. Mallison, S. F. Perry, H. Preuschoft, O. W. M. Rauhut, K. Remes, T. Tütken, O. Wings, and U. Witzel. **2011**. Biology of the sauropod dinosaurs: the evolution of gigantism. Biological Reviews 86:117–155.

Sander, P. M., and M. Clauss. **2008**. Sauropod gigantism. Science 322(5899):200–201.

Santos, V. F., J. J. Moratalla, and R. Royo-Torres. **2009**. New sauropod trackways from the Middle Jurassic of Portugal. Acta Palaeontologica Polonica 54(3):409–422.

Santos, V. F. d., M. G. Lockley, C. A. Meyer, J. Carvalho, A. Galopim de Carvalho, and J. J. Moratalla. **1994**. A new sauropod tracksite from the Middle Jurassic of Portugal. Gaia: Revista de Geociências 10:5–13.

Schanz, T., Y. Lins, H. Viefhaus, T. Barciaga, S. Läbe, H. Preuschoft, U. Witzel, and P. M. Sander. **2013**. Quantitative interpretation of tracks for determination of body mass. PLoS ONE 8(10):1–12.

Sellers, W. I., P. L. Manning, T. Lyson, K. Stevens, and L. Margetts. **2009**. Virtual palaeontology: gait reconstruction of extinct vertebrates using high performance computing. Palaeontologia Electronica 12(3):1–26.

Sellers, W. I., L. Margetts, R. A. Coria, and P. L. Manning. **2013**. March of the titans: the locomotor capabilities of sauropod dinosaurs. PLoS ONE 8(10):1–21.

Soergel, W. 1925. Die Fährten der Chirotheria: Eine paläobiologische Studie. Verlag von Gustav Fischer, Jena, 92 pp.

Stevens, K. A., S. Ernst, and D. Marty. **2016**. Uncertainty and Ambiguity in the Interpretation of Sauropod Trackways; pp. 226–242 in P. L. Falkingham, D. Marty, and A. Richter (eds.), Dinosaur Tracks - The Next Steps. Life of the Past. Indiana University Press, Bloomington, 413 pp.

Thompson, M. E., R. S. White, and G. S. Morgan. **2007**. Pace versus trot: can medium speed gait be determined from fossil trackways? New Mexico Museum of Natural History and Science Bulletin 42:309–314.

Thulborn, R. A. 1982. Speeds and gaits of dinosaurs. Palaeogeography, Palaeoclimatology, Palaeoecology 38:227–256.

Thulborn, T. 1990. Dinosaur Tracks. Chapman and Hall, New York, 410 pp.

Vila, B., O. Oms, À. Galobart, K. T. Bates, V. M. Egerton, and P. L. Manning. **2013**. Dynamic similarity in titanosaur sauropods: ichnological evidence from the Fumanya Dinosaur Tracksite (Southern Pyrenees). PLoS ONE 8(2):1–9.

Weissengruber, G. E., G. F. Egger, J. R. Hutchinson, H. B. Groenewald, L. Elsasser, D. Famini, and G. Forstenpointner. **2006**. The structure of the cushions in the feet of African elephants (*Loxodonta africana*). Journal of Anatomy 209(6):781–792.

Wilson, J. A., and M. T. Carrano. **1999**. Titanosaurs and the origin of "wide-gauge" trackways: a biomechanical and systematic perspective on sauropod locomotion. Paleobiology 25(2):252–267.

CHAPTER 6

The dinosaur scale: interpreting sauropod tracks with a soil mechanical approach for body mass estimation with thoughts on weight distribution among the limbs during walking

6.1. ABSTRACT

Body mass is one of the fundamental attributes of any organism, with sauropod dinosaurs reaching the upper limits of body mass on land. Sauropod body mass estimates range in excess of 80 tonnes and are based either on the reconstruction of the body volume or on scaling relationships between stylopodial measurements and body mass in extant quadrupedal tetrapods. Discrepancies between mass estimates based on volumetric models and those based on scaling relationships are assumed to be related to the low specific density of the sauropod body, which can be accounted for in the former but not in the latter. The low specific density of the sauropod body is inferred from strong evidence for a bird-like lung and extensive postcranial skeletal pneumaticity. Hence, a new approach for estimating the body mass is required independently from skeletal material to test the low body density hypothesis. In a novel interdisciplinary project using tracks, a third method for estimating sauropod body mass was developed by estimating the weight of a sauropod trackmaker. Footprints of sauropod dinosaurs are globally distributed in Mesozoic deposits and are of remarkable size owing to their gigantic trackmakers. Considerable paleobiological information has been gleaned from tracks, such as body dimensions and behavior of the trackmaker.

It was reasoned that each footstep of a trackmaker deforms the substrate and that this deformation can be quantitatively modelled using soil mechanical finite element analysis (FEA). Here, a case study is present based on the well-known "turning sauropod" trackway from the Copper Ridge Dinosaur tracksite (also known as Valley City site) in the Upper Jurassic Morrison Formation, Eastern Utah, USA. For the FEA, trackway parameters and footprint dimensions were obtained from photogrammetric 3D models, properties of the deformed sediment were analyzed in petrographic thin sections, and experimental soil mechanical input parameters were obtained from comparable recent river sediment. Next,

several loading conditions were applied in the FEA to model substrate deformation as observed in the Copper Ridge footprints. To calculate body weight from a single footprint, weight distribution among the limbs during locomotion has to be taken into account and can be inferred from the footfall pattern in the trackway. The resulting weight estimate for the Copper Ridge trackmaker is approximately 16 tonnes, which is in good agreement with weight estimates for probable trackmakers known from body fossils, for example, the common Morrison sauropod *Diplodocus*. By offering a novel approach for estimating the weight of extinct tetrapods, this study extends the range of paleobiological information contained in vertebrate tracks. This research started with sauropod dinosaurs because they are easily approximated in terms of kinematics and foot anatomy. This method provides a first step to obtain body masses of extinct tetrapods only known from scanty skeletal material.

6.2. INTRODUCTION

6.2.1 Body mass of sauropod dinosaurs

Paleobiological research has provided a great deal of information about the extinct group of sauropod dinosaurs, which brought them, in a broader sense, back to life. All sauropods had a similar bauplan: they were quadrupedal and graviportal with massive pillar-like limbs (Upchurch, 1995; Wilson and Sereno, 1998; Curry Rogers and Wilson, 2005). Some species of this highly diverse group of herbivorous dinosaurs evolved into gigantic forms, which apparently was a selective advantage in their evolution (Sander and Clauss, 2008; Klein et al., 2011; Sander et al., 2011). For all studies of sauropod dinosaurs and other extinct animals, the estimation of the body mass is of general interest. Sauropod dinosaurs were reaching the upper limits of body mass on land, which extended over three orders of magnitude. *Europasaurus* (Sander et al., 2006) was one of the smallest sauropods and had a reconstructed body weight of about 800 kg. This was lightweight compared to mass estimates of 120 metric tonnes for *Amphicoelias* (Carpenter, 2006), which demonstrates the gigantic proportions of this extinct group of dinosaurs.

There are two main techniques to estimate the mass of an extinct animal, including sauropods: the reconstruction of the body volume with a specific density or the scaling relationship of stylopodial dimensions. The common approach is to calculate body mass from an estimated body volume. An early attempt was performed by Colbert (1962) using reduced-scale physical models of dinosaurs. More recently, technological progress has enabled the capture of life-size skeletons with laser scanning or photogrammetry to generate three-dimensional (3D) reconstructions (Gunga et al., 2007; Gunga et al., 2008) or a numerical model for determining the volume of the animal (Henderson, 1999). Considering the specific density for a body volume, mass calculations with the convex hull method were utilized by Sellers et al. (2012). Anderson et al. (1985) established a scaling relationship of

the circumference of the long bones, which carry the weight of the animal, in relation to the body mass in extant and extinct tetrapods and birds. This approach was refined by Campione and Evans (2012).

Owing to the chosen methodology for body mass determination, the differences can be substantial. For instance for the taxon *Diplodocus*, Anderson et al. (1985) estimated a mass of 9061 kg based on long bones, whereas Seebacher (2001) calculated 19,655 kg with a volume-based method, assuming a bulk density of 1000 kg/m³ based on Alexander (1989). The different mass estimates of sauropods may be explained by the possibility of low specific density of the body. This is supported by pneumaticity in the neck and in the pelvis, and an assumed respiratory anatomy with extensive air sacs, similar to that of birds (Wedel, 2003; Wedel, 2009; Wedel and Taylor, 2013; Melstrom et al., 2016). In the volumetric approach for sauropod mass estimation by Henderson (2004), low specific densities were assumed for the neck (600 kg/m³) and the trunk (850 kg/m³) to account for lungs and air sacks. These assumed densities, similar to that of birds, lower the volumetric body mass estimates of sauropod dinosaurs. Even though pneumaticity in sauropods has been demonstrated, it is yet not quantifiable. Therefore, another approach is required to infer body mass independently from body fossils. A new method of weight estimation using tracks and trackways is shown here based on the concept of substrate deformation resulting from the loads applied by the trackmaker.

6.2.2 Dinosaur tracks

During their lifetime, dinosaurs left many tracks behind that provide valuable information for paleobiologists. Unlike bony remains, tracks allow us to study the dinosaurian trackmaker as living beings, which include, for example, size, behavior and movement. Another benefit of tracks is that they are autochthonous, indicating the original living habitat of the trackmaker (Mannion and Upchurch, 2010); in contrast, the osteological fossil record is often biased due to transportation of the material. This makes tracks very valuable not only for understanding the paleobiology of a trackmaker but also for the reconstruction of the paleoenvironment.

Fossil tracks can be thought of as petrified movement of the trackmaker, providing information about locomotion, such as footfall pattern, track depth, and walking direction. Also, biometrical information can be obtained from tracks, such as estimates of the trackmaker's hip height and body length, or the foot anatomy, such as, the number and size of the digits (Thulborn, 1990; Lockley, 1991b). From measurements of step and stride lengths in the trackway, speeds can be estimated (Alexander, 1976; Thulborn, 1990). Although tracks offer many valuable insights, it has to be kept in mind that track interpretation is often uncertain and ambiguous (Stevens et al., 2016). One complicating fact is that dinosaur tracks are often preserved as undertracks. The original track surface is not present anymore or

weathered, which might affect further interpretations (Thulborn, 1990; Lockley, 1991b; Milàn and Bromley, 2006).

The largest dinosaur tracks were produced by the gigantic sauropod dinosaurs. The first studies on sauropod tracks regarded the famous tracksites of the Glen Rose Formation, Texas, USA, by Roland T. Bird in the first half of the 20th century (Bird, 1939; Bird, 1944; Farlow et al., 2012). Sauropod tracks can be found in Triassic (Lallensack et al., submit.; Lockley et al., 2001) to Cretaceous sediments all over the globe (Wright, 2005; Mannion and Upchurch, 2010; Falkingham et al., 2012), in both cohesive (e.g., mudstones) and non-cohesive (e.g., sandstones) sediments, which indicates that they lived in a broad range of environments, such as coastal and continental habitats (Mannion and Upchurch, 2010; Falkingham et al., 2012). Sauropod tracks were divided into two categories: the wide-gauge and the narrow-gauge trackway type (Farlow, 1992; Wilson and Carrano, 1999; Wilson, 2005), but recent studies question this strict distinction based on changes from narrow to wide-gauge and vice versa that have been observed within trackways (Romano et al., 2007; Marty, 2008; Santos et al., 2009; Castanera et al., 2012). Many authors have studied and described sauropod tracks based on the explained features above, for example, *Brontopodus* (Farlow et al., 1989) and *Parabrontopodus* (Lockley et al., 1994) are just two of numerous sauropod ichnotaxa to be mentioned. The heteropody index (HI; see methods section) is used for sauropod tracks and calculated from the ratio of manus and pes track measurements (Lockley, 1989; Lockley et al., 1994; Santos et al., 1994; Santos et al., 2009). *Parabrontopodus* is the narrow-gauged, high HI (manus/pes ratio about 1/5 to 1/3) taxon attributed to non-macronarian neosauropods, and *Brontopodus* is the wide-gauged, low HI (manus/pes ratio about 1/2) taxon attributed to macronarians (Farlow, 1992; Lockley et al., 1994; Wilson and Carrano, 1999; Wilson, 2005).

6.2.3 Interpretative approaches on tracks

Apart from purely descriptive and taxonomic research on fossil footprints, a quantitative interpretation of tracks with analytical methods is of interest today (Falkingham et al., 2016a). New techniques and approaches for understanding track formation include experiments with living animals (e.g., Milàn, 2006; Platt et al., 2012), experiments under laboratory conditions (e.g., Manning, 2004; Jackson et al., 2009, 2010; White et al., 2017) or computer-assisted simulations (e.g., Henderson, 2006; Falkingham et al., 2011b; Falkingham et al., 2014). All of these studies were also focusing on substrate interactions that influence track formation. According to Falkingham (2014), a track is always a combination of three different factors, namely the substrate that bears the track (i.e., the soil or sediment), the anatomy, and the dynamical component of force exerted by the trackmaker, which also will be studied and discussed in this investigation.

An elaborate way to understand and interpret track formation is finite element analysis (FEA). FEA is a numerical method, which allows a computer-assisted simulation of physi-

cal processes. A 3D object is split up into a finite number of small elements, which are connected via nodes. The method had been often applied to biomechanical questions in paleontology (Bright, 2014), such as reconstructions of bite forces in dinosaurs (e.g., Lautenschlager, 2013; Bates and Falkingham, 2012). In soil mechanics and foundation engineering, FEA is applied to simulate the stress-strain behavior of the substrate and to determine vertical displacements (settlements), for example, in building construction sites (German Geotechnical Society, 2014). Some of these soil mechanical approaches had been applied to the study of dinosaur tracks. Margetts et al. (2005) and Margetts et al. (2006) used a method from geotechnical engineering to model theropod tracks in an elasto-plastic model. The authors found through FEA modelling that shape and depth vary in undertracks through several layers of substrate. Falkingham (2010) and Falkingham et al. (2011b) have analyzed several substrate parameters, such as shear strength, Poisson ratio or Young's modulus, to simulate dinosaur tracks with FEA and concluded that a substrate needs to have the right composition to generate and to preserve tracks. Moreover, Falkingham et al. (2011a) incorporated estimates on the position of the center of mass (CM) for the simulation of manus-only sauropod tracks. Bates et al. (2013) modeled hominin footprints to test if footprint depth is equal to the pressure exerted by the trackmaker. They found a correlation but also found many other factors that influence the track depth. A similar method to Schanz et al. (2013) and the present work was applied by Sanz et al. (2016) without the aim of mass estimation. The authors investigated sauropod tracks from the Early Cretaceous Miraflores I tracksite, Spain, and simulated them by using 3D FEA based on soil mechanical principles with the focus on sedimentological features.

By applying FEA and soil mechanical principles on footprints of a living African elephant, Schanz et al. (2013; Chapter 3) proposed a method for determining the body mass from tracks by modeling the load of the trackmaker on a simulated substrate. Although additional experimental data, such as an additional elephant and the use of different substrates, was desirable, the method itself was a valuable contribution, since the application of soil mechanical concepts has a great potential for the analysis of tracks, as it will be shown in this chapter.

6.2.4 The dynamic component in tracks

The underlying premise for the research presented here is that tracks are a result of the combination of different mechanics of the trackmaker, namely statics and dynamics, and the stiffness of the substrate material (cf. Falkingham, 2014; Margetts et al., 2005). The force exerted by the trackmaker on the substrate is a combination of a vertical component and a horizontal component, which are in equilibrium with the ground reaction force (GRF) during ground contact of the limbs (stance phase).

The body mass of the trackmaker causes substrate deformation by the action of the vertical static force. Besides the static force component, the dynamics of the trackmaker include

the kinetics and the kinematics. Kinematics refers to the speed, acceleration and deceleration of the trackmaker in the horizontal direction. It is the movement itself without any effect of force. Kinematics of the trackmaker can sometimes be inferred from its footprints, specifically from deep tracks (Gatesy et al., 1999). Kinetics refers to the accelerated moving mass of the trackmaker, which also affects track formation.

All of these mechanical components exerted by the trackmaker, represented as stress and strain in combination with the stiffness of the substrate material, produce a particular plastic deformation that we observe as the footprint. Hence, both the weight and the locomotion of the trackmaker play an important role in track formation. The relationship of stress and footprint formation has often been discussed before, since it is a general assumption that the relief of a footprint correlates with the stress exerted from the trackmaker's foot and that higher speeds cause greater stress on the substrate, which in turn causes deeper tracks (Demathieu, 1987; Manning, 2004; Bates et al., 2013). Alexander (1985) assumed that the stress exerted on the ground during walking has to be twice as high than the stress from standing.

Dinosaur tracks have often been used for studying the locomotion of the trackmaker and to determine the gait. For sauropod dinosaurs, the *pace* had been proposed by several studies as possible gait (Casanovas et al., 1997; Sellers et al., 2013; Vila et al., 2013). The pace is a two-beat rhythm gait with the ipsilateral (same side of the body) forefoot and hindfoot in ground contact at the same time according to terminology of Hildebrand (1965; 1980; 1989). Another approach to determine the gait was to reconstruct sauropod trackways with computer models based on the position of the CM (Henderson, 2006). This study confirmed that *Brachiosaurus* was the trackmaker of wide-gauge trackways and *Diplodocus* produced narrow-gauged trackways according to previous research (Farlow, 1992; Wilson and Carrano, 1999). Speed estimations based on trackways (Alexander, 1976, 1989; Thulborn, 1990; Lockley, 2007) and on limb proportions in sauropods skeletons (Christian et al., 1999) indicate slow walking with speeds of around 5 km/h. This also ties in with the general consideration that sauropod locomotion was constrained by the two aspects of safety and stability that most likely limited rapid locomotion in these gigantic animals. For a heavy sauropod, the vertical force from its mass increases faster than from the horizontal force of its movements, due to the principles of inertia. This means that the angle of excursion of the limbs has to be narrower, which results in shorter step lengths (Preuschoft et al., 2011). Consequently, sauropods might have moved in a walking locomotion, which is why the dynamic component, such as observed in gaits with aerial suspension, was very small in the case of the studied sauropod trackway.

The study by Schanz et al. (2013; Chapter 3) employed two factors for the assessment of the dynamical component of force exerted by the elephant trackmaker. First, one factor was used for weight distribution among the limbs, which was determined from empirical

weight measurements, whereby the weight fractions borne on limbs were divided by the total weight of the trackmaker. The second factor was derived from digital image correlation and video recordings of the walking elephant to determine the velocity vectors of the moving limbs. Since video recordings are not an option for evaluating the dynamics of a fossil trackmaker, another approach has to be taken. Läbe (unpubl.) introduced the adapted weight distribution factor f_{wd^*} to describe the peak load during walking. In contrast to the weight distribution factor in the study by Schanz et al. (2013), the factor f_{wd^*} was theoretically calculated for different possible positions of the CM of a sauropod trackmaker and all possible types of limb support of the limbs during the movement. This requires a rough identification of the trackmaker to assess the position of the CM and an approximation of the trackmaker's gait from trackway measurements to obtain possible types of limb support. In doing so, the dynamic component exerted by the trackmaker can be approximated. The values for the position of the CM were adapted from Henderson (2006), with a posterior CM position of 11.5% for *Diplodocus* and more anteriorly positioned CM of 37.4% for *Brachiosaurus* (given as percentages of the glenoacetabular distance).

6.2.5 Purpose of this study

The purpose of this study is to simulate loads from substrate deformation in sauropod tracks with FEA in order to estimate the mass of a sauropod trackmaker, using fossil tracks from the Jurassic Copper Ridge Dinosaur tracksite (Utah, USA) as a case study. Photogrammetric models of the original tracks provided measurements for a detailed geometry needed for the FEA model. To obtain the soil mechanical input parameters required for the FEA, such as stiffness, friction angle, and dilatancy, recent fluvial sediments were characterized as an analog to the lithified substrate of the Copper Ridge track-bearing surface. This project is based on the work of Schanz et al. (2013) on recent elephant footprints and on preliminary work by Läbe (2014). This study differs from Schanz et al. (2013), since fossil tracks are simulated for the purpose of weight estimation, and it also has a different scope than the study by Sanz et al. (2016), since it focusses more on the portion of locomotion during track formation, and the material model used in this study is more advanced. The weight estimation method here requires an interdisciplinary approach of multiple methods from paleontology, geology, biomechanics and soil mechanical engineering.

6.3. METHODS AND MATERIALS

The current interdisciplinary investigation involved methods from geosciences and engineering, like photogrammetry, sediment analysis, soil mechanical FEA, and considerations on biomechanics of sauropods. Concerning the terminology, the terms *track* and *imprint* are generally used for substrate deformation formed by both, single or multiple *pes/pedēs* (foot) or *manus/manūs* (hand). The term *trackway* is here used for a sequence of multiple imprints/tracks of one trackmaker. The term *substrate* is specific for the medium that con-

tains the tracks. Since this is a multi- and interdisciplinary approach, substrate can represent both, the *sediment* from geological view, as well as *soil* from soil mechanical view. In general, the track terminology used here follows that of Marty et al. (2016).

6.3.1 Sauropod tracks of the Copper Ridge Dinosaur tracksite

The Upper Jurassic Copper Ridge Dinosaur tracksite investigated in this study is located north of the town of Moab, close to the Arches National Park, Utah, USA (Figure 6.1, GPS coordinates: 38°49'54.1"N 109°45'43.6"W). The site offers information for visitors and is located on BLM Land (Bureau of Land Management; further information can also be obtained from the BLM office in Moab). The Copper Ridge Dinosaur tracksite, which is also known as "Valley City" was discovered in 1989 (Lockley, 1991b; Lockley and Hunt, 1995; Foster, 2015; Hunt-Foster et al., 2016; on-site information). The fluvial, ripple-bedded, reddish sandstone of the tracksite belongs to the Salt Wash Member of the Morrison Formation and is assumed to be Kimmeridgian in age. The paleoenvironment might have been a sandy braided river (Foster and Lockley, 2006; Foster, 2015). The 15 cm thick track-bearing sandstone is underlain by a layer of reddish silty mudstone with a thickness of about 30 cm. Three trackways of theropods are found on the track surface, but a sauropod trackway is particularly prominent, as it even shows a change in direction of 60° (Ishigaki and Matsumoto, 2009). The sauropod trackway was referred to as a "brontosaur" trackway by Lockley and Hunt (1995). As already seen in the field, the preservation of the sauropod tracks is poor, which might be due to decades of exposure since the discovery of the tracks. The sauropod trackway was considered to consist mainly of pes imprints with the manus imprints being overprinted. By applying the technique of vertical exaggeration to the photogrammetric 3D models of the tracks, additional manus imprints could be revealed (Läbe, in revision; Chapter 2).

Although the Copper Ridge Dinosaur tracksite is poor in preservation, there are several reasons why this tracksite was chosen for this study. First, the tracksite is well-know from multiple publications and is located in the famous Morrison Formation (Foster, 2007), from which a potential sauropod trackmaker could eventually be narrowed down from the comparison with skeletal material. In other sauropod tracksites, for example, the Barkhausen tracksite (Läbe, in revision; Kaever and de Lapparent, 1974; Friese, 1979; Lockley et al., 1994) or the Münchehagen tracksite (Hendricks, 1981; Fischer, 1998; Lockley et al., 2004), skeletal material is very rare, and thus it is not possible to know which possible sauropods could produce the tracks. And second, sauropod trackways consisting of multiple pes and manus tracks that are found in non-cohesive substrates, as required for this approach, are very rare (Falkingham et al., 2012; suppl.). Hence, the Copper Ridge Dinosaur tracksite offers the benefits of possibly identifying the trackmaker and an ideal substrate for this approach, which justifies the choice of this tracksite despite the poor preservation.

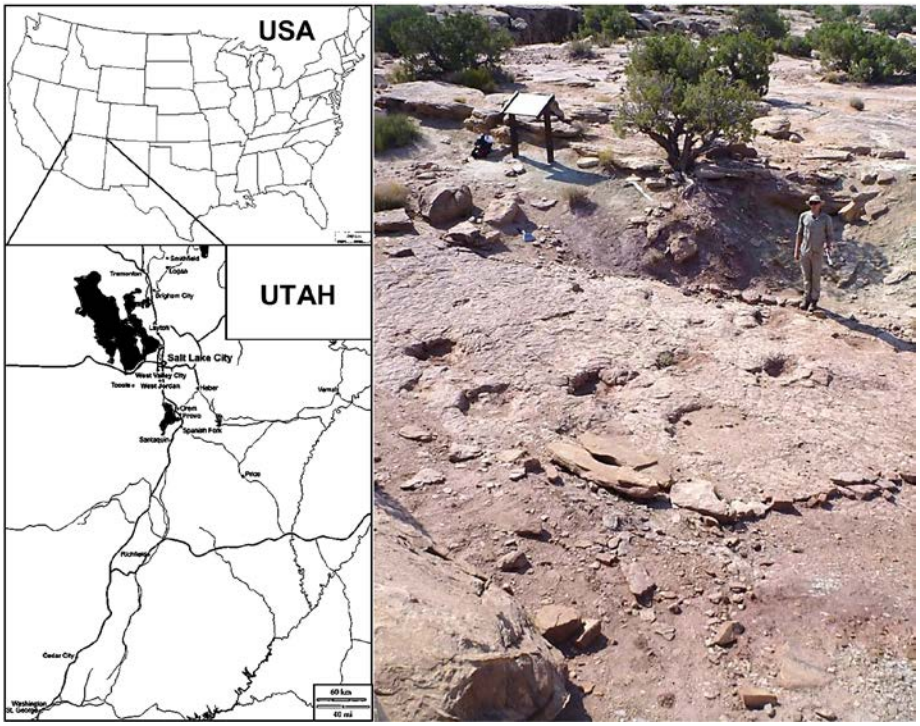

Figure 6.1: The Copper Ridge Dinosaur tracksite is located near Moab, Utah, USA. The tracksite (left) contains a sauropod trackway and several theropod trackways (person in picture is 185 cm). The sauropod trackmaker changed direction and the trackway is curved with 60°.

6.3.2 Documentation and measurements

Photogrammetry is a technique for the generation of 3D models using photos of an object. This method was used to digitize the Copper Ridge sauropod trackway (Figure 6.2; see Chapter 2). It has become the method of choice among dinosaur ichnologists when a fast, non-destructive, and effective method for digitization is needed (Falkingham, 2012; Mallison and Wings, 2014; Matthews et al., 2016). The Copper Ridge sauropod trackway was captured by over 100 photographs from different positions and angles to obtain complete coverage of the trackway. The photos were taken in two different sessions. The first session was aimed to capture the best-preserved individual footprints of the sauropod trackway and to evaluate, if the locality is suitable for this study. For that purpose, a DSLR (Canon EOS 500D) was utilized. In another photo session, the entire sauropod trackway was photographed with a consumer camera (Panasonic DMC-FT3) and was documented according to the illustration by Ishigaki and Matsumoto (2009). Compared to previous interpretations (Lockley, 1991a, Figure 6.4.; Lockley and Hunt, 1995, Figure 4.45) of the Copper Ridge sauropod trackway, not all tracks were still observable, as the first right footprint and the last left footprint are now covered by fallen rocks and debris.

The 3D models of the Copper Ridge Dinosaur tracksite were generated with the commercial software Agisoft PhotoScan 1.2.0 Professional Edition (www.agisoft.com) based on a practical guide for paleontological use of photogrammetry by Mallison and Wings (2014). The sparse point cloud consists of 288,533 points and the dense point cloud of

116,897,747 points. Using the ultra-high reconstruction settings in the software and a powerful workstation computer (Windows 10, Intel Core i7 CPU 3.60 GHz, 64 GB RAM, 2x NVIDIA Geforce GTX 690 graphics board) the calculation of the model took 8.5 hours. To better visualize the individual imprints and to improve interpretability of the model in general, further manipulation of the 3D models were undertaken (Läbe, in revision; Chapter 2). By using the freely available software CloudCompare, v. 2.5.3.beta (www.danielgm.net/cc), and ParaView, v.4.2.0. (www.paraview.org), a color depth map of the model was generated to better illustrate the topography of the trackway (Figure 6.2A). Using the open-source software Image J (www.imagej.net/ImageJ), each imprint was measured from the color depth map. To determine an accurate depth, the tracks were measured in lateral view parallel to walking direction. To determine width and length, the tracks were measured in a top-down view. From these measurements, the HI was calculated. The HI was used to determine a possible position of the CM and whether the trackway was manus or pes dominated (cf. Henderson, 2006; Lockley, 2007; Falkingham et al., 2011a), which are relevant for identifying the possible trackmaker. The speed of the trackmaker was roughly estimated using Alexander's formula $v = 0.25g^{0.5} \cdot s^{1.67} \cdot h^{-1.17}$, where v is the speed [m/s], g [m/s²] is the acceleration of gravity, s [m] is the stride length measured from the trackway, and h [m] is the hip height (Alexander, 1976). The hip height was estimated based on pes track length PL by applying the formula $h \sim 4PL$ (Alexander, 1976).

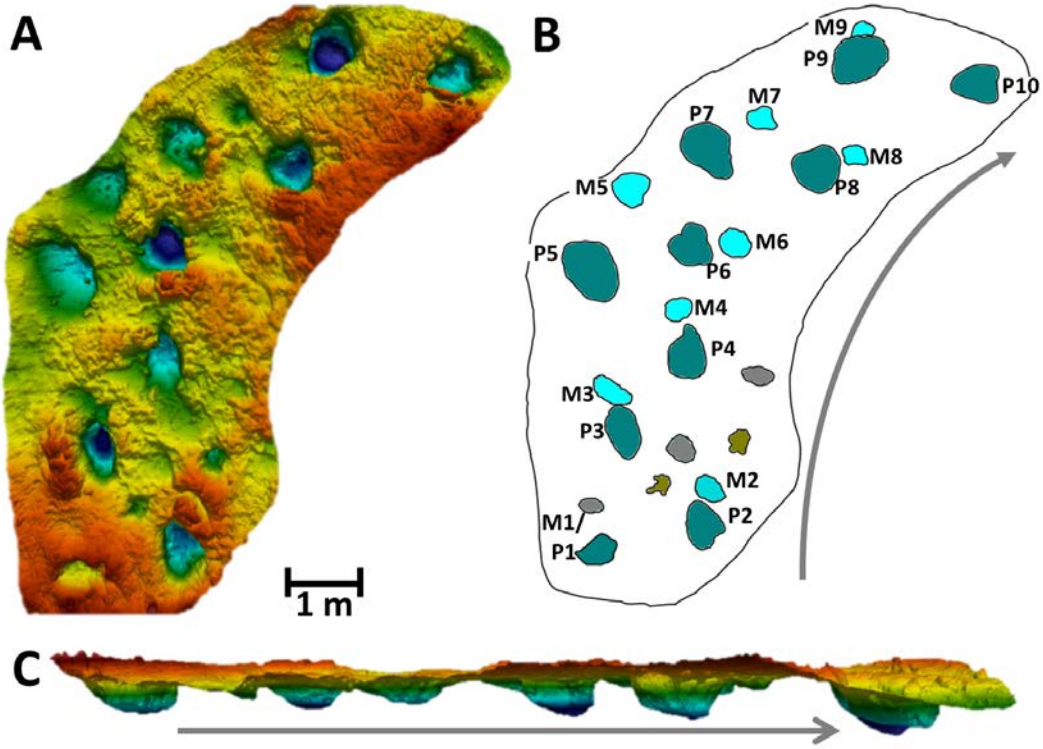

Figure 6.2: 3D models and sitemap of Copper Ridge sauropod trackway (see Läbe, in revision; Chapter 2). A. Color depth map with 5x vertical exaggeration to better visualize the individual tracks (blue = deep, red = high). B. Sitemap of the trackway (manus = light blue, pes = dark blue, tracks in other colors do not

belong to the trackway). Abbreviations: P = pes, M = manus. C. The lateral view of the 3D model shows walking direction (arrow), since the anterior part is always deeper imprinted than the posterior part.

6.3.3 Sediment analysis of the Copper Ridge sandstone and a comparable recent analog from the Moselle River

A rock sample of the track-bearing surface of the Copper Ridge Dinosaur tracksite was analyzed by classical thin section analysis. Thin sections of the sandstone were studied and documented by light microscopy with plane and cross-polarized light using a compound microscope (Leica DMLP polarizing microscope with Leica DFC420 camera). Images of the sedimentary thin sections were analyzed with Image J to determine the grain size distribution with particle analysis (Figure 6.3). The particle analysis with Image J is based on area of the grains, and not on mass. The author is aware that this method might not be as precise as in the conventional grain size analysis (sieving), but the results are sufficient for the aims of this study.

The curvature $C_c = d_{30}^2/(d_{10} \cdot d_{60})$ and the uniformity $C_u = d_{60}/d_{10}$ of the substrate are based on values d (Figure 6.3), which were determined for $d_{10} = 10\%$, $d_{30} = 30\%$ and $d_{60} = 60\%$ of grains in the grain size distribution of the sample. For the track-bearing layer of the Copper Ridge Dinosaur tracksite, the curvature was found to be $C_c = 0.95$ and the uniformity was $C_u = 2.7$, so that the sample was evaluated to be a unimodal, poorly sorted, fine sand.

For comparison with the track-bearing sandstone at Copper Ridge and to obtain input parameters needed for the numerical simulation of sauropod footprints, recent fluvial sediments were analyzed. Sediment samples were collected from a point bar deposit at the Moselle River, near the village Neef, Germany (GPS coordinates: 50°06'18.0"N 7°07'21.0"E). In total, three different samples were collected to infer the substrate parameters for the FEA with a soil mechanical test: one bulk sample for substrate classification (e.g., grain size analysis), an undisturbed sample in a steel cylinder for determining stiffness in the oedometer test and a short sediment core over the top 12 cm of the sediment. The grain size distribution was determined (DIN 18123, 1996) and is illustrated in Figure 6.3. The grain size ranges between 0.1 mm and 2 mm. Based on the mass percentage of passing grains in the grain size distribution of the sample, curvature and uniformity were determined. Uniformity ($C_u = 1.9$) and curvature ($C_c = 1.1$) of the Moselle sand indicate that it is a unimodal, moderately well sorted, medium sand. The density of the sand was determined (DIN 18126, 1996), whereby the loosest density was ρ_{min} = 1.23 g/cm³, and the densest density of the sediments was ρ_{max} = 1.56 g/cm³. From that, void ratios were calculated. The loose void ratio was found to be $e_{max} = 1.14$ and the dense void ratio was $e_{min} = 0.69$.

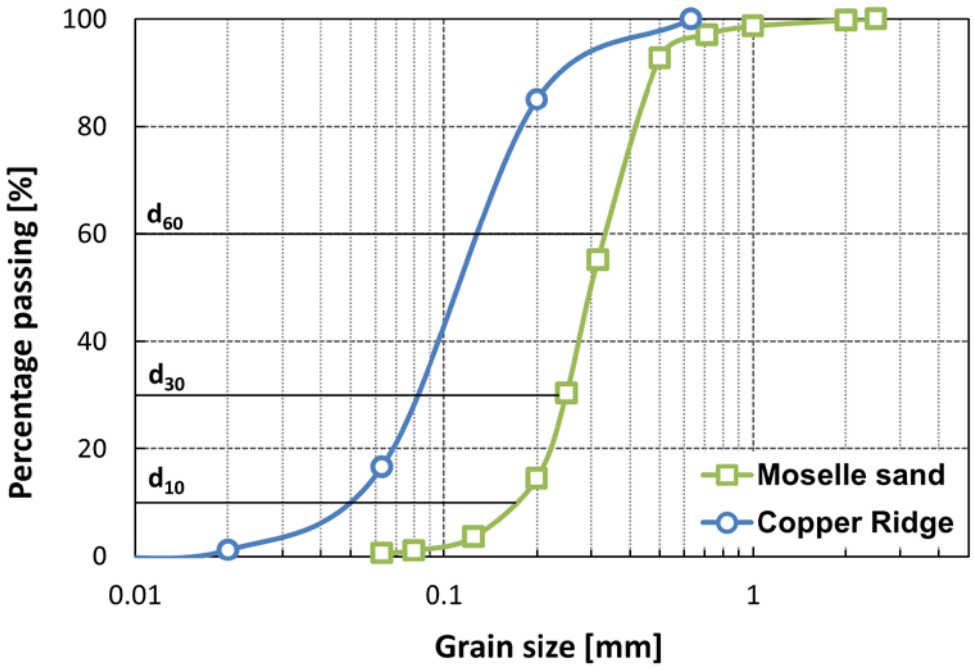

Figure 6.3: Comparison of the grain size distribution for the fossil Copper Ridge sandstone (blue circles) and the recent Moselle sand (green rectangles). The values d are determined for 10%, 30%, and 60% of the sample and required for the characterization parameters curvature and uniformity of the sample.

6.3.4 Determination of input parameters and model geometry for FEA

FEA was employed to back-calculate stresses that caused substrate deformation as observed in the tracks of the Copper Ridge Dinosaur tracksite by using the commercial software Plaxis 3D (www.plaxis.com), which is a common tool for geotechnical applications. The meshed substrate volume generated for FEA was 4.2 m in width and length, and 2.1 m in depth (Figure 6.4). A length and depth three times the average track diameter, taken from measurements of the 3D model, were chosen, because these dimensions are slightly larger than the maximum effect in each lateral direction and potential settlements in vertical direction. Otherwise, errors from strong interaction with the model margins might occur (German Geotechnical Society, 2014).

From the average area of the Copper Ridge sauropod pes tracks, a circular plate element with an equal area of 0.38 m² was used to approximate the sauropod hindfoot (Figure 6.4). The diameter of the plate element was 70 cm, according to the average length measurements from the original tracks. Although other studies (e.g., Sanz et al., 2016) aimed for a detailed model with a realistic foot shape, for the present work, it was appropriate to approach the sauropod foot by a circular plate element with a comparable area according to Schanz et al. (2013). Interfaces, which are joint elements with slightly different parameters than the volume or the plate element, were placed between the substrate volume and the circular plate element. This was done to simulate a natural pliant movement of the plate element through the substrate volume. In the numerical simulation, vertical stress, repre-

senting the load of the trackmaker, was applied to the substrate volume through the plate element, to infer deformation as observed in the Copper Ridge tracks.

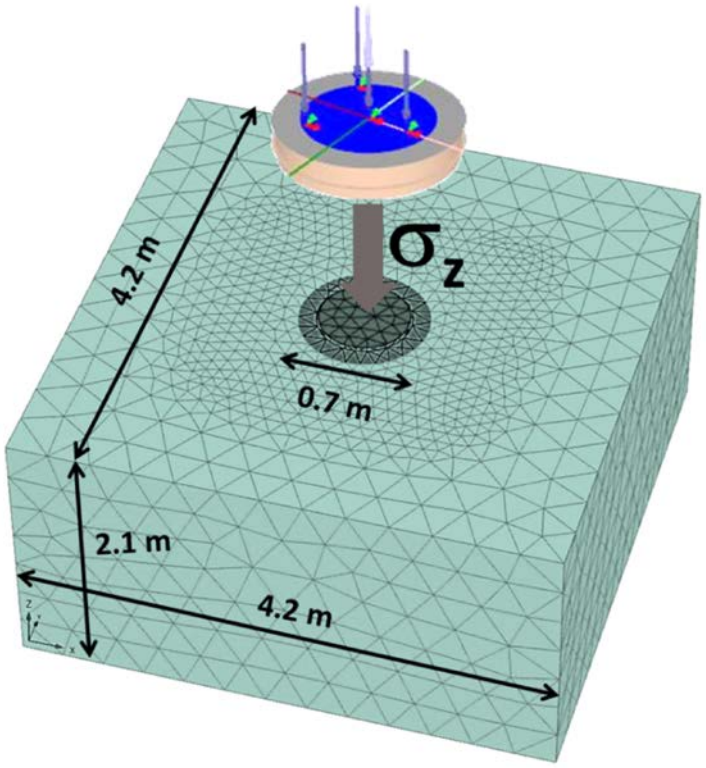

Figure 6.4: Dimensions of the meshed substrate model generated for the FEA in PLAXIS 3D. Measurements were taken from the original track geometry. The circular plate (i.e., the sauropod foot, in blue) was 70 cm in diameter and surrounded by interfaces (beige) to evoke a smooth interaction between the foot and the substrate. In the FEA simulation, vertical stresses σ_z were applied through the circular plate in order to derive settlements (i.e., a footprint).

Substrate properties were assigned to the FEA model, so that the virtual substrate behaves in a natural manner. To obtain a realistic behavior in the simulated substrate, the application of an advanced constitutive material model is crucial (Schanz et al., 2013). While other material models define, for example, a "linear elastic, perfectly plastic" and constant behavior of the material (Mohr-Coulomb material model), the so-called hardening soil model considers pre-loading, also termed the "isotropic hardening" of the soil (Schanz et al., 1999; Schanz et al., 2013). Thereby, continuous stress after initial loading results in a non-reversible plastic strain.

In soil mechanics, the behavior of a substrate is determined by how it reacts to stress, which is the directional application of force to an area, and strain, which is the deformation in the material in response to stress (e.g., compression, expansion, shrinkage, swelling). To determine the required input parameters for the FEA simulation of the footprint deformation as observed in the Copper Ridge Dinosaur tracksite, the recent Moselle sand was examined by two standard laboratory experiments from soil mechanics (Figure 6.5). For that purpose, the one-dimensional compression and rebound test (oedometer) and triaxial

test were conducted. An overview of all parameters derived from these tests and used for the FEA is given in Table 6.1. The workflow of the soil mechanical procedure and the analyses follow Schanz et al. (2013) accordingly.

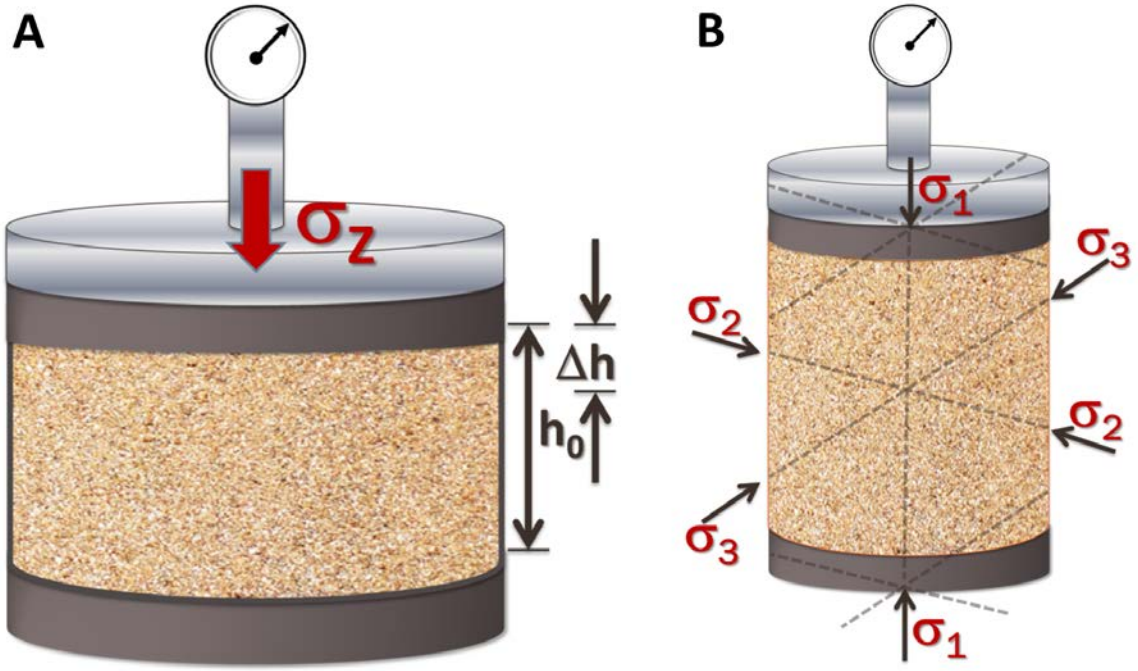

Figure 6.5: Schematic setup of the soil mechanical standard tests. A. In the one-dimensional compression and rebound test (oedometer), a substrate filled steel cylinder was exposed to vertical stress σz without any lateral strain. Changes in height (Δh) were then measured to determine the substrate stiffness for the FEA. B. The triaxial test provides shear parameters (friction angle and dilatancy) needed for the FEA. Lateral stress (σ2 = σ3) is applied on the cylindrical substrate sample placed in a rubber membrane, and the vertical stress σ1 is increased constantly.

The oedometer test is used to analyze compression behavior of a substrate. In this test, a steel cylinder filled with Moselle sand was exposed to vertical stress σ_z without any lateral strain (Figure 6.5A). Stress induced changes in height of the sample were measured to determine substrate stiffness. The parameters inferred from the oedometer test are the stiffness moduli E_{oed} [kN/m²] and E_{ur} [kN/m²] (Schanz and Vermeer, 1998). The experiment was conducted with the Moselle sand for vertical stresses of 25 kN/m^2, 50 kN/m^2, 100 kN/m^2, 200 kN/m^2, 400 kN/m^2, and 800 kN/m^2. The results of the oedometer test are illustrated in Figure 6.6. The tangent stiffness for primary oedometer loading E_{oed}^{ref} and the unloading and reloading stiffness E_{ur}^{ref} were determined from the experimental data at reference stress $\sigma_{ref} = 100$ kN/m^2 (Figure 6.6A).

The data in Figure 6.6A was linearized using the logarithm of both stress and strain with the linear regression given in the plot (Figure 6.6B). The regression analysis from Figure 6.6B is given in Equation (6.1). This term is formulated as a function of E_{oed}^{ref} in Equation (6.1) where α is the slope, β is the intersection with the ordinate and the parameter m is

determined by the slope (Ohde, 1939; Schanz, 1998). Note that the same equation works for the calculation of E_{ur}^{ref}.

$$ln(\varepsilon) = \alpha \cdot ln\left(\frac{\sigma}{\sigma_{ref}}\right) + \beta \quad \rightarrow \quad E_{oed}^{ref} = \frac{1}{\alpha} \cdot \frac{\sigma_{ref}}{e^{\beta}} \quad ; \quad \alpha = 1 - m \tag{6.1}$$

The stiffness moduli E_{oed} and E_{ur} in Equation (6.2) are derived from E_{oed}^{ref} and E_{ur}^{ref} and parameter m after renaming of the terms of Equation (6.1) (Schanz et al., 2013):

$$E_{oed} = E_{oed}^{ref} \cdot \left(\frac{\sigma}{\sigma_{ref}}\right)^{m} \quad E_{ur} = E_{ur}^{ref} \cdot \left(\frac{\sigma}{\sigma_{ref}}\right)^{m} \tag{6.2}$$

With the triaxial test (Figure 6.5B), shear parameters of the substrate were obtained for the FEA. Radial stress $\sigma_2 = \sigma_3$ is applied on a cylindrical substrate sample placed in a rubber membrane, while vertical stress σ_1 is constantly increased. The parameters inferred from the triaxial test are the deviatoric stress E_{50} [kN/m²], the friction angle ϕ [°], and the angle of dilatancy ψ [°] (Schanz and Vermeer, 1996b). The cohesion c [kN/m²] is also inferred from triaxial test, but it can be neglected for a non-cohesive clastic substrate without clay. The triaxial experiment was conducted for stresses of 50 kN/m^2, 100 kN/m^2, and 150 kN/m^2. The results of the triaxial test are illustrated in Figure 6.7. The shear stress $(\sigma_1 + \sigma_3/2)$ versus the effective normal stress $(\sigma_1 - \sigma_3/2)$ is given in Figure 6.7A, where the maximum of each stress condition plots on a linear function, which itself passes through the origin. The slope M_ϕ of the linear function defines the friction angle ϕ, as given in Equation (6.3) (DIN 18137-2, 2011):

$$M_\phi = \sin\phi \tag{6.3}$$

The axial strain (ε_1) is plotted against the deviatoric stress $(\sigma_1 - \sigma_3)$ (Figure 6.7B) to determine the secant stiffness E_{50} [kN/m^2]. The secant stiffness is a parameter describing the initial loading of the substrate (Schanz et al., 1999). E_{50} is determined as the slope of the secant through the origin and the point of 50% of the deviatoric stress at a reference stress of $\sigma_{ref} = 100$ kN/m^2 in Equation (6.4).

$$E_{50} = E_{50}^{ref} \cdot \left(\frac{\sigma_3}{\sigma_{ref}}\right)^{m} \tag{6.4}$$

In Figure 6.7C, the shear strain $(\varepsilon_1 - \varepsilon_3)$ is plotted against the volumetric strain (ε_v). In the beginning of the test, the volumetric strain decreases, as the substrate reacts contractively, but with increasing shear strain the volumetric strain increases as well, meaning that the substrate has a larger volume. The angle of dilatancy ψ of the substrate is determined as the inverse function of the sine (arcsine) of the positive slope M_ψ of the curve (Schanz and Vermeer, 1996a; Equation (6.5)).

$$\sin \psi_{(M>0)} = M_{\psi} \tag{6.5}$$

To optimize the FEA calculation, the substrate parameters obtained from the laboratory experiments were translated into input parameters for the simulation. Therefore, the SoilTest tool in Plaxis was used. The test results were modeled with the software to examine, if the modeled parameters meet the standards of the constitutive material model. The modeled results were fitted with the experimental results to find the best fitting input parameters for the FEA. This step ensures a realistic and natural substrate behavior for a reasonable simulation with FEA.

Table 6.1: Substrate parameters of the recent Moselle sand derived from soil mechanical tests (oedometer and triaxial test) and partly adapted input parameters (SoilTest) for the FEA.

	Unit	Test	Substrate parameter	Input parameter
E_{oed}^{ref}	kN/m^2	oedometer	7700	7000
E_{ur}^{ref}	kN/m^2	"	39.08 E3	-
m	[-]	"	0.578	-
E_{50}^{ref}	kN/m^2	triaxial	4900	4800
ϕ	[°]	"	35.6	36.5
ψ	[°]	"	2.63	-
c	kN/m^2	"	0	-
σ_{ref}	kN/m^2	-	100	-

6.3.5 Calculation of trackmaker weight

The FEA will provide loads, which can be transformed into a weight estimate. The load σ_{FEA}, which caused vertical displacements in the simulation as observed in the Copper Ridge tracks, includes both the static component of force exerted by the trackmaker weight and dynamic component from trackmaker locomotion. Hence, the load from the trackmakers weight σ_{TM} is dependent on the relationship of σ_{FEA} to the factor for weight distribution f_{wd^*} according to Equation (6.6).

$$\sigma_{TM} \sim \frac{\sigma_{FEA}}{f_{wd^*}} \tag{6.6}$$

To link the load to the weight of the trackmaker, two other basic equations from mechanics are needed. First, the force F[N] is determined by the maximum load $\sigma[kN/m^2]$ and the area A [m^2] in Equation (6.7), and second, the kinetic relation of force F is determined by acceleration of gravity g [m/s^2] and mass m [kg] in Equation (6.8):

$$F = \sigma \cdot A \tag{6.7}$$

$$F = m \cdot g \quad \rightarrow \quad m = F/g \tag{6.8}$$

Equations (6.6), (6.7) and (6.8) were resolved to form Equation (6.9) (cf. Schanz et al., 2013; Chapter 3, Equation 3.8) and the factor f_{wd^*} was incorporated into the equation, since the weight of the trackmaker is continuously re-distributed among the limbs during locomotion. Thereby, force F is eliminated from the equation, so that the mass of the trackmaker m_{TM} is determined by σ_{FEA} derived from the FEA for observed track depth, the area of the footprint $A_{FP} = \pi \cdot (d/2)^2$, whereby the diameter of the foot is $d = 0.7\,m^2$ according to Table 6.3, and the acceleration of gravity g=9.81 m/s²:

$$m_{TM} = \frac{\sigma_{FEA} \cdot A_{FP}}{g \cdot f_{wd^*}} \tag{6.9}$$

Table 6.2: Factors f_{wd^*} for one sauropod hindfoot calculated from the weight distribution among limbs during locomotion (Läbe, unpubl. ; Chapter 5). The factors were calculated for four different positions of the CM, given as percentage of glenoacetabular distance, and for five different types of limb support, with a calculation example for a CM position of 11.5%. Factors are given as fraction and not as percentages. Types of limb support: 1 = one limb touching the ground, 2 = two-limb support of one fore- and one hindlimb in either ipsi- and contralateral position, 3 FLP = three-limb support on the forelimb pair, 3 HLP = three-limb support on the hindlimb pair, 4 = all four limbs are in ground contact. * Center of mass for *Diplodocus* (11.5%) and *Brachiosaurus* (37.4%) after Henderson (2006).

Types of limb support	**CM**	f_{wd^*} **11.5***	**20**	**37.4***	**50**	**Calculation example for CM position of 11.5%**
1		1	1	1	1	$= 1$
2		0.885	0.8	0.626	0.5	$= 0.885$
3 FLP		0.7965	0.7	0.5634	0.45	$= (0.885/2 \cdot 0.8) + 0.885/2$
3 HLP		0.4482	0.412	0.3317	0.275	$= (0.115/2 \cdot 0.1) + 0.115/2$
4		0.4425	0.4	0.313	0.25	$= 0.885/2$

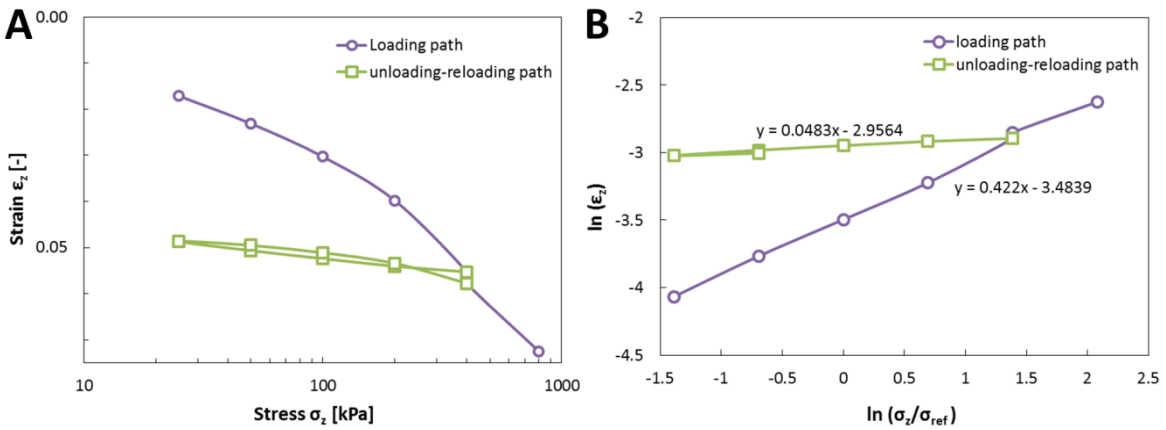

Figure 6.6: The results of the one-dimensional compression and rebound test for the Moselle sand are given for the loading path (purple line and circles) and for the unloading-reloading path (green line and rectangles). A. Data shown as stress against strain plot. The loading was conducted for values of 25 kPa, 50 kPa, 100 kPa, 200 kPa, and 400 kPa, followed by unloading back to 25kPa and reloading (green) to 400kPa. A final loading was performed to a value of 800 kPa. B. The regression analysis of the linearized oedometer data was done for determining the stress dependent stiffness moduli for loading (purple) and un-/reloading (green) needed for

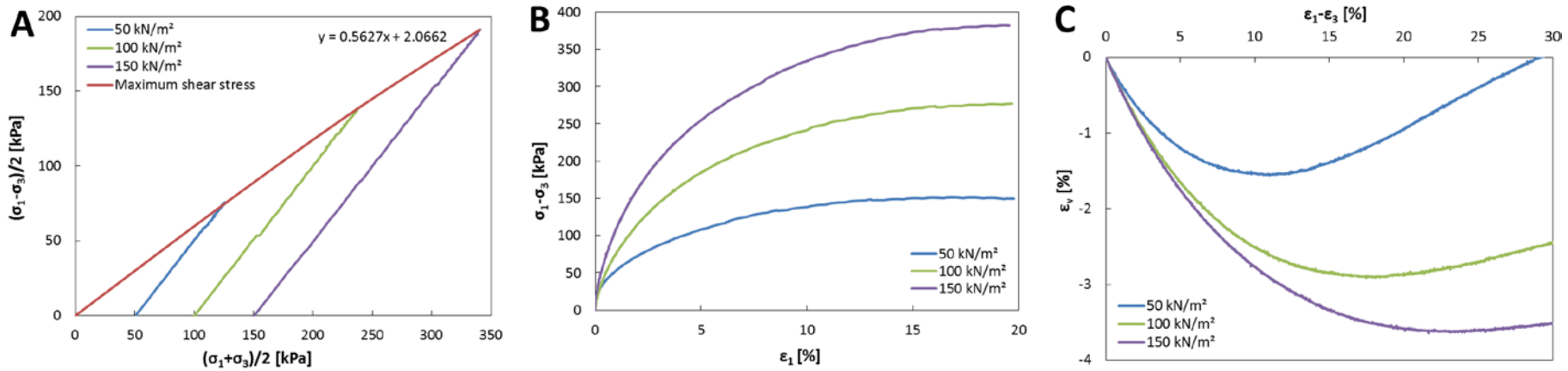

Figure 6.7: The triaxial test of the Moselle sand was conducted for 50 kN/m² (blue line), 100 kN/m² (green line), and 150 kN/m² (purple line). A. The maximum shear stress of all applied loads result in a linear function (red line), from which the friction angle ϕ is derived. B. The results of the triaxial test plotted as axial strain versus deviatoric stress for determining the secant stiffness E_{50}. C. Triaxial test data plotted as shear strain versus volumetric strain to determine the angle of dilatancy from the positive slope of the curves

6.4. RESULTS

6.4.1 Description of the Copper Ridge sauropod tracks

The shape of the individual pes imprints varies over the trackway. All pes imprints are eroded, and it is not clear if the track surface represents the actual surface on which the trackmaker was stepping. The measurements of the pes imprints (Table 6.3) were taken from the photogrammetric 3D models of the Copper Ridge sauropod trackway (Figure 6.2). Measurements were difficult to perform because of the unclear transition between the outline of the true print and the outline of the overall track, which represents the entire deformation area (cf. Falkingham et al., 2016b; Lallensack, 2016). The average length of the pes tracks is about 70 cm, which was the value used for the circular plate in the FEA (Figure 6.4). All pes imprints show elevated rims and radial cracks (cf. Nguyen-Tuan et al., 2013; Schanz et al., 2016). The average track depth was measured to be 13 cm. The floor of the imprints, which is the deformed sandstone layer, is only partially preserved and the underlying mudstone is visible. In the best-preserved tracks, P1 and P7, the floor of the imprints is partly preserved, which represents the continuing surface of the top layer. Track depth in these two footprints was measured to be 10 cm and 11 cm, respectively.

Table 6.3: Measurements of the Copper Ridge pes prints were taken from photogrammetric 3D models of the sauropod trackway. Abbreviations: P= pes, TS= track surface.

Pes print	Depth [cm]	Length [cm]	Width [cm]	Observations
P1	10	45	52	TS partly visible, but partly covered
P2	18	65	48	Deeply penetrated through TS
P3	13	76	41	Poor preservation
P4	8	70	50	TS partly visible, but filled with debris
P5	8	79	71	TS partly visible, but filled with debris
P6	18	74	53	Deeply penetrated through TS
P7	11	70	73	TS partly visible
P8	17	80	55	Deeply penetrated through TS
P9	16	75	60	Deeply penetrated through TS
P10	13	55	57	Poor preservation
Average	13.2	69	56	

Most manus prints are not overprinted by pes prints as previously assumed, but are present as very shallow imprints (Läbe, in revision; Chapter 2). Of the ten documented pes tracks, eight have corresponding manus prints. They were difficult to identify under field conditions and were highlighted with thorough investigation of the photogrammetric models using vertical exaggeration (Läbe, in revision; Chapter 2). As in the pes prints, measurements were difficult to perform. In general, the manus imprints are smaller than the pes prints. The average manus length is 29 cm and the average width is 37 cm (Table 6.4). As in the pes prints, the manus imprints might appear larger due to weathering. The best pre-

served manus prints are M1 and M9 with a length of 18 cm and 19 cm, and a width of 31 cm and 25 cm, respectively. The average HI was 1/2, which was higher than the HI of 1/3, particularly calculated for M1 and M9. The manus imprints, though present, are too eroded and faintly visible for further analysis, and thus, no FEA models were created for them. However, the pes tracks provide sufficient information for the weight estimation.

Table 6.4: Measurements of the Copper Ridge manus prints were taken from photogrammetric 3D models of the sauropod trackway. Abbreviations: M= manus.

Manus print	Length [cm]	Width [cm]
M1	18	31
M2	31	39
M3	25	53
M4	30	37
M5	44	41
M6	36	42
M7	35	34
M8	-	-
M9	19	25
M10	-	-
Average	29	37

The trackway was evaluated to be pes-dominated (cf. Falkingham et al., 2012), since the pes prints are more pronounced and more deeply impressed into the substrate than the manus prints. The walking direction is from the south-east to the north-west, as concluded by previous research (Ishigaki and Matsumoto, 2009). This can be confirmed here, since the lateral view of the trackway model shows that the anterior part of the footprints is always more deeply imprinted than the posterior one (Figure 6.2C). The distance of the pes tracks to the midline suggests intermediate-gauge with a tendency towards narrow-gauge. The step lengths are very short, and specifically in the turning section, the distance between steps is less than the length of an individual track. The calculated average speed is 3.4 km/h (0.94 m/s) according to the formula for dinosaur speeds proposed by Alexander (1976). In the turning section of the trackway, the speed is calculated to be even lower at 1.5 km/h (0.42 m/s). The hip height h of the trackmaker is calculated as 263 cm.

6.4.2 Results of the FEA

The FEA was performed to simulate the impression of one sauropod hindfoot. In four different loading steps during the simulation, vertical stresses of σ_z = 50 kN/m², 100 kN/m², 150 kN/m², and 200 kN/m² were applied to the substrate volume of the FEA model. In Figure 6.8, the main results of the FEA simulation of the sauropod pes print are illustrated. Vertical sections of the FEA model are shown at different loading steps during the simulation. The general observation is that with increasing vertical stresses σ_z the vertical deformation u is increased likewise. It was found that the Copper Ridge sauropod tracks were

generated under a load of less than 200 kN/m². The simulated vertical displacements for each loading condition are plotted in Figure 6.9. For σ_{z1} = 50 kN/m² a deformation of $u_1 = 2.1$ cm was produced, for σ_{z2} = 100 kN/m² the vertical deformation was $u_2 = 4.6$ cm, for σ_{z3} = 150 kN/m² the deformation was $u_3 = 7.6$ cm, and for vertical stress σ_{z4} = 200 kN/m² was $u_4 = 11.8$ cm. By using a regression equation (Figure 6.9), the loads for the best-preserved Copper Ridge footprints P1 and P7 were predicted: $\sigma_{10cm} = 177kN/m^2$ for the vertical deformation of 10 cm in P1 and $\sigma_{11cm} = 189kN/m^2$ for the vertical deformation of 11 cm in P7.

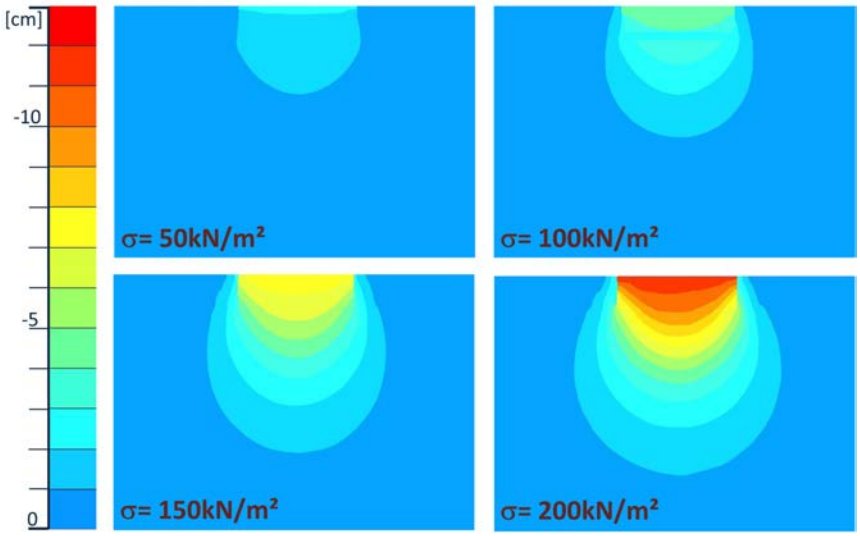

Figure 6.8: The results of the FEA show vertical sections of the model and the increase of vertical displacement during the four different loading steps (warm colours indicate large displacement). The meshed substrate volume was deformed by the applied load through the circular plate element given in Figure 6.4.

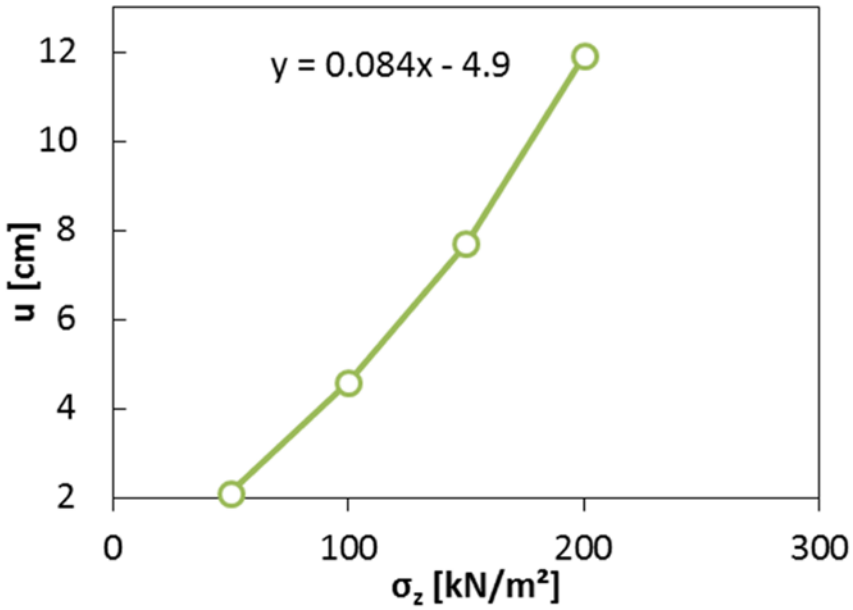

Figure 6.9: FEA results for applied loads σ_z = 50 kN/m², 100 kN/m², 150 kN/m², and 200 kN/m² and linear regression with regression equation for predicting loads for the best-preserved Copper Ridge footprints P1 and P7 with depths of 10 cm and 11 cm.

6.4.3 Calculation of trackmaker weight

Using Equation (6.9), the weight of the trackmaker was calculated using the factor f_{wd^*} (Table 6.2) for different weight distributions. The results are given in Table 6.5 for a vertical stress of $177 kN/m^2$ at a depth of 10 cm in footprint P1 and $189 kN/m^2$ for a depth of 11 cm in footprint P7, as well as for $200\ kN/m^2$ for comparison. Figure 6.10 illustrates how the calculated mass varies with different CM positions and weight distribution among limbs for different loads. The general observation is that the position of the CM influences the calculated weight. For a posterior position of the CM, such as in *Diplodocus*, the calculated weight for one-forelimb support, four-limb support and three-limb support with both forelimbs plot together, while the calculated weight for two-limb support and three-limb support with both hindlimbs plot together. The calculated weight at different CM positions consistently is lowest for one-limb support and highest for the two-limb support and three-limb support with both hindlimbs. Three-limb support with both forelimbs and four-limb support falls in between. Depending on the type of limb support and the position of the CM, the calculated mass for pes track P1 with a depth of 10 cm ranges between 6.8 tonnes and 27.2 tonnes, and for pes track P7 with a depth of 11 cm ranges between 7.3 tonnes and 29.2 tonnes (Table 6.5). In the discussion section, these ranges will be narrowed down further.

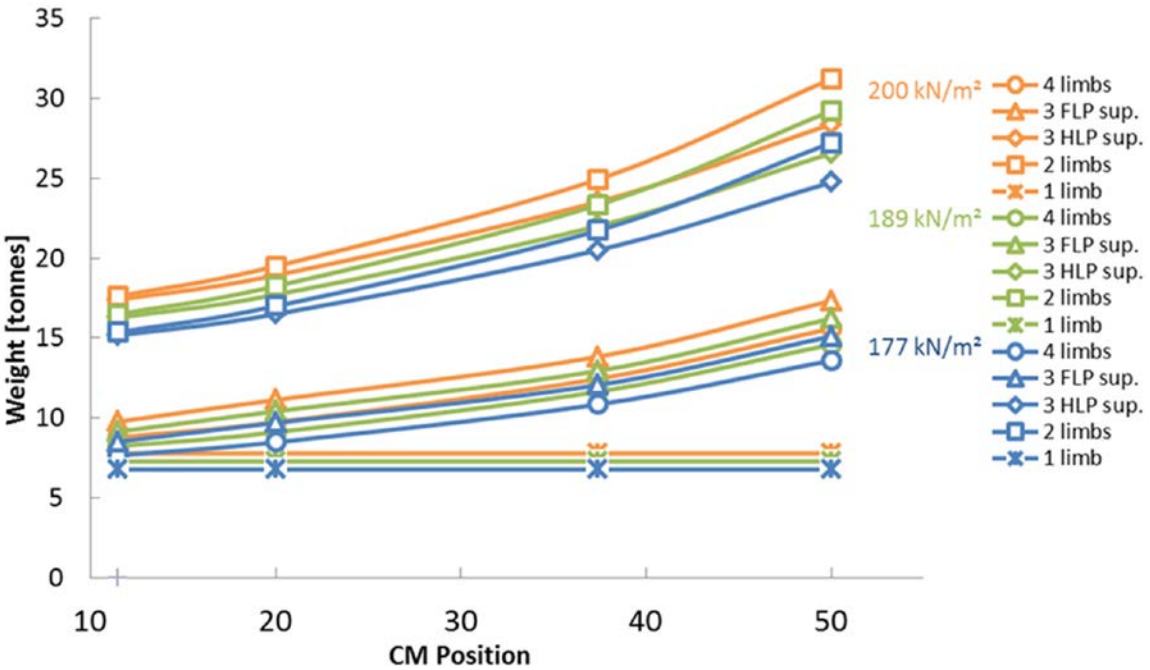

Figure 6.10: Results of the weight calculation based on FEA simulated loads (orange=200 kN/m², green=189 kN/m², blue=177 kN/m²) and considerations on weight distribution among the limbs during walking (∗=1 limb, □=2 limbs, Δ=3 FLP support with forelimbs, ◊=3 HLP support with hindlimbs, ○=4 limbs). Depending on the CM position (x-axis) and the weight (y-axis) seen for one pes track varies.

Table 6.5: Calculated masses based on different loading condition according to track depth made by one sauropod hindfoot ($\sigma_{10cm} = 177\ kN/m^2$, $\sigma_{11cm} = 189\ kN/m^2$, $\sigma_{11.8cm} = 200\ kN/m^2$), CM position of 11.5%, 20%, 37,4% and 50% (CM as percentage of glenoacetabular distance) and factors f_{wd^*} for weight distribution during locomotion among 1 limb, 2 limbs, 3 limbs with main support on the forelimb pair (3 FLP), 3 limbs with main support on the hindlimb pair (3 HLP) and 4 limbs.

	200 kN/m²				189 kN/m²				177 kN/m²			
	Mass (tonnes)				Mass (tonnes)				Mass (tonnes)			
CM	11.5	20	37.4	50	11.5	20	37.4	50	11.5	20	37.4	50
Limbs												
1	7.8	7.8	7.8	7.8	7.3	7.3	7.3	7.3	6.8	6.8	6.8	6.8
4	8.8	9.7	12.4	15.6	8.2	9.1	11.6	14.6	7.6	8.5	10.8	13.6
3 FLP	9.79	11.1	13.8	17.3	9.17	10.4	12.9	16.2	8.5	9.7	12.0	15.1
3 HLP	17.4	18.9	23.5	28.3	16.2	17.7	22.0	26.5	15.1	16.5	20.5	24.7
2	17.6	19.5	24.9	31.2	16.5	18.2	23.3	29.2	15.3	17.0	21.7	27.2

6.5. DISCUSSION

The study by Schanz et al. (2013) has paved the way for interpreting tracks quantitatively for obtaining mass estimates based on tracks of a recent trackmaker (African elephant). By using the footprint geometry and properties of the substrate for FEA simulation, the authors were able to calculate the mass of the elephant with an error of only 15%, which is an acceptable deviation for further application on extinct trackmakers. Based on the work of Schanz et al. (2013), the objective of the present chapter was to formulate an approach to estimate body mass of a sauropod trackmaker from fossil tracks. Based on footprints of the Copper Ridge Dinosaur tracksite and adapted substrate parameters, loading conditions were obtained from FEA simulated tracks to back-calculate the weight of the sauropod trackmaker. It was found that the Copper Ridge sauropod tracks were generated under a load of less than 200 kN/m².

This study shows a novel technique for weight estimation in extinct vertebrates, which may address needs for a wide range of applications among other tracksites. The “dinosaur scale" might be an alternative method to existing mass estimation approaches, which are based either on volumetric models of skeletal reconstructions or scaling relationships of stylopodial dimensions (Campione and Evans, 2012; Sellers et al., 2012), when skeletal material is scanty. It also indicates that this approach is another example, for the valuable information contained in vertebrate tracks, providing additional knowledge besides body fossils. As Schanz et al. (2013) pointed out, the accurate assessment of the substrate behavior and how simulated loads reflect the actual weight of the trackmaker have to be considered. This will be discussed in detail in the following sections.

6.5.1 Material model and substrate parameters

Previous FEA studies simulated tracks with different material models with a smaller set of parameters to define the substrate behavior in the simulation, such as the Mohr-Coulomb

material model with a linear elastic perfectly plastic behavior (Falkingham et al., 2009; Falkingham et al., 2011b; Bates et al., 2013; Sanz et al., 2016). This present thesis chapter implements the hardening soil material model (Schanz et al., 1999), which was developed for realistic simulations in geotechnics, and utilizes a larger set of parameters compared to the Mohr-Coulomb model (Table 6.1). The hardening of the soil was also considered in the simulations by Schanz et al. (2013) and Falkingham et al. (2014).

The parameters need to be acquired with care, since the input parameters influence the outcome of the simulation immensely. For the acquisition of the input parameters, the substrate has to be characterized. While the characterization of recent unconsolidated sediment is unproblematic and assessable with standard experiments, it is more difficult to assess substrate parameters of a lithified sedimentary rock. Here, the sandstone properties of the Copper Ridge track-bearing layer were analyzed with polarized microscopy and image analysis. Based on the fossil substrate, a matching recent equivalent sediment, in terms of depositional environment was found, in order to take the recent substrate properties as input parameters for the FEA. A problem with image analysis is that the thin section cuts grains randomly, and this may influence the result of the grain size distribution. In Figure 6.3, the grain size distribution of the recent Moselle sand differs slightly from the sandstone of the Copper Ridge Dinosaur tracksite. Yet it was implemented for the FEA because the Moselle sand matches nicely with the reconstructed paleoenvironment of Copper Ridge, which was evidently fluvial (Foster and Lockley, 2006; Foster, 2015).

For further studies, either micro-computed tomography (µCT) or numerical analysis of petrographic thin sections may improve interpretations of the grain size distribution of the rock. Schanz et al. (2012) used µCT analyses to address the original substrate condition before lithification. However, this requires advanced geotechnical reconstruction software, due to the high degree of cementation and similar densities in the mineral grains, which makes the separation and segmentation of individual grains difficult. Seelos and Sirocko (2005) developed a method to analyse polarized petrographic thin sections numerically to infer grain size distribution. Another approach could use soil mechanical input parameters for FEA derived from comparable, synthetic substrates in the laboratory, instead of naturally deposited ones.

Another challenge when dealing with substrate conditions and track formation is the water content of the substrate, as this was questioned in previous studies (e.g., Jackson et al., 2010; Platt et al., 2012). However, this was regarded as minor issue here, since the effect of water is negligible in siliciclastic sediments with grain sizes larger than clay. If a clastic substrate with grain size used in this study is under stress, the volumetric strain and void ratio increase, which in turn leads to drainage (Taylor, 1948). In case of clay and carbonates, water is a potential problematic factor because, for example, the swelling ability of clay minerals the excess pore water pressure.

6.5.2 Track depth

In the Copper Ridge tracks, the original track depth was difficult to measure, since most of the tracks are eroded and poorly preserved. In most pes tracks, the floor was not preserved and the underlying rock layer was visible. It is not clear if this is due to poor preservation or if the trackmaker's foot penetrated the sandstone layer so that the tracks were imprinted through the sandstone layer into the underlying mudstone. Thus, determining the track depth has to be taken with care and it remains uncertain whether the original track surface is preserved and if the present tracks are true tracks or undertracks (cf. Milàn and Bromley, 2006). This issue might have an impact on the evaluation of the true track depth, which might lead to under- or overestimation of the track depth. This in return can influence the FEA simulation, as well as the derived loads for further weight estimation. From a soil mechanical view, the settlements decrease in undertracks, while in the lateral direction the diameter of the undertrack increases. The further the track impression is transmitted into the underlying sediment layers, the less prominent the undertrack becomes, but the overall track diameter increases in size (Schanz et al., 2012). This means that the morphology of true tracks and undertracks can be different, depending on how distant in depth they are to each other. Another issue may be the compaction of the regarded track surface and a flattening of the otherwise deeper tracks due to pressure of the overburden rocks. Schanz et al. (2012) attempted to quantify the impact of overburden compaction on weight estimation of tracks and stated that it might be underestimated with approximately 7%.

6.5.3 Trackmaker identification

In general, identification of a trackmaker is difficult. The unequivocal evidence for the trackmaker would be a sensational finding of a dinosaur skeleton at the end of trackway (Thulborn, 1990). Unfortunately, no such discovery has been made so far for vertebrates. Among invertebrates, tracks of the invertebrate ichnotaxon *Kouphichnium* with the corresponding trackmaker *Mesolimulus* (horseshoe crab) at the end of the trackway from the famous Jurassic Solnhofen Lithographic Limestone, Germany, are rare exceptions (Lomax and Racay, 2012).

For the Copper Ridge tracks, "*Brontosaurus*" had formerly been regarded as the trackmaker (Lockley, 1991a; Lockley and Hunt, 1995). The tracks were also attributed to the ichnogenus *Brontopodus* (Hunt-Foster et al., 2016). Despite these taxonomical identifications, it is not clear on which synapomorphies these hypotheses are based on. According to Wright (2005), the classification of a trackmaker should be done with care and based on detailed footprint morphology. The Copper Ridge tracks unfortunately lack diagnostic and sufficient characters to align track morphology with autopodium anatomy of a sauropod skeleton from stratigraphically equivalent outcrops in the Morrison Formation.

However, it appears relatively certain that the trackmaker was a sauropod, considering the quadrupedal stance with manus and pes prints and the large size of the tracks. In case of

the Copper Ridge trackway, the trackway gauge is problematic to assess, because of the right turn in the trackway, it seems to be intermediate with a tendency to narrow. The average HI is 1/3, which is intermediate between the HI of the two ichnotaxa *Parabrontopodus* and *Brontopodus*. The HI might have a tendency to be higher, since the outline of the imprints was problematic to measure and the track dimensions might be smaller. However, the distinction between wide-gauge tracks and the narrow-gauge track type was put in question recently, since in some tracksites, gauge width has been observed to change within a single trackway (Romano et al., 2007; Marty, 2008; Santos et al., 2009; Castanera et al., 2012). Trackway gauge may not be useful as a phylogenetic signal, but just an adaption by the trackmaker to different terrains.

Another feature of the tracks is that they are pes-dominated, meaning that the pes prints are more deeply imprinted than the manus prints. This could be an argument for a higher distribution of weight on the hindlimbs due to a posterior position of the CM (cf. Henderson, 2006; Falkingham et al., 2011a).

A clear taxonomic classification based on synapomorphies is not possible for the sauropod tracks in Copper Ridge, since the preservation of the tracks is to poor. However, based on HI, intermediate-gauge and weight distribution on the hindlimbs, it might be suggested that the Copper Ridge trackmaker was probably a non-macronarian neosauropod, such as *Diplodocus*. In the Morrison Formation, *Diplodocus* is the third-most abundant sauropod, after *Camarasaurus* and *Apatosaurus* (Foster, 2007).

6.5.4 Inferring locomotion from footfall pattern

The footfall pattern in the Copper Ridge trackway shows short step lengths and ipsilateral manus and pes prints placed together. The manus prints are placed in front of the pes. According to Kienapfel et al. (2014; Chapter 4), who analyzed footfall patterns from different gaits in highly standardized horses, it was reasoned that the Copper Ridge trackmaker employed a slow walk for locomotion. The speed was estimated to be 3.4 km/h based on Alexander's formula (Alexander, 1976).

Both, the footfall pattern and speed estimate of the sauropod trackway, support a walking locomotion with low dynamics of the trackmaker. Thus, the choice of the weight distribution factor (Table 6.2; Chapter 5) for the weight calculation is affected (Equation (6.9)). The weight distribution factor is given for five different scenarios of limb support types, which might occur during a whole walk cycle.

In a walking locomotion (excluding standing on four limbs), there are three possible ways the weight on the limbs is distributed: two-limb support, three-limb support on the hindlimb pair, and three-limb support on the forelimb pair. The one-limb support can most likely be excluded, since it is assumed to happen only in gaits with higher dynamics and intercalated phase of suspension, such as running gaits.

6.5.5 Weight of the trackmaker

What we want to know is: which weight is plausible for the Copper Ridge sauropod trackmaker? Above it was reasoned that *Diplodocus* might have been a potential candidate. Henderson (2006) calculated a CM position of 11.5% for *Diplodocus*, given as percentage of the glenoacetabular distance; meaning that the CM position was located posteriorly.

In this study, the weight estimate for the pes track P1 with a depth of 10 cm and an assumed CM position of 11.5% (Table 6.5) ranges between 6.8 tonnes, for weight distribution on one hindfoot, and 15.3 tonnes, for the weight distribution on one fore- and one hindfoot. In Chapter 5, it was suggested that the highest plausible factor f_{wd^*} should be chosen for further estimation of the weight, since one footprint can experience all possible types of limb support during the entire walk cycle. In the case of the Copper Ridge trackway, which argues for a walk because of footfall pattern and speed, the weight distribution factor for the two-limb support should be taken for the weight calculation with Equation (6.9). From that, a maximum weight between 15.3 tonnes for loading conditions of 177 kN/m² and 17.63 tonnes for a load of 200 kN/m² could be estimated. This expands previous research about the Copper Ridge Dinosaur tracksite (Lockley, 1991b; Lockley and Hunt, 1995; Ishigaki and Matsumoto, 2009) with key information about the trackmaker. The weight estimate in this chapter is intermediate between other mass estimates for *Diplodocus*, for example, 10.56 tonnes by Colbert (1962), 13.42 tonnes by Henderson (2006) and 18.5 tonnes by Alexander (1985).

That means that care has to be taken when choosing weight distribution factor and CM position for estimating the weight from simulated loads. The calculated weights for loads simulated for a track of 10 cm (177 kN/m²) and 11 cm (189 kN/m²) differ by about one ton, which complies with an error of about 7%. This is similar to the calculated error for the track depth in Schanz et al. (2012).

6.5.6 Problems, future research, and conclusions

The presented approach is potentially error-prone, and a detailed sensitivity analysis should be applied to gain more confidence in this method. With such a method, it could be investigated, which of the many parameters has the greatest influence on weight estimation, and how these parameters might affect each other. In general, the outcome of a FEA simulation is highly dependent on input parameters and the chosen material model. Bright (2014) reviewed the application of FEA in paleontology and advised a careful handling of this method, since input data may vary and affect results immensely. In any case, results and implications should always be discussed thoroughly.

The dynamics is another factor to be considered and could be improved for future applications. In this research, the dynamics were reduced to a single factor. In the case of sauropods, this might not be problematic since high dynamic locomotion is not evident in the

trackways and generally not expected for sauropods (Preuschoft et al., 2011). However, Stevens et al. (2016) proposed a new computer software, Cadence, to interpret and virtually generate dinosaur trackways with a moving dinosaur model, which is controlled by internal and external constraints. With such software, the kinetics and kinematics of the trackmaker could be better quantified from track data and could benefit the presented weight estimation approach.

For the present study, tracks preserved in clastic sediments were analyzed because they are less affected by diagenesis and chemical weathering. Future work should concentrate on the application on non-clastic and cohesive sediments, as a large number of well-preserved sauropod track findings occur in carbonate sediments, which are associated with coastal paleoenvironments (Butler and Barrett, 2008; Mannion and Upchurch, 2010; Falkingham et al., 2012).

Tracks are very rarely located in homogeneous substrates. Mostly, the track-bearing layer is underlain by another layer, which might be firmer. The vertical displacement of the penetrating foot might be influenced by the underlying layer, hence it is advised to consider that for future application of the proposed method, as already mentioned by Falkingham et al. (2014) and Sanz et al. (2016).

A very interesting direction that future studies could head towards is combining morphological and track data. For example, evidence from a number of studies and specimens show sauropods were highly pneumatized in the neck, axial skeleton and pubis, which also implies an avian style lung (Wedel, 2003; Wedel, 2009; Wedel and Taylor, 2013; Melstrom et al., 2016). This pneumaticity puts very high weight estimates into question and suggests that sauropods might have been lighter than previously assumed. In addition, pneumaticity and the associated lung anatomy might also have influenced the CM position of sauropod dinosaurs (Henderson, 2004). The weight estimates produced here fall within the range of other lighter mass estimates, which indirectly support a pneumatized skeleton. With a combined approach and further development of accurate models of sauropods and further refinement of quantitative trackway analysis, greater insights into the biology of these giants, such as pneumaticity, can be gathered and better supported.

This research started with sauropod dinosaurs because they are easily approximated in terms of dynamics and foot anatomy. Although the interpretation and the simulation can be problematic (e.g., the dynamic component), the results of the present study are encouraging and should be validated with other tracksites. This method can also be expanded to other trackmakers, such as theropods, mammals, or even hominids.

6.6. ACKNOWLEDGEMENTS

I thank Prof. T. Schanz (Ruhr-Universität Bochum) for introducing me to soil mechanics. The efforts by C. Schmüdderich (Ruhr-Universität Bochum) are greatly acknowledged for support with the finite element analysis, the oedometer analysis and the improvement of the manuscript. N. Rahemi and H. Haase (both Ruhr-Universität Bochum) are thanked for the support with the triaxial and other lab tests. The soil mechanics lab at the Ruhr-Universität Bochum, specifically M. Skubisch, generously provided support and data for this study. The BLM office in Moab is thanked for providing further information about the Copper Ridge Dinosaur tracksite, since the site is managed by the BLM. I thank P. M. Sander (Universität Bonn) for providing photographs of the Copper Ridge Dinosaur tracksite, for discussion and for improving the manuscript. H. Mallison is thanked for providing an earlier version of the photogrammetry of the Copper Ridge Dinosaur tracksite. I thank T. Plogschties (Universität Bonn) for supporting data collection for photogrammetry at the Copper Ridge Dinosaur tracksite. In addition, I thank J. Lallensack and J. Mitchell for discussion and support. Finally, I wish to thank the German Academic Scholarship Foundation (Studienstiftung des deutschen Volkes) and the Andrea von Braun Foundation for generous funding of this research and related fieldwork.

6.7. REFERENCES

Alexander, R. M. 1976. Estimates of speeds of dinosaurs. Nature 261:129–130.

Alexander, R. M. 1985. Mechanics of posture and gait of some large dinosaurs. Zoological Journal of the Linnean Society 83(1):1–25.

Alexander, R. M. 1989. Dynamics of Dinosaurs and Other Extinct Giants. Columbia University Press, New York, 167 pp.

Anderson, J. F., A. Hall-Martin, and D. A. Russell. **1985**. Long-bone circumference and weight in mammals, birds and dinosaurs. Journal of Zoology 207(1):53–61.

Bates, K. T., and P. L. Falkingham. **2012**. Estimating maximum bite performance in *Tyrannosaurus rex* using multi-body dynamics. Biology Letters 8(4):660–664.

Bates, K. T., R. Savage, T. C. Pataky, S. A. Morse, E. Webster, P. L. Falkingham, L. Ren, Z. Qian, D. Collins, M. R. Bennett, J. McClymont, and R. H. Crompton. **2013**. Does footprint depth correlate with foot motion and pressure? Journal of the Royal Society Interface 10(83):1–12.

Bird, R. 1939. Thunder in his footsteps. Natural History 43:254–261.

Bird, R. T. 1944. Did *Brontosaurus* ever walk on land? Natural History 53(2):60–67.

Bright, J. A. 2014. A review of paleontological finite element models and their validity. Journal of Paleontology 88(4):760–769.

Butler, R. J., and P. M. Barrett. **2008**. Palaeoenvironmental controls on the distribution of Cretaceous herbivorous dinosaurs. Naturwissenschaften 95(11):1027–1032.

Campione, N. E., and D. C. Evans. **2012**. A universal scaling relationship between body mass and proximal limb bone dimensions in quadrupedal terrestrial tetrapods. BMC Biology 10(60):1–21.

Carpenter, K. 2006. Biggest of the big: a critical re-evaluation of the megasauropod *Amphicoelias fragillimus* Cope, 1878. New Mexico Museum of Natural History and Science Bulletin 36:131–138.

Casanovas, M., A. Fernandez, F. Perez-Lorente, and J. V. Santafe. **1997**. Sauropod trackways from site El Sobaquillo (Munilla, La Rioja, Spain) indicate amble walking. Ichnos 5(2):101–107.

Castanera, D., C. Pascual, J. I. Canudo, N. Hernández, and J. L. Barco. **2012**. Ethological variations in gauge in sauropod trackways from the Berriasian of Spain. Lethaia 45(4):476–489.

Christian, A., R. H. G. Müller, G. Christian, and H. Preuschoft. **1999**. Limb swinging in elephants and giraffes and implications for the reconstruction of limb movements and speed estimates in large dinosaurs. Mitteilungen aus dem Museum für Naturkunde in Berlin, Geowissenschaftliche Reihe 2:81–90.

Colbert, E. H. 1962. The weights of dinosaurs. American Museum Novitates 2076:1–16.

Curry Rogers, K., and J. A. Wilson (eds.). **2005**. The Sauropods - Evolution and Paleobiology. University of California Press, Berkeley, 349 pp.

Demathieu, G. R. 1987. Thickness of the Footprint-Relief and its Significance: Research on the Distribution of the Weights upon the Autopodia; pp. 61–62 in G. Leonardi (ed.), Glossary and Manual of Tetrapod Footprint Palaeoichnology. Departamento Nacional da Produção Mineral, Brazil, 137 pp.

DIN 18123. **1996**. Bestimmung der Korngrößenverteilung. Deutsches Institut für Normung e.V., 12 pp.

DIN 18126. **1996**. Bestimmung der Dichte nichtbindiger Böden bei lockerster und dichtester Lagerung. Deutsches Institut für Normung e.V., 10 pp.

DIN 18137-2. **2011**. Baugrund, Untersuchung von Bodenproben – Bestimmung der Scherfestigkeit – Teil 2: Triaxialversuch. Deutsches Institut für Normung e.V., 48 pp.

Falkingham, P. L. 2010. Computer simulation of dinosaur tracks. Ph.D. thesis, The University of Manchester, Manchester.

Falkingham, P. L. 2012. Acquisition of high resolution three-dimensional models using free, open-source, photogrammetric software. Palaeontologia Electronica 15(1):1-15.

Falkingham, P. L. 2014. Interpreting ecology and behaviour from the vertebrate fossil track record. Journal of Zoology 292(4):222–228.

Falkingham, P. L., K. T. Bates, and P. D. Mannion. **2012**. Temporal and palaeoenvironmental distribution of manus- and pes-dominated sauropod trackways. Journal of the Geological Society 169(4):365–370.

Falkingham, P. L., K. T. Bates, L. Margetts, and P. L. Manning. **2011a**. Simulating sauropod manus-only trackway formation using finite-element analysis. Biology Letters 7:142–145.

Falkingham, P. L., K. T. Bates, L. Margetts, and P. L. Manning. **2011b**. The 'Goldilocks' effect: preservation bias in vertebrate track assemblages. Journal of the Royal Society Interface 8(61):1142–1154.

Falkingham, P. L., J. Hage, and M. Baker. **2014**. Mitigating the Goldilocks effect: the effects of different substrate models on track formation potential. Royal Society Open Science 1(3):1–9.

Falkingham, P. L., L. Margetts, I. M. Smith, and P. L. Manning. **2009**. Reinterpretation of palmate and semi-palmate (webbed) fossil tracks; insights from finite element modelling. Palaeogeography, Palaeoclimatology, Palaeoecology 271(1-2):69–76.

Falkingham, P. L., D. Marty, and A. Richter (eds.). **2016a**. Dinosaur Tracks - The Next Steps. Life of the Past. Indiana University Press, Bloomington, 413 pp.

Falkingham, P. L., D. Marty, and A. Richter. **2016b**. Introduction; pp. 2–11 in P. L. Falkingham, D. Marty, and A. Richter (eds.), Dinosaur Tracks - The Next Steps. Life of the Past. Indiana University Press, Bloomington, 413 pp.

Farlow, J. O. 1992. Sauropod tracks and trackmakers: integrating the ichnological and skeletal records. Zubia 10:89–138.

Farlow, J. O., M. O'Brien, G. J. Kuban, B. Dattilo, K. T. Bates, P. L. Falkingham, L. P. Amanda Rose, C. Kumagai, C. Libben, J. Smith, and J. Whitcraft. **2012**. Dinosaur tracksites of the Paluxy River Valley (Glen Rose Formation, Lower Cretaceous), Dinosaur Valley State Park, Somervell County, Texas. Actas de V Jornadas Internacionales sobre Paleontologia de Dinosaurios y su Entorno, Salas de los Infantes, Burgos:41–69.

Farlow, J. O., J. G. Pittman, and J. M. Hawthorne. **1989**. *Brontopodus birdi,* Lower Cretaceous Sauropod Footprints from the U.S. Gulf Coastal Plain; pp. 371–394 in D. D. Gillette and M. G. Lockley (eds.), Dinosaur Tracks and Traces. Cambridge University Press, Cambridge, 476 pp.

Fischer, R. 1998. Die Saurierfährten im Naturdenkmal Münchehagen. Mitteilungen aus dem Institut für Geologie und Paläontologie der Universität Hannover 37:3–59.

Foster, J. 2007. Jurassic West: The Dinosaurs of the Morrison Formation and their World. Life of the Past. Indiana Univ. Press, Bloomington Ind., 389 pp.

Foster, J. R. 2015. Theropod dinosaur ichnogenus *Hispanosauropus* identified from the Morrison Formation (Upper Jurassic), Western North America. Ichnos 22(3-4):183–191.

Foster, J. R., and M. G. Lockley. **2006**. The vertebrate ichnological record of the Morrison Formation (Upper Jurassic, North America). New Mexico Museum of Natural History and Science Bulletin 36:203–216.

Friese, H. 1979. Die Saurierfährten von Barkhausen im Wiehengebirge. Veröffentlichungen des Landkreises Osnabrück 1:1–36.

Gatesy, S. M., K. M. Middleton, F. A. J. Jr, and N. H. Shubin. **1999**. Three-dimensional preservation of foot movements in Triassic theropod dinosaurs. Nature 399(6732):141–144.

German Geotechnical Society. **2014**. Empfehlungen des Arbeitskreises Numerik in der Geotechnik - EANG. Ernst & Sohn, Berlin, 181 pp.

Gunga, H.-C., T. Suthau, A. Bellmann, A. Friedrich, T. Schwanebeck, S. Stoinski, T. Trippel, K. Kirsch, and O. Hellwich. **2007**. Body mass estimations for *Plateosaurus engelhardti* using laser scanning and 3D reconstruction methods. Naturwissenschaften 94:623–630.

Gunga, H.-C., T. Suthau, A. Bellmann, S. Stoinski, A. Friedrich, T. Trippel, K. Kirsch, and O. Hellwich. **2008**. A new body mass estimation of *Brachiosaurus brancai* Janensch, 1914 mounted and exhibited at the Museum of Natural History (Berlin, Germany). Fossil Record 11(1):33–38.

Henderson, D. M. 1999. Estimating the masses and centers of mass of extinct animals by 3-D mathematical slicing. Paleobiology 25(1):88–106.

Henderson, D. M. 2004. Tipsy punters: sauropod dinosaur pneumaticity, buoyancy and aquatic habits. Proceedings of the Royal Society B 271(Suppl 4):180–183.

Henderson, D. M. 2006. Burly gaits: centers of mass, stability, and the trackways of sauropod dinosaurs. Journal of Vertebrate Paleontology 26(4):907–921.

Hendricks, A. 1981. Die Saurierfährte von Münchehagen bei Rehburg-Loccum (NW-Deutschland). Abhandlungen aus dem Landesmuseum für Naturkunde Münster in Westfalen 43:3–22.

Hildebrand, M. 1965. Symmetrical gaits of horses. Science 150(3697):701–708.

Hildebrand, M. 1980. The adaptive significance of tetrapod gait selection. American Zoologist 20(1):255–267.

Hildebrand, M. 1989. The quadrupedal gaits of vertebrates. Bioscience 39(11):766–775.

Hunt-Foster, R. K., M. G. Lockley, A. R. C. Milner, J. R. Foster, N. A. Matthews, B. H. Breithaupt, and J. A. Smith. **2016**. Tracking dinosaurs in BLM Canyon Country, Utah. Geology of the Intermountain West 3:67–100.

Ishigaki, S., and Y. Matsumoto. **2009**. "Off-tracking"-like phenomenon observed in the turning sauropod trackway from the Upper Jurassic of Morocco. Memoir of the Fukui Prefectural Dinosaur Museum 8:1–10.

Jackson, S. J., M. A. Whyte, and M. Romano. **2009**. Laboratory-controlled simulations of dinosaur footprints in sand: A key to understanding vertebrate track formation and preservation. Palaios 24(4):222–238.

Jackson, S. J., M. A. Whyte, and M. Romano. **2010**. Range of experimental dinosaur (*Hypsilophodon foxii*) footprints due to variation in sand consistency: how wet was the track? Ichnos 17(3):197–214.

Kaever, M., and A. F. de Lapparent. **1974**. Les traces de pas de Dinosaures du Jurassique de Barkhausen (Basse Saxe, Allemagne). Bulletin de la Société Géologique de France 16:516–525.

Kienapfel, K., S. Läbe, and H. Preuschoft. **2014**. Do tracks yield reliable information on gaits? – Part 1: The case of horses. Fossil Record 17:59–67.

Klein, N., K. Remes, C. T. Gee, and P. M. Sander (eds.). **2011**. Biology of the Sauropod Dinosaurs - Understanding the Life of Giants. Life of the Past. Indiana University Press, Bloomington, 331 pp.

Läbe, S. unpubl. . Do tracks yield reliable information on gaits? – Part 2: Thoughts on the weight distribution of sauropod dinosaurs during walking. Doctoral thesis 2017(Chapter 5).

Läbe, S. in revision. Vertical exaggeration of 3D surface models highlights additional detail in vertebrate tracks: an example from the photogrammetry of sauropod tracks. Journal of Paleontological Techniques (2017).

Läbe, S. 2014. Interpretation of fossil vertebrate tracks with a soil mechanical approach for body mass estimation. Journal of Vertebrate Paleontology (Program and Abstracts 2014):164.

Lallensack, J. N. 2016. An objective method for the generation of footprint outlines. Journal of Vertebrate Paleontology Program and Abstracts, 2016:171.

Lallensack, J. N., H. Klein, J. Milàn, O. Wings, O. Mateus, and L. B. Clemmensen. **submit.** Sauropodomorph dinosaur trackways from the Fleming Fjord Formation of East Greenland: Evidence for Late Triassic sauropods. Acta Palaeontologica Polonica (2017).

Lautenschlager, S. 2013. Cranial myology and bite force performance of *Erlikosaurus andrewsi*: a novel approach for digital muscle reconstructions. Journal of Anatomy 222(2):260–272.

Lockley, M., and A. P. Hunt. **1995**. Dinosaur Tracks and Other Fossil Footprints of the Western United States. Columbia University Press, New York, 360 pp.

Lockley, M. G. 1989. Summary and Prospectus; pp. 441–447 in D. D. Gillette and M. G. Lockley (eds.), Dinosaur Tracks and Traces. Cambridge University Press, Cambridge, 476 pp.

Lockley, M. G. 1991a. The dinosaur footprint renaissance. Modern Geology 16:139–160.

Lockley, M. G. 1991b. Tracking Dinosaurs - A New Look at an Ancient World. Cambridge University Press, Cambridge, 237 pp.

Lockley, M. G. 2007. The morphodynamics of dinosaurs, other archosaurs, and their trackways: holistic insights into relationships between feet, limbs, and the whole body. SEPM Special Publication 88:27–51.

Lockley, M. G., J. O. Farlow, and C. A. Meyer. **1994**. *Brontopodus* and *Parabrontopodus* ichnogen. nov. and the significance of wide- and narrow-gauge sauropod trackways. Gaia: Revista de Geociências 10:135–145.

Lockley, M. G., J. L. Wright, A. P. Hunt, and S. G. Lucas. **2001**. The Late Triassic sauropod track record comes into focus: old legacies and new paradigms. Guidebook New Mexico Geological Society 52:181-190.

Lockley, M. G., J. L. Wright, and D. Thies. **2004**. Some observations on the dinosaur tracks at Münchehagen (Lower Cretaceous), Germany. Ichnos 11(3-4):261–274.

Lomax, D. R., and C. A. Racay. **2012**. A long mortichnial trackway of *Mesolimulus walchi* from the Upper Jurassic Solnhofen Lithographic Limestone near Wintershof, Germany. Ichnos 19(3):175–183.

Mallison, H., and O. Wings. **2014**. Photogrammetry in paleontology - a practical guide. Journal of Paleontological Techniques 12:1–31.

Manning, P. L. 2004. A new approach to the analysis and interpretation of tracks: examples from the dinosauria. Geological Society of London Special Publications 228:94–123.

Mannion, P. D., and P. Upchurch. **2010**. A quantitative analysis of environmental associations in sauropod dinosaurs. Paleobiology 36(2):253–282.

Margetts, L., J. Leng, I. M. Smith, and P. L. Manning. **2006**. Parallel Three Dimensional Finite Element Analysis of Dinosaur Trackway Formation; pp. 743–749 in H. F. Schweiger (ed.), Numerical Methods in Geotechnical Engineering: Proceedings of the Sixth European Conference on Numerical Methods in Geotechnical Engineering. Balkema-proceedings and monographs in engineering, water and earth sciences. Taylor & Francis, London, 1678 pp.

Margetts, L., I. M. Smith, J. Leng, and P. L. Manning. **2005**. Simulating dinosaur trackway formation; pp. 1–4 in E. Oñate and D. R. J. Owen (eds.), VIII International Conference on Computational Plasticity (COMPLAS). CIMNE, Barcelona.

Marty, D. 2008. Sedimentology, taphonomy, and ichnology of Late Jurassic dinosaur tracks from the Jura carbonate platform (Chevenez—Combe Ronde tracksite, NW Switzerland): insights into the tidal-flat palaeoenvironment and dinosaur diversity, locomotion, and palaeoecology. GeoFocus 21:1–278.

Marty, D., P. L. Falkingham, and A. Richter. **2016**. Dinosaur Track Terminology: A Glossary of Terms; pp. 399–402 in P. L. Falkingham, D. Marty, and A. Richter (eds.), Dinosaur Tracks - The Next Steps. Life of the Past. Indiana University Press, Bloomington, 413 pp.

Matthews, N. A., T. A. Noble, and B. H. Breithaupt. **2016**. Close-Range Photogrammetry for 3-D Ichnology: The Basics of Photogrammetric Ichnology; pp. 28–55 in P. L. Falkingham, D. Marty, and A. Richter (eds.), Dinosaur Tracks - The Next Steps. Life of the Past. Indiana University Press, Bloomington, 413 pp.

Melstrom, K. M., M. D. D'emic, D. Chure, and J. A. Wilson. **2016**. A juvenile sauropod dinosaur from the Late Jurassic of Utah, U.S.A., presents further evidence of an avian style air-sac system. Journal of Vertebrate Paleontology 36(4):1-23.

Milàn, J. 2006. Variations in the morphology of emu (*Dromaius novaehollandiae*) tracks reflecting differences in walking pattern and substrate consistency: ichnotaxonomic implications. Palaeontology 49(2):405–420.

Milàn, J., and R. Bromley. **2006**. True tracks, undertracks and eroded tracks, experimental work with tetrapod tracks in laboratory and field. Palaeogeography, Palaeoclimatology, Palaeoecology 231:253–264.

Nguyen-Tuan, L., H. Viefhaus, M. Datcheva, and T. Schanz. **2013**. Coupled thermo-hydro-mechanical modelling of crack development along fossil dinosaur footprints in soft cohesive sediments. V International Conference on Computational Methods for Coupled Problems in Science and Engineering COUPLED PROBLEMS 2013:1–13.

Ohde, J. 1939. Zur Theorie der Druckverteilung im Baugrund. Bauingenieur 20:93–99.

Platt, B. F., S. T. Hasiotis, and D. R. Hirmas. **2012**. Empirical determination of physical controls on megafaunal footprints formation through neoichnological experiments with elephants. Palaios 27:725–737.

Preuschoft, H., B. Hohn, S. Stoinski, and U. Witzel. **2011**. Why so huge? Biomechanical Reasons for the Acquisition of Large Size in Sauropod and Theropod Dinosaurs; pp. 197–218 in N. Klein, K. Remes, C. T. Gee, and P. M. Sander (eds.), Biology of the Sauropod Dinosaurs - Understanding the Life of Giants. Life of the Past. Indiana University Press, Bloomington, 331 pp.

Romano, M., M. A. Whyte, and S. J. Jackson. **2007**. Trackway ratio: a new look at trackway gauge in the analysis of quadrupedal dinosaur trackways and its implications for ichnotaxonomy. Ichnos 14(3-4):257–270.

Sander, P. M., A. Christian, M. Clauss, R. Fechner, C. T. Gee, E.-M. Griebeler, H.-C. Gunga, J. Hummel, H. Mallison, S. F. Perry, H. Preuschoft, O. W. M. Rauhut, K. Remes, T. Tütken, O. Wings, and U. Witzel. **2011**. Biology of the sauropod dinosaurs: the evolution of gigantism. Biological Reviews 86:117–155.

Sander, P. M., and M. Clauss. **2008**. Sauropod gigantism. Science 322(5899):200–201.

Sander, P. M., O. Mateus, T. Laven, and N. Knötschke. **2006**. Bone histology indicates insular dwarfism in a new Late Jurassic sauropod dinosaur. Nature 441(7094):739–741.

Santos, V. F., J. J. Moratalla, and R. Royo-Torres. **2009**. New sauropod trackways from the Middle Jurassic of Portugal. Acta Palaeontologica Polonica 54(3):409–422.

Santos, V. F. d., M. G. Lockley, C. A. Meyer, J. Carvalho, A. Galopim de Carvalho, and J. J. Moratalla. **1994**. A new sauropod tracksite from the Middle Jurassic of Portugal. Gaia: Revista de Geociências 10:5–13.

Sanz, E., A. Arcos, C. Pascual, and I. M. Pidal. **2016**. Three-dimensional elasto-plastic soil modelling and analysis of sauropod tracks. Acta Palaeontologica Polonica 61(2):387–402.

Schanz, T. 1998. Zur Modellierung des mechanischen Verhaltens von Reibungsmaterialien. Institut für Geotechnik, Universität Stuttgart: Mitteilung 45:1–155.

Schanz, T., M. Datcheva, H. Haase, and D. Marty. **2016**. Analysis of Desiccation Crack Patterns for Quantitative Interpretation of Fossil Tracks; pp. 367–379 in P. L. Falkingham, D. Marty, and A. Richter (eds.), Dinosaur Tracks - The Next Steps. Life of the Past. Indiana University Press, Bloomington, 413 pp.

Schanz, T., Y. Lins, H. Viefhaus, T. Barciaga, S. Läbe, H. Preuschoft, U. Witzel, and P. M. Sander. **2013**. Quantitative interpretation of tracks for determination of body mass. PLoS ONE 8(10):1–12.

Schanz, T., Y. Lins, H. Viefhaus, and P. M. Sander. **2012**. Quantitative interpretation of dinosaur tracks revisited. Journal of Vertebrate Paleontology (Program and Abstracts 2012):166.

Schanz, T., and P. A. Vermeer. **1996a**. Angles of friction and dilatancy of sand. Géotechnique 46(1):145–151.

Schanz, T., and P. A. Vermeer. **1996b**. Angles of friction and dilatancy of sand. Géotechnique 46:145–151.

Schanz, T., and P. A. Vermeer. **1998**. On the Stiffness of Sands; pp. 383–387 in R. J. Jardine, M. C. R. Davies, D. W. Hight, A. K. C. Smith, and S. E. Stallebrass (eds.), Pre-failure Deformation Behaviour of Geomaterials. Thomas Telford, London.

Schanz, T., P. A. Vermeer, and P. G. Bonnier. **1999**. The Hardening Soil Model: Formulation and Verification; pp. 1–16 in R. B. J. Brinkgreve (ed.), Beyond 2000 in Computational Geotechnics - 10 Years of PLAXIS International. CRC Press, Rotterdam, 328 pp.

Seebacher, F. 2001. A new method to calculate allometric length-mass relationships of dinosaurs. Journal of Vertebrate Paleontology 21(1):51–60.

Seelos, K., and F. Sirocko. **2005**. RADIUS - rapid particle analysis of digital images by ultra-high-resolution scanning of thin sections. Sedimentology 52(3):669–681.

Sellers, W. I., J. Hepworth-Bell, P. L. Falkingham, K. T. Bates, C. A. Brassey, V. M. Egerton, and P. L. Manning. **2012**. Minimum convex hull mass estimations of complete mounted skeletons. Biology Letters 8(5):842–845.

Sellers, W. I., L. Margetts, R. A. Coria, and P. L. Manning. **2013**. March of the titans: the locomotor capabilities of sauropod dinosaurs. PLoS ONE 8(10):1–21.

Stevens, K. A., S. Ernst, and D. Marty. **2016**. Uncertainty and Ambiguity in the Interpretation of Sauropod Trackways; pp. 226–242 in P. L. Falkingham, D. Marty, and A. Richter (eds.), Dinosaur Tracks - The Next Steps. Life of the Past. Indiana University Press, Bloomington, 413 pp.

Taylor, D. W. 1948. Fundamentals of Soil Mechanics. John Wiley & Sons Inc., New York, 712 pp.

Thulborn, T. 1990. Dinosaur Tracks. Chapman and Hall, New York, 410 pp.

Upchurch, P. 1995. The evolutionary history of sauropod dinosaurs. Philosophical Transactions of the Royal Society B: Biological Sciences 349(1330):365–390.

Vila, B., O. Oms, À. Galobart, K. T. Bates, V. M. Egerton, and P. L. Manning. **2013**. Dynamic similarity in titanosaur sauropods: ichnological evidence from the Fumanya Dinosaur Tracksite (Southern Pyrenees). PLoS ONE 8(2):1–9.

Wedel, M. J. 2003. Vertebral pneumaticity, air sacs, and the physiology of sauropod dinosaurs. Paleobiology 29(2):243–255.

Wedel, M. J. 2009. Evidence for bird-like air sacs in saurischian dinosaurs. Journal of Experimental Zoology 311A(8):611–628.

Wedel, M. J., and M. P. Taylor. **2013**. Caudal pneumaticity and pneumatic hiatuses in the sauropod dinosaurs *Giraffatitan* and *Apatosaurus*. PLoS ONE 8(10):1-14.

White, M. A., A. G. Cook, and S. J. Rumbold. **2017**. A methodology of theropod print replication utilising the pedal reconstruction of *Australovenator* and a simulated paleosediment. PeerJ 5(4):1-19.

Wilson, J. A. 2005. Integrating ichnofossil and body fossil records to estimate locomotor posture and spatiotemporal distribution of early sauropod dinosaurs: a stratocladistic approach. Paleobiology 31(3):400–423.

Wilson, J. A., and M. T. Carrano. **1999**. Titanosaurs and the origin of "wide-gauge" trackways: a biomechanical and systematic perspective on sauropod locomotion. Paleobiology 25(2):252–267.

Wilson, J. A., and P. C. Sereno. **1998**. Early evolution and higher-level phylogeny of sauropod dinosaurs. Journal of Vertebrate Paleontology 18(S2):1–79.

Wright, J. L. 2005. Steps in Understanding Sauropod Biology; pp. 252–280 in K. Curry Rogers and J. A. Wilson (eds.), The Sauropods - Evolution and Paleobiology. University of California Press, Berkeley, 349 pp.

CHAPTER 7

Synthesis:

Sauropods on scales – or how vertebrate ichnology gains ground through interdisciplinarity and multi-methodology

7.1. ABSTRACT

In modern scientific endeavors, interdisciplinary research is vital for extracting novel and complex insights into various subjects. Notably, in the field of paleontology, researchers aim to understand the biology of extinct organisms and the mechanisms of preservation over millions of years, which require broad knowledge in fields such as mechanics, physiology, histology, diagenesis, and fossilization. Vertebrate ichnology particularly benefits from the cooperation with other disciplines. Although animal tracking is an ancient art, the interdisciplinary work between natural and engineering sciences has shed new light on this topic using modern, quantitative methods. This paper reviews developments in interdisciplinary track research, including updated approaches for documenting tracks. With a focus on sauropod dinosaurs, the wealth of information will be reviewed that tracks bear as "petrified movements" for inferring paleobiological features, such as locomotion and body mass. By combining paleontology with perspectives and methods from other fields, all involved parties benefit mutually. The interdisciplinary approach described here could influence future research on dinosaur ichnology, but also prehistoric anthropology and modern forensics, likewise.

7.2. INTRODUCTION

7.2.1 General introduction

Animals usually leave them in their natural habitats; we humans do too, but we do not see them very often, since we have footwear and we walk on asphalt roads. I am speaking of course of footprints and tracks. The art of describing and interpreting tracks has a long history. Foresters, hunters, tribal people, and our prehistoric ancestors have learned to read and make use of this kind of trace: What animal lives here? Where did it go and how fast was it? Was the animal traveling alone or in a herd?

Understanding tracks has been a valuable tool for our survival, but also for our general knowledge of the biology of trackmakers. Not only can we interpret footprints of extant animals, such as for tracking of endangered species (Alibhai et al., 2008), but also fossil tracks, as this has been done for hominids and early humans (Bates et al., 2013; Bennett et al., 2013; Dingwall et al., 2013; Ashton et al., 2014; Masao et al., 2016), ancient mammals (Alf, 1959, 1966; Renders, 1984; Scrivner and Bottjer, 1986; Mustoe, 2002; Bennett et al., 2014), and for dinosaurs (Gillette and Lockley, 1989; Thulborn, 1990; Lockley and Hunt, 1995; Lockley and Meyer, 2000; Falkingham et al., 2016a).

Dinosaurs were the makers of many fossil tracks from the Mesozoic time. From their first reconstructions in the 19th century until today dinosaurs underwent a complete makeover. Back then, dinosaurs were reconstructed as plump animals (Figure 7.1). Today, we have a different view on their outer appearance, weight and locomotion of dinosaurs, because paleobiology provided a great deal of insight about these animals. One has to watch modern documentaries or films (e.g., Jurassic World), to see dinosaur reconstructions moving with agility and elegance, which is mostly based on paleontological research on both body fossils and tracks. In addition, interdisciplinary approaches from other fields contributed to the modern picture of dinosaurs during the last decades.

7.2.2 Purpose of this paper

Interdisciplinarity is very important in modern paleontology. In the last century, paleontological research was often a largely descriptive pursuit rather than interpretive, which holds particularly true for dinosaur ichnology. By integrating new techniques from other disciplines, vertebrate ichnology is able to gain ground on scientific and modern approaches as well as to gain new insights to advancing research. This article focusses on sauropod tracks, which provide a prime example of the suitability and power of interdisciplinary work, particularly geology, geodesy, paleobiology, zoology, soil mechanics, and biomechanics, to make paleobiological inferences (Figure 7.2, upper gear-wheel). The formation of tracks and trackways is always influenced by three factors, anatomy, locomotion, and substrate (Padian and Olsen, 1984; Falkingham, 2014). Thus, the individual tracks, their

distribution within a trackway, and the medium that contains the tracks should always be integrated into the analyses for a holistic interpretation of tetrapod ichnofossils.

First, the following text generally describes which valuable information about a trackmaker, its anatomy, and paleobiology, can be obtained from tracks. Next, it is shown how incorporating multiple methods improve the documentation of tracks. Finally, based on the sample question of "How to estimate the weight of a sauropod trackmaker from its tracks?", in this paper I will review a sequence of interdisciplinary working steps (Figure 7.2, middle gear-wheel) to illustrate this point. The last section focusses on paleobiological features, such as weight and locomotion, which additionally are discussed based on actualistic studies on the movement and weight of extant trackmakers, such as horse and elephant.

Specifically, paleobiological interpretations about trackmakers based on evidence from disparate fields of study are of interest in this review. The paper intends to provide an innovative view on dinosaur ichnology by bringing together aspects from traditional vertebrate ichnology, not only with digitizing methods and soil mechanics but also with considerations from biomechanics.

Figure 7.1: A historical reconstruction of a megalosaur dinosaur in the Crystal Palace Grounds, London, Great Britain. This is one of the sculptures erected in the Mid-19th century. Photo by S. Läbe.

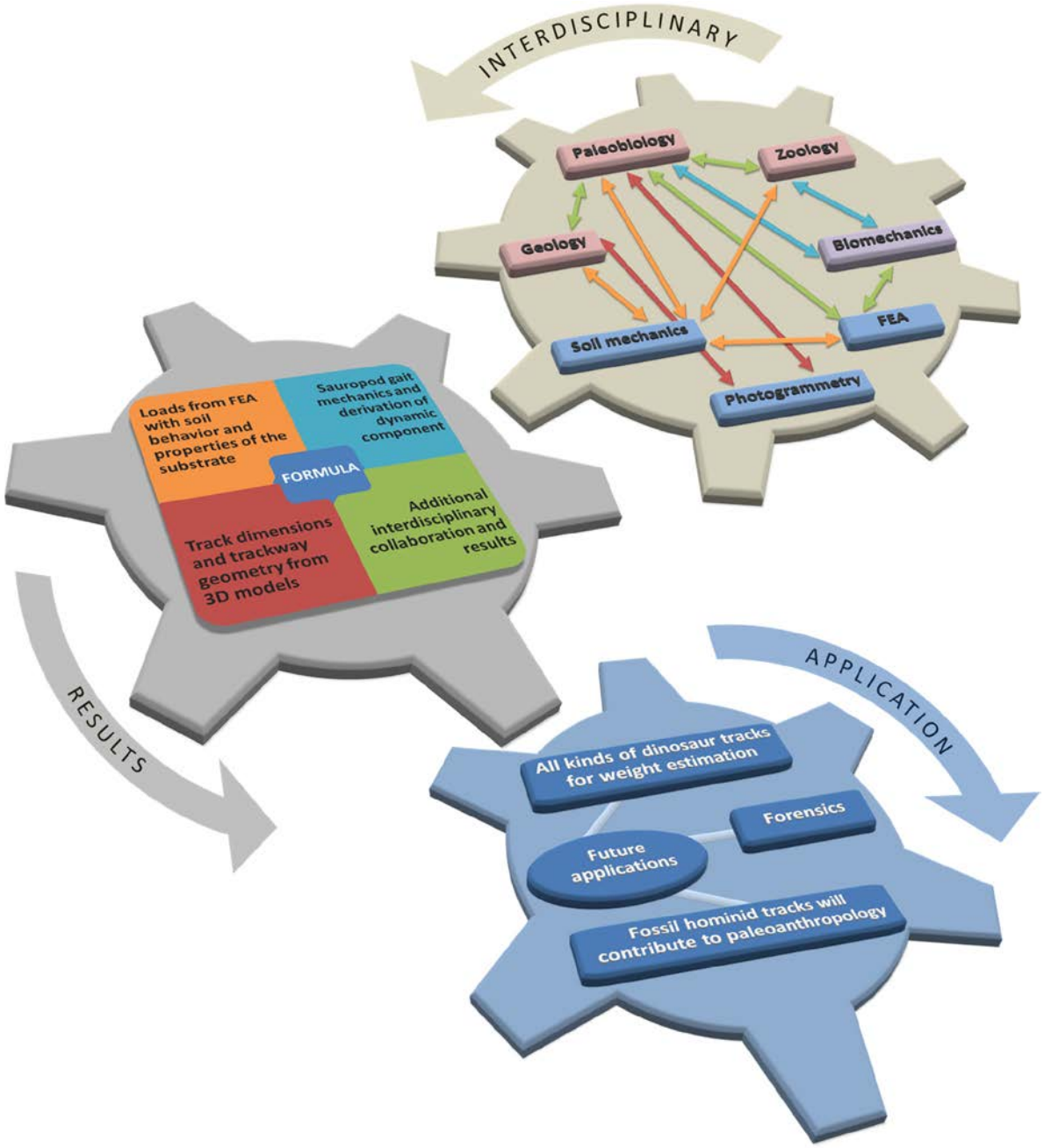

Figure 7.2: Example of an interdisciplinary and multi-methodical workflow in modern vertebrate ichnology. The basis consists of several disciplines from natural science and engineering (upper gear-wheel). The arrows are color-coded and represent several cooperations that are assigned to the results (middle gear-wheel). From the results, a formula for the weight estimation based on tracks is developed that will lead to further planned projects and potential applications (lower gear-wheel).

7.3. WHAT TRACKS CAN TELL US

7.3.1 Early research on dinosaur tracks and current state of sauropod ichnotaxonomy

Research of vertebrate tracks began in the 19th century when in England, Germany and the United States numerous petrified tracks were found and described. Tracks of the "hand-beast" found in Thuringia, Germany, were named *Chirotherium barthii* (Kaup, 1835). It was the first ichnotaxon ever to be mentioned; the importance of this particular ichnotaxon

is, for example, reflected in the name of the lithology in which these tracks are abundantly found - "Chirotheriensandstein" (cf. Haubold, 1984). The first dinosaur tracks were found in the Connecticut River Valley, USA. Although the scientist Edward Hitchcock erroneously described these traces as bird and lizard tracks, he collected and published a lot of data (Hitchcock, 1836, 1848, 1858, 1865) that were of value for future dinosaur track research. Shortly after that, three-toed tracks were found in the Early Cretaceous Wealden of Southern England (Tagart, 1846), which initially were also attributed to birds. Later, the English tracks were re-described as having been formed by *Iguanodon* (Jones, 1862). In a similar lithology in Northern Germany, three-toed tracks were named "*Ornithoidichnites*" based on their bird-like shape (Struckmann, 1880) and later correctly attributed to dinosaurs (Struckmann, 1880; Ballerstedt, 1905, 1914). The sauropod tracks from the Dinosaur Valley State Park, Texas, USA (Glen Rose Formation) were the first sauropod dinosaur tracks to be described (Bird, 1939; Bird, 1944; Farlow et al., 2012). However, Bird (1944) interpreted some of these manus-dominated sauropod tracks as swimming tracks, which is to this day a matter of controversial discussion (e.g., Ishigaki, 1989; Lockley and Rice, 1990; Henderson, 2004; Falkingham et al., 2011a; Milner and Lockley, 2016).

For a long time, dinosaur ichnology almost fell into oblivion, even though dinosaur body fossils were studied with enthusiasm and new knowledge was gained. In the 1980's, research on dinosaur track became popular again (e.g., Haubold, 1984; Leonardi, 1987; Gillette and Lockley, 1989), such that some refer to it as the "dinosaur track renaissance" (Lockley, 1986, 1991a, 1998; Falkingham et al., 2016b). This led to a wave of discoveries of dinosaur tracksites and new ichnospecies. The main contribution during this time was a proceedings volume of the First International Symposium on Dinosaur Tracks and Traces, which was held in May 1986 in Albuquerque, New Mexico, USA (Gillette and Lockley, 1989) followed by two books for general audiences that pointed out the value of dinosaur tracks (Thulborn, 1990; Lockley, 1991b).

The immense size of sauropod tracks, such as the tracks from the Lower Cretaceous Broome Sandstone, Australia, with a length of single pes prints measuring more than 150 cm (Salisbury et al., 2017), make them particularly remarkable and interesting for studies reviewed in this article. Tracks of sauropods and sauropodomorphs have since been found in sediments ranging in age from the Triassic (Lallensack et al., submit.; Lockley et al., 2001) to the Cretaceous (Wright, 2005; Mannion and Upchurch, 2010; Falkingham et al., 2012). Tracks found in both cohesive (e.g., mudstones) and non-cohesive (e.g., sandstones) sediments suggest that the trackmakers inhabited a variety of environments (Mannion and Upchurch, 2010; Falkingham et al., 2012).

For tracks, a parataxonomy (e.g., Krell, 2004) is used, similar to coprolites (e.g., Hunt et al., 2012) and dinosaur eggs (e.g., Mikhailov, 2013). This is mainly because tracks cannot unambiguously be linked to taxon known from body fossils. Since parataxonomy is a wide

field, this paper mentions only two among many other sauropod ichnotaxa: *Parabrontopodus* (Lockley, Farlow et al., 1994) and *Brontopodus* (Farlow et al., 1989) are the most common ones. Other names, such as "*Elephantopoides*" (Kaever and de Lapparent, 1974) and "*Rotundichnus*" (Hendricks, 1981) for sauropod tracks from localities in Northern Germany, were considered nomina dubia and later assigned to *Parabrontopodus* (Lockley, Farlow et al., 1994) and *Brontopodus* (Lockley et al., 2004), since these tracks lack diagnostic synapomorphies to justify new ichnotaxa.

Parabrontopodus is characterized by a narrow-gauged trackway and high heteropody (ratio of area of manus tracks to pes tracks; Lockley, 1989; Lockley, Farlow et al., 1994; Santos et al., 1994; Lockley, 2007), based on which the taxon is attributed to non-macronarian neosauropods. *Brontopodus* is a wide-gauge, low heteropody ichnotaxon attributed to macronarian sauropods (Farlow, 1992; Lockley, Farlow et al., 1994; Wilson and Carrano, 1999; Wilson, 2005). Although the two different taxa and gauge types seemed to correspond to skeletal anatomical characters, this strict distinction does not hold up anymore, since a single trackway can have alternating narrow- and wide-gauge tracks (Romano et al., 2007; Marty, 2008; Santos et al., 2009; Castanera et al., 2012).

7.3.2 Information contained in tracks

In some cases, fossil tracks are even more significant than skeletal fossils: Body fossils represent the death and final resting place of the animal, whereas tracks represent information about the trackmaker while it was alive. Although it is not usually possible to identify the trackmaker species from a track with certainty, except in rare cases. One example are horseshoe crab tracks from the Solnhofen Lithographic Limestone with the trackmaker preserved at the end of its trackway (Lomax and Racay, 2012). Tracks tell us if the animal is bipedal or quadrupedal as well as the shape of the foot and the number of digits. This information can, for instance differentiate sauropods from theropods and ornithopods, and be used for trackmaker identification (Wright, 2005). Additionally, unlike in skeletons, the foot soft part anatomy and shape of the soft parts are observable. The hip height (Alexander, 1976) and trunk length (cf. Leonardi, 1987) of the trackmaker can be roughly estimated. Within a trackway, step lengths tell the speed of the trackmaker (Alexander, 1976; Thulborn, 1990). Furthermore, tracks provide information about behavior (Day et al., 2002; Bibi et al., 2012), such as gregariousness (Lockley et al., 2002; Myers and Fiorillo, 2009; Lockley et al., 2012; McCrea et al., 2014), and even pathologies (McCrea et al., 2015; Razzolini, Vila et al., 2016). Finally, tracks tell the actual habitat which the animal lived in (Mannion and Upchurch, 2010; Falkingham et al., 2012), unlike for skeletal material which frequently experienced post-mortem transport.

After many descriptive studies on dinosaur tracks, today the question ichnologists concern themselves with is about the paleobiology of the dinosaurian trackmaker. In recent years, more effort has been undertaken to understand dinosaur track formation and to obtain

quantitative interpretations by thorough analysis and reproduction of tracks. Modern studies, for instance, include experiments with extant animals, such as birds (Milàn, 2006; Falkingham and Gatesy, 2014) and elephants (Platt et al., 2012; Schanz et al., 2013; Chapter 3), to gain information about the process of track formation; likewise laboratory experiments using indenters on various substrates have been performed (Manning, 2004; Jackson et al., 2009, 2010; White et al., 2017). These and other new interpretations and approaches are highlighted in the book "Dinosaur Tracks – Next Steps" edited by Falkingham et al. (2016a), which also summarizes current techniques, ichnotaxonomy, paleobiology and preservation from a modern point of view.

7.3.3 An advanced technique for investigating track formation: FEA

One of the promising techniques currently applied to modern track research is the finite element analysis (FEA). FEA is a numerical method from engineering sciences for the computer-based simulation of physical processes. In vertebrate paleontology, FEA is commonly used for biomechanical research, such as reconstructions of bite forces and jaw mechanics (Bell et al., 2009; Bates and Falkingham, 2012; Lautenschlager, 2013; Snively et al., 2015). In the investigation of tracks, FEA is another example of interdisciplinary research that investigates how substrate interactions influence track formation.

Early FEA work on tracks simulated the shape and depth of tracks through several layers of substrate (Margetts et al., 2005; Margetts et al., 2006). From a geotechnical point of view, this might be nothing new, but for ichnology this is very important, for example, for the understanding of undertracks (cf. Milàn and Bromley, 2006; Milàn and Bromley, 2007). In recent years, Peter Falkingham, specifically, contributed immensely to the application of FEA on the research of dinosaur tracks (Falkingham, 2010). Falkingham et al. (2009) investigated whether fossil tracks with a "webbing" between the digits occur from an actual semi-palmate or palmate foot structure, such as observed in the feet of waterfowl, or from material failure of the substrate between the digits. In Falkingham et al. (2010), the specific track depth was evaluated with FEA, which was found to be influenced by trackmaker size, foot morphology, and substrate conditions. The effect of the position of the center of mass(CM) in a sauropod trackmaker was studied by Falkingham et al. (2011a). By applying different loading conditions on virtual substrates, it was possible to produce manus-only footprints comparable to the tracks observed by Lockley, Pittman et al. (1994). In a later work, FEA revealed that tracks form only under special conditions of the substrate, as well as depending on the size and shape of the penetrating foot (Falkingham et al., 2011b). This was termed the "Goldilocks effect", since the foot constitution, load constitution, and substrate constitution have to be "just right" to produce tracks. The method was refined in Falkingham, Hage et al. (2014). In all these studies by Falkingham and colleagues, several substrate parameters such as shear strength, Poisson ratio, and Young's modulus had been addressed in the FEA simulations. Other uses of the FEA in-

clude Sanz et al. (2016), who used a soil mechanical FEA method comparable to Schanz et al. (2013; Chapter 3; to be discussed in detail below), to simulate tracks from the early Cretaceous Miraflores I tracks from Spain with focus on sedimentological characteristics.

7.4. DOCUMENTING DINOSAUR TRACKS

7.4.1 Conventional methods

Tracks and entire tracksites are often too large and fragile to remove them from the locality to a museum collection. Therefore, they usually remain *in situ*, which means proper documentation is needed for research. Before the advent of technologically advanced documentation methods, the classical way for documenting dinosaur tracks was done by sketching them on paper, taking photographs, creating plaster casts and molds, or by tracing the tracks in their original size through transparent film (Thulborn, 1990; Lockley, 1991a). While plaster and resin casts and molds provide realistic and three-dimensional (3D), though space-consuming, replicas of tracks, the other methods have potential of misinterpreting tracks because they usually incorporate a perspective distortion by the point of view of the observer.

7.4.2 Digital dinosaur tracking

A novel application of 3D methods started to be used on dinosaur tracks in the beginning of the 21st century for digital documentation. Laser scanning, as an example, proved to be valuable for accurate documentation of dinosaur footprints, trackways, and entire tracksites (Bates, Breithaupt et al., 2008; Bates, Manning et al., 2008; Bates et al., 2009; Adams et al., 2010; Bates, Falkingham et al., 2010; Platt et al., 2010).

An alternative method was photogrammetry, which had been newly adopted in paleontology (Matthews and Breithaupt, 2001; Breithaupt et al., 2004; Breithaupt et al., 2006; Matthews et al., 2006; Bates, Breithaupt et al., 2008; Breithaupt and Matthews, 2011). However, photogrammetry required expensive software and powerful computer hardware to be performed. For those reasons, laser scanning was preferred until the introduction of open-source software for photogrammetry and more reasonable costs for powerful workstations (Falkingham, 2012, 2013).

Originally, photogrammetry was a method employed in geodesy and architecture, already developed in the 19th century (Grimm, 2007; Matthews et al., 2016). The benefits of photogrammetry are that it is non-destructive, it can be applied to objects of different scales, and that it is very user-friendly, thanks to modern interfaces of computer software and even mobile phone apps. Additionally, the data collection is accelerated and more precise than for older techniques. Photogrammetry is a method now very popular in paleontology in general (Mallison and Wings, 2014), because it is also used in paleobotany (Fernández-

Lozano and Gutiérrez-Alonso, 2017), body volume reconstructions (Stoinski et al., 2011), sauropodomorph morphology (Hofmann and Sander, 2014), and geometric morphometrics on tracks (Lallensack et al., 2016). Matthews et al. (2016) comprehensively reviewed the advantages of photogrammetry in terms of dinosaur ichnology.

Recent publications of new dinosaur tracksites usually include a thorough digitization using photogrammetry, which enhances not only the interpretation of the tracks but also the traceability and makes data access easier. Investigations of the Early Cretaceous Dinosaur Ridge tracksite, Colorado, USA (Matthews and Breithaupt, 2001), the Middle Jurassic Red Gulch Dinosaur Tracksite, Wyoming, USA (Breithaupt et al., 2004), and the Early Jurassic Coste dell'Anglone tracksite in Italy (Petti et al., 2008) are just a few studies relying on the application of photogrammetry in the documentation of dinosaur tracksites.

In addition to scientific pursuits, it is worth digitizing dinosaur tracksites from a historical perspective (Santos et al., 2008; Enniouar et al., 2014; Santos, 2016). The digital tracks will still be accessible on digital archives, even when the original tracks become destroyed or eroded. Since conservation of most dinosaur tracksites is not always possible, photogrammetry is a way to "preserve" these geological heritages. In the case of Bird's Cretaceous Paluxy River tracksite (Bird, 1939; Bird, 1944), which was destroyed over a half-century ago by excavation, Falkingham, Bates et al. (2014) were able to successfully reconstruct the site based on historic photographs. Lallensack et al. (2015) were also able to reconstruct destroyed dinosaur tracks and trackways from the Upper Jurassic Langenberg Quarry, Germany, with historical photogrammetry.

A major benefit of these digital track models is their precision and realistic depiction of the original dinosaur tracks in the field. However, problems persist, since interpretation of tracks, both digital and original, is highly dependent on the experience and objectivity of the researcher. For example, one issue is the correct assessment of the tracks outline, as was discussed by Falkingham (2016) and Lallensack (2016).

7.4.3 New approaches to the digital documentation of tracks

Although photogrammetry improves the interpretation of tracks substantially, the potential of some tracksites is still not fully exploited. Tracksites with skin impressions (e.g., Platt and Hasiotis, 2006; Fondevilla et al., 2016) as an indicator for excellent track preservation are rare. Most tracksites show poor preservation of the tracks with a low numerical scale of preservation quality as described by Belvedere and Farlow (2016). Refining steps in the post-processing of the 3D models, beyond the simple application as a documentation method, can lead to improved interpretability. For a better visualization, recent publications include color depth maps of the tracksite (e.g., Lallensack et al., 2015; Razzolini, Oms et al., 2016).

In addition, Läbe (in revision; Chapter 2) introduced the visualization method of vertical exaggeration (VE) for improving the usability of 3D models of tracks not only for documentation but also for further interpretations. VE is common in geology for visualizing cross sections. In VE, 3D models are stretched along the z-axis by increasing the scale of the vertical axis relative to the horizontal axes. Läbe (in revision) employed this method for digitizing four Jurassic and Cretaceous sauropod tracksites that had formerly been classified as poorly preserved. The 3D models for these sites were edited and manipulated to highlight additional detail and to emphasize subtle features and very shallow tracks. In general, a factor of ten for the VE was evaluated as sufficient, since it is a compromise between a less effective and a too manipulative alteration of the data.

Compared to previous research on these tracksites, visibility of the tracks was enhanced in the vertical exaggerated models. In the vertically exaggerated 3D models seen in top-down view, additional tracks were revealed that could not be recognized in the field and questionable tracks were confirmed. In the case of the Copper Ridge Dinosaur tracksite (Lockley, 1991a; Lockley and Hunt, 1995; Ishigaki and Matsumoto, 2009; Foster, 2015; Hunt-Foster et al., 2016), additional manus imprints were found that were hardly recognized in the field. The confirmed manus tracks (cf. Ishigaki and Matsumoto, 2009) were important for the further interpretation of the locomotion of the trackmaker by Läbe (unpubl. b; Chapter 6). The detailed and exaggerated structure in the tracks might also help with trackmaker identification. VE 3D models of tracks can be viewed in lateral view to determine the walking direction. This is helpful because some tracksites elicited conflicting interpretations regarding the traveling direction of the trackmaker, for example, the Jurassic Barkhausen tracksite, Germany (Kaever and de Lapparent, 1974; Friese, 1979; Lockley, Farlow et al., 1994; Lockley and Meyer, 2000; Lallensack et al., 2015). This information about the trackmaker's direction of travel can be used for inferences about a preferred direction of travel in the case of multiple trackmakers or about gregarious behavior (Lockley et al., 2002; Myers and Fiorillo, 2009; Lockley et al., 2012; Fiorillo et al., 2014; McCrea et al., 2014).

7.5. INFERENCES FROM INTERDISCIPLINARY TRACK RESEARCH WITH THOUGHTS ON SAUROPOD PALEOBIOLOGY

7.5.1 The sauropod trackmaker

Sauropod dinosaurs were the largest terrestrial animals, not only among other dinosaurs (Figure 7.3). Analyzes and interpretations on the causes of gigantism of this successful, Mesozoic animal group were carried out by the DFG Research Unit 533 "Biology of the Sauropod Dinosaurs: the Evolution of Gigantism" (Klein et al., 2011; Sander, 2013). In addition to the enormous body mass of sauropods, which seem to have led to a selective

advantage, the research unit has contributed to the extension of knowledge about sauropods with modern, interdisciplinary approaches to investigate the high diversity of this animal group, its evolution and bauplan (Sander and Clauss, 2008; Klein et al., 2011; Sander et al., 2011; Sander, 2013). Not only the gigantic size was a key feature of sauropod evolution, but also reproduction with small offspring (e.g., Sander et al., 2008; Vila et al., 2010; Fowler and Sullivan, 2011), high growth rates (e.g., Werner and Griebeler, 2011; Cubo et al., 2012; Stein and Prondvai, 2014), food intake and diet (e.g., Gee, 2011; Tütken, 2011; Clauss et al., 2013; D'emic et al., 2013), and bird-like respiratory anatomy with postcranial skeletal pneumaticity (e.g., Perry et al., 2011; Yates et al., 2012; Wedel and Taylor, 2013) contributed among other traits (Sander, 2013) to the success of sauropods.

All sauropods had a similar bauplan in common (Upchurch, 1995; Wilson and Sereno, 1998; Curry Rogers and Wilson, 2005). The high body mass was borne on their massive, pillar-like limbs, which makes their quadrupedal stance graviportal (e.g., Hutchinson, 2006; Houssaye et al., 2016) and their locomotion very interesting. It may seem plausible to compare sauropods to the extant graviportal elephants (Figure 7.3), yet they differ in their articulation of the columnar limbs. While elephants have their limbs in a parasagittal plane, the glenohumeral joint of sauropods was posteroventrally oriented and suggests a non-parasagittal articulation (Bonnan, 2003; Schwarz et al., 2007; Stevens and Wills, 2009). Thus, the pectoral girdle has a ventral position which might also compensate for unequal fore- and hindlimb lengths (Stevens et al., 2016), such as in diplodocids.

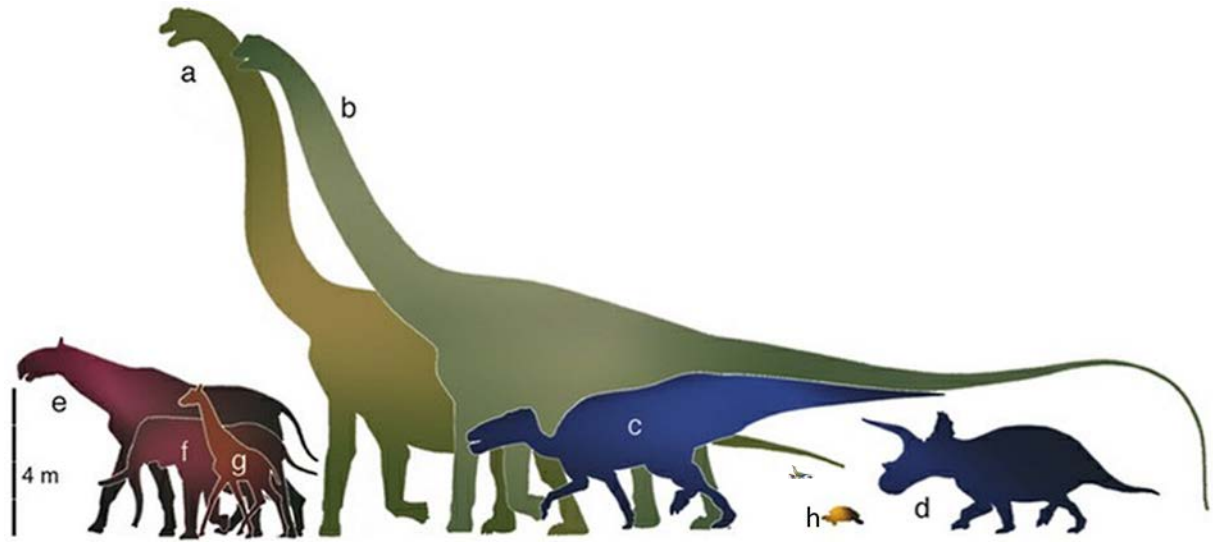

Figure 7.3: Body size in different terrestrial animals. Sauropods (a) *Brachiosaurus* and (b) *Argentinosaurus* were larger than (c) the horn-billed dinosaur *Shantungosaurus*, (d) the horned dinosaur *Triceratops*, the fossil rhinoceros (e) *Indricotherium*, (f) the African elephant, (g) the giraffe and the largest living herbivorous reptile, (h) the Galapagos tortoise (modified from Rauhut, 2007 and Sander, 2015).

7.5.2 Body mass

7.5.2.1. Body mass estimation techniques

Body mass is one of the fundamental attributes of any organism, thus it is of particular interest for the study of sauropod dinosaurs. For adult sauropods the body mass estimates extended over three orders of magnitude, starting at about 800 kg for *Europasaurus* (Sander et al., 2006) up to about 120 metric tonnes for *Amphicoelias* (Carpenter, 2006). Note that the physical term mass is often referred to as weight, which is technically a force exerted to an object by acceleration of gravity. However, it was refrained to strictly distinguish both terms, since the following weight/mass estimation approaches explicitly consider the acceleration and forces exerted on the substrate by the trackmaker during track formation. But how realistic are above-mentioned body mass estimates? Specifically, if we consider that the largest terrestrial animal today is *Loxodonta africana* (African elephant) with a weight of about 6,000 kg.

Extant animals are uncomplicated to weigh directly by using a scale. However, there are also several indirect approaches for estimating the body mass of extinct animals based on allometry and volumetry. The first one is based on a relationship between body mass and long bones that carry the weight of the animal. Anderson et al. (1985) and Campione and Evans (2012) worked on this approach and developed scaling relationships in extant and extinct tetrapods and birds. The latter one is based on reconstructions of the body volume that is multiplied by a specific density to obtain a mass estimate. Early approaches used dinosaur scale models (Colbert, 1962; Alexander, 1985), while recent studies involve computer-generated 3D models for body volume reconstruction (Henderson, 1999; Henderson, 2004; Henderson, 2006; Gunga et al., 2007; Gunga et al., 2008, 2008; Sellers et al., 2012).

Crucial for the volumetric approach is the value for the density, since it varies for different body tissues. Alexander (1983) illustrated that bone is denser (2000 kg/m³) than muscles (1050 kg/m³) and fat (900 kg/m³) and that lungs filled with air have a density of 1 kg/m³. Specifically for sauropods, the latter one is of particular interest, since parts of the vertebral column, the ribs, and the girdle bones show pneumaticity, which is associated with air sacks and an avian-style lung (Wedel, 2003; Henderson, 2004; Wedel, 2009; Yates et al., 2012; Wedel and Taylor, 2013; Melstrom et al., 2016). Postcranial skeletal pneumaticity would have decreased the overall density of a sauropod and thus has implications for body mass estimates. In addition, the distribution of skeletal and non-skeletal pneumaticity in the body affects the position of the CM and thus locomotion (Henderson, 2004). With the knowledge about pneumaticity, sauropod weight estimates may need to be revised to lower values. Re-interpretation of dinosaur body mass occurs frequently, such as in the case of the gigantic titanosaur *Dreadnoughtus* with an initial body mass estimate of about 60 tons (Lacovara et al., 2014). The sauropod, which is indeed gigantic in size, as its name refers to a battleship, was then re-examined by Bates et al. (2015): With different assumption

about body density, the titanosaur was “downsized” to a mass of about 40 tons. Such cases particularly illustrate that another method is required for inferring body mass independently from body fossils. Thus, the track record is used again to elicit information about the trackmaker.

7.5.2.2. Track-based mass estimation approach

A new method using tracks for weight estimation is based on the fact that tracks are substrate deformations resulting from the loads applied by the trackmaker. As noted in the introduction, statics, dynamics, and substrate contribute to the formation of tracks (cf. Padian and Olsen, 1984; Margetts et al., 2005; Falkingham, 2014). Thus, these three factors are important for any weight estimation approach from tracks. The force exerted on the substrate by the trackmaker is composed of a vertical component and a horizontal component. The vertical static force is caused by the weight of the trackmaker, while the horizontal component is due to the dynamics of the moving foot. Statics and dynamics are the mechanical components in the force system of track formation, which can be observed as plastic deformations, depending on the stiffness of the substrate material (e.g., Alexander, 1985; Demathieu, 1987; Manning, 2004; Bates et al., 2013).

A proof of concept for this approach was recently published by Schanz et al. (2013; Chapter 3). The weight of an elephant (with known weight) was back calculated from its footprints and the substrate that contained the tracks. After the elephant left its tracks behind in a prepared sand bed, the tracks were digitized to obtain their exact dimensions, and the subsoil was analyzed with soil mechanic laboratory experiments to determine the behavior of the soil. Based on this information, the elephant tracks were simulated using FEA. The amount of applied load required for generating a virtual elephant footprint in a substrate model with original soil properties was back-calculated to the weight of the elephant by incorporating the locomotion. Finally, the weight of the elephant was determined from the resulting forces with an error of approximately 15%.

7.5.2.3. The "sauropod scale"

Sauropod tracks from the 150-million-year-old Copper Ridge Dinosaur Tracksite, Utah, USA (Lockley, 1991b; Lockley and Hunt, 1995; Foster, 2015; Hunt-Foster et al., 2016) were used for the first ever case study for mass estimation from tracks based on the approach by Schanz et al. (2013; Chapter 3). The tracks were analyzed to estimate the weight (Läbe, unpubl. b; Chapter 6) of the trackmaker under consideration of its locomotion, resulting in a weight distribution factor that describes the peak load on any one foot during different gaits (Kienapfel et al., 2014; Chapter 4; Läbe, unpubl. a; Chapter 5). The substrate of the track-bearing surface at the Copper Ridge Dinosaur Tracksite was analyzed by sediment petrography and a comparable recent sediment was found from which the input parameter for the FEA were obtained (see also section 7.3.3). Loads were derived from the

FEA-simulated sauropod pes track. Using the load from the FEA, the area of the track, the gravity constant, and the weight distribution factor, the weight for the sauropod trackmaker was calculated to be about 16 metric tonnes (Läbe, unpubl. b; Chapter 6). This result fits within the broad range of mass estimates for this size class of sauropods from the Morrison Formation (cf. Klein et al., 2011; Appendix).

In the study by Schanz et al. (2013) on elephant tracks, the preconditions for calculating the dynamic force component exerted by the trackmaker were the knowledge of the mass of the moving limb and the speed of the trackmaker from video recordings. Obviously, both are not available for the trackmaker of fossil tracks. In general, the dynamic component in sauropod locomotion is assumed to be very low (see section 7.5.3.4), hence it was considered negligible. Instead, the locomotion of the sauropod trackmaker was approximated by weight distribution factors for the weight estimation approach by Läbe (unpubl. b; Chapter 6). The weight distribution factor (Läbe, unpubl. a; Chapter 5) has a value between 0 (low faction of body mass on a limb) and 1 (high fraction of body mass on a limb) and is calculated from the trackmaker's estimated CM and the type of limb support during a chosen hypothetical gait. The CM used to carefully approximate the type of trackmaker can be estimated from the trackway gauge (Farlow, 1992; Lockley, Farlow et al., 1994; Wilson and Carrano, 1999; Romano et al., 2007), heteropody index (Lockley, 1989; Lockley, Farlow et al., 1994; Santos et al., 1994; Santos et al., 2009), and manus versus pes domination of the track (Lockley, Pittman et al., 1994; Henderson, 2004; Henderson, 2006; Falkingham et al., 2012). The trackmaker's gait approximated from the footfall pattern in the trackway (Kienapfel et al., 2014) is used to estimate on how many limbs in ground contact weight is redistributed during locomotion (types of limb support) (Läbe, unpubl. a).

7.5.3 Sauropod locomotion

7.5.3.1. Overview on locomotion

Apart from their high body mass, the posture and locomotion of the sauropod dinosaurs is particularly interesting, since the weight was borne on pillar-like limbs during movement. The study of locomotion is a subject located intermediate between biology and mechanics; hence it has enormous potential for interdisciplinary approaches. For instance, biological insights on locomotion are applied to robotics to design machines that are modeled on nature in mobility and energy efficiency (e.g., McGhee, 1976; Alexander, 1984; Owaki et al., 2013) while on the other side the, so-called, evolutionary robotics are applied to reconstruct locomotor abilities of extinct animals (Sellers et al., 2003; Sellers et al., 2004; Sellers et al., 2005; Sellers and Manning, 2007; Bates, Manning et al., 2010).

The term locomotion is here understood as the way of legged animal movement on land. We focus on the quadrupedal locomotion, which is the movement on four legs. Among

different limb postures, such as sprawling (e.g. crocodiles), the erect limb posture is of interest, since it is present in mammalian and dinosaurian anatomy. The locomotion on land follows a cyclic movement of repeating sequences. These are termed gaits, such as walk, trot, pace, amble or gallop (i.e., canter in equine sports). According to Howell (1944) and Hildebrand (1989), gaits can either be symmetrical (harmonious locomotion, such as walk or trot, with even intervals between the footfalls), or asymmetrical (has uneven intervals, such as the gallop).

During these cycles, limbs can either be moved forward (swing phase) or remain in ground contact (stance phase) (Howell, 1944; Hildebrand, 1965, 1976, 1980). Walking and running are the two modes of cyclic terrestrial locomotion that can be distinguished in several ways (e.g., Starke et al., 2009): by the duty factor, which is the fraction of the cycle when a particular foot touches the ground (Hildebrand, 1976, 1980; Biewener, 1983; Hildebrand, 1985, 1989), the occurrence of a phase of aerial suspension (Hildebrand, 1985), the Froude number, which is a dimensionless speed measure (Alexander and Jayes, 1983; Gatesy and Biewener, 1991), and based on ground reaction forces (e.g., Li et al., 1996; Biknevicius et al., 2004; Witte et al., 2004; Balbinot and Carvalho, 2014). Obviously, most of these criteria are only available when studying a living animal in motion, but not for a fossil trackmaker from tracks.

7.5.3.2. How did extinct animals move?

For dinosaurs, it is specifically of interest how they moved, because they are only slightly comparable to any extant organism (Coombs, 1978). Although not easy to interpret (Stevens et al., 2016), tracks offer direct evidence of movement, unlike the body fossil record. In assessing locomotion, it is not only necessary to gain independent information from either tracks or bones, but also to interweave both data sources to obtain an integrated picture (e.g., Farlow, 1992; Wilson, 2005). Thus, research on animal anatomy and physiology, both extinct and extant (Hutchinson and Gatesy, 2000; Hutchinson, 2001a, 2001b, 2001c; Hutchinson and Gatesy, 2006), and computer simulation approaches (Henderson, 2006; Sellers et al., 2009; Hutchinson et al., 2011; Bates et al., 2013; Sellers et al., 2013) provided a great deal of insight into dinosaur locomotion. For instance, the locomotor abilities of *Tyrannosaurus rex* were examined by Hutchinson and Gatesy (2006) and Hutchinson et al. (2011) with 3D models of the muscles, leading to the conclusion that the locomotion of extinct theropods might have been comparable to extant ratites. In a study by Grossi et al. (2014), bipedal theropod locomotion was imitated with living birds wearing artificial theropod-like tails. The manipulation led to a shift of the CM and a vertically oriented femur, which was also assumed to characterize non-avian theropod locomotion.

7.5.3.3. Inferring locomotion from tracks

To infer locomotion from tracks, it has to be kept in mind that a track is always a combination of the static forces of the body weight and the dynamic forces of the movement of the trackmaker, as noted above. In rare cases, deep tracks reveal the limb kinematics of the trackmaker (Gatesy et al., 1999). Alexander (1976) and others (Thulborn, 1982; Alexander, 1985; Thulborn and Wade, 1989; Thulborn, 1990) proposed the formula $v = 0.25g^{0.5} \cdot s^{1.67} \cdot h^{-1.17}$ to estimate the speed v [m/s] of the trackmaker by using the acceleration of gravity g [m/s²], stride length measured from the trackway s [m], and the hip height estimated from the pes track length h [m]. For sauropod dinosaurs, speed estimations based on trackways (Alexander, 1976, 1989; Thulborn, 1990) and on limb proportions in sauropod skeletons (Christian et al., 1999) indicate slow walking with speeds of less than 5 km/h.

The accuracy of the speed formula is limited, because of numerous sources of error and the fact that it only provides relative speeds based on dynamic similarities that should not be seen as absolute speeds (Alexander, 1991). In addition, Mallison (2011) noted that speed estimates from tracks based on Alexander's formula should be understood as minimum estimates, and that dinosaurs could have combined high step frequencies with short strides to achieve higher speeds. However, an argument against Mallison's hypothesis is that in locomotion, the limbs normally do not swing outside the pendulum resonance frequency to remain energy efficient (Preuschoft et al., 1994; Preuschoft et al., 2011).
Another approach for inferring the trackmaker's locomotion is to study the footfall pattern in trackways to gain information about the employed gait. Tracks and trackways from different animals had been used for the evaluation of the gaits. For instance, for fossil camel tracks, it was proposed that the gaits trot and pace could be distinguished (Thompson et al., 2007). Renders (1984) assigned tracks of the extinct horse *Hipparion* from the volcanic ash deposits at Laetoli, Tanzania, to a running walk, by comparing them to extant horse tracks.

In a study by Kienapfel et al. (2014; Chapter 4), the tracks from highly trained horses were studied, in order to investigate if they yield reliable insights on the employed gait, at all. This was the first study to comprehensively investigate the connection of multiple gaits with the footfall pattern in trackways. And indeed, the horse trackways vary strongly in the different gaits (Figure 7.4). From the observed footfall pattern in the trackway, the step length and the placement of individual footprints in relation to each other is informative. Three possible arrangements can be seen (Figure 7.5): evenly spaced imprints along the trackway, the close placement of ipsilateral (fore- and hindlimb of same side of the body) imprints of fore- and hindfoot, and contralateral (opposite site of the body) imprints. For the ipsilateral configuration, three cases can occur: the hindfoot is placed behind the forefoot, the hindfoot is placed on top of the forefoot (overprinting), and the hindfoot is placed in front of the forefoot (overstepping).

The footfall patterns of asymmetrical gaits (canter/gallop) differ from the symmetrical ones (walk, trot, pace, and amble). However, all symmetrical gaits show similar trackways. Within the symmetrical gaits, the step lengths are considerably larger in the pace and in the trot, which is due to the higher speed. To obtain gaits from the footfall pattern, the trackmaker size and the limb length in relation to the trunk length need to be known or at least be estimated. The flow chart in Figure 7.5 summarizes the results of Kienapfel et al. (2014), illustrating different scenarios seen from the footfall pattern in horses to estimate symmetrical gaits. This chart is potentially useful to roughly estimate the gait of a quadrupedal dinosaurian trackmaker.

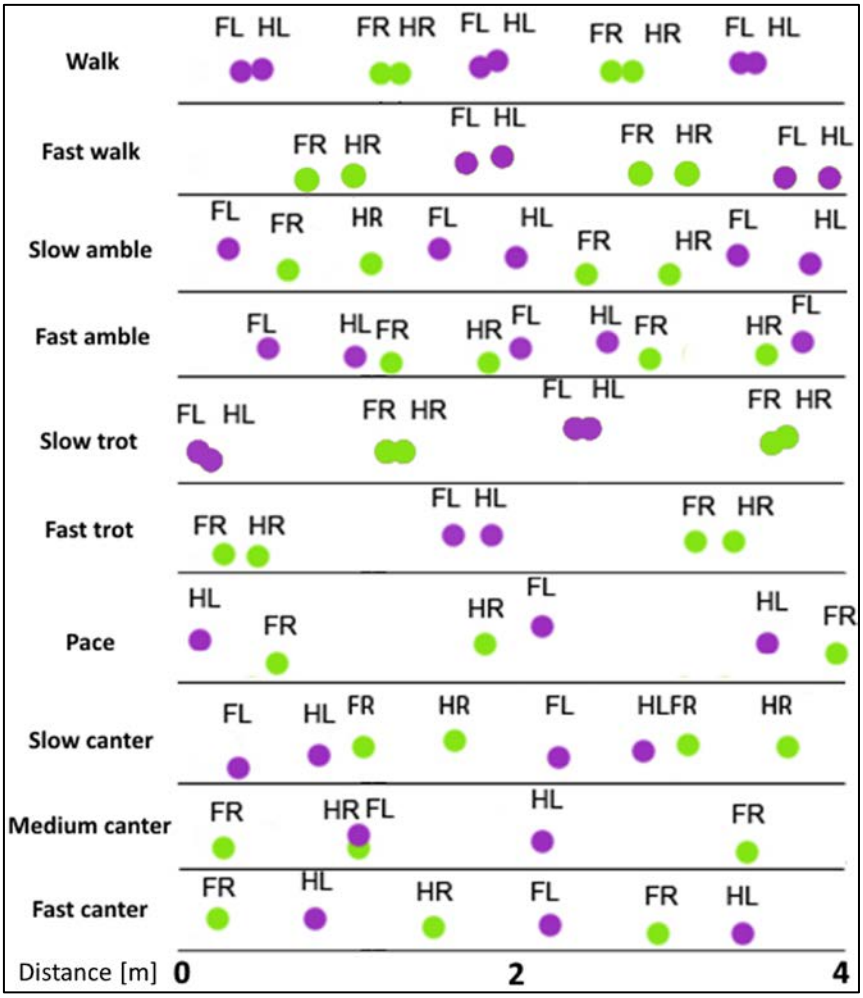

Figure 7.4: Different gaits in horses observed from footfall patterns in trackways. The tracks were measured and captured directly after they were imprinted by the horse. Each gait shows different placements of fore- and hindlimbs in the trackways. For example, in rapid gaits, such as trot and pace, the placements of the tracks (stride lengths) show larger distances. The length of each trackway is about 4 m (see bottom of image). Abbreviations: H = hindlimb, F = forelimb, purple dots = left limbs, green dots = right limbs. Modified from Kienapfel et al. (2014).

Although the excursion angle of the limbs during movement has not been discussed in depth by Kienapfel et al. (2014, Fig. 3; Chapter 4), it is an interesting aspect for distinguishing gaits from footfall patterns seen in tracks. Step length, which is the distance be-

tween footprints of the same foot, is limited by the limb length, which is approximately the hip height or height at withers, and the excursion angle. Step length and excursion angle cannot be continuously extended, since mobility in the joints of the pectoral and pelvic girdle is the limiting factor. If step length, and thus speed, should be increased further, the intercalation of an aerial suspension phase is unavoidable.

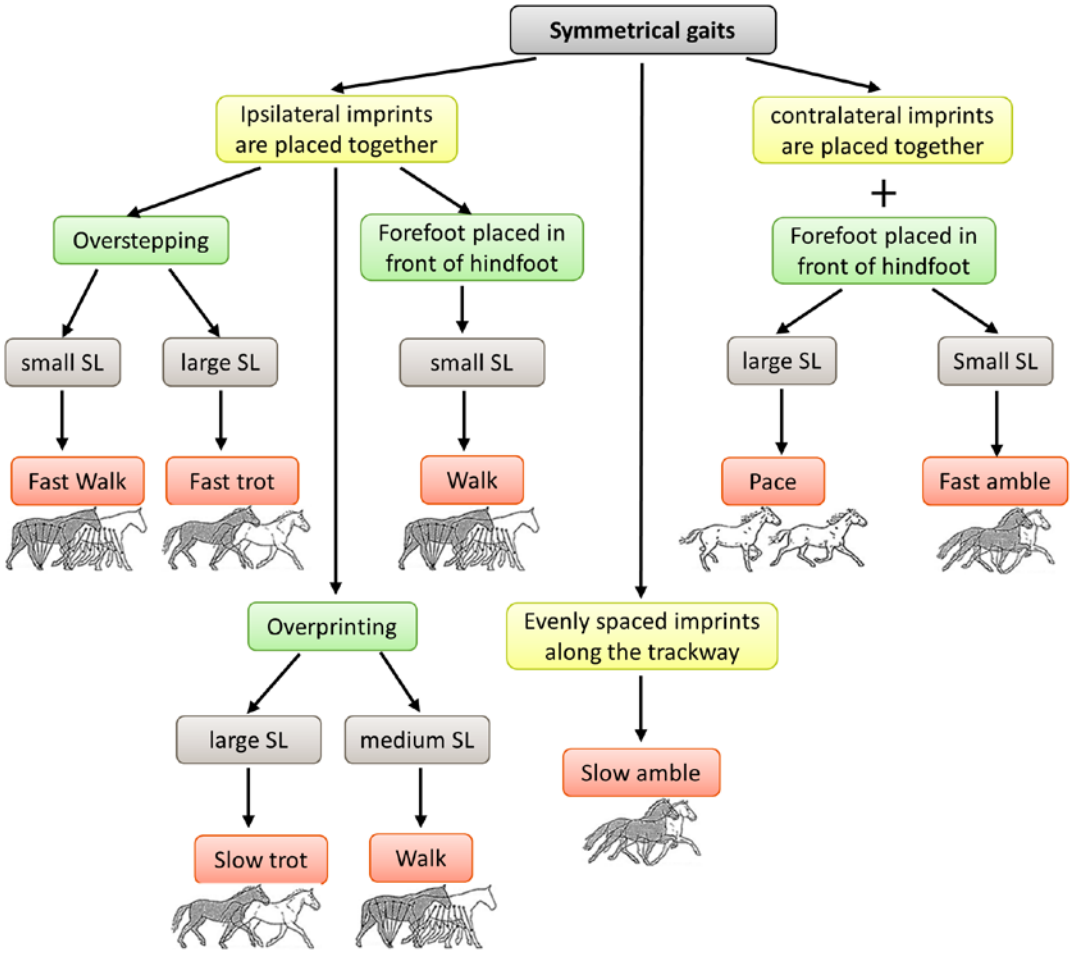

Figure 7.5: Flowchart for distinguishing trackways produced by different symmetrical gaits. SL = stride length. These are the main results from Kienapfel et al. (2014; Chapter 4); horse gait symbols were taken from Preuschoft et al. (2011).

7.5.3.4. Sauropod tracks

To study locomotion of sauropod dinosaurs, trackway evidence was included in several studies. Henderson (2006) used 3D models of sauropods constrained by the position of the CM to conclude that *Brachiosaurus* produced wide-gauge-trackways and *Diplodocus* produced narrow-gauged trackways. With that, he confirmed other studies (e.g., Farlow, 1992; Wilson and Carrano, 1999) about sauropod locomotion and posture. Other than that, the sauropod's repertoire of gaits is of interest. Sellers et al. (2013) used computer simulations constrained by speed, efficiency, and stability for investigating the locomotor capabilities of *Argentinosaurus* and proposed the pace gait. Also, prior studies concluded the pace as possible gait based on track evidence (Casanovas et al., 1997; Mezga et al., 2007; Vila et

al., 2013). According to the terminology of Hildebrand (1965, 1976, 1980, 1985, 1989), the pace is characterized by the alternating stance phases of ipsilateral limbs while the other side is in swing phase. The pace can be executed in a slow mode as a walking pace and a fast mode as a running pace, which includes a phase of aerial suspension. However, the pace is usually employed at higher speeds, since it is unstable at lower speeds (Hildebrand, 1985) due to the CM position lying outside of any support area and leading to a tipping over of the animal (Henderson, 2006). This is an argument against the proposals of sauropods employing a pace. Moreover, the studies mentioned above used formulas compiled by Leonardi (1987) and Farlow et al. (1989) based on previous work (Soergel, 1925; Baird, 1952, 1954) to estimate the trackmaker's trunk length and gait. Since these formulas had never been tested for any recent trackmaker the application, and thus the estimate gaits are speculative.

Most sauropod trackways show short step lengths, ipsilateral manus and pes prints placed together, and the manus prints are placed in front of the pes. Despite inaccuracies, such as the approximation of the trackmakers trunk length and limb length, it can be reasoned according to Kienapfel et al. (2014; Chapter 4; see also Figure 7.5) that these sauropod trackmakers were walking. As noted above, speed estimates also indicate walking.

In addition, the argument of safety and stability seems to be most important for sauropod locomotion, which most likely excludes highly dynamic gaits with an aerial phase of suspension, such as gallop (or canter in Figure 7.5), as well as running trot and fast pace (Preuschoft et al., 2011). Extant large mammals tend to move in a safe and stable way in order to minimize high bending stresses in the limbs and injuries during locomotion (McMahon, 1975; Biewener, 1989). Christian et al. (1999) concluded that the ability of fast locomotion was limited in sauropods since the high body mass would have led to enormous stress in the limbs, which would require a damping mechanism in the limbs. In extant animals, such damping structure can be observed in the autopodium of elephants (Weissengruber et al., 2006).

Consequently, sauropods probably habitually moved in a walking locomotion, which is why the dynamic component is likely to have been very small. The walk, a symmetrical gait with a four-beat rhythm gait and a duty factor of 0.5 (cf. Howell, 1944; Biewener, 1983; Hildebrand, 1985), offers the greatest stability among available gaits and may be considered as the most likely gait for sauropods (Läbe, unpubl. a; Chapter 5). Alternating supporting phases of two limbs and three limbs that are touching the ground during the stance phase are characteristic for the walk. Stability is created because the areas of support during the stance phase of three supporting limbs are larger than in other gaits (Gray, 1944; Hildebrand, 1980). It is likely that sauropods had a wider repertoire of gaits than the walk, which they used depending on speed or terrain, just like recent tetrapods. However, this repertoire is not sufficiently recorded in sauropod trackways.

7.6. CONCLUSION AND FUTURE APPLICATION

Vertebrate ichnology benefits from combining paleontological methods with methods from other disciplines, such as soil mechanics, geodesy, geology, paleobiology, and zoology (Figure 7.2, upper gear-wheel). The interdisciplinary approaches described for inferring estimates of body mass and locomotion from tracks can influence future research on dinosaur ichnology, but also prehistoric anthropology and modern forensics, likewise (Figure 7.2, lower gear-wheel). The dinosaur scale (see section 7.5.2.3; Läbe, unpubl. b; Chapter 6) is an interdisciplinary project based on tracks (Figure 7.2, middle gear-wheel) that provides a possible, yet elaborate approach for estimating body mass for sauropod dinosaurs. Although the soil mechanical analysis of the substrate and the setup of FEA simulation are worthwhile for the determination of dinosaur's mass, the method is error-prone. The crux of matter is the assessment of the dynamical component in generation of the tracks. This problem was attempted to be bypassed by applying information for weight distribution from the estimated gait (Läbe, unpubl. a; Chapter 5). Future research should focus on providing a simplified approach to mass estimation, which may be possible by using soil mechanical standard equation for settlements (Boussinesq, 1885) and a more detailed acquisition of the dynamical component, for example by virtually generated trackways from moving dinosaur models (cf. Stevens et al., 2016). Once the dinosaur scale is technically mature, it will be able to provide sufficient data for multiple extant and extinct trackmakers, for example, early hominids. Such information might be of value for statistical analyses to obtain, for example, composition and distribution of different trackmakers in a paleoenvironment.

7.7. ACKNOWLEDGEMENTS

I thank P. M. Sander, J. Mitchell, and T. Plogschties (all University of Bonn) for discussions and improving the manuscript. The German Academic Scholarship Foundation (Studienstiftung des deutschen Volkes) and the Andrea von Braun Foundation are acknowledged for funding.

7.8. REFERENCES

Adams, T. L., C. Strganac, M. J. Polcyn, and L. L. Jacobs. **2010**. High resolution three-dimensional laser-scanning of the type specimen of *Eubrontes* (?) *glenrosensis* Shuler, 1935, from the Comanchean (Lower Cretaceous) of Texas: implications for digital archiving and preservation. Palaeontologia Electronica 13(3):1–11.

Alexander, R. M. 1976. Estimates of speeds of dinosaurs. Nature 261:129–130.

Alexander, R. M. 1983. Animal Mechanics. Blackwell Scientific, Oxford.

Alexander, R. M. 1984. The gaits of bipedal and quadrupedal animals. The International Journal of Robotics Research 3(2):49-59.

Alexander, R. M. 1985. Mechanics of posture and gait of some large dinosaurs. Zoological Journal of the Linnean Society 83(1):1–25.

Alexander, R. M. 1989. Dynamics of Dinosaurs and Other Extinct Giants. Columbia University Press, New York, 167 pp.

Alexander, R. M. 1991. Doubts and assumptions in dinosaur mechanics. Interdisciplinary Science Reviews 16(2):175–181.

Alexander, R. M., and A. S. Jayes. **1983**. A dynamic similarity hypothesis for the gaits of quadrupedal mammals. Journal of Zoology 201:135–152.

Alf, R. M. 1959. Mammal footprints from the Avawatz Formation, California. Bulletin of the Southern California Academy of Sciences 58(1):1-10.

Alf, R. M. 1966. Mammal trackways from the Barstow Formation, California. Bulletin of the Southern California Academy of Sciences 65(4):258–264.

Alibhai, S. K., Z. C. Jewell, and P. R. Law. **2008**. A footprint technique to identify white rhino *Ceratotherium simum* at individual and species levels. Endangered Species Research 4:205–218.

Anderson, J. F., A. Hall-Martin, and D. A. Russell. **1985**. Long-bone circumference and weight in mammals, birds and dinosaurs. Journal of Zoology 207(1):53–61.

Ashton, N., S. G. Lewis, I. de Groote, S. M. Duffy, M. Bates, R. Bates, P. Hoare, M. Lewis, S. A. Parfitt, S. Peglar, C. Williams, and C. Stringer. **2014**. Hominin footprints from Early Pleistocene deposits at Happisburgh, UK. PLoS ONE 9(2):1–13.

Baird, D. 1952. Revision of the Pennsylvanian and Permian footprints *Limnopus*, *Allopus* and *Baropus*. Journal of Paleontology 26(5):832–840.

Baird, D. 1954. *Chirotherium lulli*, a pseudosuchian reptile from New Jersey. Bulletin of the Museum 111:166–194.

Balbinot, G., and A. B. de Carvalho. **2014**. Determination of ground reaction force peaks from human footprint depths. International Jounal of Basic and Applied Sciences 3(1):30–34.

Ballerstedt, M. 1905. Über Saurierfährten der Wealdenformation Bückeburgs. Naturwissenschaftliche Wochenschrift 4(31):481–485.

Ballerstedt, M. 1914. Bemerkungen zu den älteren Berichten über Saurierfährten im Wealdensandstein und Behandlung einer neuen, aus 5 Fußabdrücken bestehenden Spur. Centralblatt für Mineralogie, Geologie und Paläontologie 2:48–64.

Bates, K. T., B. H. Breithaupt, P. L. Falkingham, N. A. Matthews, D. Hodgetts, and P. L. Manning. **2008**. Integrated LiDAR and photogrammetric documentation of the Red Gulch Dinosaur Tracksite (Wyoming, USA); pp. 101–103 in S. E. Foss, L. Cavin, T. Brown, J. I. Kirkland, and V. L. Santucci (eds.), Proceedings of the Eighth Conference on Fossil Resources, St. George, Utah. BLM Regional Paleontologist, Salt Lake City, Utah.

Bates, K. T., and P. L. Falkingham. **2012**. Estimating maximum bite performance in *Tyrannosaurus rex* using multi-body dynamics. Biology Letters 8(4):660–664.

Bates, K. T., P. L. Falkingham, D. Hodgetts, J. O. Farlow, B. H. Breithaupt, M. O'Brien, N. Matthews, W. I. Sellers, and P. L. Manning. **2009**. Digital imaging and public engagement in palaeontology. Geology Today 25(4):134–139.

Bates, K. T., P. L. Falkingham, S. Macaulay, C. Brassey, and S. C. R. Maidment. **2015**. Downsizing a giant: re-evaluating *Dreadnoughtus* body mass. Biology Letters 11(6):20150215.

Bates, K. T., P. L. Falkingham, F. Rarity, D. Hodgetts, A. Purslow, and P. L. Manning. **2010**. Application of high-resolution laser scanning and photogrammetric techniques to data acquisition, analysis and interpretation in palaeontology. International Archives of Photogrammetry, Remote Sensing and Spatial Information Sciences 38:68–73.

Bates, K. T., P. L. Manning, L. Margetts, and W. I. Sellers. **2010**. Sensitivity analysis in evolutionary robotic simulations of bipedal dinosaur running. Journal of Vertebrate Paleontology 30(2):458–466.

Bates, K. T., P. L. Manning, B. Vila, and D. Hodgetts. **2008**. Three-dimensional modelling and analysis of dinosaur trackways. Palaeontology 51(4):999–1010.

Bates, K. T., R. Savage, T. C. Pataky, S. A. Morse, E. Webster, P. L. Falkingham, L. Ren, Z. Qian, D. Collins, M. R. Bennett, J. McClymont, and R. H. Crompton. **2013**. Does footprint depth correlate with foot motion and pressure? Journal of the Royal Society Interface 10(83):1–12.

Bell, P. R., E. Snively, and L. Shychoski. **2009**. A comparison of the jaw mechanics in hadrosaurid and ceratopsid dinosaurs using finite element analysis. Anatomical Record 292(9):1338–1351.

Belvedere, M., and J. O. Farlow. **2016**. The Numerical Scale for Quantifying the Quality of Preservation of Vertebrate Tracks; pp. 92–98 in P. L. Falkingham, D. Marty, and A. Richter (eds.), Dinosaur Tracks - The Next Steps. Life of the Past. Indiana University Press, Bloomington, 413 pp.

Bennett, M. R., P. L. Falkingham, S. A. Morse, K. Bates, and R. H. Crompton. **2013**. Preserving the impossible: conservation of soft-sediment hominin footprint sites and strategies for three-dimensional digital data capture. PLoS ONE 8(4):1–15.

Bennett, M. R., S. A. Morse, and P. L. Falkingham. **2014**. Tracks made by swimming hippopotami: an example from Koobi Fora (Turkana Basin, Kenya). Palaeogeography, Palaeoclimatology, Palaeoecology 409:9–23.

Bibi, F., B. Kraatz, N. Craig, M. Beech, M. Schuster, and A. Hill. **2012**. Early evidence for complex social structure in Proboscidea from a late Miocene trackway site in the United Arab Emirates. Biology Letters 8(4):670–673.

Biewener, A. A. 1983. Allometry of quadrupedal locomotion: the scaling of duty factor, bone curvature and limb orientation to body size. Journal of Experimental Biology 105:147–171.

Biewener, A. A. 1989. Scaling body support in mammals: limb posture and muscle mechanics. Science 245(4913):45–48.

Biknevicius, A. R., D. R. Mullineaux, and H. M. Clayton. **2004**. Ground reaction forces and limb function in tölting Icelandic horses. Equine Veterinary Journal 36(8):743–747.

Bird, R. 1939. Thunder in his footsteps. Natural History 43:254–261.

Bird, R. T. 1944. Did *Brontosaurus* ever walk on land? Natural History 53(2):60–67.

Bonnan, M. F. 2003. The evolution of manus shape in sauropod dinosaurs: implications for functional morphology, forelimb orientation, and phylogeny. Journal of Vertebrate Paleontology 23(3):595–613.

Boussinesq, J. 1885. Application des potentiels à l'étude de l'équilibre et du mouvement des solides élastiques, principalement au calcul des déformations et des pressions que produisent, dans ces solides, des efforts quelconques exercés sur une petite partie de leur surface ou de leur intérieur: Mémoire suivi de notes étendues sur divers points de physique mathématique et d'analyse. Gauthier-Villars, Paris.

Breithaupt, B. H., and N. A. Matthews. **2011**. Photogrammetric ichnology: state-of-the-art digital data analysis of paleontological resources in North America, Europe, Asia, and Africa. Journal of Vertebrate Paleontology Program and Abstracts 2011:77.

Breithaupt, B. H., N. A. Matthews, and T. A. Noble. **2004**. An integrated approach to three-dimensional data collection at dinosaur tracksites in the Rocky Mountain West. Ichnos 11(1-2):11–26.

Breithaupt, B. H., E. H. Southwell, T. Adams, and N. A. Matthews. **2006**. The Red Gulch dinosaur tracksite: public participation in the conservation and management of a world-class paleontological site. New Mexico Museum of Natural History and Science Bulletin 34:10.

Campione, N. E., and D. C. Evans. **2012**. A universal scaling relationship between body mass and proximal limb bone dimensions in quadrupedal terrestrial tetrapods. BMC Biology 10(60):1–21.

Carpenter, K. 2006. Biggest of the big: a critical re-evaluation of the megasauropod *Amphicoelias fragillimus* Cope, 1878. New Mexico Museum of Natural History and Science Bulletin 36:131–138.

Casanovas, M., A. Fernandez, F. Perez-Lorente, and J. V. Santafe. **1997**. Sauropod trackways from site El Sobaquillo (Munilla, La Rioja, Spain) indicate amble walking. Ichnos 5(2):101–107.

Castanera, D., C. Pascual, J. I. Canudo, N. Hernández, and J. L. Barco. **2012**. Ethological variations in gauge in sauropod trackways from the Berriasian of Spain. Lethaia 45(4):476–489.

Christian, A., R. H. G. Müller, G. Christian, and H. Preuschoft. **1999**. Limb swinging in elephants and giraffes and implications for the reconstruction of limb movements

and speed estimates in large dinosaurs. Mitteilungen aus dem Museum für Naturkunde in Berlin, Geowissenschaftliche Reihe 2:81–90.

Clauss, M., P. Steuer, D. W. H. Muller, D. Codron, and J. Hummel. **2013**. Herbivory and body size: allometries of diet quality and gastrointestinal physiology, and implications for herbivore ecology and dinosaur gigantism. PLoS ONE 8(10):1-16.

Colbert, E. H. 1962. The weights of dinosaurs. American Museum Novitates 2076:1–16.

Coombs, W. P. J. 1978. Theoretical aspects of cursorial adaptations in dinosaurs. The Quarterly Review of Biology 53:393–418.

Cubo, J., N. Le Roy, C. Martinez-Maza, and L. Montes. **2012**. Paleohistological estimation of bone growth rate in extinct archosaurs. Paleobiology 38(02):335–349.

Curry Rogers, K., and J. A. Wilson (eds.). **2005**. The Sauropods - Evolution and Paleobiology. University of California Press, Berkeley, 349 pp.

Day, J. J., P. Upchurch, D. B. Norman, A. S. Gale, and H. P. Powell. **2002**. Sauropod trackways, evolution, and behavior. Science 296(5573):1659.

Demathieu, G. R. 1987. Thickness of the Footprint-Relief and its Significance: Research on the Distribution of the Weights upon the Autopodia; pp. 61–62 in G. Leonardi (ed.), Glossary and Manual of Tetrapod Footprint Palaeoichnology. Departamento Nacional da Produção Mineral, Brazil, 137 pp.

D'emic, M. D., J. A. Whitlock, K. M. Smith, D. C. Fisher, and J. A. Wilson. **2013**. Evolution of high tooth replacement rates in sauropod dinosaurs. PLoS ONE 8(7):1-7.

Dingwall, H. L., K. G. Hatala, R. E. Wunderlich, and B. G. Richmond. **2013**. Hominin stature, body mass, and walking speed estimates based on 1.5 million-year-old fossil footprints at Ileret, Kenya. Journal of Human Evolution 64(6):556–568.

Enniouar, A., A. Lagnaoui, and A. Habib. **2014**. A Middle Jurassic sauropod tracksite in the Argana Basin, Western High Atlas, Morocco: an example of paleoichnological heritage for sustainable geotourism. Proceedings of the Geologists' Association 125(1):114–119.

Falkingham, P. L. 2010. Computer simulation of dinosaur tracks. Ph.D. thesis, The University of Manchester, Manchester.

Falkingham, P. L. 2012. Acquisition of high resolution three-dimensional models using free, open-source, photogrammetric software. Palaeontologia Electronica 15(1):1-15.

Falkingham, P. L. 2013. Low cost 3D scanning using off the shelf video gaming peripherals. Journal of Paleontological Techniques 11:1–9.

Falkingham, P. L. 2014. Interpreting ecology and behaviour from the vertebrate fossil track record. Journal of Zoology 292(4):222–228.

Falkingham, P. L. 2016. Applying Objective Methods to Subjective Track Outlines; pp. 73–80 in P. L. Falkingham, D. Marty, and A. Richter (eds.), Dinosaur Tracks - The Next Steps. Life of the Past. Indiana University Press, Bloomington, 413 pp.

Falkingham, P. L., K. T. Bates, and J. O. Farlow. **2014**. Historical photogrammetry: Bird's Paluxy River dinosaur chase sequence digitally reconstructed as it was prior to excavation 70 years ago. PLoS ONE 9(4):1–5.

Falkingham, P. L., K. T. Bates, and P. D. Mannion. **2012**. Temporal and palaeoenvironmental distribution of manus- and pes-dominated sauropod trackways. Journal of the Geological Society 169(4):365–370.

Falkingham, P. L., K. T. Bates, L. Margetts, and P. L. Manning. **2011a**. Simulating sauropod manus-only trackway formation using finite-element analysis. Biology Letters 7:142–145.

Falkingham, P. L., K. T. Bates, L. Margetts, and P. L. Manning. **2011b**. The 'Goldilocks' effect: preservation bias in vertebrate track assemblages. Journal of the Royal Society Interface 8(61):1142–1154.

Falkingham, P. L., and S. M. Gatesy. **2014**. The birth of a dinosaur footprint: subsurface 3D motion reconstruction and discrete element simulation reveal track ontogeny. Proceedings of the National Academy of Sciences of the United States of America 111(51):18279–18284.

Falkingham, P. L., J. Hage, and M. Baker. **2014**. Mitigating the Goldilocks effect: the effects of different substrate models on track formation potential. Royal Society Open Science 1(3):1–9.

Falkingham, P. L., L. Margetts, and P. L. Manning. **2010**. Fossil vertebrate tracks as paleopenetrometers: confounding effects of foot morphology. Palaios 25(6):356–360.

Falkingham, P. L., L. Margetts, I. M. Smith, and P. L. Manning. **2009**. Reinterpretation of palmate and semi-palmate (webbed) fossil tracks; insights from finite element modelling. Palaeogeography, Palaeoclimatology, Palaeoecology 271(1-2):69–76.

Falkingham, P. L., D. Marty, and A. Richter (eds.). **2016a**. Dinosaur Tracks - The Next Steps. Life of the Past. Indiana University Press, Bloomington, 413 pp.

Falkingham, P. L., D. Marty, and A. Richter. **2016b**. Introduction; pp. 2–11 in P. L. Falkingham, D. Marty, and A. Richter (eds.), Dinosaur Tracks - The Next Steps. Life of the Past. Indiana University Press, Bloomington, 413 pp.

Farlow, J. O. 1992. Sauropod tracks and trackmakers: integrating the ichnological and skeletal records. Zubia 10:89–138.

Farlow, J. O., M. O'Brien, G. J. Kuban, B. Dattilo, K. T. Bates, P. L. Falkingham, L. P. Amanda Rose, C. Kumagai, C. Libben, J. Smith, and J. Whitcraft. **2012**. Dinosaur tracksites of the Paluxy River Valley (Glen Rose Formation, Lower Cretaceous), Dinosaur Valley State Park, Somervell County, Texas. Actas de V Jornadas Internacionales sobre Paleontologia de Dinosaurios y su Entorno, Salas de los Infantes, Burgos:41–69.

Farlow, J. O., J. G. Pittman, and J. M. Hawthorne. **1989**. *Brontopodus birdi,* Lower Cretaceous Sauropod Footprints from the U.S. Gulf Coastal Plain; pp. 371–394 in D.

D. Gillette and M. G. Lockley (eds.), Dinosaur Tracks and Traces. Cambridge University Press, Cambridge, 476 pp.

Fernández-Lozano, J., and G. Gutiérrez-Alonso. **2017**. The Alejico Carboniferous forest: a 3D-terrestrial and UAV-assisted photogrammetric model for geologic heritage preservation. Geoheritage 9(2):163–173.

Fiorillo, A. R., S. T. Hasiotis, and Y. Kobayashi. **2014**. Herd structure in Late Cretaceous polar dinosaurs: A remarkable new dinosaur tracksite, Denali National Park, Alaska, USA. Geology 42(8):719–722.

Fondevilla, V., B. Vila, O. Oms, and À. Galobart. **2016**. Skin impressions of the last European dinosaurs. Geological Magazine 154(2):393–398.

Foster, J. R. 2015. Theropod dinosaur ichnogenus *Hispanosauropus* identified from the Morrison Formation (Upper Jurassic), Western North America. Ichnos 22(3-4):183–191.

Fowler, D. W., and R. M. Sullivan. **2011**. The first giant titanosaurian sauropod from the Upper Cretaceous of North America. Acta Palaeontologica Polonica 56(4):685–690.

Friese, H. 1979. Die Saurierfährten von Barkhausen im Wiehengebirge. Veröffentlichungen des Landkreises Osnabrück 1:1–36.

Gatesy, S. M., and A. A. Biewener. **1991**. Bipedal locomotion: effects of speed, size and limb posture in birds and humans. Journal of Zoology 224(1):127–147.

Gatesy, S. M., K. M. Middleton, F. A. J. Jr, and N. H. Shubin. **1999**. Three-dimensional preservation of foot movements in Triassic theropod dinosaurs. Nature 399(6732):141–144.

Gee, C. T. 2011. Dietary Options for the Sauropod Dinosaurs from an Integrated Botanical and Paleobotanical Perspective; pp. 34–56 in N. Klein, K. Remes, C. T. Gee, and P. M. Sander (eds.), Biology of the Sauropod Dinosaurs - Understanding the Life of Giants. Life of the Past. Indiana University Press, Bloomington, 331 pp.

Gillette, D. D., and M. G. Lockley (eds.). **1989**. Dinosaur Tracks and Traces. Cambridge University Press, Cambridge, 476 pp.

Gray, J. 1944. Studies in the mechanics of the tetrapod skeleton. Journal of Experimental Biology 20(2):88–116.

Grimm, A. 2007. The origin of the term photogrammetry. Photogrammetric Week '07 51:53–60.

Grossi, B., J. Iriarte-Díaz, O. Larach, M. Canals, and R. A. Vásquez. **2014**. Walking like dinosaurs: chickens with artificial tails provide clues about non-avian theropod locomotion. PLoS ONE 9(2):1–6.

Gunga, H.-C., T. Suthau, A. Bellmann, A. Friedrich, T. Schwanebeck, S. Stoinski, T. Trippel, K. Kirsch, and O. Hellwich. **2007**. Body mass estimations for *Plateosaurus engelhardti* using laser scanning and 3D reconstruction methods. Naturwissenschaften 94:623–630.

Gunga, H.-C., T. Suthau, A. Bellmann, S. Stoinski, A. Friedrich, T. Trippel, K. Kirsch, and O. Hellwich. **2008**. A new body mass estimation of *Brachiosaurus brancai* Janensch, 1914 mounted and exhibited at the Museum of Natural History (Berlin, Germany). Fossil Record 11(1):33–38.

Haubold, H. 1984. Saurierfährten, 2nd edition. Die neue Brehm-Bücherei 479. Ziemsen, Wittenberg Lutherstadt, 231 pp.

Henderson, D. M. 1999. Estimating the masses and centers of mass of extinct animals by 3-D mathematical slicing. Paleobiology 25(1):88–106.

Henderson, D. M. 2004. Tipsy punters: sauropod dinosaur pneumaticity, buoyancy and aquatic habits. Proceedings of the Royal Society B 271(Suppl 4):180–183.

Henderson, D. M. 2006. Burly gaits: centers of mass, stability, and the trackways of sauropod dinosaurs. Journal of Vertebrate Paleontology 26(4):907–921.

Hendricks, A. 1981. Die Saurierfährte von Münchehagen bei Rehburg-Loccum (NW-Deutschland). Abhandlungen aus dem Landesmuseum für Naturkunde Münster in Westfalen 43:3–22.

Hildebrand, M. 1965. Symmetrical gaits of horses. Science 150(3697):701–708.

Hildebrand, M. 1976. Analysis of Tetrapod Gaits: General Consideration on Symmetrical Gaits; pp. 203–236 in R. M. Herman, S. Grillner, P. S. G. Stein, and D. G. Stuart (eds.), Neural Control of Locomotion. Plenum Press, New York.

Hildebrand, M. 1980. The adaptive significance of tetrapod gait selection. American Zoologist 20(1):255–267.

Hildebrand, M. 1985. Walking and Running; pp. 38–57 in M. Hildebrand, D. M. Bramble, L. F. Liem, and D. B. Wake (eds.), Functional Vertebrate Morphology. Harvard University Press, Cambridge Mass., 430 pp.

Hildebrand, M. 1989. The quadrupedal gaits of vertebrates. Bioscience 39(11):766–775.

Hitchcock, E. 1836. Ornithichnology – description of the foot marks of birds (Ornithichnites) on New Red Sandstone in Massachusetts. American Journal of Science 29:307–340.

Hitchcock, E. 1848. An attempt to discriminate and describe the animals that made the fossil footmarks of the United States, and especially of New England. Memoirs of the American Academy of Arts and Science 3:129–256.

Hitchcock, E. 1858. Ichnology of New England: A Report on the Sandstone of the Connecticut Valley, Especially its Fossil Footmarks. W. White, Boston, Mass., 232 pp.

Hitchcock, E. 1865. Supplement to the Ichnology of New England. Wright and Potter State Printers, Boston, Mass., 96 pp.

Hofmann, R., and P. M. Sander. **2014**. The first juvenile specimens of *Plateosaurus engelhardti* from Frick, Switzerland: isolated neural arches and their implications for developmental plasticity in a basal sauropodomorph. PeerJ 2:1-40.

Houssaye, A., K. Waskow, S. Hayashi, R. Cornette, A. H. Lee, and J. R. Hutchinson. **2016**. Biomechanical evolution of solid bones in large animals: a microanatomical investigation. Biological Journal of the Linnean Society 117(2):350–371.

Howell, A. B. 1944. Speed in Animals. University of Chicago Press, Chicago, 270 pp.

Hunt, A. P., S. G. Lucas, J. Milàn, and J. A. Spielmann. **2012**. Vertebrate coprolite studies: status and prospectus. New Mexico Museum of Natural History and Science Bulletin 57:5–24.

Hunt-Foster, R. K., M. G. Lockley, A. R. C. Milner, J. R. Foster, N. A. Matthews, B. H. Breithaupt, and J. A. Smith. **2016**. Tracking dinosaurs in BLM Canyon Country, Utah. Geology of the Intermountain West 3:67–100.

Hutchinson, J. R. 2001a. Dinosaur Locomotion; in Encyclopedia of Life Sciences. John Wiley & Sons, Ltd, London.

Hutchinson, J. R. 2001b. The evolution of femoral osteology and soft tissues on the line to extant birds (Neornithes). Zoological Journal of the Linnean Society 131(2):169–197.

Hutchinson, J. R. 2001c. The evolution of pelvic osteology and soft tissues on the line to extant birds (Neornithes). Zoological Journal of the Linnean Society 131(2):123–168.

Hutchinson, J. R. 2006. The evolution of locomotion in archosaurs. Comptes Rendus Palevol 5(3-4):519–530.

Hutchinson, J. R., K. T. Bates, J. Molnar, V. Allen, and P. J. Makovicky. **2011**. A computational analysis of limb and body dimensions in *Tyrannosaurus rex* with implications for locomotion, ontogeny, and growth. PLoS ONE 6(10):1–20.

Hutchinson, J. R., and S. M. Gatesy. **2000**. Adductors, abductors, and the evolution of archosaur locomotion. Paleobiology 26(4):734–751.

Hutchinson, J. R., and S. M. Gatesy. **2006**. Beyond the bones. Nature 440:292–294.

Ishigaki, S. 1989. Footprints of Swimming Sauropods from Morocco; pp. 83–86 in D. D. Gillette and M. G. Lockley (eds.), Dinosaur Tracks and Traces. Cambridge University Press, Cambridge, 476 pp.

Ishigaki, S., and Y. Matsumoto. **2009**. "Off-tracking"-like phenomenon observed in the turning sauropod trackway from the Upper Jurassic of Morocco. Memoir of the Fukui Prefectural Dinosaur Museum 8:1–10.

Jackson, S. J., M. A. Whyte, and M. Romano. **2009**. Laboratory-controlled simulations of dinosaur footprints in sand: A key to understanding vertebrate track formation and preservation. Palaios 24(4):222–238.

Jackson, S. J., M. A. Whyte, and M. Romano. **2010**. Range of experimental dinosaur (*Hypsilophodon foxii*) footprints due to variation in sand consistency: how wet was the track? Ichnos 17(3):197–214.

Jones, T. R. 1862. Trails, tracks, and surface-markings. The Geologist 5(04):128–139.

Kaever, M., and A. F. de Lapparent. **1974**. Les traces de pas de Dinosaures du Jurassique de Barkhausen (Basse Saxe, Allemagne). Bulletin de la Société Géologique de France 16:516–525.

Kaup, J. J. 1835. Mittheilungen, an Professor Bronn gerichtet. Thier-Fährten von Hildburghausen: *Chirotherium* oder *Chirosaurus.* Neues Jahrbuch für Mineralogie, Geognosie, Geologie und Petrefaktenkunde:327–328.

Kienapfel, K., S. Läbe, and H. Preuschoft. **2014**. Do tracks yield reliable information on gaits? – Part 1: The case of horses. Fossil Record 17:59–67.

Klein, N., K. Remes, C. T. Gee, and P. M. Sander (eds.). **2011**. Biology of the Sauropod Dinosaurs - Understanding the Life of Giants. Life of the Past. Indiana University Press, Bloomington, 331 pp.

Krell, F.-T. 2004. Parataxonomy vs. taxonomy in biodiversity studies – pitfalls and applicability of 'morphospecies' sorting. Biodiversity and Conservation 13(4):795–812.

Läbe, S. unpubl. a. Do tracks yield reliable information on gaits? – Part 2: Thoughts on the weight distribution of sauropod dinosaurs during walking. Doctoral thesis 2017(Chapter 5).

Läbe, S. unpubl. b. The dinosaur scale: interpreting sauropod tracks with a soil mechanical approach for body mass estimation with thoughts on weight distribution among the limbs during walking. Doctoral thesis 2017(Chapter 6).

Läbe, S. in revision. Vertical exaggeration of 3D surface models highlights additional detail in vertebrate tracks: an example from the photogrammetry of sauropod tracks. Journal of Paleontological Techniques (2017).

Lacovara, K. J., M. C. Lamanna, L. M. Ibiricu, J. C. Poole, E. R. Schroeter, P. V. Ullmann, K. K. Voegele, Z. M. Boles, A. M. Carter, E. K. Fowler, V. M. Egerton, A. E. Moyer, C. L. Coughenour, J. P. Schein, J. D. Harris, R. D. Martinez, and F. E. Novas. **2014**. A gigantic, exceptionally complete titanosaurian sauropod dinosaur from southern Patagonia, Argentina. Scientific reports 4:6196.

Lallensack, J. N. 2016. An objective method for the generation of footprint outlines. Journal of Vertebrate Paleontology Program and Abstracts, 2016:171.

Lallensack, J. N., H. Klein, J. Milàn, O. Wings, O. Mateus, and L. B. Clemmensen. **submit.** Sauropodomorph dinosaur trackways from the Fleming Fjord Formation of East Greenland: Evidence for Late Triassic sauropods. Acta Palaeontologica Polonica (2017).

Lallensack, J. N., P. M. Sander, N. Knötschke, and O. Wings. **2015**. Dinosaur tracks from the Langenberg Quarry (Late Jurassic, Germany) reconstructed with historical photogrammetry: evidence for large theropods soon after insular dwarfism. Palaeontologia Electronica 18.2.31A:1–34.

Lallensack, J. N., A. H. van Heteren, and O. Wings. **2016**. Geometric morphometric analysis of intratrackway variability: a case study on theropod and ornithopod dinosaur trackways from Münchehagen (Lower Cretaceous, Germany). PeerJ 4:1-52.

Lautenschlager, S. 2013. Cranial myology and bite force performance of *Erlikosaurus andrewsi*: a novel approach for digital muscle reconstructions. Journal of Anatomy 222(2):260–272.

Leonardi, G. (ed.). **1987**. Glossary and Manual of Tetrapod Footprint Palaeoichnology. Departamento Nacional da Produção Mineral, Brazil, 137 pp.

Li, Y., R. H. Crompton, R. M. Alexander, M. M. Günther, and W. J. Wang. **1996**. Characteristics of ground reaction forces in normal and chimpanzee-like bipedal walking by humans. Folia Primatologica 66:137–159.

Lockley, M., and A. P. Hunt. **1995**. Dinosaur Tracks and Other Fossil Footprints of the Western United States. Columbia University Press, New York, 360 pp.

Lockley, M., A. S. Schulp, C. A. Meyer, G. Leonardi, and D. Kerumba Mamani. **2002**. Titanosaurid trackways from the Upper Cretaceous of Bolivia: evidence for large manus, wide-gauge locomotion and gregarious behaviour. Cretaceous Research 23(3):383–400.

Lockley, M. G. 1986. The paleobiological and paleoenvironmental importance of dinosaur footprints. Palaios 1(1):37–47.

Lockley, M. G. 1989. Summary and Prospectus; pp. 441–447 in D. D. Gillette and M. G. Lockley (eds.), Dinosaur Tracks and Traces. Cambridge University Press, Cambridge, 476 pp.

Lockley, M. G. 1991a. The dinosaur footprint renaissance. Modern Geology 16:139–160.

Lockley, M. G. 1991b. Tracking Dinosaurs - A New Look at an Ancient World. Cambridge University Press, Cambridge, 237 pp.

Lockley, M. G. 1998. The vertebrate track record. Nature 396(6710):429–432.

Lockley, M. G. 2007. The morphodynamics of dinosaurs, other archosaurs, and their trackways: holistic insights into relationships between feet, limbs, and the whole body. SEPM Special Publication 88:27–51.

Lockley, M. G., J. O. Farlow, and C. A. Meyer. **1994**. *Brontopodus* and *Parabrontopodus* ichnogen. nov. and the significance of wide- and narrow-gauge sauropod trackways. Gaia: Revista de Geociências 10:135–145.

Lockley, M. G., M. Huh, S.-G. Gwak, K. G. Hwang, and I. S. Paik. **2012**. Multiple Tracksites with Parallel Trackways from the Cretaceous of the Yeosu City Area Korea: Implications for Gregarious Behavior in Ornithopod and Sauropod Dinosaurs. Ichnos 19(1-2):105–114.

Lockley, M. G., and C. Meyer. **2000**. Dinosaur Tracks and Other Fossil Footprints of Europe. Columbia University Press, New York, 341 pp.

Lockley, M. G., J. G. Pittman, C. A. Meyer, and V. F. d. Santos. **1994**. On the common occurrence of manus-dominated sauropod trackways in Mesozoic carbonates. Gaia: Revista de Geociências 10:119–124.

Lockley, M. G., and A. Rice. **1990**. Did "*Brontosaurus*" ever swim out to sea?: evidence from brontosaur and other dinosaur footprints. Ichnos 1(2):81–90.

Lockley, M. G., J. L. Wright, A. P. Hunt, and S. G. Lucas. **2001**. The Late Triassic sauropod track record comes into focus: old legacies and new paradigms. Guidebook New Mexico Geological Society 52:181-190.

Lockley, M. G., J. L. Wright, and D. Thies. **2004**. Some observations on the dinosaur tracks at Münchehagen (Lower Cretaceous), Germany. Ichnos 11(3-4):261–274.

Lomax, D. R., and C. A. Racay. **2012**. A long mortichnial trackway of *Mesolimulus walchi* from the Upper Jurassic Solnhofen Lithographic Limestone near Wintershof, Germany. Ichnos 19(3):175–183.

Mallison, H. 2011. Fast moving dinosaurs: why our basic tenet is wrong. Journal of Vertebrate Paleontology (Program and Abstracts 2011):150.

Mallison, H., and O. Wings. **2014**. Photogrammetry in paleontology - a practical guide. Journal of Paleontological Techniques 12:1–31.

Manning, P. L. 2004. A new approach to the analysis and interpretation of tracks: examples from the dinosauria. Geological Society of London Special Publications 228:94–123.

Mannion, P. D., and P. Upchurch. **2010**. A quantitative analysis of environmental associations in sauropod dinosaurs. Paleobiology 36(2):253–282.

Margetts, L., J. Leng, I. M. Smith, and P. L. Manning. **2006**. Parallel Three Dimensional Finite Element Analysis of Dinosaur Trackway Formation; pp. 743–749 in H. F. Schweiger (ed.), Numerical Methods in Geotechnical Engineering: Proceedings of the Sixth European Conference on Numerical Methods in Geotechnical Engineering. Balkema-proceedings and monographs in engineering, water and earth sciences. Taylor & Francis, London, 1678 pp.

Margetts, L., I. M. Smith, J. Leng, and P. L. Manning. **2005**. Simulating dinosaur trackway formation; pp. 1–4 in E. Oñate and D. R. J. Owen (eds.), VIII International Conference on Computational Plasticity (COMPLAS). CIMNE, Barcelona.

Marty, D. 2008. Sedimentology, taphonomy, and ichnology of Late Jurassic dinosaur tracks from the Jura carbonate platform (Chevenez—Combe Ronde tracksite, NW Switzerland): insights into the tidal-flat palaeoenvironment and dinosaur diversity, locomotion, and palaeoecology. GeoFocus 21:1–278.

Masao, F. T., E. B. Ichumbaki, M. Cherin, A. Barili, G. Boschian, D. A. Iurino, S. Menconero, J. Moggi-Cecchi, and G. Manzi. **2016**. New footprints from Laetoli (Tanzania) provide evidence for marked body size variation in early hominins. eLife 5.

Matthews, N. A., and B. H. Breithaupt. **2001**. Close-range photogrammetry experiments at Dinosaur Ridge. The Mountain Geologist 38(3):147–153.

Matthews, N. A., T. A. Noble, and B. H. Breithaupt. **2006**. The application of photogrammetry, remote sensing and geographic information systems (GIS) to fossil resource management. New Mexico Museum of Natural History and Science Bulletin 34:119–131.

Matthews, N. A., T. A. Noble, and B. H. Breithaupt. **2016**. Close-Range Photogrammetry for 3-D Ichnology: The Basics of Photogrammetric Ichnology; pp. 28–55 in P. L. Falkingham, D. Marty, and A. Richter (eds.), Dinosaur Tracks - The Next Steps. Life of the Past. Indiana University Press, Bloomington, 413 pp.

McCrea, R. T., L. G. Buckley, J. O. Farlow, M. G. Lockley, P. J. Currie, N. A. Matthews, and S. G. Pemberton. **2014**. A 'Terror of Tyrannosaurs': the first trackways of tyrannosaurids and evidence of gregariousness and pathology in tyrannosauridae. PLoS ONE 9(7):1–13.

McCrea, R. T., D. H. Tanke, L. G. Buckley, M. G. Lockley, J. O. Farlow, L. Xing, N. A. Matthews, C. W. Helm, S. G. Pemberton, and B. H. Breithaupt. **2015**. Vertebrate ichnopathology: pathologies inferred from dinosaur tracks and trackways from the Mesozoic. Ichnos 22(3-4):235–260.

McGhee, R. B. 1976. Robot Locomotion; pp. 237–264 in R. M. Herman, S. Grillner, P. S. G. Stein, and D. G. Stuart (eds.), Neural Control of Locomotion. Plenum Press, New York.

McMahon, T. A. 1975. Allometry and biomechanics: limb bones in adult ungulates. The American Naturalist 109(969):547-563.

Melstrom, K. M., M. D. D'emic, D. Chure, and J. A. Wilson. **2016**. A juvenile sauropod dinosaur from the Late Jurassic of Utah, U.S.A., presents further evidence of an avian style air-sac system. Journal of Vertebrate Paleontology 36(4):1-23.

Mezga, A., B. C. Tešović, and Z. Bajraktarević. **2007**. First record of dinosaurs in the Late Jurassic of the Adriatic-Dinaridic Carbonate Platform (Croatia). Palaios 22(2):188–199.

Mikhailov, K. E. 2013. Eggshell structure, parataxonomy and phylogenetic analysis: some notes on articles published from 2002 to 2011. Historical Biology 26(2):144–154.

Milàn, J. 2006. Variations in the morphology of emu (*Dromaius novaehollandiae*) tracks reflecting differences in walking pattern and substrate consistency: ichnotaxonomic implications. Palaeontology 49(2):405–420.

Milàn, J., and R. Bromley. **2006**. True tracks, undertracks and eroded tracks, experimental work with tetrapod tracks in laboratory and field. Palaeogeography, Palaeoclimatology, Palaeoecology 231:253–264.

Milàn, J., and R. G. Bromley. **2007**. The impact of sediment consistency on track and undertrack morphology: experiments with emu tracks in layered cement. Ichnos 15(1):19–27.

Milner, A. R. C., and M. G. Lockley. **2016**. Dinosaur Swim Track Assemblages: Characteristics, Contexts, and Ichnofacies Implications; pp. 152–180 in P. L. Falkingham, D. Marty, and A. Richter (eds.), Dinosaur Tracks - The Next Steps. Life of the Past. Indiana University Press, Bloomington, 413 pp.

Mustoe, G. E. 2002. Eocene bird, reptile and mammal tracks from the Chucknut Formation, Northwest Washington. Palaios 17:403–413.

Myers, T. S., and A. R. Fiorillo. **2009**. Evidence for gregarious behavior and age segregation in sauropod dinosaurs. Palaeogeography, Palaeoclimatology, Palaeoecology 274(1-2):96–104.

Owaki, D., T. Kano, K. Nagasawa, A. Tero, and A. Ishiguro. **2013**. Simple robot suggests physical interlimb communication is essential for quadruped walking. Journal of the Royal Society, Interface 10(78):20120669.

Padian, K., and P. E. Olsen. **1984**. The fossil trackway *Pteraichnus*: not pterosaurian, but crocodilian. Journal of Paleontology 58(1):178–184.

Perry, S. F., T. Breuer, and N. Pajor. **2011**. Structure and Function of the Sauropod Respiratory System; pp. 83–93 in N. Klein, K. Remes, C. T. Gee, and P. M. Sander (eds.), Biology of the Sauropod Dinosaurs - Understanding the Life of Giants. Life of the Past. Indiana University Press, Bloomington, 331 pp.

Petti, F. M., M. Avanzini, M. Belvedere, M. de Gasperi, P. Ferretti, S. Girardi, F. Remondino, and R. Tomasoni. **2008**. Digital 3D modelling of dinosaur footprints by photogrammetry and laser scanning techniques: integrated approach at the Coste dell'Anglone tracksite (Lower Jurassic, Southern Alps, Northern Italy). Studi Trentini di Scienze Naturali - Acta Geologica 83:303–315.

Platt, B. F., and S. T. Hasiotis. **2006**. Newly discovered sauropod dinosaur tracks with skin and foot-pad impressions from the Upper Jurassic Morrison Formation, Bighorn Basin, Wyoming, U.S.A. Palaios 21(3):249–261.

Platt, B. F., S. T. Hasiotis, and D. R. Hirmas. **2010**. Use of low-cost multistripe laser triangulation (MLT) scanning technology for three-dimensional, quantitative paleoichnological and neoichnological studies. Journal of Sedimentary Research 80(7):590–610.

Platt, B. F., S. T. Hasiotis, and D. R. Hirmas. **2012**. Empirical determination of physical controls on megafaunal footprints formation through neoichnological experiments with elephants. Palaios 27:725–737.

Preuschoft, H., B. Hohn, S. Stoinski, and U. Witzel. **2011**. Why so huge? Biomechanical Reasons for the Acquisition of Large Size in Sauropod and Theropod Dinosaurs; pp. 197–218 in N. Klein, K. Remes, C. T. Gee, and P. M. Sander (eds.), Biology of the Sauropod Dinosaurs - Understanding the Life of Giants. Life of the Past. Indiana University Press, Bloomington, 331 pp.

Preuschoft, H., H. Witte, A. Christian, and S. Recknagel. **1994**. Körpergestalt und Lokomotion bei großen Säugetieren. Verhandlungen der Deutschen Zoologischen Gesellschaft 87(2):147–163.

Rauhut, O. W. M. 2007. Gigantismus bei Dinosauriern. Freunde der Bayerischen Staatssammlung für Paläontologie und Historische Geologie München e.V. Jahresbericht 2006 und Mitteilungen(35):47–62.

Razzolini, N. L., O. Oms, D. Castanera, B. Vila, V. F. d. Santos, and A. Galobart. **2016**. Ichnological evidence of megalosaurid dinosaurs crossing Middle Jurassic tidal flats. Scientific reports 6:1–15.

Razzolini, N. L., B. Vila, I. Díaz-Martínez, P. L. Manning, and À. Galobart. **2016**. Pes shape variation in an ornithopod dinosaur trackway (Lower Cretaceous, NW Spain): New evidence of an antalgic gait in the fossil track record. Cretaceous Research 58:125–134.

Renders, E. 1984. The gait of *Hipparion* sp. from fossil footprints in Laetoli, Tanzania. Nature 308:179–181.

Romano, M., M. A. Whyte, and S. J. Jackson. **2007**. Trackway ratio: a new look at trackway gauge in the analysis of quadrupedal dinosaur trackways and its implications for ichnotaxonomy. Ichnos 14(3-4):257–270.

Salisbury, S. W., A. Romilio, M. C. Herne, R. T. Tucker, and J. P. Nair. **2017**. The dinosaurian ichnofauna of the Lower Cretaceous (Valanginian–Barremian) Broome Sandstone of the Walmadany Area (James Price Point), Dampier Peninsula, Western Australia. Journal of Vertebrate Paleontology 36(6, suppl.):1–152.

Sander, P. M. 2013. An evolutionary cascade model for sauropod dinosaur gigantism - overview, update and tests. PLoS ONE 8(10):1–23.

Sander, P. M. 2015. Gigantism: sauropod dinosaur gigantism and the evolution of maximum body size in other dinosaurs and mammals. DFG Research Unit 533. Steinmann-Institut, Bonn. Available at www.sauropod-dinosaurs.uni-bonn.de.

Sander, P. M., A. Christian, M. Clauss, R. Fechner, C. T. Gee, E.-M. Griebeler, H.-C. Gunga, J. Hummel, H. Mallison, S. F. Perry, H. Preuschoft, O. W. M. Rauhut, K. Remes, T. Tütken, O. Wings, and U. Witzel. **2011**. Biology of the sauropod dinosaurs: the evolution of gigantism. Biological Reviews 86:117–155.

Sander, P. M., and M. Clauss. **2008**. Sauropod gigantism. Science 322(5899):200–201.

Sander, P. M., O. Mateus, T. Laven, and N. Knötschke. **2006**. Bone histology indicates insular dwarfism in a new Late Jurassic sauropod dinosaur. Nature 441(7094):739–741.

Sander, P. M., C. Peitz, F. D. Jackson, and L. M. Chiappe. **2008**. Upper Cretaceous titanosaur nesting sites and their implications for sauropod dinosaur reproductive biology. Palaeontographica Abteilung A 284(4-6):69–107.

Santos, V. 2016. Dinosaur tracksites in the Middle Jurassic of Maciço Calcário Estremenho (west-central Portugal): a geoheritage to be enhanced. Comunicações Geológicas 103(Especial I):55–58.

Santos, V. F., J. J. Moratalla, and R. Royo-Torres. **2009**. New sauropod trackways from the Middle Jurassic of Portugal. Acta Palaeontologica Polonica 54(3):409–422.

Santos, V. F. d., M. G. Lockley, C. A. Meyer, J. Carvalho, A. Galopim de Carvalho, and J. J. Moratalla. **1994**. A new sauropod tracksite from the Middle Jurassic of Portugal. Gaia: Revista de Geociências 10:5–13.

Santos, V. F. d., C. M. d. Silva, and L. A. Rodrigues. **2008**. Dinosaur track sites from Portugal: scientific and cultural significance. Oryctos 8:77–88.

Sanz, E., A. Arcos, C. Pascual, and I. M. Pidal. **2016**. Three-dimensional elasto-plastic soil modelling and analysis of sauropod tracks. Acta Palaeontologica Polonica 61(2):387–402.

Schanz, T., Y. Lins, H. Viefhaus, T. Barciaga, S. Läbe, H. Preuschoft, U. Witzel, and P. M. Sander. **2013**. Quantitative interpretation of tracks for determination of body mass. PLoS ONE 8(10):1–12.

Schwarz, D., E. Frey, and C. A. Meyer. **2007**. Novel reconstruction of the orientation of the pectoral girdle in sauropods. Anatomical Record 290(1):32–47.

Scrivner, P. J., and D. J. Bottjer. **1986**. Neogene avian und mammalian tracks from the Death Valley National Monument, California: their context, classification and preservation. Palaeogeography, Palaeoclimatology, Palaeoecology 57:285–331.

Sellers, W. I., G. M. Cain, W. Wang, and R. H. Crompton. **2005**. Stride lengths, speed and energy costs in walking of *Australopithecus afarensis*: using evolutionary robotics to predict locomotion of early human ancestors. Journal of the Royal Society, Interface 2(5):431–441.

Sellers, W. I., L. A. Dennis, and R. H. Crompton. **2003**. Predicting the metabolic energy costs of bipedalism using evolutionary robotics. The Journal of Experimental Biology 206:1127–1136.

Sellers, W. I., L. A. Dennis, W. W-J, and R. H. Crompton. **2004**. Evaluating alternative gait strategies using evolutionary robotics. Journal of Anatomy 204(5):343–351.

Sellers, W. I., J. Hepworth-Bell, P. L. Falkingham, K. T. Bates, C. A. Brassey, V. M. Egerton, and P. L. Manning. **2012**. Minimum convex hull mass estimations of complete mounted skeletons. Biology Letters 8(5):842–845.

Sellers, W. I., and P. L. Manning. **2007**. Estimating dinosaur maximum running speeds using evolutionary robotics. Proceedings of the Royal Society B 274(1626):2711–2716.

Sellers, W. I., P. L. Manning, T. Lyson, K. Stevens, and L. Margetts. **2009**. Virtual palaeontology: gait reconstruction of extinct vertebrates using high performance computing. Palaeontologia Electronica 12(3):1–26.

Sellers, W. I., L. Margetts, R. A. Coria, and P. L. Manning. **2013**. March of the titans: the locomotor capabilities of sauropod dinosaurs. PLoS ONE 8(10):1–21.

Snively, E., J. M. Fahlke, and R. C. Welsh. **2015**. Bone-breaking bite force of *Basilosaurus isis* (Mammalia, Cetacea) from the late Eocene of Egypt estimated by finite element analysis. PLoS ONE 10(2):1-23.

Soergel, W. 1925. Die Fährten der Chirotheria: Eine paläobiologische Studie. Verlag von Gustav Fischer, Jena, 92 pp.

Starke, S. D., J. J. Robilliard, R. Weller, A. M. Wilson, and T. Pfau. **2009**. Walk-run classification of symmetrical gaits in the horse: a multidimensional approach. Journal of the Royal Society, Interface 6(33):335–342.

Stein, K., and E. Prondvai. **2014**. Rethinking the nature of fibrolamellar bone: an integrative biological revision of sauropod plexiform bone formation. Biological Reviews 89(1):24–47.

Stevens, K. A., S. Ernst, and D. Marty. **2016**. Uncertainty and Ambiguity in the Interpretation of Sauropod Trackways; pp. 226–242 in P. L. Falkingham, D. Marty, and A. Richter (eds.), Dinosaur Tracks - The Next Steps. Life of the Past. Indiana University Press, Bloomington, 413 pp.

Stevens, K. A., and E. D. Wills. **2009**. Non-parasagittal yet efficient: the role of the pectoral girdles and trunk in the walk of *Triceratops* and *Apatosaurus*. Journal of Vertebrate Paleontology 29(3, Suppl. A):185.

Stoinski, S., T. Suthau, and H.-C. Gunga. **2011**. Reconstructing Body Volume and Surface Area of Dinosaurs Using Laser Scanning and Photogrammetry; pp. 94–104 in N. Klein, K. Remes, C. T. Gee, and P. M. Sander (eds.), Biology of the Sauropod Dinosaurs - Understanding the Life of Giants. Life of the Past. Indiana University Press, Bloomington, 331 pp.

Struckmann, C. 1880. Vorläufige Nachricht über das Vorkommen großer, vogelähnlicher Thierfährten (Ornithoidichnites) im Hastingssandsteine von Bad Rehburg bei Hannover. Neues Jahrbuch für Mineralogie, Geologie und Paläontologie 1:125–128.

Tagart, E. 1846. On markings in the Hastings Sand Beds near Hastings, supposed to be the footprints of birds. Quarterly Journal of the Geological Society 2(1-2):267.

Thompson, M. E., R. S. White, and G. S. Morgan. **2007**. Pace versus trot: can medium speed gait be determined from fossil trackways? New Mexico Museum of Natural History and Science Bulletin 42:309–314.

Thulborn, R. A. 1982. Speeds and gaits of dinosaurs. Palaeogeography, Palaeoclimatology, Palaeoecology 38:227–256.

Thulborn, R. A., and M. Wade. **1989**. A Footprint as a History of Movement; pp. 51–56 in D. D. Gillette and M. G. Lockley (eds.), Dinosaur Tracks and Traces. Cambridge University Press, Cambridge, 476 pp.

Thulborn, T. 1990. Dinosaur Tracks. Chapman and Hall, New York, 410 pp.

Tütken, T. 2011. The Diet of Sauropod Dinosaurs: Implications of Carbon Isotope Analysis on Teeth, Bones, and Plants; pp. 57–82 in N. Klein, K. Remes, C. T. Gee, and P. M. Sander (eds.), Biology of the Sauropod Dinosaurs - Understanding the Life of Giants. Life of the Past. Indiana University Press, Bloomington, 331 pp.

Upchurch, P. 1995. The evolutionary history of sauropod dinosaurs. Philosophical Transactions of the Royal Society B: Biological Sciences 349(1330):365–390.

Vila, B., F. D. Jackson, J. Fortuny, A. G. Selles, and A. Galobart. **2010**. 3-D modelling of megaloolithid clutches: insights about nest construction and dinosaur behaviour. PLoS ONE 5(5):1-13.

Vila, B., O. Oms, À. Galobart, K. T. Bates, V. M. Egerton, and P. L. Manning. **2013**. Dynamic similarity in titanosaur sauropods: ichnological evidence from the Fumanya Dinosaur Tracksite (Southern Pyrenees). PLoS ONE 8(2):1–9.

Wedel, M. J. 2003. Vertebral pneumaticity, air sacs, and the physiology of sauropod dinosaurs. Paleobiology 29(2):243–255.

Wedel, M. J. 2009. Evidence for bird-like air sacs in saurischian dinosaurs. Journal of Experimental Zoology 311A(8):611–628.

Wedel, M. J., and M. P. Taylor. **2013**. Caudal pneumaticity and pneumatic hiatuses in the sauropod dinosaurs *Giraffatitan* and *Apatosaurus*. PLoS ONE 8(10):1-14.

Weissengruber, G. E., G. F. Egger, J. R. Hutchinson, H. B. Groenewald, L. Elsasser, D. Famini, and G. Forstenpointner. **2006**. The structure of the cushions in the feet of African elephants (*Loxodonta africana*). Journal of Anatomy 209(6):781–792.

Werner, J., and E. M. Griebeler. **2011**. Reproductive biology and its impact on body size: comparative analysis of mammalian, avian and dinosaurian reproduction. PLoS ONE 6(12):1-12.

White, M. A., A. G. Cook, and S. J. Rumbold. **2017**. A methodology of theropod print replication utilising the pedal reconstruction of *Australovenator* and a simulated paleosediment. PeerJ 5(4):1-19.

Wilson, J. A. 2005. Integrating ichnofossil and body fossil records to estimate locomotor posture and spatiotemporal distribution of early sauropod dinosaurs: a stratocladistic approach. Paleobiology 31(3):400–423.

Wilson, J. A., and M. T. Carrano. **1999**. Titanosaurs and the origin of "wide-gauge" trackways: a biomechanical and systematic perspective on sauropod locomotion. Paleobiology 25(2):252–267.

Wilson, J. A., and P. C. Sereno. **1998**. Early evolution and higher-level phylogeny of sauropod dinosaurs. Journal of Vertebrate Paleontology 18(S2):1–79.

Witte, T. H., K. Knill, and A. M. Wilson. **2004**. Determination of peak vertical ground reaction force from duty factor in the horse (*Equus caballus*). The Journal of Experimental Biology 207(Pt 21):3639–3648.

Wright, J. L. 2005. Steps in Understanding Sauropod Biology; pp. 252–280 in K. Curry Rogers and J. A. Wilson (eds.), The Sauropods - Evolution and Paleobiology. University of California Press, Berkeley, 349 pp.

Yates, A. M., M. J. Wedel, and M. F. Bonnan. **2012**. The early evolution of postcranial skeletal pneumaticity in sauropodomorph dinosaurs. Acta Palaeontologica Polonica 57(1):85–100.

List of Figures

List of Tables

This dissertation presents analyses of recent and fossil tracks with quantitative and interdisciplinary methods for estimating the body mass and locomotion of a sauropod trackmaker. By employing methods from natural and engineering sciences, this research demonstrates that interdisciplinary research on tetrapod tracks can provide insights beyond conventional paleontological research. The novelty in this dissertation is that it brings aspects from traditional vertebrate ichnology together with modern methods and considerations from biomechanics and soil mechanics to gain additional information about sauropod paleobiology.

**Dissertation zur Erlangung des Doktorgrades (Dr. rer. nat.)
der Mathematisch-Naturwissenschaftlichen Fakultät
der Rheinischen Friedrich-Wilhelms-Universität Bonn**